Cortical and Thalamic Innervation of Striatum

by

Natalie M. Doig

Keble College

A thesis submitted to the University of Oxford

in fulfilment of the requirements for the degree of

Doctor of Philosophy

University of Oxford,

MRC Anatomical Neuropharmacology Unit,

Department of Pharmacology,

June 2012

Cortical and thalamic innervation of striatum

Natalie M. Doig
Keble College, Oxford

Thesis submitted for degree of Doctor of Philosophy
Trinity Term, 2012

Abstract

The basal ganglia are a collection of sub-cortical nuclei involved in the execution of a range of motor and cognitive behaviours. The striatum is the input nucleus of the basal ganglia, receiving major excitatory innervation from the cerebral cortex and intralaminar thalamic nuclei. The main target of these two pathways are the principal striatal neurons, the medium-sized spiny neurons (MSNs), which are subdivided based on their axonal targets and the expression of molecular markers. Direct pathway neurons project to the output nuclei of the basal ganglia and express the D_1 dopamine receptor subtype, whereas indirect pathway MSNs project to the output nuclei via the globus pallidus, and express the D_2 receptor. The striatum also contains interneurons that are essential in processing information within striatum; the cholinergic interneuron is of particular interest due to its role in reward-related behaviour. The aim of this study was to examine the cortical and thalamic innervation of subtypes of striatal neurons.

To examine whether the cortical or thalamic afferents selectively innervate direct or indirect pathway neurons, transgenic mice expressing GFP under either the D_1 or D_2 receptor promoter were used. Striatal sections from these mice were immunostained to reveal the GFP and selective markers of the cortical and thalamic afferents, VGluT1 and VGluT2, respectively. A quantitative electron microscopic examination of synaptic connectivity was carried out. The results indicate that there is no selectivity of either the cortical or thalamic pathway for D_1 or D_2 expressing MSNs. Thus both direct and indirect pathway MSNs are involved in the processing of both cortical and thalamic information

The cortical and thalamic innervation to cholinergic interneurons was also examined. Stimulation of cortex and thalamus *in vivo* in anaesthetised rats resulted in short-latency excitatory responses in identified cholinergic interneurons, indicative of monosynaptic connections. After recording, cholinergic interneurons were filled with neurobiotin. The synaptic innervation from cortex and thalamus was then examined in two individual, electrophysiologically characterised, and neurochemically identified cholinergic interneurons. One neuron received input from both cortex and thalamus, whereas the other neuron received input from the thalamus only. These results provide anatomical and physiological data illustrating how the excitatory inputs to striatum innervate cholinergic interneurons.

Acknowledgements

I would like to thank Professor Somogyi for his vision of the Unit. Working in the MRC Unit has been a privilege, and every day has brought me intellectual stimulation from a really talented group of people. I have had access to fantastic range of resources, for which I am very grateful.

I would like to thank my supervisor Professor Paul Bolam, who has been supportive, kind and encouraging throughout the time I have been in Oxford. It has been a really great experience to work with you; I have learned so much, I can't thank you enough.

I would like to thank Dr. Pete Magill for his encouragement throughout the years I have worked in the lab. Thank you for always providing me with sensible advice about all things science and DPhil related. And thank you for helping me along in my quest to learn electrophysiology.

I would like to thank Dr. Andrew Sharott. Thank you for teaching me *in vivo* physiology and being so patient and encouraging throughout.

I would like to thank Mrs Liz Norman for always being supportive and accommodating with everything personal license and animal related. Thank you for always helping me, despite how busy you are.

I would like to thank Gareth Hazell for all his help, and hard work in the lab.

Thank you to all the members of the Bolam and Magill labs, and indeed the Unit. It has been an excellent experience all round. There was always someone there whenever I had a question or needed a hand, which is invaluable.

Thank you to my family for being there always.

This thesis is dedicated to my grandmother, Dr Maisie Millar, and my mother, Julia, for their continuous support and encouragement.

Table of Contents

Abstract ..... **i;**

Acknowledgements ..... **ii;**

Table of Contents ..... **iv;**

List of Tables ..... **viii;**

List of Figures ..... **ix;**

List of Abbreviations ..... **xi;**

Preface ..... **xii**

Chapter One: General Introduction **1**

1.1. Functional Organisation of the Basal Ganglia **2**

1.1.1. An overview of the basal ganglia 2;

1.1.2. Striatum 5;

1.1.3. Globus pallidus (pars externa) 7;

1.1.4. Substantia nigra pars compacta 8;

1.1.5. Subthalamic nucleus 10;

1.1.6. The output nuclei of the basal ganglia 11;

1.1.7. Summary 12

1.2. Microcircuitry of the Striatum **14**

1.2.1. Medium-sized spiny neurons 14;

1.2.2. Striatal interneurons 20

1.2.2.1. Parvalbumin-expressing interneurons 20;

1.2.2.2. Nitric oxide synthase-expressing interneurons 22;

1.2.2.3. Calretinin-expressing interneurons 25;

1.2.2.4. Cholinergic interneurons 25

1.2.3. Summary 29

1.3. Corticostriatal Projection **30**

1.3.1. Overview 30;

1.3.2. Neurons that give rise to the corticostriatal projection 30;

1.3.3. Synaptic organisation of the corticostriatal pathway 31;

1.3.4. Functional organisation of the corticostriatal projection 33

1.3.4.1. Corticostriatal plasticity 36

1.3.5. Summary 38

1.4. Thalamostriatal Projection 39

1.4.1. Overview 39;

1.4.2. Neurons that give rise to the thalamostriatal projection 39;

1.4.3. Synaptic organisation of the thalamostriatal projection 44;

1.4.4. Functional organisation of the thalamostriatal system 46;

1.4.5. Summary 48

1.5. Aims 49

1.5.1. Cortical and thalamic innervation of MSNs 49;

1.5.2. Cortical and thalamic innervation of cholinergic interneurons 49

1.5.2.1. Cortical and thalamic input to cholinergic interneurons in vivo. 49;

1.5.2.2. Cortical and thalamic synaptic input to an individual cholinergic interneuron. ... 50

Chapter Two: Cortical and thalamic innervation of medium-sized spiny neurons in the mouse striatum 51

2.1. Introduction 52

2.1.1. Aims 53

2.2. Materials and Methods 54

2.2.1. Tissue preparation 54;

2.2.2. Immunohistochemistry 54;

2.2.3. Electron microscopic analysis 57

2.2.3.1. Tissue single-labelled for VGluT1 or VGluT2 in D_1 and D_2 mice 57;

2.2.3.2. Tissue double-labelled for VGluT1 or VGluT2 and GFP in D_1 and D_2 mice 59

2.2.4. Statistical analysis 60

2.3. Results 61

2.3.1. Postsynaptic targets of corticostriatal and thalamostriatal afferents in D_1 and D_2 transgenic mice. 61;

2.3.2. Morphological characteristics of corticostriatal and thalamostriatal terminals in D_1 and D_2 transgenic mice 63;

2.3.3. Innervation of direct and indirect pathway MSNs by corticostriatal and

thalamostriatal afferents 63;

2.3.4. Divergence and convergence of afferents derived from the cortex and thalamus in the striatum 69

2.4. Discussion 74

2.4.1. Cortical and thalamic input to direct and indirect pathway MSNs 74;

2.4.2. Technical considerations..... 78

Chapter Three: Cortical and thalamic inputs to cholinergic interneurons..... 80

3.1. Introduction 81

3.1.1. Aims..... 83

3.2. Methods and Materials 85

3.2.1. Electrophysiological recordings 85;

3.2.2. Stimulation of cortex and thalamus 86;

3.2.3. Juxtacellular labelling of single neurons 87;

3.2.4. Histochemistry and immunohistochemistry 87;

3.2.5. Data acquisition and analysis 88

3.3. Results..... 92

3.3.1. Electrophysiological recordings of striatal neurons 92;

3.3.2. Responses of cholinergic interneurons to cortical stimulation 95;

3.3.3. Responses of cholinergic interneurons to thalamic stimulation 102;

3.3.4. Responses of cholinergic interneurons to both cortical and thalamic stimulation 110

3.4. Discussion 119

3.4.1. Cortical and thalamic stimulation of cholinergic interneurons 119;

3.4.2. Technical considerations..... 126

Chapter Four: Cortical and thalamic synaptic innervation of cholinergic interneurons..... 127

4.1. Introduction 128

4.1.1. Aims..... 129

4.2. Methods and Materials 131

4.2.1. Tissue 131;
4.2.2. Immunohistochemistry 131;
4.2.3. Digital reconstruction and analysis 133;
4.2.4. Re-embedding and ultramicrotoming 134;
4.2.5. Electron microscopy 135;
4.2.6. Analysis 135
4.3. Results 138
4.3.1. Dendritic organisation of cholinergic interneurons 138;
4.3.2. Synaptic innervation of cholinergic interneurons 144
4.4. Discussion 156
4.4.1. Dendritic structure of cholinergic interneurons 156;
4.4.2. Synaptic innervation of cholinergic interneurons 157;
4.4.3. Technical considerations 162
Chapter Five: General Discussion 163
5.1. General Discussion 164
5.1.1. Future work 170;
5.1.2. General conclusions 172
References 174

List of Tables

Table 2.1. Postsynaptic targets of individual VGluT1- and VGluT2-positive terminals in D_1 and D_2 transgenic mice, in comparison to previous studies 62

Table 3.1. Reagents and antibodies used for histochemistry and immunohistochemistry. 91

Table 3.2. Summary of neurons recorded and stimulation protocols applied. 97

Table 4.1. Summary of the antibodies used during processing. 136

Table 4.2 Summary of the processing of the neurons 137

Table 4.3. Dendritic properties of reconstructed cholinergic interneurons. 142

Table 4.4. Synaptic input to each fragment of dendrite examined for an indivdidual cholinergic interneuron, neuron H. 147

Table 4.5 Synaptic input to each fragment of dendrite examined for an individual cholinergic interneuron E. 148

List of Figures

Figure 1.1. The basal ganglia: connectivity of the major nuclei. 4

Figure 1.2. Synaptic connectivity between subtypes of striatal neurons. 19

Figure 1.3. Projection from the intralaminar thalamic nuclei to the striatum in the rat. 43

Figure 2.1. D1- and D2- expressing MSNs in the striatum, as revealed by immunoperoxidase labelling for EGFP. 66

Figure 2.2. D_1 and D_2 MSNs receive synaptic input from VGluT1-postive terminals and with VGluT2-positive terminals. 67

Figure 2.3. Quantitative analysis of the cortical and thalamic innervation of direct and indirect pathway MSNs in the striatum. 68

Figure 2.4. Divergent cortical and thalamic input to direct and indirect pathway MSN spines. 71

Figure 2.5. An individual direct pathway MSN may receive synaptic input from both thalamic (VGluT2-positive) and putative cortical (VGluT2-negative) terminals. . 72

Figure 2.6. Summary of the patterns of innervation from cortex and thalamus to direct and indirect pathway neurons. 73

Figure 3.1 Experimental set-up. 90

Figure 3.2. Physiological and morphological properties of an identified cholinergic interneuron. 94

Figure 3.3. Cortical stimulation of an identified cholinergic interneuron. 98

Figure 3.4. Average response to a single cortical stimulus. 99

Figure 3.5. Paired cortical stimulation of an identified cholinergic interneuron. . 100

Figure 3.6. Average response to paired cortical stimulation. 101

Figure 3.7. Thalamic stimulation of an identified cholinergic interneuron. 103

Figure 3.8. Average responses to a single thalamic stimulus. 104

Figure 3.9. Paired thalamic stimulation of an identified cholinergic interneuron. 105

Figure 3.10. Average response to paired thalamic stimulation. 106

Figure 3.11. 40 Hz thalamic stimulation of an identified cholinergic interneuron. 108

Figure 3.12. Average responses to 40 Hz thalamic stimulation. 109

Figure 3.13. Responses of an individual identified cholinergic interneuron to cortical and thalamic stimulation. 112

Figure 3.15. Responses of individual identified cholinergic interneurons to cortical and thalamic stimulation. 113

Figure 3.14. Responses of five identified cholinergic interneuron to both cortical and thalamic stimulation. 116

Figure 3.16. Response of two identified cholinergic interneurons to both paired cortical and thalamic stimulation. 117

Figure 3.17. Response of one identified cholinergic interneuron to 40Hz stimulation of cortex and thalamus. 118

Figure 3.18. Schematic diagram indicating connectivity between the cortex, striatum and Pf nucleus. 124

Figure 4.1. Schematic diagram illustrating the methods used. 136

Figure 4.2. Analysis of the dendritic of an individual cholinergic interneuron, neuron H. 139

Figure 4.3.Analysis of the dendritic of an individual cholinergic interneuron, neuron E..... 140

Figure 4.4. Analysis of the dendritic of an individual cholinergic interneuron, neuron L..... 141

Figure 4.5. Sholl analysis of the dendrites of the reconstructed cholinergic interneurons. 143

Figure 4.6. VGluT2-positive terminals form asymmetric synapses with the dendrites of a cholinergic interneuron. 149

Figure 4.7. VGluT1 and VGluT2-positive terminals form synapses with the dendrites of an individual cholinergic interneuron. 150

Figure 4.8. Unlabelled terminals form asymmetric and symmetric synapses with the dendrites of a cholinergic interneuron, neuron H. 151

Figure 4.9. Unlabelled terminals form asymmetric and symmetric synapses with the dendrites of a cholinergic interneuron, neuron E. 152

Figure 4.10. Proportions of synapses onto the dendrites of two cholinergic interneurons, neurons H and E. 153

Figure 4.11. Synaptic density of symmetric and asymmetric synapses in the different dendritic compartments, examined for two cholinergic interneurons 154

Figure 4.12. Average proportion and distribution of all synapses examined. 155

List of Abbreviations

5-HT: 5-hydroxytryptamine
6-OHDA: 6-hydroxydopamine
ABC: avidin biotin peroxidase complex
AHP: after hyperpolarisation
BAC: bacterial artificial chromosome
cAMP: cyclic adenosine monophosphate
ChAT: choline acetyltransferase
CM: centre médian nucleus
CNS: central nervous system
CR: calretinin
CST: crossed corticostriatal
EEG: electroencephalogram
EM: electron microscopy
EP: entopeduncular nucleus
EPSC: excitatory post synaptic current
FS: fast spiking
GABA: gamma amino butyric acid
GAD: glutamic acid decarboxylase
GP: globus pallidus
GPe: globus pallidus pars externa
GPi: globus pallidus pars interna
HB: habenula
ICSS: intracranial self stimulation
IKir: inward rectifying potassium channel
Ih: hyperpolarisation activated cation current
ITN: intralaminar thalamic nuclei
IP3: inositol tri-phosphate
IPSC: inhibitory post synaptic current
LTD: long term depression
LTP: long term potentiation
LTS: low threshold spiking
MSN: medium-sized spiny neuron
NAcc: nucleus accumbens
NGS: normal goat serum
NO: nitric oxide
NOS: nitric oxide synthase
NPY: neuropeptide Y
OCD: obsessive compulsive disorder
PB: phosphate buffer
PBS: phosphate buffer saline pH 7.4
Pf: parafascicular nucleus
PPE: pre-proenkephalin
PPN: pedunculopontine nucleus
PT: pyramidal tract
PV: parvalbumin
RF: reticular formation
SC: superior colliculus
SD: standard deviation
SEM: standard error of the mean
SN: substantia nigra
SNpc: substantia nigra pars compacta
SNpr: substantia nigra pars reticulata
SS: somatostatin
STN: subthalamic nuclei
SWA: slow wave activity
TH: tyrosine hydroxylase
VGluT1: vesicular glutamate transporter sub-type 1
VGluT2: vesicular glutamate transporter sub-type 2
VTA: ventral tegmental area

Chapter Two of this thesis is based on the publication:

Cortical and Thalamic Innervation of Direct and Indirect Pathway Medium-Sized Spiny Neurons in Mouse Striatum

by Natalie M. Doig, Jonathan Moss, and J. Paul Bolam, (2010),

The Journal of Neuroscience, **30**:14610 –14618.

Research carried out by the DPhil candidate contributed to the following publication, but was not included in this thesis:

Functional Alterations to the Nigrostriatal System in Mice Lacking All Three Members of the Synuclein Family.

by Anwar, S., Peters, O., Millership, S., Ninkina, N., **Doig, N**., Connor-Robson, N., Threlfell, S., Kooner, G., Deacon, R.M., Bannerman, D.M., Bolam, J.P., Chandra, S.S., Cragg, S.J., Wade-Martins, R. & Buchman, V.L. (2011)

The Journal of Neuroscience, **31:** 7264-7274.

Chapter One: General Introduction

1.1. Functional Organisation of the Basal Ganglia

1.1.1. An overview of the basal ganglia

The basal ganglia are a collection of sub-cortical nuclei that are involved in a range of motor and cognitive processes. One of the major roles of the basal ganglia is in the integration of sensorimotor information and the elicitation of specific behaviours. Information to the basal ganglia arises from all areas of the cerebral cortex, and the thalamus. The way in which the basal ganglia assimilate this information in order to carry out their role is an area of active research. The significance of the role of the basal ganglia is illustrated in the devastating neurological disorders associated with this brain region, such as the motor deficits that result from Parkinson's disease. Although, historically it was believed that the basal ganglia are exclusively involved in motor processing, it is now recognised that the basal ganglia are involved in a much more extensive range of functions such as reward-based learning.

The dorsal division of the basal ganglia, which is primarily associated with sensorimotor processing, includes the striatum[1], the globus pallidus pars externa[2] (GPe), the globus pallidus pars interna[3] (GPi), the subthalamic nucleus (STN) and the substantia nigra (SN), which can be divided into two major regions: the substantia nigra pars compacta (SNpc) and the more ventral substantia nigra pars reticulata (SNpr). The SNpc contains dopaminergic neurons that project to the striatum via the nigrostriatal pathway. The ventral division of the basal ganglia, generally associated with limbic functions, consists of the nucleus accumbens[4] (NAcc), the ventral pallidum, and the ventral tegmental area (VTA) (Bolam *et al.*, 2000). Although the main focus of this thesis is the dorsal division of the basal ganglia the division of the striatum into functionally distinct regions is an important

1 In primates and other mammals the striatum is made up of the putamen and caudate nucleus which is divided by the internal capsule.

2 In rodents the globus pallidus pars externa is simply the globus pallidus.

3 The globus pallidus pars interna is given the name the entopeduncular nucleus in several species including rodents

4 The nucleus accumbens is the ventral division of the striatum.

feature of its organisation.

The striatum is the main recipient of inputs to the basal ganglia. The entire cortical mantle projects to the striatum, although there is also a notable cortical projection to the STN (Nambu *et al.*, 2002). The striatum receives a significant input from the thalamus, mainly originating in the intralaminar thalamic nuclei (ITN). In a classical view of basal ganglia function the striatum receives input in a topographical manner, from specific regions of cortex, the striatum then 'processes' this information and sends it through the basal ganglia network to the GPi and SNpr, the output nuclei of the basal ganglia. Information can then be transmitted to the targets of the basal ganglia, such as the thalamus, superior colliculus (SC), pedunculopontine nucleus (PPN), reticular formation (RF), and the lateral habenula (HB) which then results in the execution of particular behaviours such as movement, in a context-dependent manner (See Figure 1.1; Alexander *et al.*, 1986). Each of the sub-nuclei of the basal ganglia have specific anatomical and physiological features which allow them to carry out their particular roles within the network.

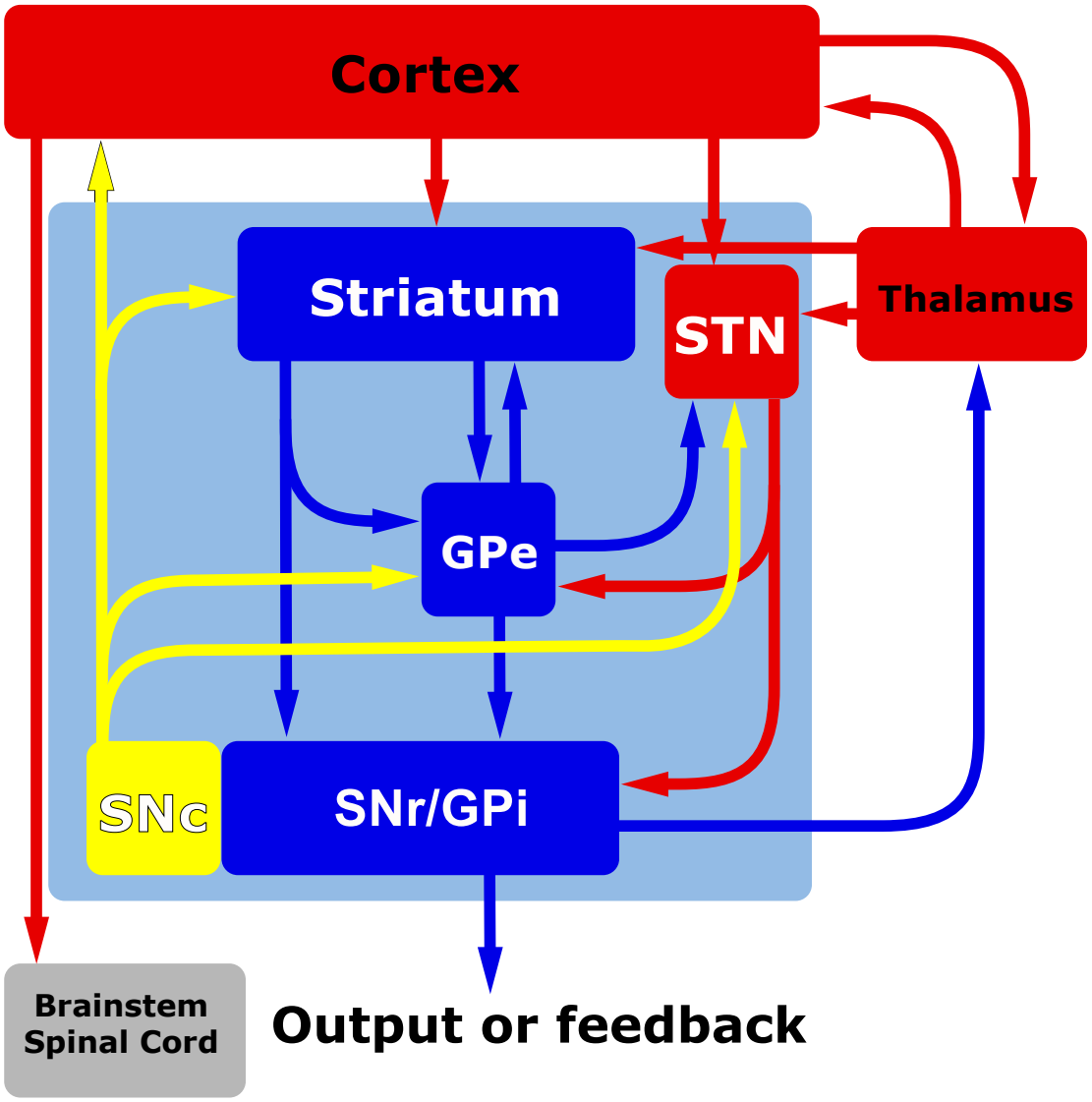


Figure 1.1. The basal ganglia: connectivity of the major nuclei.

The component nuclei of the basal ganglia (within the light blue box), and the major inputs to the basal ganglia. Inhibitory (GABAergic) nuclei are shown in blue, excitatory (glutamatergic) nuclei are in red and dopaminergic nuclei are in yellow (Bolam et al., 2009). Information is transmitted from the striatum to the ouput nuclei via two pathways; the 'direct pathway' is composed of neurons that project directly to the output nuclei of the basal ganglia (SNr/GPi), whereas neurons that give rise to the 'indirect pathway' project to the output nuclei via the GPe.

1.1.2. Striatum

The striatum is the input nucleus of the basal ganglia, receiving massive innervation from both the cortex and the thalamus. The principal neuronal cell type within the striatum is the medium-sized spiny neuron (MSN), which is a GABAergic projection neuron. The population of MSNs are subdivided based on their axonal projections, as well as the expression of certain molecular markers. Neurons that make up the so called "direct pathway" project directly to the output nuclei of the basal ganglia (GPi and SNpr); whereas neurons of the "indirect' pathway" project to the output nuclei via the GPe (See Figure 1.1). The separation of MSNs into two populations is a central tenet of our understanding of the organisation and function of the basal ganglia and will be discussed in more detail.

Although the MSNs are the primary cell type, there are also four main types of interneuron within the striatum. There are three subsets of GABAergic interneurons which can be separated based on their expression of certain molecular markers: i) parvalbumin- (PV) expressing interneurons, ii) calretinin- (CR) expressing interneurons, and iii) nitric oxide synthase- (NOS) expressing interneurons. The fourth group is the cholinergic interneuron, which releases the neurotransmitter acetylcholine (Kawaguchi, 1997). Although striatal interneurons are greatly outnumbered by the MSNs they possess specific anatomical and physiological features which put them in a position to significantly influence the output of the striatum and thus shape the function of the basal ganglia. Interneurons are therefore of particular interest in the study of the striatum and will be discussed in more detail.

The striatum also exhibits a structural organisation in the form of certain regions called 'patches' (also known as 'striosomes') which show high levels of expression of specific molecular markers. Striatal patch compartments exhibit dense μ-opioid expression and low levels of acetylcholinesterase (Gerfen, 1992). The matrix compartment, in which the patches are embedded, can be defined by the presence of neurons that express calbindin (Gerfen, 1992). The separation of the striatum into patch and matrix compartments is

particularly important in relation to the afferent and efferent organisation of striatum. Cortical neurons that give rise to the corticostriatal pathway are mainly located in layers III and V (McGeorge & Faull, 1989). The patch compartments receive innervation from cortical neurons in deep layer V, whereas the matrix compartments receive input from superficial layer V and layer III (Gerfen, 1992). This specific functional organisation is maintained in the output of striatum. The MSNs within the patch compartment send their axons to SNpc, whereas matrix MSNs project to SNpr (Gerfen, 1992). The SNpc is of particular interest in understanding the role of the striatum in reward-related behaviour, therefore the specificity of patch neurons innervating the SNpc indicates a precise role of patch MSNs in the dopaminergic circuitry (Fujiyama *et al.*, 2011). The organisation of striatal neurons into different compartments and the specificity of afferent and efferent connectivity are important for the way in which the striatum assimilates and processes information, although the functional implications of this organisation remain difficult to elucidate.

The actions of neuromodulators within the striatum are central in shaping the dynamics of this microcircuit. Of the neuromodulators that influence striatal circuitry, the most studied are dopamine and acetylcholine. Dopamine is released from axons that originate in the SNpc; acetylcholine is released locally by interneurons within the striatum, the influence of these will be discussed later. Aside from dopamine and acetylcholine, the striatum also receives other neuromodulatory inputs including serotonergic innervation from the dorsal raphé nucleus and histaminergic innervation from the tuberomamillary nucleus of the posterior hypothalamus. Serotonin (5-hydroxytryptamine; 5-HT) in the CNS is important for normal brain function; disorders of the serotonin system are known to underlie several neurological disorders such as depression and obsessive compulsive disorder (OCD), for example (Graybiel & Rauch, 2000). The striatum receives a notable serotonergic innervation, and indeed expresses an abundance of serotonin receptors (Barnes & Sharp, 1999). The role of serotonin within the basal ganglia is complex and inextricably linked to an interaction with dopamine (Di Giovanni *et al.*, 2008; Navailles & De Deurwaerdere, 2011). Neurons of the raphé nucleus also innervate other nuclei of

the basal ganglia, as well as the striatum, including the SNpc and can thus elicit their effects on the basal ganglia through different routes. Within the striatum, serotonin is able to excite two of the four subtypes of interneuron which in turn can modify the behaviour of the MSNs (Blomeley & Bracci, 2005; Blomeley & Bracci, 2009).

Histamine has an important role in the regulation of circadian rhythms as well as other behaviours. In the CNS, histamine acts on H_3 receptors which are most abundant within the striatum (Pollard *et al.*, 1993). Histamine H_3 receptors are located on axon terminals and can thus act presynaptically as auto receptors, thereby modulating the release of neurotransmitters. In the striatum, histamine can modulate the release of several neurotransmitters such as dopamine, serotonin, and glutamate (Pollard *et al.*, 1993; Molina-Hernandez *et al.*, 2001). Recently, histamine has been shown to have a suppressive role on the excitatory inputs to the striatum, as well as decreasing the lateral inhibition between MSNs (Ellender *et al.*, 2011). Histamine, like serotonin, is thus in a position to be able to alter processing within the striatum. Neuromodulation within striatum is complex and widely recognised to be essential to the functional circuitry. The striatum is the focus of this thesis and will be discussed in greater detail.

1.1.3. Globus pallidus (pars externa)

The external part of the globus pallidus (GPe), simply known as the globus pallidus (GP) in rodents, is a GABAergic structure located medial and caudal to the striatum. The GPe is the primary target of striatal neurons that make up the indirect pathway (Smith *et al.*, 1998). In addition to the neurons of the indirect pathway that project to the GPe, neurons of the direct pathway also have axonal collaterals which innervate the GPe as they project to the SNpr/GPi (Kawaguchi *et al.*, 1990; Fujiyama *et al.*, 2011). The GPe also receives a glutamatergic input from the STN (Kita, 2007), and to a lesser extent, the GPe also receives input from the SNpc (Kita, 2007).

The GPe sends a GABAergic output to many of the nuclei within the basal ganglia, including the STN and the output nuclei (See Figure 1.1) (Kita, 2007). A subset of neurons within the GPe also project back to the striatum, where they can selectively innervate

interneurons (Kita & Kitai, 1994; Bevan *et al.*, 1998). GPe neurons also give rise to local axon collaterals within the GPe (Bevan *et al.*, 1998; Sadek *et al.*, 2007).

Neurons of the GPe which project to striatum have spiny dendrites, and are PV-negative but express preproenkephalin (PPE), whereas the non-striatal projecting neurons have aspiny dendrites and express PV (Kita, 2007). *In vivo* recordings of GPe neurons have shown that there are at least two types of GPe neuron which can be differentiated on firing rate, pattern and waveform; although the use of anaesthesia appears to have a dramatic effect on the spontaneous nature of these neurons (Gardiner & Kitai, 1992; Kelland *et al.*, 1995; Magill *et al.*, 2000; Kita, 2007). The GPe is highly interconnected with the other nuclei of the basal ganglia and therefore in a central position to alter the processing and output of the basal ganglia network.

1.1.4. Substantia nigra pars compacta

The substantia nigra pars compacta (SNpc) is located in the midbrain and the dopaminergic neurons within this area are referred to as cell group A9. The SNpc provides dopaminergic innervation to the striatum, forming the nigrostriatal projection. Neurons in the ventral tegmental area (VTA; A10) also project to the striatum, forming the mesostriatal pathway. The SNpc provides dopaminergic input to the dorsal, sensorimotor part of striatum, whereas the VTA provides input to the limbic-related areas of striatum (Smith & Kieval, 2000); therefore the SNpc is the focus here.

The SNpc receives input from striatum, neurons of the direct pathway innervate dopaminergic neurons, as shown by the co-localisation of substance P and GABA in presynaptic terminals forming synapses with TH-positive neurons in the SNpc (Bolam & Smith, 1990). The SNpc also receives notable innervation from the GPe (Smith & Bolam, 1990b), and the GABAergic neurons of the SNpr (Mailly *et al.*, 2003). Striatal neurons which project to the SNpc are anatomically segregated from those which project to the substantia nigra pars reticulata (SNpr) as only the direct pathway MSNs which are located within the patch compartment of the striatum project to the SNpc (Fujiyama *et al.*, 2011).

The dopaminergic neurons in the SNpc which project to striatum have huge axonal arborisations (an average axon length of almost 0.5 m), which innervate both the patch and matrix compartments of striatum (Matsuda *et al.*, 2009). Neurons of the SNpc preferentially innervate the striatum, although some of them do have axon collaterals which innervate GPe and STN (Hassani *et al.*, 1997; Matsuda *et al.*, 2009). The way in which dopaminergic axons innervate the striatum is non selective with all striatal structures being within 1 μm of a TH-positive synapse (Moss & Bolam, 2008). Due to this pattern, and the sheer size of the neurons, all subtypes of neurons within striatum are in a position to be modulated by dopamine.

Dopaminergic neurons of the SNpc have a firing rate of about 5 Hz *in vivo,* in the anaesthetised rat, and can exhibit a variety of firing patterns including random, pacemaker and bursting activity (Brown *et al.*, 2009). The SNpc is not a homogeneous structure, but can be divided into dorsal and ventral tiers, neurons in the dorsal tier are positive for calbindin (Smith & Kieval, 2000). Calbindin-expressing and calbindin-negative neurons exhibit different spontaneous firing activity *in vivo*; calbindin-positive neurons have a slightly slower firing rate (Brown *et al.*, 2009). These neurons also display different levels of susceptibility in Parkinson's disease. Calbindin-positive neurons have some level of protection against the neuropathological processes involved in the degeneration of dopaminergic neurons; this is observed in both patients and in animal models of the disease (Yamada *et al.*, 1990).

Dopamine is involved in many functions in the brain including reward-related behaviour, movement, cognition, mood, sleep, attention, memory and learning. The nigrostriatal pathway is greatly diminished in Parkinson's disease, and it is this that initially identified it as a crucial element in basal ganglia motor loop. Dopamine has also received attention in relation to its role in reward, and at the extreme end of this, addiction. Dopaminergic neurons in the SNpc exhibit distinctive firing patterns in relation to reward, and the cues that predict reward, during behavioural tasks in the primate. Dopaminergic neurons will respond with an increase in firing when a reward is given (with no cue),

will respond to a cue that has become associated with a reward, will show no response if there is a cue which predicts a reward and the reward is given as predicted, and finally, dopaminergic neurons will show a decrease in firing if a predicted reward is omitted, which is often termed the 'reward error prediction signal' (Schultz, 1998). In this way dopamine neurons have been considered to be neural substrates for the coding of reward (Bromberg-Martin *et al.*, 2010).

The effects of dopamine within the striatum are heterogeneous and complex, and dependent on the receptors expressed and the level of dopamine available (Gerfen & Surmeier, 2011). Dopamine acts via the D_1-like[5] or D_2-like[6] families of receptors to mediate its effects. In the striatum, dopamine is essential for the induction, maintenance and reversal of plasticity (Calabresi *et al.*, 2007). Dopamine acts via second messenger cascades to activate or inhibit specific currents and intracellular messengers in order influence processing within striatum. The role of dopamine in corticostriatal plasticity will be discussed.

1.1.5. Subthalamic nucleus

The STN is the only glutamatergic nucleus within the basal ganglia, and is thought to 'drive' the other nuclei (Bevan *et al.*, 2007). Neurons of the STN project to the GPe and the GPi/SNpr, and are capable of exerting considerable influence over these target nuclei. However, the STN is under tight regulatory control as it forms a reciprocal network with the GPe (Shink *et al.*, 1996; Bevan *et al.*, 2007). This network is important in normal basal ganglia functioning, and abnormal activity is thought to underlie neurological dysfunction (Plenz & Kital, 1999). The STN has been of particular interest in the study of neurological diseases, as direct manipulation of this nucleus, in the form of 'deep brain stimulation', can improve the symptoms of specific motor disorders such as Parkinson's disease.

The STN also receives glutamatergic input from both motor cortex and the

---

5 The D1 family of receptors (D_1, D_5) are GPCRs which *activate* adenylyl cyclase and cAMP production.

6 The D2 family of receptors (D_2, D_3, D_4) are GPCRs which *inhibit* adenylyl cyclase and cAMP production.

intralaminar thalamic nucleus, and a dopaminergic input from the SNpc. Neurons of the STN fire tonically at about 5-15Hz, displaying autonomous pacemaker activity (Bevan *et al.*, 2007). This tonic firing is altered by the many afferent inputs to the STN, and importantly in terms of Parkinson's disease, dopamine (Bevan *et al.*, 2002). Thus the role of the STN in integrating these multiple inputs places it in a central position to alter network activity within the basal ganglia.

1.1.6. The output nuclei of the basal ganglia

The SNpr and the GPi form the output nuclei of the basal ganglia, and as such are the last stage for information processing in the basal ganglia. In rodents the GPi is not as developed as it is in primates, and is referred to as the entopeduncular nucleus (EP). The EP/GPi and SNpr are the main targets of the neurons that make up the direct pathway, and since the striatum contains many more neurons than within these two nuclei there is likely to be a high degree of convergence (Smith *et al.*, 1998). The SNr/GPi receives a projection from the STN, providing the only glutamatergic influence over the output nuclei (Smith *et al.*, 1998). The SNr also receives a GABAergic input from the GPe (Smith *et al.*, 1998). The output nuclei are thus able to receive processed information via the indirect pathway. In this way the GPe is able to exert an additional inhibitory influence over the output nuclei (Deniau *et al.*, 2007).

The SNr and GPi contain GABAergic cells that project to nuclei within the thalamus and other subcortical structures. These neurons fire tonically *in vivo* and *in vitro* exerting an overall tonic inhibition on the neurons that they innervate (Hikosaka, 2007). The neurons of the SNr and GPi/EP send an innervation to the thalamus, mainly to the ventromedial-ventrolateral complex, which has a diffuse cortical projection (Hauber, 1998). The SNr and GPi/EP also innervate nuclei of the intralaminar thalamic nucleus, the region of thalamus which projects to striatum (Hauber, 1998). The output nuclei also project to the superior colliculus (SC) and the pedunculopontine nucleus (PPN) (Hauber, 1998).

In order to understand the output of the basal ganglia and its role in eliciting

certain behaviours Hikosaka and colleagues (2007) have studied the control of the SNr over the SC which is known to be highly involved in the oculomotor system. Neurons in the SNr show a decrease in overall firing rate that is directly related to the preparation of a saccade in the primate (Hikosaka, 2007). This causes a disinhibition of neurons in the SC, which elicits a spike which allows the saccade to be executed (Hikosaka, 2007). Although this is over-simplified here, this gives us insight into a particular way in which information coming from the basal ganglia can have a direct role in the execution of a specific motor action.

1.1.7. Summary

The functional organisation of the basal ganglia is well-conserved over evolution. Indeed all amphibians, amniotes, jawed fish and lamprey have functioning basal ganglia which exhibit some of the classical cellular and neurochemical features of the basal ganglia (Reiner *et al.*, 1998), including a complex connectivity with a direct and indirect pathway present in the lamprey (Stephenson-Jones *et al.*, 2011). This conservation in vertebrates indicates that the basal ganglia are involved in processes that are central to survival, such as the selection of an action in the presence of competing sensory inputs and conflicting motor systems (Redgrave *et al.*, 1999; Grillner *et al.*, 2005; Stephenson-Jones *et al.*, 2011).

The neural substrates of the basal ganglia are organised in a way that provides evidence for parallel processing of functionally segregated circuits, a concept put forward by Alexander, DeLong and Strick (1986). This concept incorporates the inputs to the basal ganglia, the organisation within the separate nuclei of the basal ganglia and the output regions to form a comprehensive model which takes into account at least five separate functional circuits; motor, oculomotor, dorsolateral, lateral orbitofrontal, and anterior cingulate, in the non-human primate (Alexander *et al.*, 1986; Alexander & Crutcher, 1990). This theory provides explanation for how the basal ganglia are involved in such a wide range of neural processes. However, anatomical evidence has accumulated which demonstrates that the basal ganglia circuitry is much more complex than the parallel

processing theory would suggest. The basal ganglia are involved in several neurological diseases, including motor diseases such as Parkinson's disease and Huntington's disease, research into these disorders has provided great insight into the function of the basal ganglia (Albin *et al.*, 1989). Insight into the clinical manifestations of these diseases has allowed functional models of basal ganglia organisation to be proposed, and have established a basis for experimental work (Albin *et al.*, 1989).

The basal ganglia are involved in a wide range of behaviours, and indeed neurological disorders. In order to understand the role of the basal ganglia in this extensive array of neurological processes it is essential to examine the underlying organisation of the basal ganglia. This is emphasised by fact that most of the therapeutic advances for Parkinson's disease have stemmed from basic scientific research. The cortex and thalamus provide the major innervation to the basal ganglia; the way in which the striatum processes and transmits this information is key in shaping the overall output of the basal ganglia network.

1.2. Microcircuitry of the Striatum

1.2.1. Medium-sized spiny neurons

Medium-sized spiny neurons (MSNs) are the principal neuronal cell type, and constitute the primary computational unit of the striatum. The MSNs assimilate the inputs to striatum and transmit this information through the basal ganglia network, thereby shaping the functional output. The population of MSNs are GABAergic, and are so called because of their size, and the fact that their dendrites are densely spiny (Smith & Bolam, 1990a). Over 95% of the total cell population in striatum is composed of MSNs, the remaining percentage consisting of striatal interneurons (Oorschot, 1996; Rymar *et al.*, 2004). The division of MSNs into two separate projection pathways is a central principle of the model of basal ganglia function. MSNs of the 'direct pathway', which project to the output nuclei of the basal ganglia (GPi, SNr), express the dopamine D_1 receptor subtype, and contain the neuropeptides substance P and dynorphin[7] (Gerfen *et al.*, 1990; Yung *et al.*, 1995). MSNs that project to the output nuclei via the GPe constitute the '*indirect pathway*' and express the dopamine D_2 receptor subtype and contain the neuropeptide enkephalin[8] (Gerfen *et al.*, 1990; Yung *et al.*, 1995). The direct/indirect pathway model is central to the functional organisation of basal ganglia, and has provided a framework for the comprehension and examination of disorders of the basal ganglia, as proposed by Albin and colleagues (1989). This model was motivated by the clinical manifestations of basal ganglia disorders in human patients and presents a description of basal ganglia functional organisation in both the diseased and normal states. In this model hypo- and hyper-kinetic disorders are explained by an imbalance in the output from striatum. In hypo-kinetic disorders, such as Parkinson's disease, this imbalance results in an increase in the inhibitory output of the basal ganglia to motor regions of the thalamus. An increase in this inhibition can be explained by over-activity in the indirect pathway which leads to increased inhibition of the GPe, and in turn a disinhibition of the output nuclei, and

7 This pathway is also known as the striatonigral pathway, as the neurons innervate the SNr.

8 This pathway is also known as the striatopallidal pathway as the primary target is the GPe.

increased excitation through the disinhibition of STN, resulting in a suppression of motor output (Albin *et al.*, 1989). Conversely, an increase in activity of the direct pathway can result in an increase in motor output, such as seen in hyper-kinetic disorders. Increased activity in the direct pathway (or decreased activity in the indirect pathway) leads to increased inhibition of the basal ganglia output, and thus a disinhibition of the motor related targets of basal ganglia output. Thus imbalances in the direct/indirect pathways can explain the changes in motor output as seen in clinical disorders of the basal ganglia (Albin *et al.*, 1989). Although greatly oversimplified here, this model has provided an essential paradigm for the examination of basal ganglia function, and indeed one that has been examined at many different levels.

The functional separation of the direct and indirect pathways is maintained in their innervation of the output nuclei of the basal ganglia, however studies in monkeys and rodents has shown that it is not clear cut (Kawaguchi *et al.*, 1990; Parent *et al.*, 1995; Wu *et al.*, 2000). Examination of striatofugal neurons in the rodent has shown that *all* MSNs project to the GPe (i.e.. both those that make up the direct and indirect pathways) (Kawaguchi *et al.*, 1990; Wu *et al.*, 2000). MSNs that project to the output nuclei (direct pathway) *also* send axon collaterals to the GPe, although the axonal arborisation within the output nuclei is much greater than within the GPe (Kawaguchi *et al.*, 1990; Wu *et al.*, 2000). These direct pathway neurons may be classified into two groups, i) those that arborise in the GPe and have a focused arborisation pattern in the SNr, and ii) neurons that arborise in both the GPe and the GPi/EP and show a more profuse terminal arborisation in the SNr (Wu *et al.*, 2000). Neurons of the indirect pathway exclusively project to the GPe but show a greater level of arborisation within this nuclei compared with the neurons of the direct pathway (Wu *et al.*, 2000). Thus, an important feature of the direct/indirect pathway model of basal ganglia function is that both classes of MSNs are in a position to influence both the GPe and the output nuclei, albeit to different extents.

Although the main targets of MSN axons are within other nuclei of the basal ganglia, outside the striatum, MSNs have extensive local axon collaterals within the

striatum (Wilson & Groves, 1980). These local axon collaterals form symmetric synapses with other MSNs within the striatum (Wilson & Groves, 1980; Somogyi *et al.*, 1981). Furthermore, neurons of the direct pathway form symmetrical (Grays Type II) synapses with neurons of the indirect pathway (Yung *et al.*, 1996). Similarly, neurons of the indirect pathway have been shown to form synapses with neurons of the direct pathway (Somogyi *et al.*, 1982; Aronin *et al.*, 1986; Yung *et al.*, 1996). Neurons within each of these two subpopulations have also been shown to be inter-connected. Direct pathway neurons form synapses with other direct pathway neurons (Bolam & Izzo, 1988), and the same is true for indirect pathway neurons (DiFiglia *et al.*, 1982; Pickel *et al.*, 1992) (See Figure 1.2 for a summary of anatomical connectivity between striatal neurons). In all cases mentioned the location of these synapses is onto the dendritic shafts and spine necks (Wilson, 2007). This local synaptic connectivity means that the two populations of MSNs are functionally inter-connected and in a position to influence each other. *In vitro* paired recordings have shown that MSNs can inhibit one another but that the resulting IPSC is small (Koos *et al.*, 2004), which is of functional significance. It is also important to note here that the MSNs are able to release other neurotransmitters, aside from GABA, which presents another mechanism whereby MSNs can influence each other. Direct pathway neurons are able to release substance P, which is a neuropeptide that mediates its actions via the neurokinin receptor[9]. In the striatum, substance P has been shown to be excitatory and facilitate glutamatergic inputs to other MSNs (Blomeley & Bracci, 2008; Blomeley *et al.*, 2009). The two populations of MSNs are also capable of releasing opioids; direct pathway neurons can release dynorphin, and indirect pathway neurons are able to release enkephalin. Opioids have been shown to have an overall inhibitory effect in the striatum, and are able to inhibit the glutamatergic inputs to neighbouring MSNs (Jiang & North, 1992; Blomeley & Bracci, 2011). When considering the interactions within the MSN network, it is vital to remember that GABA is not the only neurotransmitter at play and that the interactions can be both inhibitory and excitatory and the MSNs can influence each other over a longer time course via several different mechanisms.

9 Neurokinin receptor 1 (NK1) is a GPCR and is the endogenous receptor for substance P.

Although MSNs are sub-divided on the basis of their axonal targets, and expression of particular receptors, they have many similar features, and are often considered as one group. The MSNs are capable of exhibiting a variety of firing rates and patterns. In general, they have a low basal firing rate (0.1 – 5 Hz) and can fire both phasically and tonically, as well as remaining completely silent (Wilson & Groves, 1981). The intrinsic properties of these neurons include a hyperpolarised resting membrane potential (~ -70 mV), low input resistance and a strong rectification when hyperpolarised (Kita *et al.*, 1984; Kawaguchi *et al.*, 1989). An inward rectifying potassium current (I_{Kir}) has been shown to be responsible for this inward rectification and to contribute to the hyperpolarised resting membrane potential (Nisenbaum & Wilson, 1995).

A distinct feature of MSNs is the ability of these neurons to periodically shift between two differing membrane states; from a hyperpolarised 'Down state' (-90 to -70mV) to the slightly more depolarised 'Up state' (-60 to -40mV) where the MSN can, but does not necessarily, fire action potentials (Wilson & Kawaguchi, 1996). Murer and colleagues (2002), describe the Up states as 'enabling events' which allow the processing of information through basal ganglia circuitry. The origin and role of the state transitions in MSNs has been debated. In the anaesthetised rat, the state transitions in MSNs are coupled to the cortical electro-encephalogram (EEG) activity, indicating that the cortex has a central role in altering the state of MSNs (Mahon *et al.*, 2001; Kasanetz *et al.*, 2002). Indeed, decortication results in the abolition of state transitions in MSNs (Wilson, 1993). Thus, it is thought that cortical input to the striatum is able to induce state transitions within MSNs. It is important to note, however, that the state transitions are prominent during anaesthesia (and slow-wave sleep) but during wakefulness MSNs are capable of a greater range of patterns of spontaneous activity (Mahon *et al.*, 2006). Stern and colleagues (1998) showed that state transitions in striatum can be correlated amongst groups of MSNs, suggesting that cortical activity leads to synchronous activity in striatum, via the activation of specific cell assemblies (Stern *et al.*, 1998). There are other factors which can influence state transitions, including the levels of neuromodulators in striatum, such as dopamine (Murer *et al.*, 2002). Although the exact roles of the up and down state

transitions remain unclear, they represent a method, following cortical excitation, by which particular groups of MSNs can be activated and thus process and transmit information.

Overall the MSNs have a distinct role to play in the striatum, as integrators and transmitters of information. Their differential expression of dopamine receptors and axonal targets highlights the separation of the roles of the two subtypes of MSN. The MSNs share many of their properties, and are often considered to be a homogeneous population, although recently there has been some indication that there are important differences in their physiology and somatodendritic architecture (Gertler *et al.*, 2008). Recent technological advances, such as the availability of bacterial artificial chromosome (BAC) transgenic mice which express eGFP under the control of either the D_1 or the D_2 receptors has allowed these differences to be explored with more ease (Gong *et al.*, 2003; Valjent *et al.*, 2009). The output of MSNs can be modulated by the activity of interneurons within the striatum; which is important to consider when examining the ways in which MSNs process information in order to influence the output of the basal ganglia.

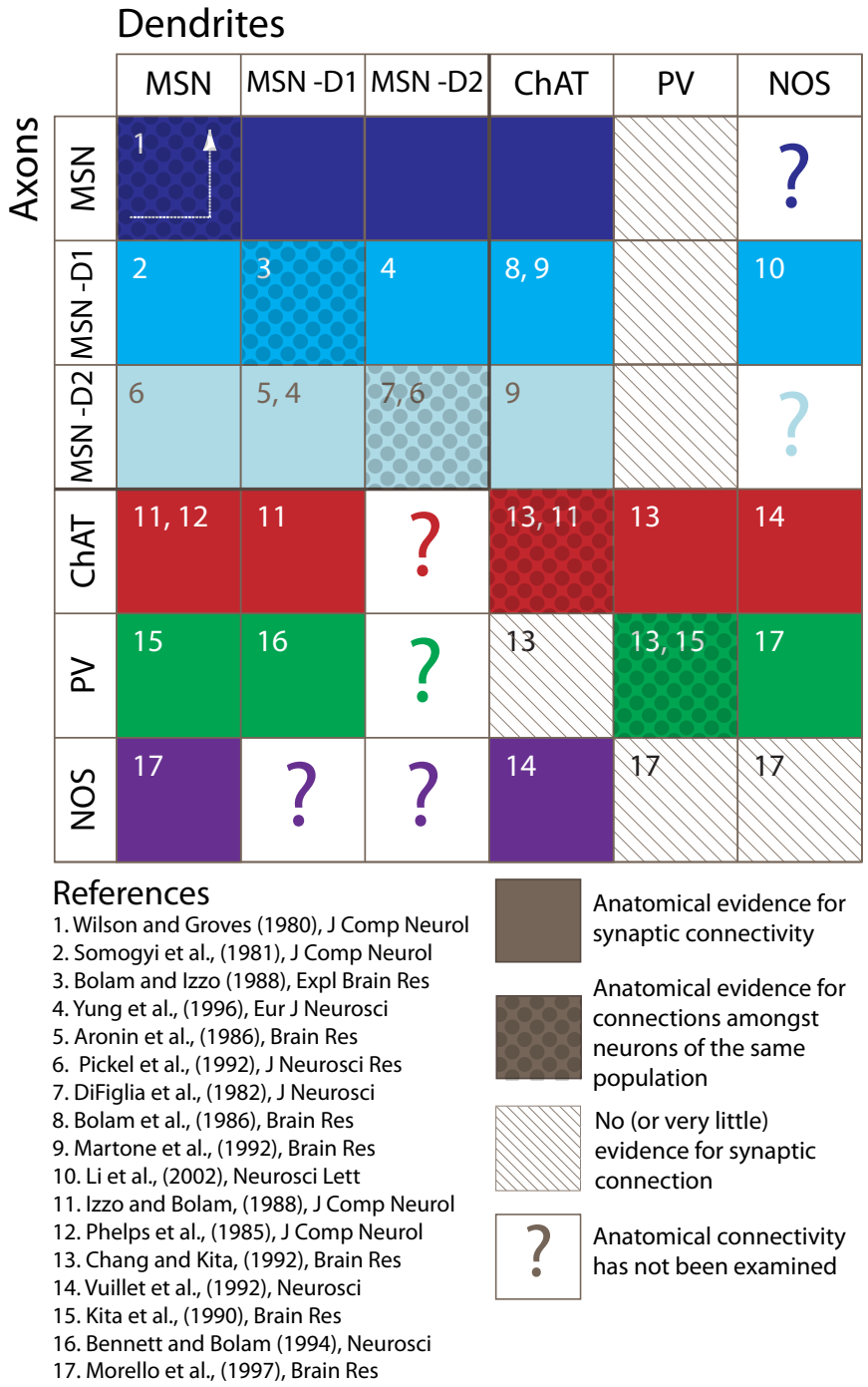


Figure 1.2. Synaptic connectivity between subtypes of striatal neurons.

Schematic diagram illustrating the known synaptic connections between the different types of neurons within striatum. The output of the neuronal subtype is on the left (axons), and input is at the top (dendrites). The arrow indicates directionality. To see the output of a neuronal subtype follow it from left to right, and to see the input follow it from top to bottom.

1.2.2. Striatal interneurons

The remaining 5% of the total cell population in the striatum is composed of interneurons, all of which are predominantly aspiny. There are four main recognised populations of striatal interneurons. There are three subsets of GABAergic interneurons, which express specific markers: parvalbumin- (PV) expressing interneurons, calretinin- (CR) expressing interneurons, and nitric oxide synthase- (NOS), somatostatin- (SS) and neuropeptide Y- (NPY) expressing interneurons (Kawaguchi *et al.*, 1995). Finally, there are the 'giant' cholinergic interneurons which have large cell bodies and express the acetylcholine synthesising enzyme, choline acetyltransferase (ChAT). Despite the fact that striatal interneurons are hugely outnumbered by the MSNs there are several lines of evidence which highlight the importance of their contribution to striatal processing, as is the case in several different brain regions. Each subset of striatal interneuron will be discussed in further detail.

1.2.2.1. Parvalbumin-expressing interneurons

Parvalbumin (PV) specifically labels a subset of striatal neurons, neurons that are also strongly positive for GABA, or GAD[10] (Kawaguchi *et al.*, 1995). The PV interneurons have medium-sized cell bodies (slightly larger than MSNs), are aspiny, and have varicose dendrites (Cowan *et al.*, 1990). The axons of PV interneurons exhibit dense local arborisations, which can form 'basket-like' synapses on somata of other striatal neurons (Kawaguchi *et al.*, 1995). The population of PV interneurons are interconnected through gap-junctions between dendrites (Kita *et al.*, 1990). PV-interneurons are present in both the patch and matrix compartments of the striatum (Cowan *et al.*, 1990). The density of PV interneurons is not even over the entire striatum, it is higher in the lateral striatum relative to medial striatum (Bennett & Bolam, 1994).

PV interneurons are also called 'fast-spiking' (FS) interneurons when referring to their electrophysiological properties. *In vivo* recordings of FS interneurons (which

10 Glutamic acid decarboxylase (GAD), an enzyme which catalyses the decarboxylation of glutamate to GABA.

were then confirmed as being PV-positive) in the anaesthetised rat have shown that these neurons have a very short action potential width (< 1ms), which is quicker than all other striatal neurons (Mallet *et al.*, 2005). The FS interneurons show differential spontaneous firing patterns in different brain states; during slow wave activity[11] (SWA) FS interneurons show a firing rate of about 0.5 Hz which is not that much greater than the spontaneous firing rate of MSNs as seen in the anaesthetised rat, whereas in an 'activated' brain state[12] FS interneurons have a higher firing rate of about 3.5 Hz (Mallet *et al.*, 2005). In the awake behaving rat, FS interneurons show a characteristic short waveform, have a spontaneous firing frequency of ~15 Hz, and exhibit changes in firing pattern dependent on brain state (Berke *et al.*, 2004).

A major role of PV neurons in the striatum is considered to be the regulation of striatal output through *feed-forward inhibition*. It has been shown that PV interneurons form symmetric synapses with MSNs (Kita *et al.*, 1990; Bennett & Bolam, 1994). The population of PV interneurons are also interconnected within striatum; not only electrically by gap junctions, but also synaptically (Kita *et al.*, 1990). Thus, the PV interneurons are in a position to alter the activity of MSNs in a synchronous manner. *In vitro,* Koos and Tepper (1999) showed that FS interneurons can exert a very powerful inhibition over MSNs; one FS interneuron spike can produce a profound IPSP and can significantly delay the firing of the post-synaptic neuron. Furthermore, an individual FS cell can inhibit neighbouring MSNs of the direct and indirect pathway with similar dynamics (Planert *et al.*, 2010); although there is evidence that FS interneurons preferentially target direct-pathway MSNs (Gittis *et al.*, 2010). Compared to the inter connectivity between MSNs the FS → MSN connection is much more homogeneous and provides a reliable inhibition (Planert *et al.*, 2010). It is estimated that one FS interneuron contacts 3000 MSNs whereas one MSN is estimated to contact 728 other MSNs (Humphries *et al.*, 2010). This is a possible explanation for the relatively greater robustness of the FS → MSN connection compared

11 The dominant brain state in urethane anaesthesia; exhibiting a cortical field potential characterised by large amplitude slow waves at about 1Hz.

12 Activated brain states occur in the anaesthetised rat, and can be defined by the absence of the slow wave oscillation.

to the MSN → MSN connection. *In vivo,* FS interneurons respond rapidly to cortical stimulation (faster than MSNs on average) which allows them to then inhibit MSNs, thus an essential role of the FS interneuron is in the integration of cortical input (Mallet *et al.*, 2005). Recordings from FS interneurons in awake-behaving rats found that these neurons have a role in choice-execution and that their firing (in a synchronous manner) can suppress unwanted actions (Gage *et al.*, 2010). This evidence indicates that whilst the role of FS interneurons in feed-forward inhibition appears to be central in the striatal circuitry, it is not as clear in the awake-behaving animal (Berke, 2011).

1.2.2.2. Nitric oxide synthase-expressing interneurons

A subset of neurons in the striatum are positive for NADPH-diaphorase, a coenzyme involved in several oxidative-reduction and anabolic processes; in the nervous system NADPH is equivalent to nitric oxide synthase (NOS) as it is required for the production of nitric oxide (NO) from L-arginine (Hope *et al.*, 1991). Striatal neurons expressing NADPH were also found to be positive for neuropeptide Y (NPY) and somatostatin (SS) (Vincent *et al.*, 1983). In the cat and squirrel monkey these neurons do not project outside of the striatum, identifying them as a population of interneurons (Smith & Parent, 1986). For some time it remained unclear as to whether the NOS/NPY/SS interneurons utilised a classical neurotransmitter, however it was shown that they could also exhibit GABA-immunoreactivity (Aoki & Pickel, 1990). In the rat, 73% percent of this population of interneurons contain all three molecular markers: SS, NPY, and nNOS[13], 16% contain SS and nNOS, and 6% contained only nNOS (Figueredo-Cardenas *et al.*, 1996). Understanding the significance of these different subpopulations is difficult, there is evidence which suggests that the NPY interneurons in the mouse can be separated based on electrophysiological, morphological and neurochemical properties (Ibanez-Sandoval *et al.*, 2011). Overall, however, the functional relevance of these subpopulations remains unclear, and thus will not be considered further here and this population will simply be referred to as NOS interneurons.

13 The neuronal (n) isoform of NOS.

Interneurons which express NOS have medium-sized cell bodies, long, straight aspiny dendrites which can traverse up to 1 mm, and axonal arborisations which are less dense than those of the PV-interneurons (Kawaguchi *et al.*, 1995). *In vitro* recordings of NPY-positive striatal neurons (as shown by the expression of GFP in a BAC-NPY mouse) illustrate that these neurons exhibit heterogeneous spontaneous firing patterns (Partridge *et al.*, 2009). The spontaneous firing rate is between 4 and 12 Hz, depending on the recording method and, in agreement with previous studies in the rat, these neurons showed low-threshold spiking (LTS) patterns and high-input resistances (Koos & Tepper, 1999; Partridge *et al.*, 2009). However, these neurons have not been recorded and identified in the rat.

Out of all the interneurons in the striatum the NOS interneurons are capable of releasing the largest variety of neurotransmitters, which is central to the complexity of their role in striatum. NO is an atypical neurotransmitter and can have several effects, at many different levels, such as modifying long-term potentiation (LTP) and long-term depression (LTD), enhancement of neurotransmitter release, regulation of gene expression and interactions with many other neurotransmitter systems in the brain, and is thought to be important in motor behaviour (for review see Del Bel *et al.*, 2005). In the striatum, it has been demonstrated that NO (specifically the NO/cGMP pathway[14]) is required for formation of corticostriatal LTD, which is a form of plasticity important for motor learning (Calabresi *et al.*, 1999). Indeed, stimulation of the ipsilateral frontal cortex *in vivo* causes a robust increase in levels of NO in striatum (Sammut *et al.*, 2007). NO also has an interactive role with dopamine, NO can act to facilitate the release of dopamine within striatum (West *et al.*, 2002). The way in which NO increases dopaminergic release seems to be through multiple pathways, including action on glutamatergic receptors (West *et al.*, 2002). The role of NO in regulation of DA release (at both the terminal and cellular level) is important in regards to normal motor behaviour, and in disorders of the basal ganglia.

Aside from NO, NOS interneurons can also release NPY, SS and GABA. In

14 NO elevates cGMP via activation of guanylyl cyclase (GC), which can then stimulate cGMP-dependent protein kinase (PKG)

comparison to the FS interneurons, the NOS neurons seem to have a weak GABAergic influence over MSNs (Tepper *et al.*, 2010). There is anatomical evidence for NOS-interneurons forming synapses with MSNs (Morello *et al.*, 1997). Gittis and colleagues (2010) found that an examination of 60 pairs of neurons, the presynaptic neuron exhibiting LTS (putative NOS neuron), and the post-synaptic neuron being a putative MSN, revealed that only 2 pairs were synaptically connected. And indeed, the connection was weak and variable (Gittis *et al.*, 2010). Furthermore, they found that the LTS neurons were not synaptically connected to interneurons; they examined connections with FS interneurons, cholinergic interneurons, and other LTS neurons, and found no evidence for synaptic connectivity (Gittis *et al.*, 2010). However, there is some anatomical evidence to suggest a synaptic connection with ChAT neurons (Vuillet *et al.*, 1992). Overall the electrophysiological evidence indicates that the NOS interneurons are not major contributors to GABAergic feed-forward inhibition within striatum, especially relative to FS interneurons.

The effects of SS and NPY within striatum are not well understood. SS is a peptide involved in a wide range of biological functions, both in the central and peripheral nervous system; its effect is mediated via a family of five metabotropic receptors (Patel, 1999). In striatum, it has been shown that SS can have differential effects on calcium dependent potassium currents (Galarraga *et al.*, 2007). Specifically, SS can enhance the BK-current[15], and depress the SK-current[16] in MSNs (Galarraga *et al.*, 2007). Due to the role of these currents in the after-hyperpolarisation (AHP), SS can alter the firing pattern of MSNs; in particular SS can change the temporal nature of the firing to a more 'stuttering' pattern (Galarraga *et al.*, 2007). Besides a post-synaptic effect, there is evidence that SS can have a presynaptic role in modulating the level of lateral inhibition between MSNs (Lopez-Huerta *et al.*, 2008). Using an *in vitro* preparation Lopez-Huerta *et al*., (2008) showed that SS can decrease the IPSC between MSNs in striatum, but not the IPSCs coming from interneurons. Therefore, due to both pre- and post-synaptic mechanisms, SS can alter

15 Large conductance Ca^{2+} mediated K channel

16 Small conductance Ca^{2+} mediated K channel

the integration of inputs and the output of MSNs, and can thus contribute to information processing in the striatum.

Neuropeptide Y (NPY) is a 36 amino acid peptide which exerts its effect via a family of five metabotropic GPCRs (Y_1-Y_5). Although there is little research about the exact role of NPY within striatum, it has been shown that it seems to have a role in the regulation of dopamine release (Adewale *et al.*, 2005). By measuring the DOPA content of a rat brain slice, Adewale *et al.,* (2005) showed that NPY can have both a facilitatory and inhibitory effect on dopamine release from terminals in the striatum. It was found that this effect is mediated via the different subtypes of NPY receptor, although the intricate details of this effect remain to be elucidated (Adewale *et al.*, 2005). A role for NPY in dopamine modulation means that it is not only important in normal striatal processing but could also be a target for Parkinson's disease treatments.

1.2.2.3. Calretinin-expressing interneurons

In the striatum calretinin (CR) immunoreactivity specifically labels a separate population of GABAergic interneurons, distinct from the PV and NOS interneurons. Calretinin-positive neurons in the striatum are located preferentially in rostral portions of rat striatum (Bennett & Bolam, 1993). These neurons are aspiny, have small-medium cell bodies, and long, infrequently branching dendrites (Bennett & Bolam, 1993). The presence of CR-positive terminals forming synapses onto dendritic spines and shafts indicates that they are a part of the striatal microcircuit, although some of the terminals examined formed asymmetric synaptic specialisations and are thus likely to originate from outside of the striatum (Bennett & Bolam, 1993). In the rodent the CR interneurons are relatively sparse, however in the primate (Squirrel monkey) they are the most abundant interneuron type (Wu & Parent, 2000). Of all the main classes of striatal interneuron, the least is known about the CR interneurons; and indeed no identified CR interneuron has been recorded in any preparation.

1.2.2.4. Cholinergic interneurons

Acetylcholine is an important neuromodulator in striatum. Acetylcholine is

released by a specific neuronal cell type within striatum, the cholinergic interneuron. Cholinergic interneurons are also known as 'giant' aspiny interneurons due to their large somatic size (~20 to 50 μm in diameter) (Bolam *et al.*, 1984; Kawaguchi *et al.*, 1995). These neurons have large dendritic arbors that can extend up to a 1 mm away from the cell body and large, dense axonal arborisations which can extend as far as the dendrites (Wilson *et al.*, 1990). Cholinergic interneurons account for 1-2% of striatal neurons in the rat (Wilson *et al.*, 1990). These interneurons have received specific interest because of the roles of acetylcholine in reward-related behaviour and the pathophysiology of Parkinson's disease.

Cholinergic interneurons have broad action potentials (1.7 to 4 ms), and a characteristic waveform shape, which allows them to be distinguished from MSNs (Wilson *et al.*, 1990). These neurons exhibit distinctive firing patterns *in vivo*, most notably a tonic firing rate at about 3-10 Hz, but can also display irregular, and 'bursty' firing patterns (Wilson *et al.*, 1990). These firing patterns are intrinsic and are present in the absence of synaptic input (Bennett & Wilson, 1999). The tonic firing of these neurons has led them to be referred to as 'tonically active neurons' or TANs in the literature[17]. There are several different currents which contribute to the tonic firing of the cholinergic interneurons. The combined effects of a sub-threshold sodium current and a hyperpolarisation activated cation current (I_h) can drive the neurons to spike threshold and maintain spontaneous firing *in vitro* (Bennett *et al.*, 2000). Cholinergic interneurons also exhibit a prominent after-hyperpolarisation (AHP) following depolarisation that is complex and produced by a combination of currents (Wilson & Goldberg, 2006). The after hyperpolarisation can be divided into distinct parts, a fast-AHP, medium-AHP and slow-AHP, each of which can be attributed to the contribution of different currents (Wilson & Goldberg, 2006). The fast- and medium-AHPs are mainly attributed to the persistent sodium channel and both large and small conductance calcium activated potassium channels (Wilson & Goldberg, 2006). The slow-AHP, which is activated by rhythmic bursting or driven depolarisation,

17 It is important to note that neurons referred to as TANs are not necessarily confirmed as being positive for ChAT, especially in the case of research carried out in behaving primates.

is attributed to a low voltage calcium activated potassium current which shows maximal activation after more than 300 ms of depolarisation and occurs at ~1 s after depolarisation onset (Wilson & Goldberg, 2006). Cholinergic neurons have distinctive and unique properties which shape their firing pattern and contribute to their role in striatum.

The role of cholinergic neurons in the striatum is of particular importance as they are the sole source of acetylcholine within striatum. Acetylcholine, along with dopamine, is a major striatal neuromodulator and mediates its effects via activation of nicotinic[18] and muscarinic[19] receptors. In striatum, the nicotinic receptors are in a position to be able to enhance dopamine release from the terminals of dopaminergic neurons (Zhou *et al.*, 2002). The muscarinic receptors have differing effects, and are expressed by different neurons. Muscarinic receptors M_1, M_3 and M_5 are G_q-coupled; activation of these receptors results in activation of phospholipase C, and the inositol triphosphate (IP_3) signal transduction pathway. Whereas activation of M_2 and M_4 (G_i-coupled) results in a decrease in cAMP and thus overall inhibitory effects. In striatum, all MSNs express the M_1 receptor, but only MSNs of the direct pathway express the M_4 muscarinic receptor subtype (Kreitzer, 2009). Cholinergic interneurons express the M_2 receptor which can work as an auto-receptor regulating the release of acetylcholine (Kreitzer, 2009). It is also important to note here that acetylcholine is very rapidly degraded by acetylcholinesterase, and therefore the tonic firing and thus continuous release of acetylcholine does not desensitise the receptors (Zhou *et al.*, 2002). Due to the expression of receptors on different neuronal subtypes in the striatum, and its interaction with dopamine, acetylcholine has a particular role in modulating the dynamics of the striatal microcircuit.

Although it has been postulated that acetylcholine, like dopamine, may work via volume transmission, the large axonal arbor of the cholinergic interneuron forms synapses with other neurons in the striatal microcircuit. Cholinergic interneurons have been shown to form symmetric synapses with MSNs (Wainer *et al.*, 1984; Phelps *et al.*, 1985; Izzo &

---

18 Ligand-gated ion channels composed of five subunits.

19 There are five major subtypes of muscarinic receptor: M_1-M_5. All are GPCRs, each with individual properties.

Bolam, 1988); including MSNs that make up the direct pathway (Izzo & Bolam, 1988, see Fig 1.2). Cholinergic interneurons are also connected with other interneurons. The axon terminals of cholinergic interneurons form symmetric synapses with PV-positive neurons in the striatum, and it appears that this is a unidirectional relationship as there is no evidence for PV-positive terminals forming synapses with ChAT-positive dendrites (Chang & Kita, 1992). There is also some evidence to suggest that cholinergic interneurons form synapses with NOS interneurons (NPY-positive) and that this synaptic relationship is reciprocal, with NPY-positive terminals forming symmetric synapses onto ChAT-positive dendrites (Vuillet *et al.*, 1992). The population of cholinergic interneurons have also been shown to be interconnected synaptically (Izzo & Bolam, 1988; Chang & Kita, 1992). This connectivity, and the expression of particular receptors, put the cholinergic interneurons in a unique place within the striatal microcircuit. However the detailed studies of cholinergic interneurons in rodents are still difficult to interpret in the light of work done in behaving primates.

Experiments in behaving primates have shown that TANs are involved in reward-related behaviour. It has been demonstrated that TANs can respond to the presentation of a reward, or a sensory stimuli that is associated with a reward (cue), and that the response is characterised by a *pause* in tonic firing (Kimura *et al.*, 1984). Importantly, when the association between cue and reward is altered the TANs lose their responsiveness to the initial cue and can then acquire a response to a newly introduced cue (Aosaki *et al.*, 1994b). The response has also been shown to be linked to the availability of dopamine within the basal ganglia (Aosaki *et al.*, 1994a), although dopaminergic neurons code reward in a differential manner (Morris *et al.*, 2004). Joshua and colleagues (2008) found that during an instrumental conditioning task in monkeys dopaminergic neurons in the SNpc can discriminate between rewarding and aversive events whilst TANs do not distinguish between them. Dopaminergic neurons can also differentiate between a high and low probability of reward, whereas the TANs do not robustly encode reward probability (Joshua *et al.*, 2008). Therefore the 'conditioned pause response' is related to the motivational significance, or salience, of the stimulus whether it is rewarding or aversive (Goldberg &

Reynolds, 2011). There still remain questions about the exact role of the TANs in reward-related behaviour; such as a possible role in the integration of contextual information and movement control (Apicella, 2007). Another issue is elucidating the possible mechanisms for the generation of the pause (Goldberg & Reynolds, 2011). Altogether, TANs have a role to play in the neural encoding of reward-related events, and this is intricately linked to the balance of acetylcholine and dopamine within the striatum.

1.2.3. Summary

The striatum is a computational hub within the basal ganglia. The MSNs are the main functional unit within the striatum, and are subdivided based on their expression of dopamine receptors. This division has functional consequences and indeed our working hypotheses of striatal function are based on this division, both for the normal and the diseased basal ganglia. Striatal interneurons are in a position to be able to modify the processing of information by the MSNs. The four major types of interneuron have distinctive molecular, anatomical and electrophysiological phenotypes which underlie their role within the striatum. The PV-interneurons are fast-spiking GABAergic neurons which are considered to be the main contributors to feed-forward inhibition within the striatum, and they can rapidly inhibit the MSNs in response to cortical input. The NOS-interneurons can release several different neurotransmitters and can thus affect the dynamics of striatal connectivity through a variety of mechanisms. Very little is known about the calretinin interneurons both in terms of anatomical connectivity and electrophysiology. The cholinergic interneurons are of great interest due to their role in reward-related behaviour and the pathophysiology of Parkinson's disease. They are solely responsible for the release of acetylcholine within striatum which has an intricate interaction with dopamine. The distinctive and unique firing patterns of the cholinergic interneurons contribute to their role. It is important to note however that the functional roles of all the striatal neurons are shaped by their afferent innervation. The striatum receives major innervation from both the cortex and the thalamus; these inputs have distinct roles and patterns of innervation which will be discussed.

1.3. Corticostriatal Projection

1.3.1. Overview

The cortical projection to striatum is central to the motor and cognitive functions that are now recognised as the fundamental roles of the basal ganglia. Although the striatum is a GABAergic structure there are many more asymmetric, glutamatergic synapses in the striatum, relative to GABAergic synapses (Wilson, 2007). The cortical projection originates from all areas of the cerebral cortex and projects to striatum in a topographical manner. The major target of the cortical projection is the MSN; however inputs to interneurons have also been described, as will be discussed. The exact 'role' of the cortex in basal ganglia functioning will be examined briefly, although many specific roles have been described, and there is often no reason why the broad range of functions cannot coexist. The plasticity of the corticostriatal projection is essential in shaping information processing within striatum, and can modify how the system works both normally and in disorders of the basal ganglia.

1.3.2. Neurons that give rise to the corticostriatal projection

Early studies using axonal degeneration showed that the striatum receives projections from all areas of cortex, in small mammals (rats, rabbits and cats) and in primates (Kemp & Powell, 1970). The cerebral cortex is arranged in layers, with most areas having 6 distinctive layers (I-VI), although primary motor cortex lacks a layer IV and as such is also known as agranular[20] cortex. Layers III and V contain pyramidal cells, which are the output neurons of the cortex, and it is these cells that project to striatum. A study by McGeorge and Faull (1989) examining the corticostriatal projection in the rat using anterograde labelling showed that the pyramidal cells which project to striatum are located in layer V, and in particular layer Va, with a few cells in layers III and/or IV. The neurons that project to the dorsolateral striatum are located within the sensory and

20 Layer IV is called the internal granule cell layer due to the presence of the small spherical granule cell bodies.

motor areas of cortex, whereas the ventromedial portion of striatum receives innervation from limbic areas as well as auditory and visual cortical areas (McGeorge & Faull, 1989). Cortical neurons projecting to dorsolateral striatum do so in a bilateral manner, with a predominance of ipsilateral projecting neurons, and importantly this projection is topographically organised (McGeorge & Faull, 1989).

Corticostriatal projecting neurons can be subdivided into three major classes depending on their axonal projections (Cowan & Wilson, 1994). First, cortical neurons that project to both the brainstem and also to the striatum; second, neurons which project to both the thalamus and the striatum, and third, cortical neurons which project to other parts of cortex, and also have collaterals that innervate striatum. It is important to note that this is a general subdivision and does not hold across all areas of cortex and cortical layers (Cowan & Wilson, 1994). Cowan and Wilson (1994) examined corticostriatal neurons in motor cortex and showed that there are two main types which can be separated based on their anatomical properties: pyramidal tract (PT) neurons[21], and crossed corticostriatal (CST) neurons[22]. PT neurons are mainly located in deep layer V, and most of them show relatively greater axonal arborisation within cortex as compared to striatum. CST neurons are located in superficial layer V (and deep layer III), and have extensive axonal arborisations within both the cortex and the contralateral striatum (Cowan & Wilson, 1994). It is important to note that striatal- projecting neurons are not homogeneous; however, the functional relevance of different types of corticostriatal neurons remains unclear.

1.3.3. Synaptic organisation of the corticostriatal pathway

There is a massive convergence of cortical afferents onto the striatum; these inputs are then integrated by striatal neurons. The main target of the corticostriatal pathway is the dendritic spines of MSNs (Kemp & Powell, 1971b; Somogyi *et al.*, 1981). One MSN receives ~10,000 asymmetric synapses (Kincaid *et al.*, 1998); a proportion of these are of

21 Neurons that respond to antidromic stimulation of the ipsilateral pyramidal tract

22 Neurons that respond to antidromic stimulation of the contralateral striatum

cortical origin, and a proportion are of thalamic origin, which will be discussed later.

Besides innervating the MSNs, the corticostriatal projection also innervates the dendrites of striatal interneurons. Electrical stimulation of motor cortex causes the PV interneurons to spike, with a shorter latency and a greater probability relative to nearby MSNs (Mallet *et al.*, 2005). Cortical afferents form asymmetric synapses with the somata and dendrites of PV interneurons (Lapper *et al.*, 1992; Bennett & Bolam, 1994). Moreover, PV interneurons can receive input from two distinct cortical areas; axons from primary motor and primary somatosensory cortices can converge onto the dendrites an individual PV interneuron (Ramanathan *et al.*, 2002). This means that cortical information from two distinct functional cortical regions can be integrated by PV interneurons.

There is also evidence for cortical innervation of the NOS interneurons. Stimulation of the ipsilateral and contralateral frontal cortex of rats *in vivo* can induce an increase in NO efflux within striatum (Sammut *et al.*, 2007; Ondracek *et al.*, 2008). This indicates that a corticostriatal pathway has influence over the NOS interneurons in a functional way that can influence the levels of NO in striatum. Anatomical evidence for a cortical innervation of NOS interneurons is sparse. Vuillet *et al*., (1989) found that only a few cortical terminals were seen to be in the vicinity of the NPY interneurons. Thomas *et al.,* (2000) investigated cortical input to M_2-immunoreactive striatal neurons; the M_2 muscarinic receptor is expressed on the dendrites of both SS and cholinergic interneurons. Using anterograde markers for the cortical input combined with M_2-immunohistochemistry; the labelled cortical terminals were seen to form asymmetric synapses with M_2 labelled dendrites, as well as with spine-like structures (Thomas *et al.*, 2000). Although, it is important to note that it was not possible to distinguish between NOS and ChAT neurons in this study. The cortical innervation to NOS neurons needs to be examined further.

There is evidence to suggest that cholinergic interneurons receive direct innervation from the cortex. Intracellular recordings from TANs *in vivo* show that TANs respond to stimulation of the cortex with latencies that are indicative of monosynaptic innervation (Wilson *et al.*, 1990; Reynolds & Wickens, 2004). Indeed, the TANs could respond to

stimulation of the contralateral cortex with a shorter latency relative to the latencies of putative MSNs recorded in the same preparation (Reynolds & Wickens, 2004). The anatomical evidence to support this connection has been debated. Lapper and Bolam (1992) found that there was no evidence to indicate a direct synaptic cortical innervation of cholinergic interneurons in rat striatum, using anterograde labelling of cortical neurons. Although they suggest that the technical limitations of the study meant that there was a possibility of poor labelling of distal dendrites, therefore cortical innervation could selectively innervate the distal dendrites of the cholinergic interneurons (Lapper & Bolam, 1992). Dimova *et al.,* (1993) found that, although rare, degenerating cortical terminals formed asymmetric synapses with ChAT-positive structures, and indeed, in agreement with Lapper and Bolam (1992), the terminals were seen to form on the more distal regions of the ChAT dendrites (Dimova *et al.*, 1993). Meredith and Wouterlood (1990) found that, in the nucleus accumbens, cholinergic interneurons formed asymmetric synapses with afferent fibres from the hippocampus. However, these were also onto the distal dendrites of the cholinergic interneurons, and also only a few were found, only 3 out of 164 hippocampal terminals examined were in contact with ChAT-positive structures, whilst the rest contacted spine-like structures, presumably belonging to MSNs (Meredith & Wouterlood, 1990). Altogether there is some evidence which suggests that cholinergic interneurons of the striatum receive synaptic input from the cortex, although it appears that this innervation is sparse, and likely to target the more distal dendrites.

1.3.4. Functional organisation of the corticostriatal projection

The corticostriatal pathway has been known to be topographically organised for over 50 years (Webster, 1961). The corticostriatal pathway is spatially organised in a topographical manner, such that motor areas which produce movement of the forelimb when stimulated project to the dorsolateral striatum, whereas motor regions that are responsible for facial movement project more ventrally, in the rat (e.g.. Ebrahimi *et al.*, 1992). This topographically organised innervation from motor and somatosensory cortices supports the idea of multiple parallel segregated cortico-basal ganglia- thalamo-

cortical loops, as presented by Alexander et al., (1986). However, further examination of the corticostriatal pathway has shown that it is more complex than a purely spatial topographical projection, which in part is due to the fact that there is a large amount of convergence of cortical input, and the degree of 'overlap' is essential to the functional organisation of the corticostriatal projection.

Firstly, there is specificity in the organisation of the corticostriatal pathway in relation to the patch-matrix organisation of the striatum. Cortical neurons in deep layer V and layer VI project principally to the patches, although neurons in this layer do also project to the matrix (Gerfen, 1989; Kincaid & Wilson, 1996). Neurons in superficial layer V and layer II/III project mainly to the matrix compartment of striatum (Gerfen, 1989; Kincaid & Wilson, 1996). There are, therefore, distinct classes of corticostriatal neurons which project to specific compartments within striatum, indicating that there is a functional specificity to this system, which is based on more than the topographical innervation.

Using a combination of physiological and anatomical techniques, Flaherty and Graybiel (1991) found that a tracer injection into a physiologically mapped area of the somatosensory cortex in the squirrel monkey resulted in a 'patchy' innervation of the putamen. Tracer injections into single body part representations in cortex led to a divergent staining of the putamen (Flaherty & Graybiel, 1991). Moreover, multiple tracer injections into separate cortical body part representations could result in a pattern of convergence within the putamen, although the level of convergence was also determined by the areas of cortex that were labelled; related body part representations showed more overlap than unrelated parts (Flaherty & Graybiel, 1991). This implies a functional, rather than spatial organisation.

A further investigation of this, combined with retrograde labelling of the GPe and GPi, examined the input and output organisation (Flaherty & Graybiel, 1994). They confirmed their previous findings that projections from a single body part representation can innervate specific foci within the putamen, called 'matrisomes', as they are within

the matrix of the striatum (Flaherty & Graybiel, 1994). They also showed that despite the fact that the projections from cortex can diverge within striatum, they can then *re-converge* at the level of the pallidum (Flaherty & Graybiel, 1994). This indicates that the divergence within striatum may have a particular functional mechanism such as allowing sensorimotor learning, but does not mean that the information from the cortex ultimately forms a new distinct output pathway.

Kincaid and colleagues (1998) analysed corticostriatal neurons from the agranular cortex, and found that a cortical axon forms between 20-40 synapses within a sphere of striatum with a radius of 400 μm which is equivalent to the volume of striatum occupied by the dendritic arbor of an MSN (Kincaid *et al.*, 1998). From this data, as well as data previously published, they estimated that ~381,180 cortical axons would be required to innervate the volume occupied by one spiny neuron in order to reach the cortical synaptic density (Kincaid *et al.*, 1998). Previous data indicates that there are ~2845 neurons within the volume of a spiny neuron's dendritic arbor, therefore the contribution of one cortical axon to one MSN must represent a very small fraction of the total innervation from cortex (Kincaid *et al.*, 1998). If a cortical axon is totally selective, and therefore forms all its 40 synapses (in the given area) with one neuron, then the average number of cortical cells innervating one MSN would be 134; whereas if the cortical projecting is nonselective then 5360 neurons would be required to innervate one MSN (Kincaid *et al.*, 1998). Regardless of whether the innervation is totally selective or nonselective, the percentage of cortical axons that are shared by two MSNs is very low (≤ 1.4%), indicating a low level of redundancy (Kincaid *et al.*, 1998). This indicates that even though the projection to striatum is topographical, two MSNs within a small area are receiving different information, coming from different cortical neurons. An extension of this work, by Zheng and Wilson (2002) examined the arborisation of corticostriatal neurons. They found that, on average, one corticostriatal neuron could occupy ~4% of the striatal volume in the rat (Zheng & Wilson, 2002). The discontinuous innervation of striatum, as illustrated by the anterograde labelling studies was also reflected in the innervation of a single cortical neuron (Zheng & Wilson, 2002). Although they describe the corticostriatal neurons as

being heterogeneous this work supports the concept that the input to two neighbouring MSNs is not shared (Zheng & Wilson, 2002). This supports the idea that activation of a single striatal neuron can occur via the co-ordinated activation of distributed ensembles of cortical neurons (Zheng & Wilson, 2002). The authors suggest that either cortical input to striatum is overwhelmingly redundant or that several cortical representations must be rejected (Zheng & Wilson, 2002).

1.3.4.1. Corticostriatal plasticity

Fundamental to the role of the corticostriatal system in basal ganglia mediated behaviour is plasticity of the synaptic connections. The classical forms of plasticity, long-term potentiation (LTP) and long-term depression (LTD) have been described throughout the brain, there are, however, several aspects of these that are specific to the corticostriatal synapse. In the striatum, the interaction between glutamate and dopamine is essential for plasticity, although acetylcholine, nitric oxide (NO) and endocannabinoids are also important contributors (Calabresi *et al.*, 2007).

One of the features of plasticity at the corticostriatal synapse is that the direction of plasticity is primarily negative, that is LTD as opposed to LTP. High frequency stimulation, such as 100 Hz (which can cause LTP in other brain regions) results in a long-lasting depression of excitatory synaptic transmission in striatum *in vitro* (Calabresi *et al.*, 1992). Calabresi *et al.,* (1992) also showed that blockade of NMDA receptors did not alter the amplitude and time course of the evoked EPSPs, indicating that NMDA receptors are not necessary for LTD. However, an antagonist of metabotropic glutamate receptors significantly reduced LTD, indicating that glutamate metabotropic receptors are required for the induction of LTD in striatum (Calabresi *et al.*, 1992). Examination of this in animals where D_1 or D_2 receptors were antagonised or in animals with 6-OHDA lesions, found that LTD induction was blocked, signifying the necessity for dopamine in order to induce LTD in striatum (Calabresi *et al.*, 1992). The specific role that dopamine plays is complex, the necessity of co-activation of both D_1 and D_2 receptors is difficult to comprehend as they are expressed in separate populations of neurons, although the role

of the cholinergic interneuron has been implicated here (Wickens, 2009). The timing of dopamine release is also important to consider, as it has implications for reward-related behaviour (Wickens, 2009). In striatum there is a delicate balance between acetylcholine and dopamine, and indeed acetylcholine is implicated in the modulation of corticostriatal plasticity. Acetylcholine can induce the release of dopamine via nicotinic receptors on dopaminergic terminals, and indeed cholinergic interneurons express the D_2 dopamine receptor subtype (Wang *et al.*, 2006; Calabresi *et al.*, 2007). Furthermore, the cortical terminals in striatum express muscarinic receptors and are inhibited by acetylcholine; in this way the cholinergic interneurons are able to decrease the excitatory input to MSNs (Pakhotin & Bracci, 2007). The complex interactions between dopamine and acetylcholine are an active area of research, and the mechanisms have been greatly oversimplified here, but it is important to note that in order to discuss corticostriatal plasticity in striatum dopamine and acetylcholine must be considered.

It has also been shown that endocannabinoids have an important role in striatal plasticity. Endocannabinoids are retrograde messengers; in striatum the induction of LTD is dependent on the activation of the CB_1 receptor (Surmeier *et al.*, 2007). It is clear that corticostriatal plasticity is complex within striatum, and there are different striatal neurons and several neuromodulators involved. The preference for LTD in striatum is also coming under scrutiny, Shen *et al.,* (2008) show that spike-timing dependent LTP can be induced in D_2 MSNs, and it is dependent on both the NMDA and the adenosine A_{2A} receptor. Whereas LTD could also be induced in the D_2 MSNs, and this was dependent on the metabotropic glutamate receptors and Cav1.3 Ca^{2+} channels (Shen *et al.*, 2008). This indicates that the specific timing and different contributions of different receptors can alter the direction of plasticity.

Although the specific details of corticostriatal plasticity are most easily elucidated using an *in vitro* preparation, the link between behaviour and plasticity are more closely linked in the *in vivo* model (despite the many caveats of anaesthesia use). Charpier and Deniau (1997) found evidence for LTP of the corticostriatal synapse *in vivo.* Moreover

they found that the direction of plasticity was positive *in vivo*, which was in contrast with the *in vitro* work at that time (Charpier & Deniau, 1997), although we know now that corticostriatal plasticity is complex and requires many different mediators. A study by Reynolds *et al.,* (2001) used a combination of behaviour and intracellular recordings. Electrodes were planted in the SNpc and rats performed intra-cranial self stimulation (ICSS), and then were anaesthetised and striatal neurons were recorded from (Reynolds *et al.*, 2001). During recordings the SNpc was stimulated using the same parameters as developed during ICSS, and it was found that there was significant potentiation of corticostriatal synapses, presenting a putative mechanism for reward based learning which incorporates the involvement of dopaminergic innervation from the SNpc (Reynolds *et al.*, 2001).

1.3.5. Summary

The corticostriatal system is implicated in all basal ganglia function from movement to habit formation (Graybiel, 2008). The corticostriatal pathway innervates the MSNs and the striatal interneurons, with a functional topography. Plasticity in the corticostriatal pathway is important for normal function, and changes in this pathway are apparent in disorders of the basal ganglia, from movement disorders to schizophrenia and obsessive compulsive disorder (OCD) (Calabresi *et al.*, 1996; Foerde *et al.*, 2008; Graybiel, 2008). As has been discussed, dopamine has a crucial role in corticostriatal plasticity, and understanding the underlying rules of dopamine dependent plasticity has uncovered a wide range of complex mechanisms that are a potential molecular and cellular substrate for learning in the basal ganglia. It is important to note here, however, that the cortex is not the only glutamatergic innervation of the striatum; the thalamostriatal system will now be discussed.

1.4. Thalamostriatal Projection

1.4.1. Overview

The thalamostriatal projection to striatum originates predominantly in the intralaminar thalamic nuclei (Jones, 2007). The number of terminals forming synapses in the striatum of thalamic origin are of an equal magnitude to those originating in cortex (Lacey *et al.*, 2005). The different nuclei within the intralaminar thalamus show differing patterns of innervation within striatum, and indeed the synaptic innervation of MSNs is heterogeneous dependent on the thalamic nuclei. Axonal projections from the thalamus innervate MSNs and striatal interneurons, excluding the calretinin-positive interneurons (Sidibé & Smith, 1999). The intralaminar thalamus receives innervation from subcortical structures and is important for attention and arousal. There are contrasts between cortical and thalamic innervation of striatum which give us some insight into their relative roles in basal ganglia function.

1.4.2. Neurons that give rise to the thalamostriatal projection

The vast majority of neurons that give rise to the thalamostriatal projection are located in the intralaminar thalamic nuclei (ITN). The groups of nuclei within the intralaminar thalamus are within, and medial to, the internal medullary lamina. The existence of a thalamostriatal projection was not apparent until the 1940s when lesions in the striatum caused severe retrograde degeneration in some of the nuclei within the intralaminar thalamus, this was confirmed in a study by Vogt and Vogt in 1941 (Jones, 2007). The projection was still contested until the 70s when retrograde tracing techniques were introduced and showed, after injections into striatum, the labelling of thalamic cells (Jones, 2007). It is now widely accepted that the ITN project heavily to the striatum. This projection was first referred to as being ‘non-specific’ as, in comparison to other thalamic nuclei, resulted in a widespread distribution of efferent fibres within the cortex, as well as a wide range of varying effects when electrically stimulated (Groenewegen and Berendse, 1994). As such, the ITN have a unique organisation, that is different from the organisation

of the major thalamocortical pathways (Sherman and Guillery, 1996).

The ITN can be subdivided into a rostral and caudal group of intralaminar nuclei (Jones, 1985). The rostral group is made of the 'central medial', 'paracentral', 'central lateral' and 'rhomboid nuclei[23]' (Jones, 1985). The caudal group is composed of the 'centre médian nucleus', and the 'parafascicular nucleus', which cannot be reliably separated in rodents and are frequently considered as one, and collectively referred to as the parafascicular nucleus (Van der Werf *et al.*, 2002). In rodents, the lateral part of the parafascicular (Pf) nucleus is considered to be equivalent to the primate centre médian (CM) nucleus, whilst the medial Pf nucleus is considered to be equivalent to the primate Pf nucleus (Figure 1.3; Van der Werf *et al.*, 2002).

The results of a thorough anatomical characterisation of the thalamostriatal pathway carried out by Berendse and Groenewegen (1990) using anterograde labelling in rats found that the projections have a particular topography. The rostral intralaminar nuclei project to the caudate- putamen: the central medial nucleus projects to a medial zone of the caudate putamen and to dorsal parts of the nucleus accumbens, rostral parts of the paracentral nucleus project to dorsal parts of the caudate-putamen and the caudal parts project more ventrally, the central lateral (CL) nucleus shares a similar topographical projection as with the paracentral nucleus (Fig. 1.3; Berendse & Groenewegen, 1990). The caudal intralaminar nucleus also exhibit a topographical projection: the medial Pf projects to the medial part of the caudate putamen, and dorsolateral nucleus accumbens, the lateral Pf (equivalent to CM) projects to the lateral part of caudate-putamen (Fig. 1.3; Berendse & Groenewegen, 1990). They found that the midline thalamic nuclei including the rhomboid nucleus project primarily to the nucleus accumbens, and overall to the most ventral and medial areas of striatum (Berendse & Groenewegen, 1990). The focus here will be on the nuclei of the ITN that project to dorsolateral striatum, and more specifically in the rat, the CL and Pf.

---

23 The rhomboid nucleus can also be considered part of the midline nuclei of the thalamus, along with the paraventricular, parataenial, intermediodorsal and reunions nuclei.

As well as projecting to the striatum, neurons in the ITN also project to the cortex. Deschênes *et al.* (1996b) examined neurons within the CL nucleus and their projections by injecting biocytin into the CL which labelled 4-20 neurons around the injection site. It was found that these neurons had somata of between 15 – 20 μm, and 10 – 15 primary dendrites (Deschênes *et al.*, 1996b). The axons gave rise to a few branches within the reticular complex and then entered striatum and had one to four collaterals with long varicose axonal branches which appeared to form 'en passant' contacts with striatal neurons (Deschênes *et al.*, 1996b). The axons then enter motor cortex, where they terminate in a 'patchy' manner primarily within layers Va and III (Deschênes *et al.*, 1996b). From this data, the authors surmised that all CL neurons which innervate striatum also innervate the cerebral cortex. Deschênes *et al.,* (1996a) also examined the neurons which originate in the Pf nucleus, using biocytin injections and juxtacellular labelling of individual neurons. These neurons had ovoid or polygonal somata and 4 – 5 thick, long and poorly branched dendrites (Deschênes *et al.*, 1996a). The axons of these neurons branched in the reticular complex, and then projected to the GP, striatum and cortex (Deschênes *et al.*, 1996a). In the GP, the Pf axons gave off one or two collaterals which appeared to make en passant connections (Deschênes *et al.*, 1996a). The striatal projection seen was very widespread and terminated in several clusters, with multiple terminations in each cluster (Deschênes *et al.*, 1996a). The Pf neurons also had axons which, after innervating striatum, continued into the cerebral cortex, terminating in layer VI; although the innervation to cortex was very sparse, especially in comparison to the striatal innervation (Deschênes *et al.*, 1996a). From this work it can be concluded that, in the rat, the CL and Pf predominantly innervate striatum the same neurons may also send axons into cerebral cortex.

Neurons of the CL and Pf not only have distinctive morphology, but also have distinct physiological properties (Lacey *et al.*, 2007). Extracellular recordings *in vivo* found that CL neurons fired LTS bursts in a similar fashion to thalamic relay neurons whereas Pf neurons fired single spikes (Lacey *et al.*, 2007). This study also examined, and extended, the contrasting morphological characteristics of CL and Pf neurons, concluding that CL neurons exhibited the 'bushy' like appearance attributed to thalamic

relay neurons, whereas Pf neurons were more reticular-like (Lacey *et al.*, 2007). This study also found differing synaptic connectivity within striatum (Lacey *et al.*, 2007), which will be discussed further.

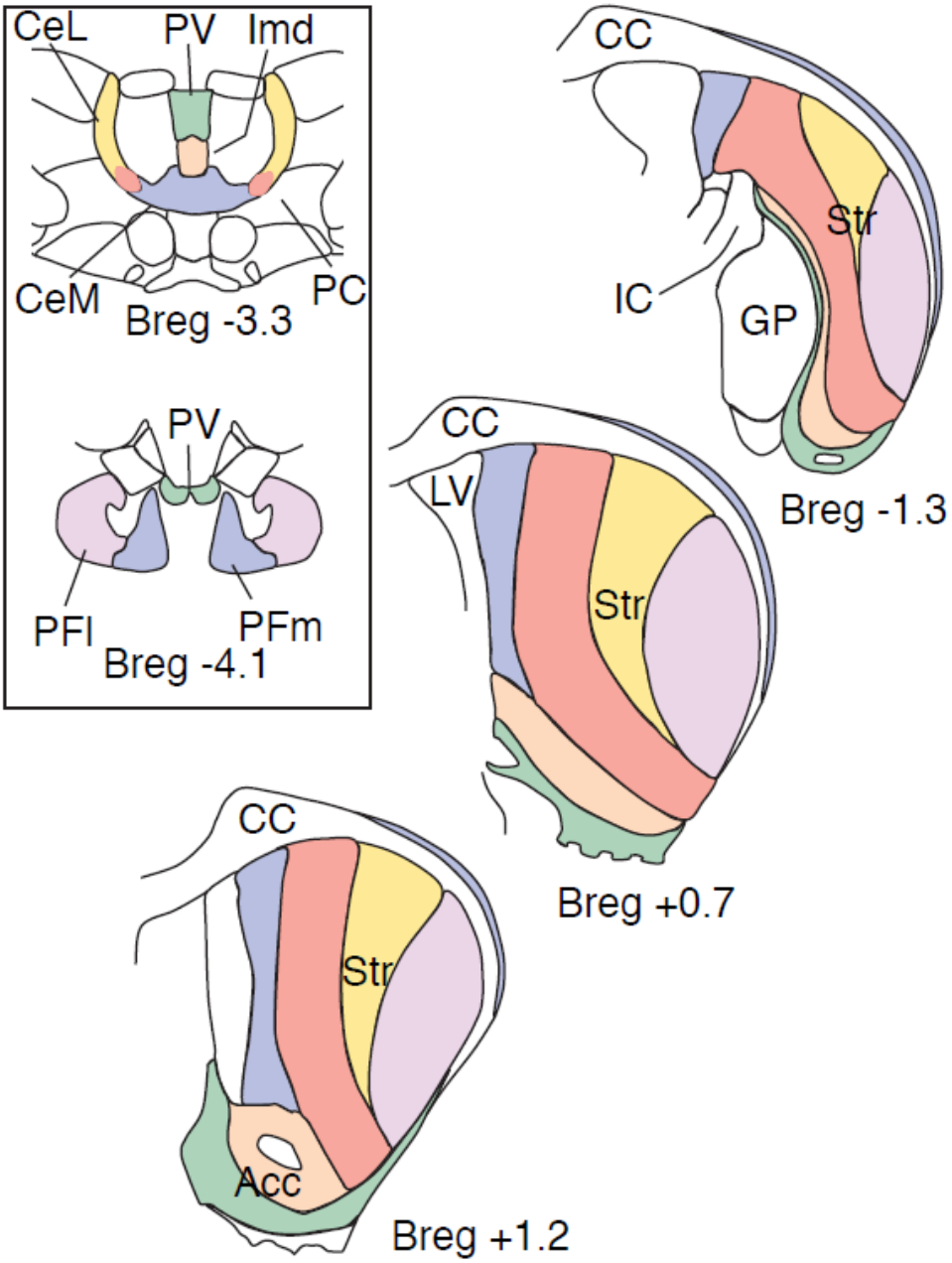


Figure 1.3. Projection from the intralaminar thalamic nuclei to the striatum in the rat.

Schematic diagram illustrating the projection from the intralaminar thalamic nuclei (inset) to the striatum (Str) in the rat. Projections from the central lateral thalamic nucleus (CeL; yellow) and the paracentral nucleus (PC; pink) terminate in the central part of the lateral striatum. Projections from the central median (CeM; blue) and the medial parafasciular nucleus (PFm; blue) terminate the rostro-caudal extent of the medial third of striatum. Projections from the lateral parafascicular nucleus (PFl; purple) terminate in the most lateral part of striatum. *Breg, bregma; CC, corpus callosum; GP, globus pallidus; IC, internal capsule; Imd intermediodorsal nculeus, LV, lateral ventricle.* (Figure from Smith *et al*., 2004)

1.4.3. Synaptic organisation of the thalamostriatal projection

As is the case with the corticostriatal projection, the main target of the thalamostriatal pathway is the MSN. Kemp and Powell (1971a, b) found that lesions in cortex and thalamus caused a decrease in the number of spines on MSNs. Furthermore, the decrease in spines was equal for cortical and thalamic lesions, indicating that the innervation from these structures are of similar magnitudes (Kemp & Powell, 1971b). However, the techniques used are now outdated, and these experiments were carried out in the cat. It is also now recognised that the different nuclei of the ITN have different anatomical properties. Dubé *et al.,* (1988) made lesions in either the cortex or Pf and showed that, in contrast to cortical axons, axonal projections originating in the Pf formed asymmetric synaptic contacts exclusively with the dendritic shafts of MSNs in the rat. In the squirrel monkey, Pf projections formed 81% of their synaptic contacts with dendritic shafts (12% with spines); whereas the CM projections formed 66% on dendritic shafts and 29% with spines (Sadikot *et al.*, 1992b). This indicates that the innervation pattern may be different amongst different species, and that there is heterogeneity between thalamic nuclei.

Recent usage of the vesicular glutamate transporter 2 (VGluT2) as a selective marker for the thalamostriatal projection from the ITN has allowed further examination of the pattern of synaptic connectivity within striatum (Fremeau *et al.*, 2001; Herzog *et al.*, 2001; Fujiyama *et al.*, 2004). A study by Lacey *et al*., (2005) showed that out of all the VGluT2-labelled terminals examined 72% formed synapses with dendritic spines, and 28% with dendritic shafts, in the rat. This indicates that although CM/Pf may preferentially innervate dendritic shafts, when the thalamostriatal projection is considered as a whole, the majority of synapses are formed with the spines of MSNs, albeit to a lesser extent than the cortical projection. When the innervation from the thalamus is considered in light of the different striatal compartments the pattern becomes more complex. Thalamostriatal axons have differing preferences for forming synapses with spines or shafts depending on whether they innervate the patch or matrix compartment (Raju *et al.*, 2006). In the matrix

compartment, VGluT2-positive terminals formed almost 90% of synapses with dendritic spines, whereas in the patch compartment the synapses with spines and shafts were almost equal (Raju *et al.*, 2006). This study also showed that, in agreement with previous work, the Pf preferentially innervates dendritic shafts, whereas the CL, midline and other striatal projecting nuclei from the ITN formed mainly axospinous synaptic contacts (Raju *et al.*, 2006). Lacey *et al.,* (2007) examined the synaptic connectivity of individually labelled CL and Pf neurons, and found that whilst the CL neurons did almost exclusively innervate dendritic spines (91%) there was much more heterogeneity in regards to the innervation from Pf. Overall, Pf neurons innervated shafts preferentially (61%), although one neuron (out of the six studied) showed a preference for innervating dendritic spines (97%), which indicates that axospinous contacts *can* be formed by Pf neurons, and that there is heterogeneity even between neurons that originate from a particular thalamic nuclei (Lacey *et al.*, 2007).

Aside from MSNs the thalamostriatal projection has also been shown to innervate striatal interneurons. In the monkey, projections from the CM were shown to form synaptic contacts with PV-positive dendrites within striatum (67 out of the 160 terminals examined) (Sidibé & Smith, 1999). A similar study in the rat showed that projections from the Pf formed the majority of synapses with unlabelled dendrites (75.9%), some with spines (22.5%) and very few with PV-positive dendrites (1.3%) (Rudkin & Sadikot, 1999). In the same study, when the PV-dendrites were examined, only four out of 100 presynaptic terminals were of thalamic origin (Rudkin & Sadikot, 1999). This indicates that the majority of input, that forms asymmetric synapses with PV interneurons is not from the thalamus but most likely of cortical origin. This is also dependent on the data which indicates that the input to dendritic shafts is from the Pf and therefore the majority of the input to interneurons is most likely to originate in the Pf. Sidibé and Smith (1999) also showed that, in the monkey, projections from the CM formed synapses with dendrites that were positive for SS (62 out of 167 terminals examined) (Sidibé & Smith, 1999). This has however not been examined in the rat. This same study concluded that there was no evidence for thalamic innervation of calretinin-positive dendrites in striatum (Sidibé &

Smith, 1999).

Out of all striatal interneurons the thalamic innervation to the cholinergic interneurons has received the most attention. Lapper and Bolam (1992) examined the cortical and thalamic innervation of ChAT-positive structures in striatum; evidence for thalamic input was described, which was in direct contrast to the cortical input, for which there was a lack of evidence. Out of the 33 terminals from Pf forming synapses with ChAT neurons, 55% were with distal dendrites, 24% with more proximal dendrites and 21% with perikarya (Lapper & Bolam, 1992). Cholinergic interneurons also receive innervation from the CM in the monkey, 55 out of the 104 terminals studied formed synaptic contacts with ChAT-positive dendrites (Sidibé & Smith, 1999). The functional significance of the thalamic innervation of ChAT neurons will be discussed further.

1.4.4. Functional organisation of the thalamostriatal system

As well as the corticostriatal pathway the thalamostriatal pathway also maintains a general functional topography. The projections to the specific regions of striatum are reflected in their cortical projections (Haber & Calzavara, 2009). For example, the midline and medial intralaminar nuclei project to limbic related areas of the cortex such as the amygdala and hippocampus; and project to the more limbic-associated areas of striatum (Haber & Calzavara, 2009). Francois *et al.,* (1991) injected tracers into the CM-Pf or into the leg area of motor cortex in monkeys. The staining of both the cortical and thalamic injections resulted in a corresponding pattern of innervation within the dorsolateral striatum, indicating that sensorimotor regions of cortex and the CM-Pf have overlapping areas of innervation (Francois *et al.*, 1991). The CM-Pf projects to pre-motor and sensorimotor areas of cortex, indicating that these circuits could provide the basis for closed sensorimotor loops (Francois *et al.*, 1991; Sadikot & Rymar, 2009). This functional topography is also illustrated in the afferent connections to the thalamic nuclei; the CM receives innervation from the somatosensory cortices, whereas the Pf receives innervation from pre-motor and cingulate cortices which is reflected in their

relative innervation of the cortex (Sadikot & Rymar, 2009). Therefore there is anatomical evidence for functional regions of the striatum receiving innervation from cortical and thalamic areas that are functionally related (Francois *et al.*, 1991; Sadikot *et al.*, 1992a; Sadikot *et al.*, 1992b; Haber & Calzavara, 2009; Sadikot & Rymar, 2009).

Besides innervation from the cortex the ITN also receive input from subcortical structures, which is central to the functional roles of the thalamostriatal system. The CL nucleus receives a dense input from the brainstem, the reticular formation, the raphé nuclei and the superior colliculus (SC), and from the output nuclei of the basal ganglia (SNpr) (Van der Werf *et al.*, 2002). The CM-Pf receives innervation from the spinal cord, the reticular formation (including the locus coeruleus and the raphé nuclei), brainstem nuclei, deep cerebellar nuclei and the vestibular nuclei, as well as from the SNpr (Van der Werf *et al.*, 2002). As these inputs would suggest, the ITN are involved in the 'reticular activating system', a system that regulates arousal and attention (Van der Werf *et al.*, 2002). The majority of the outputs of the CM and Pf project to the basal ganglia, which suggests that they are not only involved in sensory awareness but also involved in motor processes (Van der Werf *et al.*, 2002). This is also highlighted in evidence from Parkinson's disease patients where the CM-Pf undergoes significant degeneration (Galvan & Smith, 2011).

Research carried out in behaving primates has highlighted the role of the CM-Pf complex in attention. Recordings from the CM-Pf during an attention task revealed that the neurons respond significantly to visual stimuli that signify the onset (cue) and target of an attentional task, and that the response is greatest when the stimulus is on the contralateral side and unexpected (Minamimoto & Kimura, 2002). Moreover, neurons of the CM also display activity that suggests that they are involved in reward-related behaviour (Minamimoto *et al.*, 2005). In a reward-based movement task, neurons of the CM responded with increased probability when a small (vs. large) reward was given, and that this effect was more evident when a large reward was expected (Minamimoto *et al.*, 2005). Matsumoto and colleagues (2001) also showed that the CM-Pf provides task dependent information to TANs. Neurons in both the CM-Pf and the striatum were

recorded from whilst stimuli, both with and without rewards, were presented to monkeys (Matsumoto *et al.*, 2001). The authors found that injection of muscimol into the CM-Pf abolished the response of TANs to a cue and reward (Matsumoto *et al.*, 2001). This demonstrates that the responsiveness of TANs is dependent on innervation from the ITN (Matsumoto *et al.*, 2001). The thalamostriatal system is thus able to transmit information to the basal ganglia about sensory events and reward-related information.

1.4.5. Summary

The major innervation from thalamus to the striatum originates in the intralaminar thalamus. The thalamic projection is however, very heterogeneous. The different nuclei within the ITN project to different compartments of the striatum, and form synapses with different parts of the MSN. Furthermore, the neurons within these nuclei have differing physiological and morphological characteristics. The projection maintains a functional topography that related to the functional innervation from the cortex. The ITN, and in particular, the CM-Pf have been shown to have a role in attention and attentional shifting. The innervation from the CM-Pf also has been shown to have a role in reward-related behaviour and may provide motivational signals to the cholinergic interneurons. Although the cortex and thalamus both provide a major glutamatergic innervation to the striatum, there are clearly many dissimilarities between the two systems.

1.5. Aims

The overall aim of this thesis was to examine cortical and thalamic innervation to subtypes of striatal neurons, using a combination of techniques.

1.5.1. Cortical and thalamic innervation of MSNs

MSNs are the main target of cortical and thalamic innervation to the striatum, the aim of this study was to determine whether there is any selectivity of these two excitatory afferents in their innervation of direct and indirect pathway MSNs. In order to address this, bacterial artificial chromosome (BAC) transgenic mice were used, in which enhanced green fluorescent protein (EGFP) reports the presence of D_1 or D_2 dopamine receptor subtypes, markers of direct and indirect pathway MSNs, respectively. Excitatory afferents were identified by the selective expression of vesicular glutamate transporter type 1 (VGluT1) by corticostriatal afferents, and vesicular glutamate transporter type 2 (VGluT2) by thalamostriatal afferents. A quantitative electron microscopic analysis was performed on striatal tissue from D_1 and D_2 mice that were double immunolabelled to reveal the EGFP and either VGluT1 or VGluT2.

1.5.2. Cortical and thalamic innervation of cholinergic interneurons

Cholinergic interneurons are the source of acetylcholine within striatum, and thus in a position to modify plasticity within the striatal microcircuit. The aim of this study was to examine and compare the inputs to cholinergic interneurons from both cortex and thalamus. In order to examine this, two complementary methods were employed:

1.5.2.1. Cortical and thalamic input to cholinergic interneurons in vivo.

Extracellular recordings from cholinergic interneurons were carried out in the anaesthetised rat. Stimulating electrodes were placed in motor cortex and the parafascicular nucleus of the ITN. A variety of stimulation protocols were applied to examine and compare the responses of individual cholinergic interneurons to cortical and thalamic stimulation. Using the juxtacellular method neurons which exhibited firing patterns indicative of TANs

were filled with neurobiotin after recording. The neurons could then be neurochemically identified *post-mortem* using the known molecular markers for striatal neuron subtypes.

1.5.2.2. Cortical and thalamic synaptic input to an individual cholinergic interneuron.

Individual, identified cholinergic interneurons which had been examined physiologically *in vivo* were processed for electron microscopy. In order to examine the synaptic input from cortex and thalamus onto individual cholinergic interneurons, adjacent sections were labelled for markers of cortical and thalamic terminals, VGluT1 and VGluT2, respectively. The relative contribution of cortical and thalamic synaptic inputs to two cholinergic interneurons was examined in all parts of the dendritic arbor.

Chapter Two: Cortical and thalamic innervation of medium-sized spiny neurons in the mouse striatum

2.1. Introduction

One of the primary roles of the striatum is to integrate glutamatergic afferents which originate in the cortex and the thalamus (Smith & Bolam, 1990a; Gerfen, 1992; Bolam *et al.*, 2000; Smith *et al.*, 2004; Graybiel, 2005). The predominant targets of the corticostriatal and thalamostriatal projections are the dendritic spines of the medium-sized spiny neurons (MSNs), the main neuronal cell-type and principal projection neuron of the striatum (Kemp & Powell, 1971b; a; Somogyi *et al.*, 1981; Dubé *et al.*, 1988; Xu *et al.*, 1989; Smith & Bolam, 1990a; Xu *et al.*, 1991; Sadikot *et al.*, 1992b; Smith *et al.*, 1994; Bolam *et al.*, 2000; Smith *et al.*, 2004; Lacey *et al.*, 2005; Raju *et al.*, 2006; Moss & Bolam, 2008; Raju *et al.*, 2008).

Medium-sized spiny neurons are divided into two major subpopulations based on projection targets and the expression of dopamine receptor subtypes, as well as a variety of other molecular markers (Gerfen *et al.*, 1990; Smith *et al.*, 1998). Given that the excitatory inputs to the striatum from the cortex and thalamus are fundamental in the expression of basal ganglia function, it is critical to elucidate the pattern of innervation of the two subpopulations of MSNs. Both direct and indirect pathway MSNs have been shown to receive synaptic input from the cortex (Somogyi *et al.*, 1981; Hersch *et al.*, 1995; Lei *et al.*, 2004). Light microscopic studies have suggested that the same is true for thalamostriatal afferents (Lanciego *et al.*, 2004; Castle *et al.*, 2005). Electron microscopic studies in primates have suggested that afferents from the centromedian nucleus (CM) of the thalamus preferentially innervate direct pathway MSNs (Sidibé & Smith, 1996). Furthermore, *in vivo* electrophysiological analyses have demonstrated that striatonigral neurons, at least, receive excitatory input after both cortical and thalamic stimulation (Kocsis *et al.*, 1977; Vandermaelen & Kitai, 1980), and *in vitro* studies in transgenic mice have shown that individual direct and indirect pathway neurons respond to cortical and thalamic stimulation (Ding *et al.*, 2008).

2.1.1. Aims

The aim of the present experiments was to define the rules of connectivity of corticostriatal and thalamostriatal afferents in relation to MSNs that give rise to the direct and indirect pathways. The development of transgenic mice which express EGFP under the D_1 and D_2 dopamine receptor promoters (Gong *et al.*, 2003; Valjent *et al.*, 2009) and thus identify direct and indirect pathway MSNs respectively allowed us to address this issue. Previous to the development of these animals it has been difficult to reliably separate MSNs of the direct and indirect pathways based on the selective expression of dopamine receptors. This could then be combined with the fact that subtypes of vesicular glutamate transporters are selective molecular markers of cortical and intralaminar thalamic afferents (VGluT1 and VGluT2, respectively; Fremeau *et al.*, 2001; Herzog *et al.*, 2001; Kaneko & Fujiyama, 2002; Fremeau *et al.*, 2004; Fujiyama *et al.*, 2004; Raju *et al.*, 2006; Barroso-Chinea *et al.*, 2008; Raju *et al.*, 2008). Thus, the selective expression of subtypes of molecular markers allowed us to address the issue of selective innervation of direct and indirect pathway MSNs by either cortical or thalamic afferents. Thus, a quantitative analysis of the connectivity of the two glutamatergic afferents in relation to the subpopulations of MSNs was performed.

2.2. Materials and Methods

All experimental procedures were conducted in accordance with the Animals (Scientific Procedures) Act 1986 (UK), and the Society for Neuroscience policy on the use of animals in research. Experimental procedures were carried out on twenty-eight adult BAC transgenic mice that report subtypes of the dopamine receptor, either D_1 or D_2, by the presence of EGFP (28-58g; Mutant Mouse Regional Resource Centers, MMRRC). Pilot and control experiments were conducted on fourteen of the BAC transgenic mice to establish the optimal staining conditions, and the detailed quantitative analysis on the remaining fourteen. Details of the methods of BAC mice production have been published and can be found on the GENSAT website (Gong *et al.*, 2003; GENSAT, 2009).

2.2.1. Tissue preparation

The D1 and D_2 EGFP mice were anaesthetised with sodium pentobarbitone (200 mg/kg; Rhône Mérieux, Dublin, Republic of Ireland) then perfused via the aorta with approximately 30 ml of phosphate buffered saline (PBS; 0.1 M phosphate buffer [PB], pH 7.4, 0.876% NaCl, 0.02% KCl) followed by 50 ml fixative (0.1 M PB, pH 7.4, 3% paraformaldehyde, 0.1% glutaraldehyde) over about 15 min. Free fixative was removed by post-perfusion with PBS. The brain was removed and cut into 50-60 μm sagittal sections (1 in 6 series) using a vibrating blade microtome (VT1000S; Leica Microsystems, Wetzlar, Germany).

2.2.2. Immunohistochemistry

All sections were washed three times in PBS and placed into a cryoprotectant (0.05 M PB, 25% sucrose, 10% glycerol) for a minimum of 2 h before freeze-thawing. Each section was immersed in chilled isopentane and then liquid nitrogen for a few seconds, left to thaw at about 25ºC for approximately 5 min and then washed 3 times in PBS.

The sections were then either single- or double-immunolabelled. All sections were immunolabelled to reveal either VGluT1 or VGluT2, as markers of cortical and thalamic terminals, respectively. Double-labelled sections were then immunolabelled to reveal

the EGFP (which reports expression of either the D_1 or D_2 receptor subtypes, markers of direct or indirect pathway MSNs, respectively). Primary antibodies for the double-immunolabelling experiments were added sequentially. Normal goat serum in PBS (NGS-PBS; Vector Laboratories, Peterborough, UK) was used to block (10% NGS) and wash (2% NGS) sections prior to the addition of primary antibodies. Antibodies against VGluT1 or VGluT2, raised in rabbits (VGluT1, MAb Technologies, Stone Mountain, GA; VGluT2, Synaptic Systems, Göettingen, Germany) were used at a dilution of 1:2000 in 2% NGS-PBS and the sections were incubated overnight (approximately 14 h), shaking at room temperature or over three nights (approximately 64 h) at 4°C. They were then washed once in 2% NGS-PBS, three times in PBS and once in 1% NGS-PBS. The sections were then incubated for 2 h in anti-rabbit gold-conjugated antibody (1.4 nm colloidal gold, Nanoprobes, Yaphank, NY) at a dilution of 1:100 in 1% NGS-PBS. This was followed by one wash in 1% NGS-PBS and three washes each in PBS and acetate buffer (0.1 M sodium acetate 3-hydrate, pH 7.0-7.5) in preparation for silver intensification of the conjugated gold particles. Silver reagent (1 ml; HQ Silver kit, Nanoprobes) was added to each section and allowed to react for 4 min, washed three times each in acetate buffer and PBS, and once in 2% NGS-PBS. The sections were then incubated in a biotinylated antibody against GFP, raised in goat (BA-0702, Vector Laboratories, Peterborough, UK), at a dilution of 1:500 (for D_1 mouse sections) or 1:1000 (for D_2 mouse sections) in 2% NGS-PBS overnight, shaking at room temperature, or over three nights (approximately 64 h) at 4°C. Washes of once in 2% NGS-PBS and three times in PBS preceded the incubation in avidin-biotin-peroxidase complex (ABC; Vector Laboratories, prepared according to the manufacturer's instructions) with shaking for 90 min at about 25ºC.

After the ABC incubation, the sections were washed three times in PBS followed by three washes in 0.1 M PB (pH 6.0). A peroxidase reaction using tetramethylbenzidine (TMB) as the chromogen was then carried out to reveal EGFP in striatal tissue taken from D_1 and D_2 BAC mice. The TMB-tungstate method was used because of its increased sensitivity when compared to other peroxidase reactions (Bolam, 1992; Llewellyn-Smith et al., 1993). Sections were placed for 20 min in a pre-incubation solution of: 80 ml 0.1

M PB (pH 6.0), 4 ml ammonium paratungstate (1% in deionised H2O), 1 ml TMB (0.2% dissolved in absolute ethanol; Sigma-Aldrich T5525, Dorset, UK), 800 µl ammonium chloride (NH4Cl; 0.4% in deionised H2O), and 800 µl D-Glucose (20% in deionised H2O). All steps, from pre-incubation onwards were carried out on ice. To perform the reaction the pre-incubation solution was removed and replaced with the reaction solution, which consisted of 2 ml of the pre-incubation solution (as above) plus 2 µl glucose oxidase (Sigma G6891). The reaction was allowed to continue for 2-8 min, until dark blue staining of MSN cell bodies in the striatum was clearly seen under the dissecting microscope, and was stopped with cold 0.1 M PB (pH 6.0). Sections were then washed three times for 10 min with 0.1 M PB (pH 6.0). The reaction was then stabilized using diaminobenzidine (DAB) and cobalt (II) chloride. Sections were incubated in a stabilization solution of: 400 µl ammonium chloride (0.4% in deionised H2O), 400 µl D-glucose (20% in deionised H2O), 800 µl cobalt (II) chloride (1% in deionised H2O), and 40 mg DAB dissolved in 40 ml 0.1 M PB (pH 6.0). The stabilization solution was filtered and stored at about -20°C before use. Sections were incubated for 10-15 min. The stabilization solution was then removed with three 10 min washes of 0.1 M PB (pH 6.0). During stabilization, the blue-staining colour from the reaction step changes to a darker magenta colour and background staining is reduced. Sections were then washed three times in 0.1 M PB (pH 7.4).

The sections were then placed flat on the bottom of glass petri dishes and post-fixed in osmium tetroxide (1% in PB; Oxkem, Oxford, UK) for 7 min. They were then washed in 0.1 M PB and dehydrated in an ascending series of ethanol dilutions (15 min in 50% ethanol, 35 min in 70% ethanol which included 1% uranyl acetate [TAAB, Reading, UK], 15 min in 95% ethanol, and twice 15 min in absolute ethanol). Following absolute ethanol, sections were washed twice in propylene oxide (Sigma) for 15 min and lifted, using modified forceps, into resin (Durcupan ACM, Fluka, Gillingham, UK) in crafted foil boats and left overnight (approximately 15 h) at room temperature. The resin was then warmed to reduce its viscosity and sections were placed on microscope slides, a coverslip applied and the resin cured at 65°C for about 70 h.

The GFP primary antibody, raised in goat, shows high affinity for wild-type, recombinant or any variants of Aquorea victorea GFP (BA-0702 Vector Laboratories, Peterborough, UK). Immunoperoxidase staining of the GFP antibody showed a precise correlation with EGFP fluorescence in D_1 and D_2 BAC-EGFP mice. The VGluT primary antibodies were raised against rat VGluT1 and VGluT2 (amino acids 543-560 and 510-582, respectively). The distribution of immunolabelling at the light and electron microscopic levels was distinct for each primary antibody and consistent with previous observations by ourselves (Lacey et al., 2005; Moss & Bolam, 2008) and others, using the same or different antibodies (Fremeau et al., 2001; Herzog et al., 2001; Kaneko & Fujiyama, 2002; Fujiyama et al., 2004; Fujiyama et al., 2006; Raju et al., 2006; Raju et al., 2008). No immunolabelling was observed following omission of the primary antibodies or when tissue from wild-type litter mates (D_1 BAC-EGFP negative) was processed using the anti-GFP antibody followed by a tungstate-stabilised TMB reaction.

2.2.3. Electron microscopic analysis

All sections were examined in the light microscope and areas from the dorsolateral striatum were cut from the slide, glued to the top of a resin block and trimmed with razor blades. Serial sections, about 50 nm thick (silver/grey), were then cut using an ultramicrotome (Leica EM UC6, Leica Microsystems) and were collected on pioloform-coated, single-slot copper grids (Agar Scientific, Stansted, UK). The sections were then lead-stained to improve contrast for electron microscopic examination. A Philips CM10 electron microscope was used to examine sections of tissue. All analyses were performed at a minimum of 5 μm from the tissue-resin border (i.e. the surface of the section). The maximum distance from the tissue-resin border examined was determined by the penetration of the gold conjugated antibody together with the angle at which the tissue-resin was sectioned, and was therefore variable.

2.2.3.1. Tissue single-labelled for VGluT1 or VGluT2 in D_1 and D_2 mice

In order to establish whether the VGluT1 or VGLut2 terminals showed a similar pattern of innervation in the transgenic mice as has been previously described for the rat and

monkey, VGluT-immunopositive synapses were systematically analysed in one of the serial sections on an electron microscope grid. One section out of the serial sections on the grid was selected at random, using randomly generated integers. At a magnification where it is not possible to clearly visualize synapses (×1,950), an area was chosen, which generally comprised of the entire tissue/resin border. The magnification was then increased to ×10,500 and positively labelled VGluT terminals forming asymmetric synapses were identified and digitally recorded at an indicated magnification of ×25,000 (Gatan multiscan CCD camera, Gatan, Oxfordshire, UK). The criterion for an immunopositive structure was three or more silver-intensified immunogold particles (hereafter simply referred to as immunogold particles). Asymmetric synapses (Gray's type 1) were identified by the presence of presynaptic vesicle accumulation, a thick postsynaptic density, a widened synaptic cleft and cleft material. Asymmetric synapses were identified and imaged, continuing systematically in straight lines across the section. This systematic process was continued within the same section until the entire selected area had been covered. The process was then repeated on sections on different grids until 50 VGluT-immunopositive synapses were analysed per animal for each group: VGluT1 labelling in D_1 and D_2 mouse tissue, VGluT2 labelling in D_1 and D_2 mouse tissue, (n = 3 animals per group). This resulted in a total of 150 VGluT-positive synapses per group and an overall total of 600 asymmetric synapses. In these images, the postsynaptic target(s) of the VGluT-positive terminals were characterized. Dendritic shafts were identified by their relatively large size when compared to spines, the presence of mitochondria and, although not essential, the protrusion of spines from their shaft. Spines were identified by their shape and relatively small size when compared to dendritic shafts, the lack of mitochondria within their cytoplasm and, although not essential, the presence of spiny apparatus. Subsequently, any other immunopositive terminals seen within the frame were also analysed. Any immunopositive terminals not fully within the frame were excluded. Postsynaptic structures, such as large dendrites that extended beyond the borders of the frame, were only examined within the frame. Digital images were analysed using the publicly available software, ImageJ (http://rsbweb.nih.gov/ij/). and they were adjusted

for contrast and brightness using Adobe Illustrator and Photoshop (Version CS3, Adobe Systems Incorporated, San Jose, CA).

In view of the fact that the probability of the release of glutamate at thalamostriatal synapses is less than at corticostriatal synapses in these two lines of mice (Ding et al., 2008), we analysed quantitative aspects of the VGluT1- and VGluT 2-positive terminals in the data set from the double labelled tissue (see below). A total of 56 VGluT1 and 59 VGluT2 terminals forming axospinous synapses were analysed in single sections that were systematically taken from the double-labelled tissue data set (n=6 animals per group). Cross sectional area, length of synaptic specializations, number of vesicles and distance of vesicles from the active zone were measured using ImageJ and the ImageJ plug-in PointDensitySyn (Larsson & Broman, 2005).

2.2.3.2. Tissue double-labelled for VGluT1 or VGluT2 and GFP in D_1 and D_2 mice

In order to examine VGluT1- and VGLuT2- positive terminals forming synapses with D_1 or D_2 structures, EGFP immunopositive postsynaptic structures forming asymmetric synapses were randomly selected and followed in 7 serial sections. The postsynaptic structures were examined and the presynaptic terminal was then described as being positive or negative for the particular VGluT-marker under study. The analysis was performed this way in order to ensure that no EGFP- false negative structures were included in the study. Serial sections on one electron microscope grid were numbered from 1 to 7 at a low magnification (×58). The analysis always began from the middle section (number 4). The tissue/resin border was located at a magnification of ×5,800 (where synapses cannot be clearly visualized) and an area was then randomly selected. The magnification was then increased (×10,500) and the tissue was scanned until the first EGFP-positive structure was identified, as indicated by the presence of TMB crystals and/or DAB staining within spines or dendrites. If the EGFP-positive structure was seen to be forming an asymmetric synapse, it was then examined, and images were captured, in

the seven serial sections at a magnification of ×25,000, keeping the profile central within the frame. After acquisition these images were analysed and the presynaptic terminals forming asymmetric synapses with EGFP-positive structures were identified as being either VGluT-immunopositive (3 or more immunogold particles) or negative over the 7 serial sections. It was also determined whether the structure received any other synaptic input, and whether the presynaptic terminal formed more than one asymmetric synapse with the same or different postsynaptic structures. This was repeated until 50 EGFP-positive synapses had been identified and imaged in tissue from the same animal, using several grids from up to two blocks. This procedure was carried out for each group (D_1 tissue labelled for VGluT1 or VGluT2, and D_2 tissue labelled for VGluT1 or VGluT2), resulting in a total of 150 EGFP-positive postsynaptic structures per group (n = 3 animals per group), and an overall total of 600 EGFP postsynaptic structures. To control for the fact that immunogold staining within the tissue/resin border is variable, due to the penetration of the immunogold secondary antibody, only sets of images (7 serial sections) containing at least one VGluT-immunopositive structure were included in the study. Any other EGFP-positive profiles receiving asymmetric synapses seen within the frame were also analysed and counted, providing the entire presynaptic terminal was within the frame border.

2.2.4. Statistical analysis

All statistical calculations were performed using the statistical software R (version 2.10.1; R Development Core Team, 2009, Vienna, Austria) and PASW Statistics (v18.0; SPSS, 2010, Surrey, UK). For statistical analyses, either the Fisher's exact test or the Mann–Whitney U test were used, all p-values described are two tailed. Differences were considered significant when $p < 0.05$.

2.3. Results

2.3.1. Postsynaptic targets of corticostriatal and thalamostriatal afferents in D_1 and D_2 transgenic mice.

The targets of cortical and thalamic innervation of the striatum, as indicated by labelling for VGluT1 or VGluT2, respectively, have been studied extensively in rat and non-human primate (Lacey et al., 2005; Fujiyama et al., 2006; Raju et al., 2006; Moss & Bolam, 2008; Raju et al., 2008). In order to determine whether the synaptic architecture in the D_1 and D_2 transgenic mice is comparable to that in other species, we analysed tissue from the D_1 and D_2 BAC EGFP mice single-immunolabelled for VGluT1 or VGluT2. Light microscopic (LM) analysis revealed that the patterns of VGluT1 and VGluT2 immunogold labelling were consistent with previous reports, with intense VGluT1 labelling in the cortex and hippocampus, and VGluT2 labelling most intense in the thalamus (Fremeau et al., 2004). Electron microscopic (EM) analysis revealed that VGluT1 and VGluT2 immunogold labelling was concentrated within axons and axon terminals forming asymmetric synapses. Consistent with previous studies in rat (Lacey et al., 2005; Fujiyama et al., 2006; Raju et al., 2006; Moss & Bolam, 2008) and Rhesus monkey (Raju et al., 2008; see Table 1), VGluT1-positive terminals in striatal tissue from both D_1 and D_2 transgenic mice, formed asymmetric synapses almost exclusively with spines (98.8% and 98.2%, respectively), with only a small proportion in synaptic contact with dendritic shafts (Table 2.1). Likewise, VGluT2-positive terminals in the D_1 and D_2 tissue had a similar distribution to other species: with about 77% to 80% in contact with spines and the remainder (~21%) in contact with dendritic shafts (Table 2.1). Statistical analysis revealed that the difference between the proportions of VGluT1- and VGluT2-positive terminals forming synapses with dendritic spines is significant ($p < 0.001$; Fisher's exact test). These data demonstrate that the pattern of glutamatergic innervation of MSNs in the striatum of the D_1 and D_2 BAC EGFP transgenic mice is not markedly different from other species.

Table 2.1. Postsynaptic targets of individual VGluT1- and VGluT2-positive terminals in D_1 and D_2 transgenic mice, in comparison to previous studies

VGluT1		**VGluT2**	
Study	**Percentage of VGluT-positive terminals forming axospinous synapses (±SEM)**	**Study**	**Percentage of VGluT-positive terminals forming axospinous synapses (±SEM)**
Mouse D_1 (Present study)	98.8 (±1.1; n=3)	Mouse D_1 (Present study)	77.6 (±1.6; n=3)
Mouse D_2 (Present study)	98.2 (±1.0; n=3)	Mouse D_2 (Present study)	80.1 (±4.8; n=3)
Rat (Moss & Bolam, 2008)	95.9	Rat (Moss & Bolam, 2008)	70.5
Rat (Lacey et al., 2005)	98.9	Rat (Lacey et al., 2005)	71.9
Rat (Raju et al., 2006)	>90	Rat (Raju et al., 2006)	80-90 (patch), 50-60 (matrix)
Rat (Fujiyama et al., 2006)	82 (patch), 81 (matrix)	Rat (Fujiyama et al., 2006)	84 (patch), 30 (matrix)
Rhesus Monkey (Raju et al., 2008)	94 - 98	Rhesus Monkey (Raju et al., 2008)	50 - 65

2.3.2. Morphological characteristics of corticostriatal and thalamostriatal terminals in D_1 and D_2 transgenic mice

A previous study revealed no differences in the cross-sectional area of VGluT1- and VGluT2-positive synaptic terminals or length of the synaptic membrane in the rat (Lacey et al., 2005). Similarly, no differences were observed in the diameter of VGluT-positive synaptic terminals in primate (Raju et al., 2008), although there is an indication that VGluT1-positive terminals may have a larger volume (Smith et al., 2009b). In this study no significant differences in the cross-sectional area of VGluT1- and VGluT2-positive synaptic terminals were observed (mean±SD, VGluT1, 0.30 ±0.0495 μm^2; VGluT2, 0.30 ± 0.0548 μm^2; $p > 0.05$; n = 6 animals per group; Mann–Whitney U test in this and subsequent comparisons) nor in the length of the synaptic membrane (VGluT1, 0.18 ± 0.05 μm; VGluT2, 0.16 ± 0.01 μm; $p > 0.05$). Analysis of the distribution of vesicles revealed no significant differences in the number (mean ± SD, VGluT1, 26.56 ± 7.68; VGluT2, 31.74 ± 6.51; $p > 0.05$), density of vesicles (VGluT1, 87.77 ± 15.65 per μm 2; VGluT2, 108.40 ± 29.92 per μm 2; $p>0.05$), mean distance from active zone (VGluT1, 241.13 ± 52.31 nm; VGluT2, 254.06 ± 43.58 nm; $p > 0.05$), and inter-vesicle distance as an indicator of clustering (VGluT1, 300.48 ± 41.07 nm; VGluT2, 295.35 ± 59.44 nm; $p > 0.05$). There were also no significant differences in the morphological characteristics of terminals when pooled to reflect whether the terminal was forming a synapse with either a D_1- or D_2-positive spine (all p values > 0.05, Mann–Whitney U test). These findings indicate that there are no differences in the morphological characteristics of corticostriatal and thalamostriatal terminals and their vesicle distributions that could account for their different electrophysiological properties (Ding et al., 2008).

2.3.3. Innervation of direct and indirect pathway MSNs by corticostriatal and thalamostriatal afferents

In double-labelled tissue, cortical or thalamic terminals were identified by immunogold labelling for VGluT1 or VGluT2 respectively and EGFP, which reports the expression of D_1 or D_2 receptors, was used to differentiate the direct and indirect pathway MSNs and was revealed by immunoperoxidase labelling. Light microscopic examination

of immunolabelling for EGFP in sections from D_1 and D_2 mice, showed intense labelling in the striatum and distinct labelling of the direct and indirect pathways, respectively (i.e. intense staining in the substantia nigra pars reticulata and entopeduncular nucleus [D_1 mice], and the globus pallidus externa [D_2 mice]), as has been reported previously (for review see Valjent et al., 2009). High magnification light microscopy revealed that labelling for EGFP was localized within MSN cell bodies, dendrites and spine-like structures, and was intermingled with unlabelled cells (Fig 2.1). Electron microscopic analysis revealed that immunoperoxidase reaction product (TMB-DAB) was consistently located within MSN dendrites and dendritic spines (Figures 2.2, see also Figs. 2.4, 2.5).

Initial qualitative electron microscopic analysis of the double-labelled tissue revealed that D_1 (EGFP-positive) structures receive synaptic input from both VGluT1-positive terminals (Figure 2.2a) and VGluT2-positive terminals (Figure 2.2b). Similarly, D_2 (EGFP-positive) structures receive synaptic input from both VGluT1-positive terminals (Figure 2.2c), and VGluT2-positive terminals (Figure 2.2d). This demonstrates that both cortical and thalamic afferents innervate both direct pathway MSNs and indirect pathway MSNs.

Quantitative electron microscopic analysis of the tissue double-labelled for EGFP (D_1 or D_2) and VGluT1 or VGluT2 was carried out. Immunopositive (D_1 or D_2) postsynaptic structures were randomly selected and analysed, and the presynaptic terminals forming asymmetric synapses were characterized as being VGluT-positive or negative. Thus, we were able to determine what proportion of terminals forming synaptic contact with neurons of the direct (D_1) and indirect (D_2) pathways were derived from the cortex (VGluT1-postive) or the thalamus (VGluT2-positive) (Fig. 2.3). Examination of D_1 tissue labelled for VGluT1 revealed that, out of the 150 asymmetric synapses examined, 63 of the presynaptic terminals were positive for VGluT1, (average percentage of 42% ± 11.5%; n = 3; Fig. 2.3). In D_1 tissue labelled for VGluT2, out of the 150 synapses examined, 66 of the presynaptic terminals were VGluT2 positive, (average percentage of 44% ± 7.02%; n = 3; Fig. 2.3). Similarly, for D_2 tissue labelled for VGluT1, 57 presynaptic terminals

forming synapses were positively labelled, (average percentage of 38% ± 12.7%; n=3; Fig 2.3). For D_2 tissue labelled for VGluT2, a total of 50 out of the 150 presynaptic terminals forming synapses were positive, (average percentage of 33% ± 7.42%; n = 3; Fig. 2.3). The statistical analyses revealed that the postsynaptic D_1 or D_2 (EGFP-positive) structures do not receive significantly different proportions of synaptic inputs from either VGluT1- or VGluT2-positive terminals ($p = 0.82$ and $p = 0.47$ respectively, Fisher's exact test). Moreover, neither VGluT1- nor VGluT2-positive terminals showed any significant differences in the proportions of synapses formed with either D_1 or D_2 MSNs ($p = 0.56$ and $p = 0.08$ respectively, Fisher's exact test).

Although the synaptic contacts made by VGluT1- and VGluT2-positive terminals with D_1- or D_2-positive neurons were analysed in separate sections we conclude that at least a proportion of the terminals immunonegative for one of the VGluTs, in fact, expressed the other VGluT, demonstrating a convergence of cortical and thalamic input to both direct and indirect pathway neurons (see below also). However, if all VGluT-immunopositive terminals in contact with D_1 or D_2 neurons are considered as a whole, the total does not account for all terminals forming asymmetric synapses (15-30% negative). Although false-negatives cannot be ruled out, previous studies have shown that approximately 20-30% of terminals forming asymmetric synapses are negative for both VGluT1 and VGluT2. This indicates that a proportion of terminals that form asymmetric synapses may not be glutamatergic or may express an hitherto unidentified vesicular glutamate transporter (Lacey et al., 2005; Raju et al., 2008; Smith et al., 2009a; Moss et al., 2011).

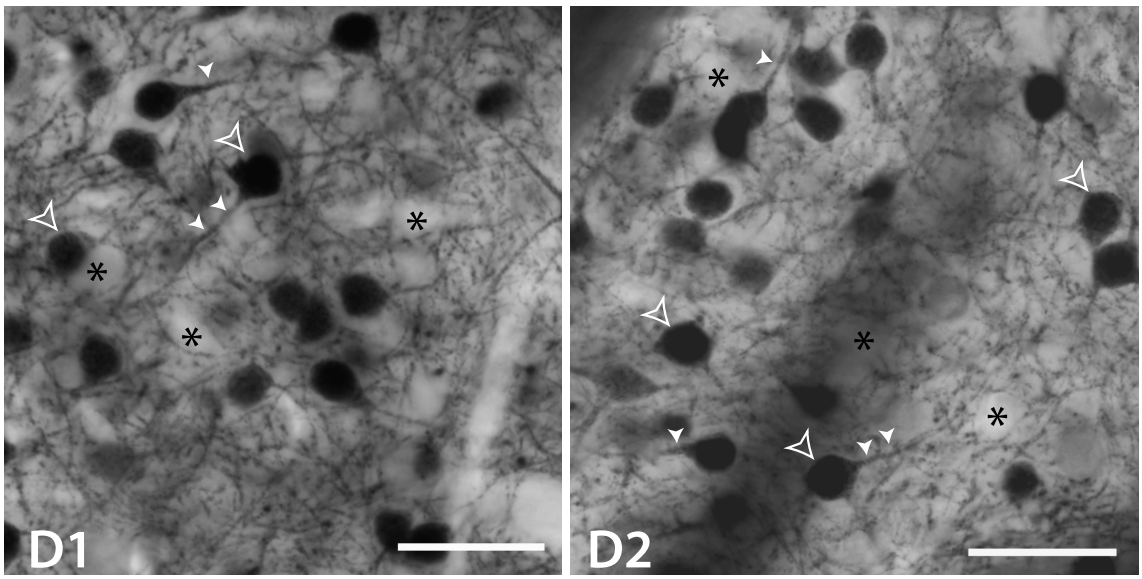


Figure 2.1. D1- and D2- expressing MSNs in the striatum, as revealed by immunoperoxidase labelling for EGFP.

Light microscopic images showing neuronal cell-bodies (some indicated by open arrowheads) and dendrites (some indicated by filled arrowheads) of MSNs labelled for EGFP (immunoperoxidase reaction product; TMB-DAB) in tissue from D_1 (left) and D_2 (right) BAC-EGFP mice. Note that the outlines of negative MSN cell bodies can be seen (some indicated by asterisks). Note also the dense meshwork of dendritic labelling in the neuropil. Scale bars, 50 μm.

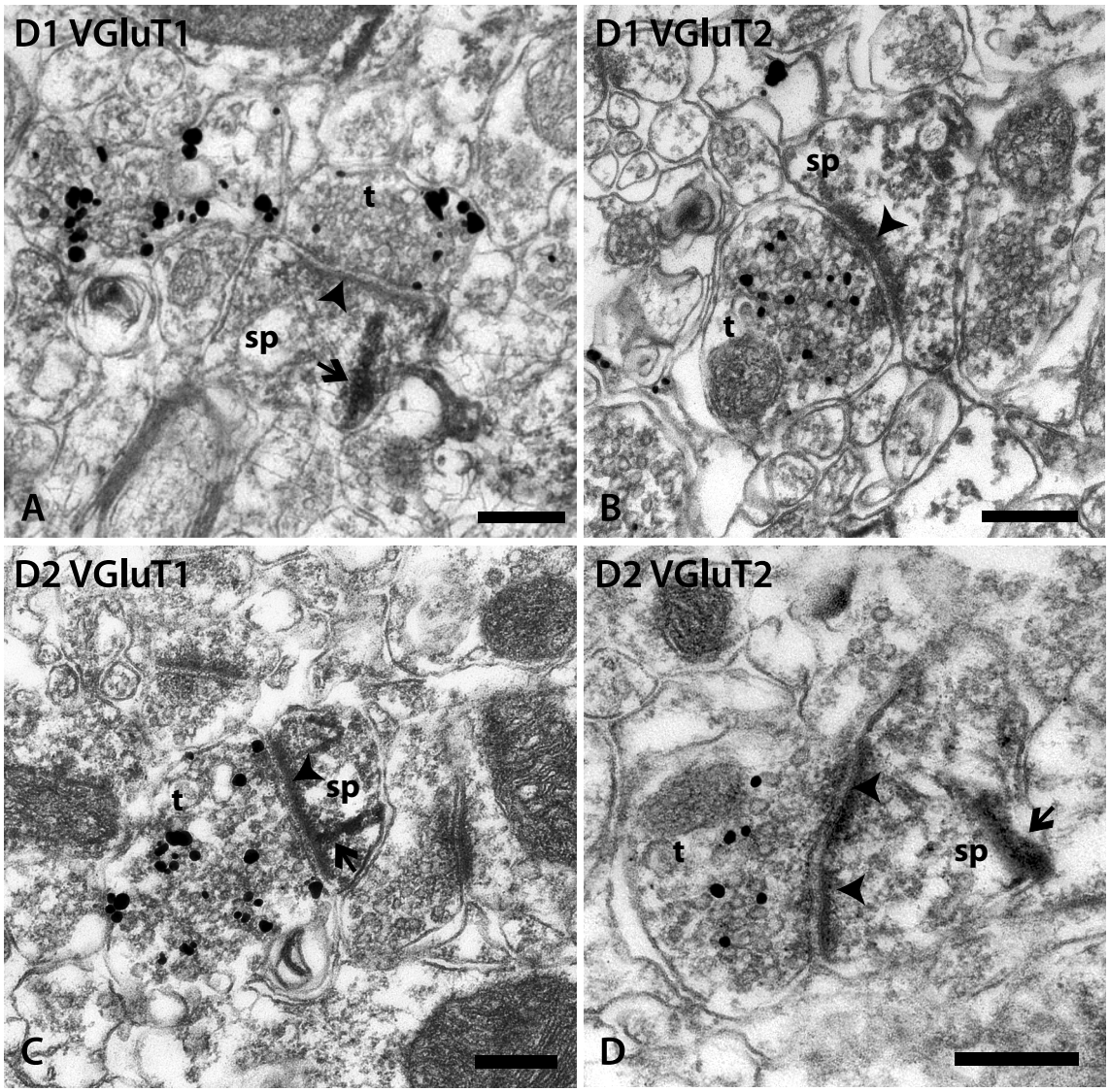


Figure 2.2. D_1 and D_2 MSNs receive synaptic input from VGluT1-postive terminals and with VGluT2-positive terminals.

A, A spine (sp) of a D_1 MSN, identified by peroxidase immunolabeling for EGFP, receiving asymmetric synaptic input (arrowhead) from a VGluT1-positive terminal (t), identified by immunogold labelling. Note the large crystal-like reaction product formed by TMB (small arrows). ***B,*** A spine (sp) of a D_1 MSN, identified by immunoperoxidase labelling for EGFP, receiving asymmetric synaptic input (arrowhead) from a VGluT2-positive terminal (t), identified by immunogold labelling. Note the floccular electron dense peroxidase reaction product. ***C,*** A spine (sp) of a D_2 MSN identified by peroxidase labelling for EGFP receiving asymmetric synaptic input (arrowhead) from a VGluT1-positive terminal (t) identified by immunogold labelling. Note the large crystal-like reaction product formed by TMB (small arrow). ***D,*** A spine (sp) of D_2 MSN, identified by peroxidase labelling for EGFP, receiving asymmetric synaptic input (arrowheads) from a VGluT2-positive terminal (t) identified by immunogold labelling. Note the large crystal-like reaction product formed by TMB (small arrows). Scale bars, 250 nm.

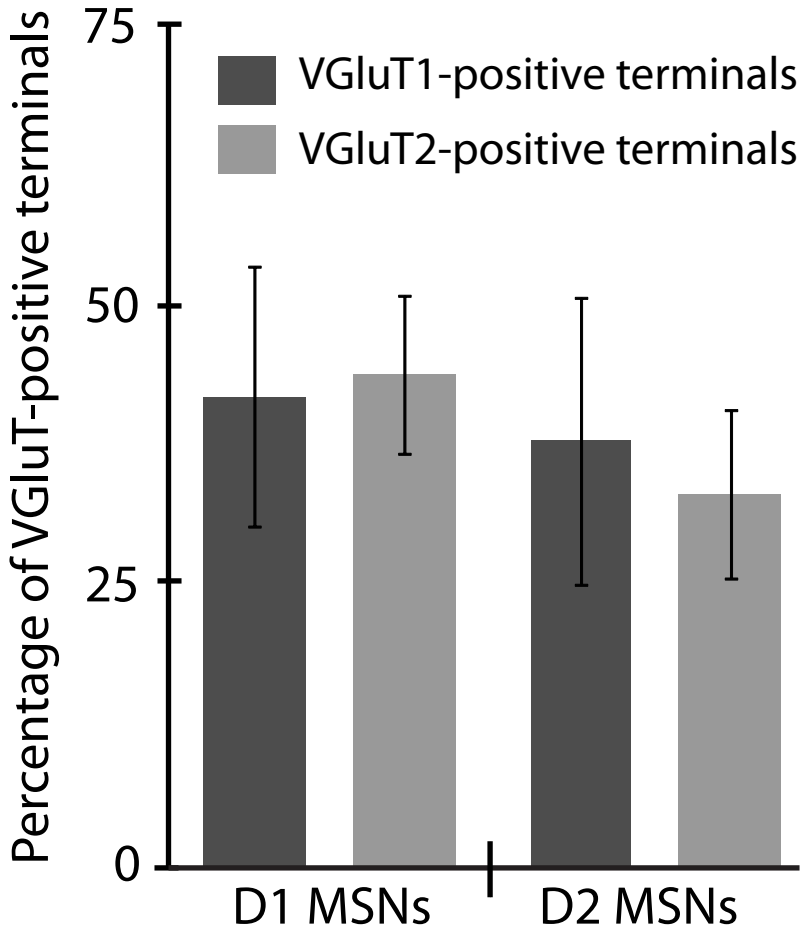


Figure 2.3. Quantitative analysis of the cortical and thalamic innervation of direct and indirect pathway MSNs in the striatum.

A histogram showing the average percentage of VGluT-positive terminals forming asymmetric synapses with EGFP-positive (D_1 or D_2) structures out of a total of 150 synapses per set of tissue (D_1 VGluT1, D_1 VGluT2, D_2 VGluT1 or D_2 VGluT2; n = 3 animals per group). Of the 300 D_1-positive structures, 63 had presynaptic structures that were VGluT1-positve, and 66 that were VGluT2-positive, in their respectively labelled tissue. Similarly, for D_2-positive structures, 57 had presynaptic structures that were VGluT1-positve, and 50 that were VGluT2-positive. D_1-positive or D_2-positive structures did not form significantly different numbers of synapses with VGluT1 or VGluT2 terminals ($p > 0.05$, Fisher's exact test). Additionally, neither VGluT1- nor VGluT2-positive afferents formed significantly different numbers of synapses with D_1 or D_2-positive structures ($p > 0.05$, Fisher's exact test).

2.3.4. Divergence and convergence of afferents derived from the cortex and thalamus in the striatum

The fact that single VGluT-positive terminals occasionally formed more than one synapse enabled examination, at a qualitative level, of the issue of divergence of cortical and thalamic afferents with direct or indirect pathway neurons. Similarly, as EGFP-positive dendrites and spines may receive more than one synapse, and we followed them in seven serial sections, we were able to examine convergence of cortical and thalamic afferent synapses formed with an individual direct or indirect pathway neuron. Of course, these data can only be considered as qualitative principally because of the possibility of false-negatives.

It was observed that individual VGluT-positive terminals formed asymmetric synapses with both an EGFP-positive spine (D_1 or D_2) as well as an EGFP-negative spine (Fig. 2.4). Out of the 63 VGluT1-positive terminals observed to form asymmetric synapses with D_1-positive spines, 9 also formed asymmetric synapses with D_1-negative spines (Fig 2.4a). Similarly, 8 out of the 66 VGluT2-positive terminals that formed asymmetric synapses with D_1-positive spines also formed a synapse with a D_1-negative spine (Fig. 2.4b). A similar situation was observed for VGluT-positive terminals forming synapses in D_2 tissue; out of the 57 VGluT1-positive terminals observed to form synapses with D_2-positive spines, 9 also formed a synapse with a D_2-negative spine (Fig. 2.4c), and 8 out the 50 VGluT2-positive terminals forming synapses with a D_2-positive spine also contacted a D_2-negative spine (Fig. 2.4d). These observations demonstrate that individual cortical and thalamic axons form divergent synaptic contact with both direct and indirect pathway MSNs.

In addition to the divergence of cortical and thalamic afferents, it was observed that an individual D_1-positive neuron received asymmetric synaptic input from both a VGluT2-positive and a VGluT2-negative terminal (Fig. 2.5). Similarly, this was observed for a D_2-positive neuron. On these occasions, VGluT2-negative synapses were formed with the heads of dendritic spines, whereas VGluT2-positive synapses were formed with

the dendritic shafts from which these spines emerged. Although it cannot be concluded with certainty that the VGluT2-negative terminal is of cortical origin, this indicates a convergence of excitatory inputs, from different origins, onto both direct and indirect pathway neurons. The patterns of innervation from the cortex and thalamus to neurons of the direct and indirect pathways are summarised in Figure 2.6.

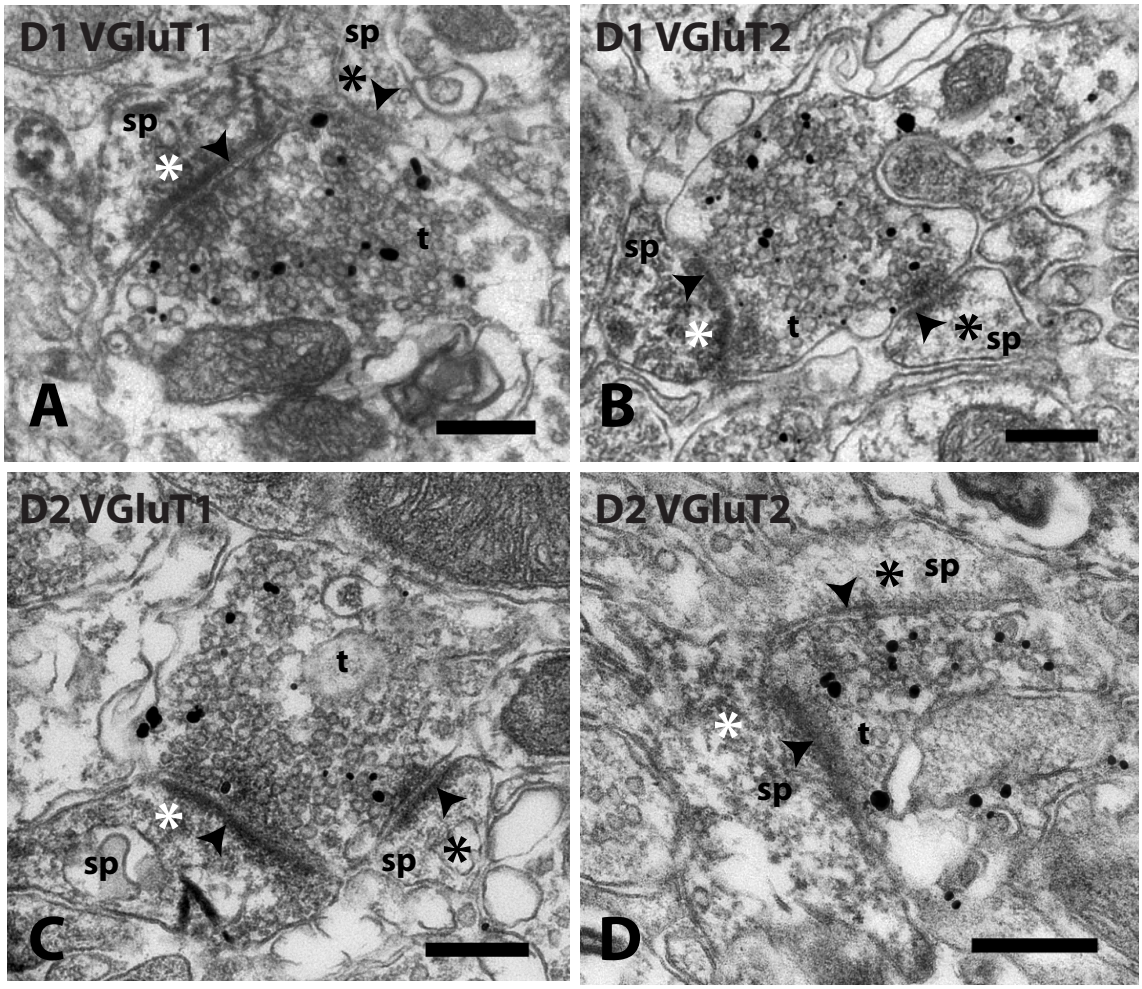


Figure 2.4. Divergent cortical and thalamic input to direct and indirect pathway MSN spines.

A, A VGluT1-positive terminal (t) makes asymmetric synaptic contact (arrowheads) with a D_1-positive spine (sp; white asterisk) and a D_1-negative spine (sp; black asterisk). ***B,*** A VGluT2-positive terminal (t) makes asymmetric synaptic contact (arrowheads) with a D_1-positive spine (sp; white asterisk) and a D_1-negative spine (sp; black asterisk). ***C,*** A VGluT1-positive terminal (t) makes asymmetric synaptic contact (arrowheads) with a D_2-positive spine (sp; white asterisk) and a D_2-negative spine (sp; black asterisk). ***D,*** A VGluT2-positive terminal (t) makes asymmetric synaptic contact (arrowheads) with a D_2-positive spine (sp; white asterisk) and a D_2-negative spine (sp; black asterisk). D_1- and D_2-positive spines are identified by the presence of peroxidase reaction product; clear synaptic specializations were seen over the seven serial sections. Scale bars, 250 nm.

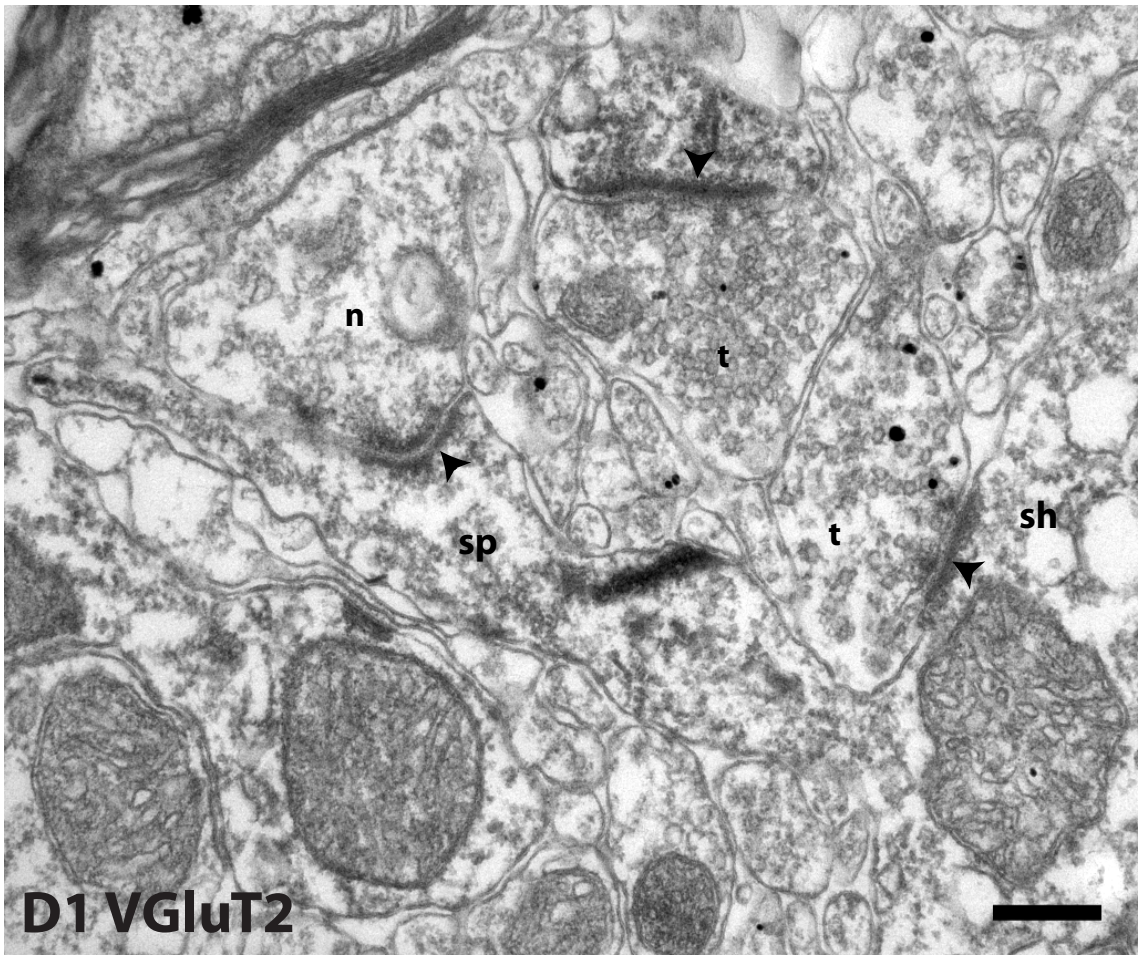


Figure 2.5. An individual direct pathway MSN may receive synaptic input from both thalamic (VGluT2-positive) and putative cortical (VGluT2-negative) terminals.

A D1-positive dendritic shaft (sh) receives asymmetric synaptic input (arrowhead) from a VGluT2-positive terminal (t). A spine (sp) emerging from this shaft receives asymmetrical synaptic input (arrowhead) from a VGluT2-negative terminal (n). Scale bar, 250 nm.

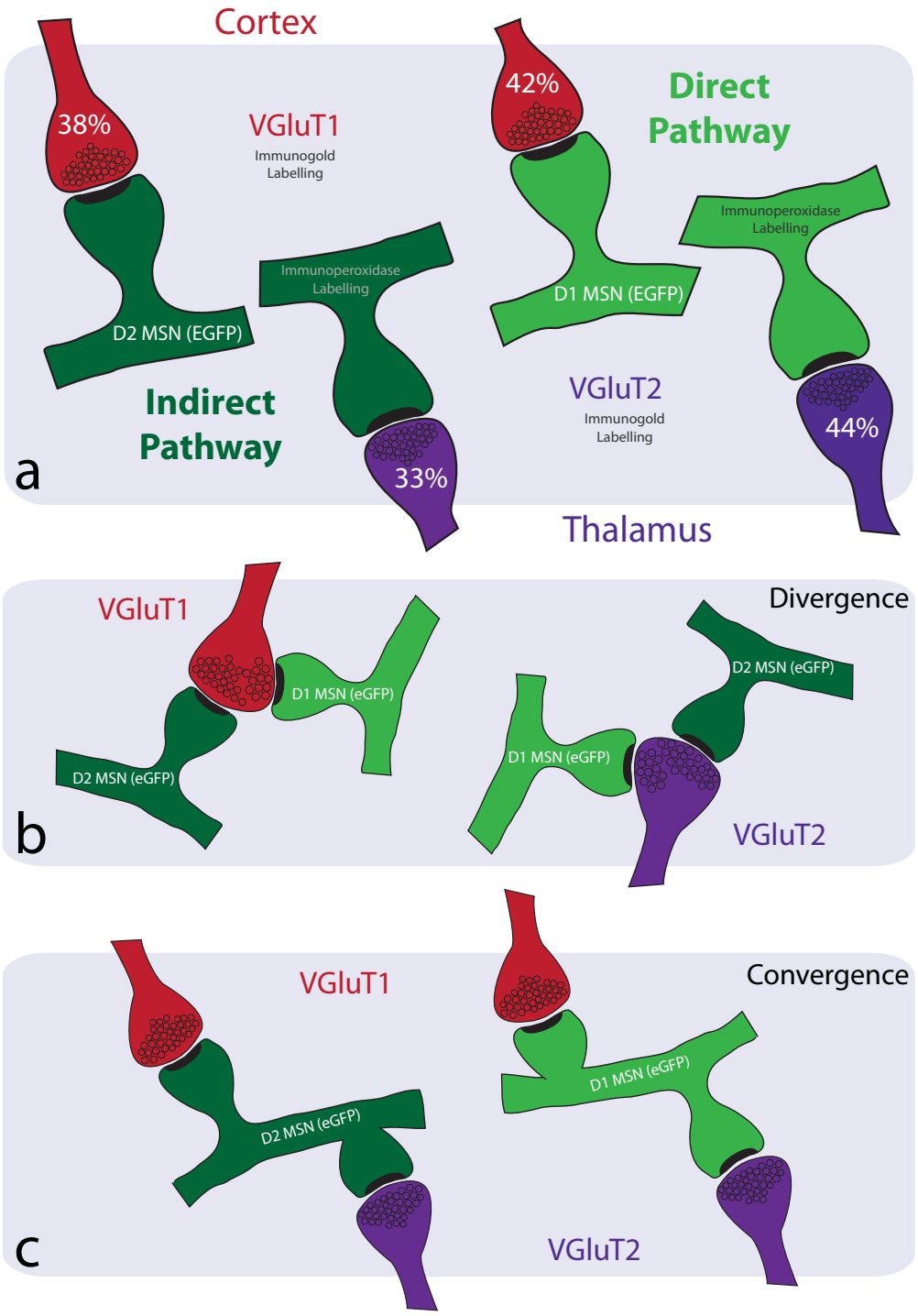


Figure 2.6. Summary of the patterns of innervation from cortex and thalamus to direct and indirect pathway neurons.

a) Direct pathway neurons receive input from both the cortex (42%) and the thalamus (44%); indirect pathway neurons receive input from the cortex (38%) and the thalamus (33%). ***b)*** Divergence of information: cortical terminals form synapses with neurons of the direct and indirect pathway; thalamic terminals form synapses with neurons of the direct and indirect pathway. ***c)*** Convergence of information: neurons of the direct pathway receive input from the cortex and thalamus; neurons of the indirect pathway receive input from the cortex and thalamus.

2.4. Discussion

The corticostriatal and thalamostriatal pathways, which mainly target the spines of MSNs, are critical in the expression of basal ganglia function. Furthermore, the transmission of information through the two separate, but intermingled populations of MSNs (i.e. those that give rise to the direct and indirect pathways), is one of the fundamental rules in the organization of the neuronal networks of the basal ganglia. In this study, both corticostriatal and thalamostriatal afferents were seen to innervate MSNs that give rise to the direct pathway *and* MSNs that give rise to the indirect pathway. Indeed, the quantitative analyses reveal that, when considering the proportions of excitatory afferents of MSNs, the corticostriatal and thalamostriatal afferents innervate the two populations of MSNs to a similar degree. The analyses also revealed that *individual* cortical and thalamic axons can innervate *both* direct and indirect pathway MSNs. Furthermore, the data suggest that individual direct or indirect pathway MSNs receive input from both the cortex and thalamus. Thus, a principle of basal ganglia circuitry is that the two major excitatory inputs to the basal ganglia innervate, to equal degrees, *both* MSNs that give rise to the direct pathways and those that give rise to the indirect pathway. Our findings are in agreement with previous electrophysiological data (Kocsis *et al.*, 1977; Vandermaelen & Kitai, 1980; Ding *et al.*, 2008) and reinforce the concept that subcortical inputs to the basal ganglia are as important as cortical afferents in the expression of basal ganglia function (Redgrave *et al.*, 1999; Smith *et al.*, 2004; McHaffie *et al.*, 2005).

2.4.1. Cortical and thalamic input to direct and indirect pathway MSNs

The development of BAC transgenic mice in which EGFP reports the expression of dopamine D_1 or D_2 receptors and hence direct or indirect pathway MSNs has been critical in the elucidation of the properties of these subpopulations of MSNs (Gong et al., 2003; Lobo et al., 2006; Kreitzer & Malenka, 2007; Surmeier et al., 2007; Ade et al., 2008; Cepeda et al., 2008; Day et al., 2008; Gertler et al., 2008; Shen et al., 2008; Shuen et al., 2008; Janssen et al., 2009). This development, together with the discovery

that VGluT1 and VGluT2 selectively label corticostriatal and thalamostriatal afferents (Fremeau et al., 2004), enabled direct assessment and quantification of the relationship between excitatory afferents and the principal neurons of the striatum. Both corticostriatal and thalamostriatal projections make synaptic contact with both direct and indirect pathway neurons to similar degrees. Our findings thus suggest that despite heterogeneities in neurochemistry, morphology and connections of the two populations of MSNs, when using molecular markers to study the projections, the corticostriatal and thalamostriatal afferents are relatively uniform in their innervation of MSNs. It is possible, however, that there is heterogeneity when considering sub-divisions of the corticostriatal or thalamostriatal pathways. Indeed, previous anterograde labelling studies have indicated that subpopulations of cortical afferents show selectivity for direct or indirect pathway MSNs (Hersch et al., 1995; Lei et al., 2004) and afferents from the CM nucleus of the squirrel monkey selectively innervate neurons of the direct pathway (Sidibé & Smith, 1996). Furthermore, microstimulation of sensorimotor cortex and local disinhibition of primary motor cortex both result in up-regulation of early-gene expression primarily within indirect pathway neurons (Berretta et al., 1997; Parthasarathy & Graybiel, 1997). Moreover, lesioning of the intralaminar thalamic nuclei has been shown to preferentially down-regulate enkephalin mRNA, thus indicating an increased influence over the indirect pathway (Salin & Kachidian, 1998). Our study does not obviate these findings but demonstrates that, when the projections are considered as a whole, there is uniformity in the innervation of the two populations of MSNs by excitatory afferents and hence both direct and indirect pathways neurons are likely to be similarly influenced by cortical and thalamic afferents.

It is critical to determine whether the homogeneity of the excitatory innervation of MSN subpopulations is reflected in the innervation of single cells, i.e. do individual direct or indirect pathway MSNs receive convergent input from both the cortex and the thalamus and, if so, what are the relative proportions of these afferents? The electron microscopic analyses provided qualitative data on this issue. On the basis that a terminal that is negative for, say VGluT2, is likely to be a cortical terminal (i.e. presumably expressing

VGluT1) and vice versa, it was identified that individual direct pathway MSNs or indirect pathway MSNs received input from both the cortex and thalamus. However, the caveat to this is that a terminal negative one of the VGluTs may of course, not necessarily express the other VGluT. The fact that it was observed that about 56-67% of terminals forming asymmetric synapses with D_1 or D_2 MSNs are negative for the VGluT under study implies convergence of cortical and thalamic terminals on individual neurons, because together VGluT1- or VGluT2-positive terminals account for 70-85% of asymmetric synapses in the striatum. Thus at least some of the negative boutons will express the other VGluT. Direct analysis of this issue requires the combination of VGluT immunolabelling together with the labelling of single, identified, direct or indirect pathway MSNs. Our findings thus confirm and extend in vivo electrophysiological analyses that have revealed that individual MSNs frequently respond to both cortical and thalamic stimulation and in vitro analyses demonstrating both cortical and thalamic input to direct and indirect pathway neurons (Kocsis et al., 1977; Vandermaelen & Kitai, 1980; Ding et al., 2008; Smeal et al., 2008).

A second critical issue in the organization of the corticostriatal and thalamostriatal pathways is the divergence of cortical and thalamic afferents to the striatum. Do individual cortical or thalamic axons innervate both direct and indirect pathway MSNs? Again, the observations reported here threw light upon this issue. Individual cortical terminals were identified forming synapses with both direct pathway MSNs in the D_1 mice and presumed indirect pathway MSNs that were immunonegative for EGFP. This suggests that an individual cortical axon provides divergent input to the striatum with respect to subpopulations of MSNs, a conclusion that was also made from the analysis of the D_2 mice. On the basis of similar analyses, it can also be concluded that individual thalamic axons provide divergent input to subpopulations of MSNs. The precise quantitative aspects of convergence and divergence remain to be established.

The classical view of the functional organization of the basal ganglia is that corticostriatal projections provide the major inputs to the basal ganglia and the role of

thalamus is transmission of information back to the cortex. Recently, the sub-cortical inputs to the basal ganglia have received more attention within the field, and are now more widely recognised as being important in action selection and the reticular activating system (McHaffie *et al.,* 2005; Smith *et al.,* 2011). Prominent, and probably most important of the sub-cortical inputs, is that from the thalamus (Groenewegen & Berendse, 1994; Smith *et al.*, 2004), principally, but not exclusively, from the intralaminar thalamic nuclei. Indeed, there are many similarities between the thalamostriatal and the corticostriatal pathways in addition to their glutamatergic phenotype. Quantitative analysis has demonstrated that the number of synapses in the striatum derived from the thalamus is of the same order of magnitude as derived from the cortex (Lacey *et al.*, 2005; Raju *et al.*, 2008). Furthermore, their synaptic targets are largely similar, in that most cortical and thalamic terminals innervate dendritic spines with a smaller proportion innervating the dendritic shafts of interneurons (Kemp & Powell, 1971b; Somogyi *et al.*, 1981; Dubé *et al.*, 1988; Xu *et al.*, 1989; Smith & Bolam, 1990a; Xu *et al.*, 1991; Sadikot *et al.*, 1992b; Bennett & Bolam, 1994; Smith *et al.*, 2004). Of course, a notable exception is the thalamostriatal pathway originating in the parafascicular nucleus which principally innervates dendritic shafts of both MSNs and interneurons (Lapper & Bolam, 1992; Raju *et al.*, 2006; Lacey *et al.*, 2007). The spatial relationship between thalamostriatal synapses and dopaminergic synapses is similar to the relationship between corticostriatal and dopaminergic synapses, thus both are in a position to be modulated by released dopamine to a similar degree (Moss & Bolam, 2008). Despite differences in the response to stimulation of corticostriatal and thalamostriatal afferents (Smeal *et al.*, 2007; Smeal *et al.*, 2008), which do not vary between direct and indirect pathway neurons (Ding *et al.*, 2008), they are both excitatory and give rise to EPSPs. Any specific differences between corticostriatal and thalamostriatal projections are likely to be underscored by the particular neurons within different functional regions of the cortex or sub-nuclei thalamus that give rise to the projections. The thalamostriatal projection, in particular, is highly heterogeneous with respect to the somatodendritic morphology of the projecting neurons, their electrophysiological activity, synaptic targets, and patterns of innervation of the

matrix and patch/striosomes (Herkenham & Pert, 1981; Deschênes *et al.*, 1996a; Smith *et al.*, 2004; Raju *et al.*, 2006; Lacey *et al.*, 2007).

The neuronal networks that constitute the basal ganglia and the regions that are connected to the basal ganglia, are organized in such a way that excitatory inputs to the striatum 'select' which individual MSNs, or groups of MSNs, are depolarised from the relatively hyperpolarized resting state. With sufficient convergent excitatory input, and appropriate modulatory influence of released dopamine, the 'selected' population of MSNs, which likely constitute both direct and indirect pathway neurons, will fire action potentials, and it is this that underlies basal ganglia-associated behaviour. Our findings, together with those of others, suggest that, although the thalamostriatal pathway carries different functional information from that of the corticostriatal pathway and encodes it in an heterogeneous manner (Lacey *et al.*, 2007) that is distinct from the cortex in terms of receptor profiles, release probability, and short-term plasticity (Ding *et al.*, 2008; Smeal *et al.*, 2008), it is likely to be equally involved in the selection of individual or populations of MSNs of both the direct and indirect pathways.

2.4.2. Technical considerations

A major consideration is the possibility that transgenic mice examined in this study have been altered as a consequence of genetic manipulation. Two recent studies found that the introduction of the BAC-EGFP under the control of either the D_1 or D_2 receptor promoters can cause physiological and behavioural changes that are not seen in the wild-type mice (Bagetta *et al.*, 2011; Kramer *et al.*, 2011). In D_1-EGFP mice, there are changes in plasticity and an increase in anxiety in animals which are positive for expression of EGFP (Bagetta *et al.,* 2011). In D_2-EGFP, the D_2 receptor is over-expressed and as a result of this increase the mice showed fundamental changes in their dopaminergic systems and this was accompanied by behavioural changes (Kramer *et al.*, 2011). These results promote caution when using animals which have undergone genetic manipulation, as both D_1 and D_2 BAC-EGFP mice appear to have significant changes in their dopaminergic systems. However, in terms of gross anatomical changes, no significant alterations have

been described due to introduction of EGFP under the promoter of the D_1 or D_2 receptors. Although, this is an issue which needs be considered further. In terms of the present study the increase in D_2 receptor should not alter the results as long as the D_2 receptor remains solely expressed by the indirect pathway neurons.

Chapter Three: Cortical and thalamic inputs to cholinergic interneurons

Responses to cortical and thalamic stimulation in vivo

3.1. Introduction

Cholinergic interneurons release acetylcholine in the striatum, an important neuromodulator, and play a principal role in reinforcement learning. Cholinergic interneurons, or TANs in behaving primates, exhibit a 'conditioned pause response' which is a suppression of normal firing activity in relation to the presentation of particular cues or outcomes during reward-related learning tasks (Goldberg & Reynolds, 2011). The conditioned pause response has been shown to be linked to dopamine release; neurons in the SNpc show a coincident increase in discharge rate during reward-related behaviour tasks (Morris *et al.*, 2004). There are, however, differences between the firing properties of dopaminergic neurons in the SNpc and the cholinergic interneurons in the striatum, in relation to reward trials in behaving primates. Dopaminergic neurons increase their activity in response to the presentation of cues that are linked to rewards; and their activity is related to the probability of presentation of a reward, with a greater increase in firing rate when there is a greater probability of reward (Joshua *et al.,* 2008). In the same task, TANs showed a coincident decrease in firing rate which did not code the probability of reward (Joshua *et al.,* 2008). Furthermore whereas dopaminergic neurons encoded the difference between aversive and rewarding events; TANs could encode the difference between rewarding events and the omission of an expected reward (Joshua *et al.,* 2008). This indicates that although there is a clear link between the activity of dopaminergic and TANs, they are able to differentially encode rewarding and aversive events in behavioural trials.

Although dopamine is important for the acquisition of the pause response, MPTP lesions in the monkey do not completely eliminate all TAN pauses, indicating that dopamine, whilst necessary, is not the only contributor (Aosaki *et al.*, 1994a). The conditioned pause response has behavioural relevance and highlights the importance of the cholinergic interneurons in reward-related learning, but the origin, or the underlying mechanisms, of the pause are not entirely understood (Goldberg & Reynolds, 2011). The way(s) in which the cholinergic interneurons are able to contribute to striatal processing

needs further examination, and to this end the afferent inputs to the cholinergic neurons need to be assessed.

Besides dopamine, thalamic innervation of cholinergic interneurons is also important for the conditioned pause response. The infusion of muscimol[24] into the CM/Pf of monkeys greatly reduces the pause response and rebound facilitation of TANs during a behavioural task (Matsumoto *et al.*, 2001). This indicates that the thalamic innervation to the TANs is important for providing sensory information relevant to reward-related behaviour. Further evidence for the importance of sensory input is demonstrated by the fact that visual stimuli can induce a pause-like response in putative cholinergic interneurons recorded *in vivo* in the rat, and this is reliant on the disinhibition of the superior colliculus, which implicates the tecto-thalamostriatal pathway (Schulz *et al.*, 2011). Besides the thalamostriatal input, TANs recorded *in vivo* in the rat also receive cortical innervation that has different response characteristics to those exhibited by neighbouring putative MSNs (Wilson *et al.*, 1990; Reynolds & Wickens, 2004). The role of the corticostriatal input to the cholinergic interneurons is less clear, but is a possible mechanism for plasticity of the pause response, such altering the sensitivity of the response (Goldberg & Reynolds, 2011).

Responses of cholinergic interneurons to cortical and thalamic stimulation have been examined *in vivo* and *in vitro*. Wilson and colleagues (1990), found that stimulation in the ipsi- or contra-lateral frontal cerebral cortex, or the intralaminar thalamic nuclei resulted in short latency EPSPs in TANs recorded *in vivo*, indicative of monosynaptic inputs. Reynolds and Wickens (2004) further examined the cortical input to the cholinergic interneurons *in vivo*. The latencies of the EPSPs in the giant aspiny neurons (putative cholinergic interneurons) to contralateral cortical simulation were significantly shorter than those measured in the MSNs in the same preparation, 5.1 ms and 9.3 ms, respectively (Reynolds & Wickens, 2004). In a slice preparation where the cortical and thalamic innervation of striatum is preserved, Ding and colleagues (2010) examined the

24 $GABA_A$ agonist

integration of these inputs by putative cholinergic interneurons. They found that a high frequency stimulus train delivered to the thalamus could evoke a burst - pause pattern of activity in the recorded interneurons (Ding *et al.*, 2010). Conversely, the same stimulation train delivered to the cortex resulted in a lesser increase in firing, and no pause (Ding *et al.*, 2010). Furthermore the pause, but not the burst, was dependent on dopaminergic activation of the D_2 receptor (Ding *et al.*, 2010), which is consistent with evidence that suggests that both thalamic stimulation and dopamine are necessary for TANs to pause in behaving primates. This study also examined the differences between cortical and thalamic stimulation of putative cholinergic interneurons; whilst the thalamic train of stimulation was facilitating, the cortical train was not, which indicates that these synapses have distinct properties (Ding *et al.*, 2010). However, in the studies described here, the neurons were not identified as being positive for ChAT although the physiological and morphological characteristics suggests that, in all likeliness, they are cholinergic interneurons (Wilson *et al.*, 1990; Reynolds & Wickens, 2004; Ding *et al.*, 2010). An understanding of how individual cholinergic interneurons integrate input from both the thalamus and cortex is essential for elucidating the role of these neurons in striatal function.

3.1.1. Aims

The way in which cholinergic interneurons integrate their afferent inputs is central to their role in the striatum. Examination of the responses of cholinergic interneurons to cortical and thalamic stimulation *in vivo* can provide insight into how these neurons assimilate information from different sources. The responses of cholinergic interneurons to cortical (Reynolds & Wickens, 2004), and to cortical and thalamic stimulation (Wilson *et al.,* 1990) has been examined previously, although the neurons that were recorded from were not identified as being positive for ChAT. Wilson and colleagues (1990) found that cholinergic interneurons could respond to stimulation of ipsi- and contra- lateral cortical stimulation, and to stimulation of the ITN with response latencies indicative of monosynaptic connections, however the paper does not state whether the responses to cortical and thalamic stimulation were recorded from the *same* neurons. Therefore a particular aim of this study was to examined the way in which *individual,*

electrophysiologically characterised, and neurochemically identified cholinergic interneurons respond to stimulation of both cortex and thalamus. Reynolds and Wickens (2004) also examined the responses of putative cholinergic interneurons *in vivo* to cortical stimulation. It was found that cholinergic interneurons could respond to cortical stimulation with a shorter latency response compared to MSNs recorded in the same preparation (Reynolds and Wickens, 2004).

A recent study *in vitro* has shown that cholinergic interneurons exhibit distinctive responses to cortical and thalamic stimulation, that is relevant to their role in reward-related behaviour. Ding and colleagues (2010), have shown that whilst high frequency thalamic stimulation results in an increase in spiking followed by a decrease in activity (lasting from 360 to 1300 ms), cortical stimulation could cause the initial increase in firing but that this increase was not followed by a decrease in activity. This indicates that there are important differences in the responses of cholinergic interneurons to cortical and thalamic stimulation (Ding *et al.,* 2010). However, this study was conducted *in vitro* and therefore the network is not intact and GABAergic synaptic connectivity was blocked, and cholinergic interneurons were identified by their physiology and size but were not confirmed as being positive for ChAT.

In this study cholinergic interneurons were identified *in vivo* by their unique physiological characteristics and stimulation to the motor cortex and/or the Pf nucleus was then applied and the responses of the cholinergic interneurons were examined. A particular aim was to examine the responses of individual neurons to stimulation of both cortex and thalamus. A variety of stimulation protocols were used to examine the responses of these neurons further. The neurons could then be filled using the juxtacellular method and subsequently identified with an antibody against choline acetyltransferase (ChAT).

3.2. Methods and Materials

3.2.1. Electrophysiological recordings

Experimental procedures were performed on adult male Sprague Dawley rats (Charles River) and were conducted in accordance with the Animals (Scientific Procedures) Act, 1986 (United Kingdom), and the European Communities Council Directive (86/609/EEC).

Electrophysiological recordings were made in 36 rats (250 g - 340 g). Anaesthesia was induced with isoflurane (Isoflo, Schering-Plough) and maintained with urethane (1.3 g/kg, i.p.; ethyl carbamate, Sigma), and supplemental doses of ketamine (30 mg/kg, i.p.; Ketaset, Willows Francis) and xylazine (3 mg/kg, i.p.; Rompun, Bayer), as described previously (Brown *et al.*, 2009). All wound margins were infiltrated with the local anaesthetic bupivacaine (0.75% w/v; Astra) and corneal dehydration was prevented by the application of Hypromellose eye drops (Norton Pharmaceuticals). Animals were then placed in a stereotaxic frame. Body temperature was maintained at 37 ± 0.5°C using a homoeothermic heating device (Harvard Apparatus). Anaesthesia levels were assessed by examination of the electrocorticogram (ECoG, see below), and by testing reflexes to a cutaneous pinch. Saline solution (0.9% w/v NaCl) was applied to all areas of exposed cortex to prevent dehydration.

Parallel bipolar stimulating electrodes (constructed from nylon coated stainless steel wires; California Fine Wire, Grover City, CA), with tip diameters of ~100 μm, a tip separation of ~150 μm, and an impedance of ~10 kΩ, were implanted into the ipsilateral (right) motor cortex and intralaminar thalamus and then fixed to the skull with dental acrylic cement (Associated Dental Products, Swindon, UK). The coordinates of the cortical stimulation site (AP: 2.5 mm, ML: 3.0 mm, bregma reference, and a depth of 2.2 mm below the dura) correspond to primary motor cortex (Paxinos & Watson, 1986). The coordinates of the thalamic stimulation site (AP: -3.7 mm, ML: 1.3 mm, and a depth of ~5.5 mm below the dura) correspond to the parafascicular nucleus of the intralaminar

thalamus (Paxinos & Watson, 1986; see Fig 3.1 for experimental setup).

The ECoG was recorded via a 1 mm diameter steel screw juxtaposed to the dura mater above the right frontal cortex (AP: +4.2 mm, ML: 2.0 mm in relation to bregma) (Paxinos & Watson, 1986) and was referenced against another screw implanted in the skull above the cerebellum. Raw ECoG was band pass filtered (0.3–1500 Hz, -3 dB limits) and amplified (2000X, DPA-2FS filter/amplifier; Scientifica) before acquisition. A discrete craniotomy was performed above the right striatum (AP: +0.5 mm, ML: 3.0 mm in relation to bregma) (Paxinos & Watson, 1986), and the dura mater removed for insertion of recording electrodes. Extracellular recordings of action potentials of striatal neurons were made using 12–30 MΩ glass electrodes (tip diameter 1.5-2.0 μm), which contained saline solution (0.5 M NaCl) and Neurobiotin (1.5% w/v, Vector Laboratories). Electrode signals were amplified (10X) through the active bridge circuitry of an Axoprobe-1A amplifier (Molecular Devices Corp.), bifurcated, then differentially filtered to extract local field potentials (LFPs) and unit activity. Spikes were often several millivolts in amplitude and always exhibited a biphasic waveform with an initial positive deflection. The LFPs were recorded after further amplification (100X; DPA-2FS; Scientifica) and "wideband" filtering (between 0.3 and 5000 Hz; DPA-2FS; Scientifica). Single units were recorded after alternating current coupling, further amplification (100X; DPA-2FS; Scientifica), and standard band pass filtering (between 300 and 5000 Hz; DPA-2FS; Scientifica). A Humbug (Quest Scientific) was used to eliminate mains noise at 50 Hz. Neuronal firing was recorded during slow-wave activity (SWA), which accompanies deep anaesthesia and is similar to activity observed during natural sleep, and during episodes of cortical activation, which contain patterns of activity that are more analogous to those observed during the awake, behaving state (Steriade, 2000). Transition from SWA to the activated brain state is exemplified by obliteration of the cortical slow oscillation (~1 Hz), as well as δ (1–4 Hz) and spindle (7–14 Hz) oscillations (Steriade, 2000).

3.2.2. Stimulation of cortex and thalamus

Electrical stimuli, which consisted of single square-wave current pulses of 0.3 ms

duration and variable amplitude (100 – 900 μA), were delivered to either the motor cortex or to the intralaminar thalamic nucleus (Pf) at a frequency of 0.5 Hz using a constant current isolator (A360D; World Precision Instruments, Stevenage, UK) that was gated by a programmable pulse generator controlled using Spike 2 (v 7.0, Cambridge Electronic Design). Three different stimulation protocols were applied to cortex and then thalamus or vice versa depending on the individual response of the neuron: i) a single stimulation to cortex/thalamus, ii) a paired stimulus given with a 100 ms interval, and iii) a 40 Hz train of 5 stimuli given with a 25 ms interval.

3.2.3. Juxtacellular labelling of single neurons

To locate the recorded neurons and enable an analysis of their morphological and neurochemical properties, they were then labelled with Neurobiotin (Vector Laboratories) by the juxtacellular method (Pinault, 1996; Brown *et al.*, 2009). Briefly, the electrode was advanced towards the neuron slowly while a microiontophoretic current was applied (1–10 nA positive current, 200 ms duration, 50% duty cycle). The optimal position of the electrode was identified when the firing of the neuron was robustly modulated by the current injection. It was necessary to modulate the neuronal firing by the microiontophoretic current for ~1 - 5 min, to obtain reliable labelling. The Neurobiotin (NB) was then left to transport along neuronal processes for up to 5 h. After the recording and labelling sessions, the animals were given a lethal dose of ketamine (150 mg/kg) and perfused via the ascending aorta with ~100 ml of 0.01 M PBS at pH 7.4, followed by 300 ml of 0.1% w/v glutaraldehyde and 4% w/v paraformaldehyde in 0.1 M phosphate buffer, pH 7.4, and then by 200 ml 4% w/v paraformaldehyde in 0.1 M phosphate buffer. Brains were then left in fixative solution at 4°C for <12 h and then in PBS until they were sectioned 24–72 h later.

3.2.4. Histochemistry and immunohistochemistry

The fixed brains were sectioned at 50 μm in the parasagittal plane on a vibrating blade microtome (VT1000S; Leica Microsystems); sections were collected in a 1 in 6 series. All sections were then washed in PBS (X3) and incubated in a fluorescent

conjugated streptavidin (streptavidin-CY3; 1:1000, 4°C, overnight; Zymed in 0.1M PBS with 0.3% Triton-X100) to bind to the Neurobiotin and hence allow visualisation of the labelled neuron(s). This was carried out in the absence of Triton when neurons were to be examined by electron microscopy. Sections containing the neurons were then examined using an epi-fluorescence microscope, and according to the physiological and morphological characteristics of the neuron(s) an appropriate marker was chosen, such as an antibody against ChAT. The section containing the soma of the neuron was then isolated and incubated in primary antibody overnight at room temperature (See Table 3.1 for details of the antibodies used). The sections were then washed in PBS (X3) and a fluorescent secondary antibody was then applied, either 488 or Cy5, (See Table 3.1). If the neuron was negative for the first primary antibody applied, then another marker was tested using a different antibody against the marker but derived from a different species; followed by application of a fluorescent conjugated secondary antibody, until the molecular identity of the neuron could be established. Only neurons positive for both neurobiotin (NB) and ChAT have been included in this study.

In order to determine the placement of the thalamic stimulating electrode an antibody against cerebellin 1 (CBLN 1) was used on sections where the electrode track was apparent. CBLN1 is a selective marker of the Pf nucleus (Kusnoor *et al.*, 2010); this was combined with Nissl staining (classical method for delineating the thalamic nuclei) (Table 3.1). Using this method it was possible to determine whether the tip of the stimulating electrode is within the Pf nucleus (Fig 3.1).

3.2.5. Data acquisition and analysis

Evoked LFPs and unit activity were sampled at 5 and 10 kHz, respectively. The EEG signal was sampled at 5 kHz. All bio-potentials were digitized on-line with a PC running Spike2 acquisition and analysis software (version 7.0; Cambridge Electronic Design, Cambridge, UK). Data from Spike 2 was analysed using Spike2 or exported and the analysed using Microsoft Excel (2007).

Peri-stimulus time histograms (PSTHs) were constructed from 100-200 consecutive

stimulation trials, with bins of either 2.5 ms (for figures) or 1 ms (for analysis). The "peak response" was defined as the bin with the highest spike count, the time that this peak occurs was taken as the "latency to peak response". Probability of response was the peak response from the PSTH normalised for the number of stimulation trials. The "average latency to first spike" was the latency to the first spike following each stimulus, which was then averaged. All results are mean (± SEM) unless otherwise stated. For statistical analysis non parametric tests were used: Mann-Whitney U test for unpaired data (comparisons of responses from different neurons) and Wilcoxon signed-rank test for paired data (comparisons of responses from an individual neuron).

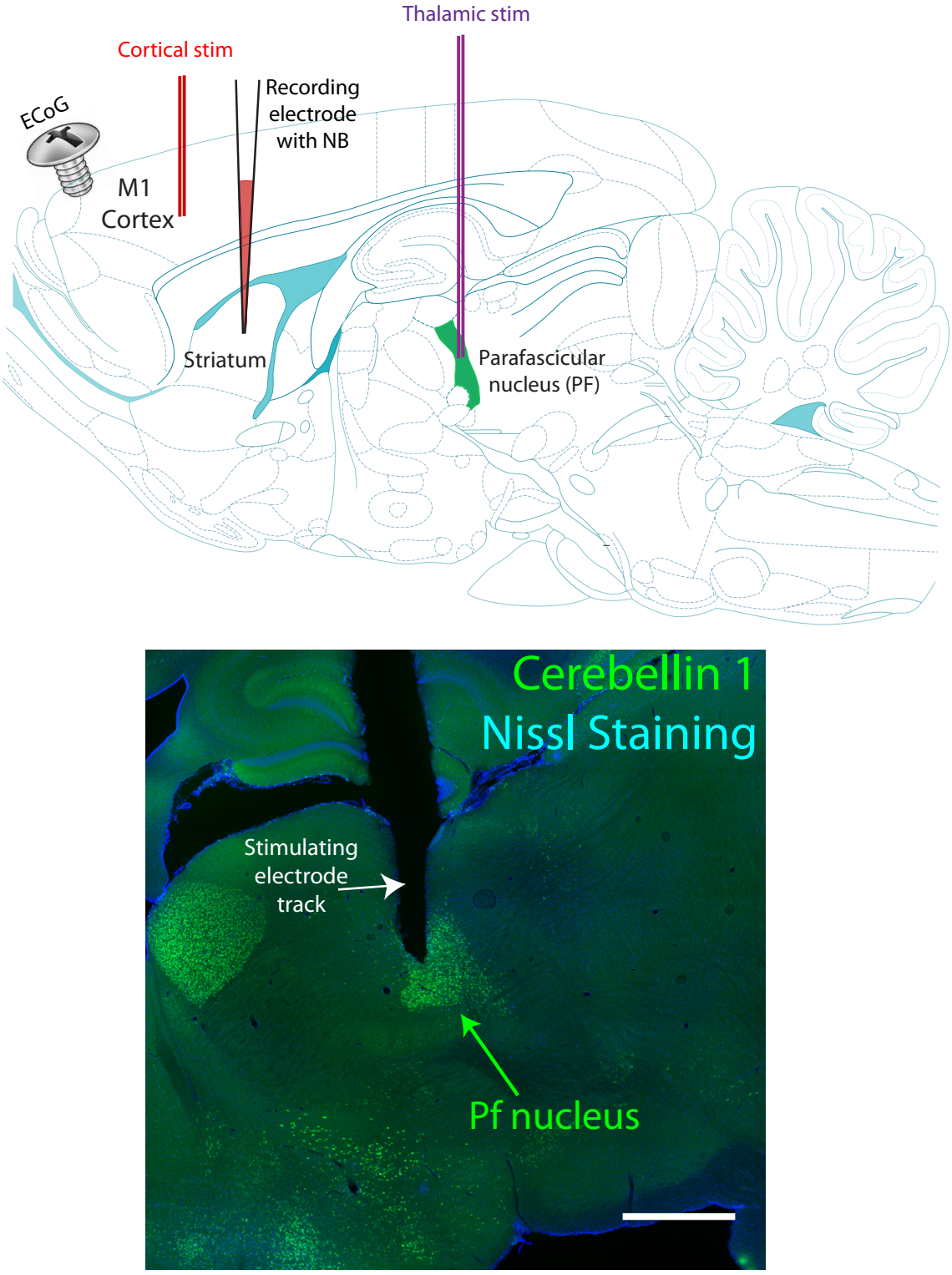


Figure 3.1 Experimental set-up.

a) Sagittal plate of rat brain showing the placement of stimulating electrodes in motor cortex and parafascicular nucleus. The recording electrode is filled with neurobiotin and lowerd into the striatum. The ECoG is recorded using a screw placed over frontal cortex. ***b)*** Confocal image of the thalamus, Cerebellin1 was used as a marker for parafascicular nucleus, combined with Nissl staining. The placement of the stimulating electrode is shown. Scale bar, 1000 μm.

Table 3.1. Reagents and antibodies used for histochemistry and immunohistochemistry.

	Species of origin	Manufacturer	Cat No	Dilution
Histochemistry				
Streptavidin CY3	n/a	Invitrogen	43-8315	1 in 1000
Nissl (NeuroTrace)	n/a	Molecular Probes	N-21479	1 in 100
Immunohistochemistry				
Antigen to which primary antibody binds				
ChAT	Goat	Chemicon	AB144P	1 in 500
DARPP-32	Rabbit	Cell Signalling	2302	1 in 100
Mu Opioid Receptor	Rabbit	Immunostar	24216	1 in 5000
Parvalbumin	Guinea Pig	Synaptic Systems	195004	1 in 1000
NOS	Rabbit	Millipore	AB5380	1 in 1000
Calretinin	Rabbit	Synaptic Systems	214102	1 in 1000
Cerebellin-1	Rabbit	Gift. J Morgan (Kusnoor *et al*., 2010)	N/A	1 in 3000
Fluorescent-conjugated secondary antibodies				
Alexa Fluor 488	Variety of species	Jackson Immuno Research		1 in 1000
Cy5	Variety of species	Jackson Immuno Research		1 in 500

3.3. Results

3.3.1. Electrophysiological recordings of striatal neurons

Extracellular recordings were made from striatal neurons during both slow-wave activity (SWA) and cortical activation. Subtypes of striatal neurons were putatively identified by their electrophysiological activity (Wilson *et al.*, 1990; Reynolds & Wickens, 2004; Mallet *et al.*, 2005; Kreitzer, 2009; Inokawa *et al.*, 2010). Extracellular recordings were made from 93 striatal neurons. Neurons with higher firing rates were preferentially recorded, as these were more likely to be interneurons (Kreitzer, 2009). Electrophysiological recordings were made from different types of striatal neurons including MSNs, FS interneurons, TANs, and low threshold spiking neurons. The focus of this study was the TANs in striatum, and therefore data recorded from other striatal neurons will be described briefly but not included in this thesis.

A total of 41 putative MSNs were recorded, and labelling was attempted for 7 of these neurons. Putative MSNs were recognised by their low basal firing rates of ~0.1-1 Hz during both SWA and cortical activation. After putative MSNs were filled with neurobiotin they were examined and confirmed as such by the presence of spines on the dendrites. In cases where there was still uncertainty, the MSNs were tested for DARPP-32 immunoreactivity. The 7 neurons that were recorded and labelled were recovered and confirmed as MSNs. Data recorded from these neurons will not be included in this thesis.

A total of 20 FS interneurons were recorded, and labelling was attempted on 13 of these. FS interneurons were identified by their high frequency discharge during cortical activation, and a short action potential width (< 1 ms). The neurons were then recovered post-mortem and a primary antibody against parvalbumin (PV) was used to confirm their identity. A total of 6 of the FS interneurons recorded and labelled were successfully recovered and identified as PV-positive. Data recorded from these neurons will not be included in this thesis.

A total of 21 TANs were recorded and labelling was attempted for 16 of these neurons. TANs were identified by their tonic firing rate of ~2-10 Hz during both SWA and cortical activation (Figure 3.2). Following recording, cholinergic neurons were filled with neurobiotin, and the molecular identity of the neurons could then be confirmed using a primary antibody against ChAT (Fig 3.2). A total of 11 of the TANs that were recorded and labelled were successfully recovered and identified as immunopositive for ChAT. Data recorded from these neurons will be examined in more detail.

A total of 5 neurons were recorded that exhibited low threshold spiking (LTS) and labelling was attempted on 2 of these, however labelling was unsuccessful and they could not be recovered. For 6 neurons that were not able to be identified by their electrophysiological characteristics labelling was not attempted. Likewise, 3 neurons that were recorded and labelled could not be identified using the standard molecular markers for striatal neurons. Data recorded from these neurons will not be included in this thesis.

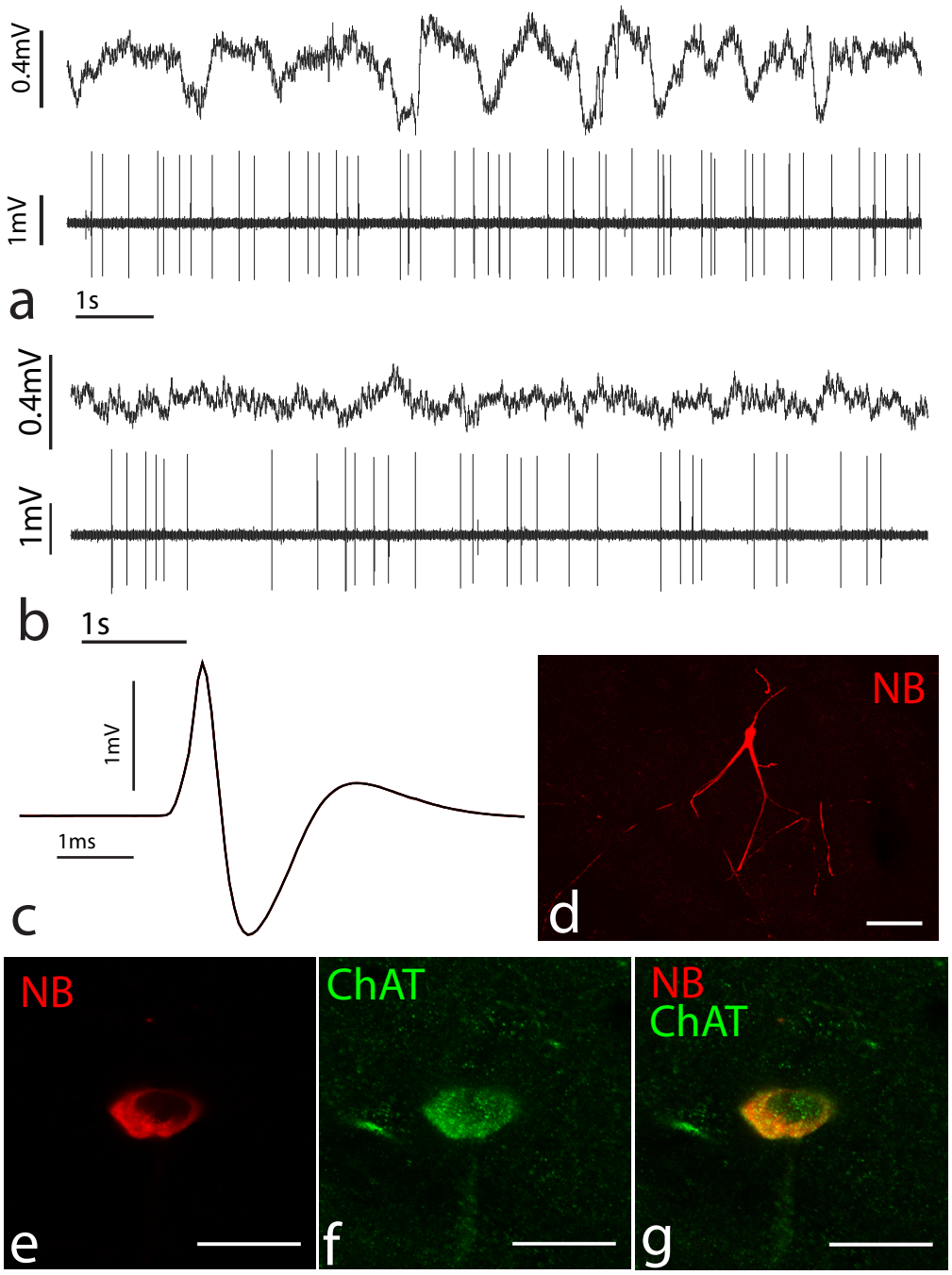


Figure 3.2. Physiological and morphological properties of an identified cholinergic interneuron.

a) Electrophysiological recording (lower trace) showing the spontaneous activity of a cholinergic interneuron during cortical slow-wave activity (upper trace). ***b)*** Electrophysiological recording showing spontaneous activity of the same cholinergic interneuron (lower trace) during cortical activation (upper trace). ***c)*** The average waveform of the cholinergic interneuron. ***d)*** Z-projection of a stack of confocal micrographs showing the dendrites of the neurobiotin filled neuron (NB). ***e)*** Single plane confocal micrograph showing the soma of the NB-filled neuron. ***f)*** The soma of the neuron immunopositive for ChAT. ***g)*** The soma of the neuron positive for both NB and ChAT. Scale bars, d, 50 µm; e, f, g, 25 µm.

3.3.2. Responses of cholinergic interneurons to cortical stimulation

Cortical stimulation protocols were applied to 9 out of the 11 identified cholinergic interneurons that were recorded and labelled. A further 7 cholinergic interneurons where cortical stimulation was attempted were included in this study; these neurons were recorded by Dr Andrew Sharott as part of a wider study. A summary of the neurons recorded and the stimulation protocols applied is presented in Table 3.2.

Out of the 16 identified neurons that were recorded and cortical stimulation was applied, 9 of these neurons responded to the cortical stimulation with a short latency increase in firing probability (at about ~ 0 to 20 ms following stimulation; Table 3.2). The response was generally composed of an initial excitatory phase followed by an overall reduction in firing rate (40-200 ms post stimulation) and then a rebound excitation (Fig 3.3). An averaged PSTH of all the identified cholinergic interneurons which responded to cortical stimulation (n=9), shows that the multiphasic response is consistent and composed of an initial excitation, followed by a reduction in firing rate, and a rebound excitation at about 300 ms after stimulation (Fig 3.4a). The averaged peak probability of firing occurs at 8.15 ms following cortical stimulation (bins of 1 ms; Fig 3.4b).

Various stimulation protocols were used to further examine the nature of the responses of cholinergic interneurons. A paired stimulation protocol was used as FS interneurons and MSNs have been shown to respond differently to the first and second pulses (Mallet *et al.*, 2005). A time interval of 100 ms between stimulations was chosen because this is the most comparable with data from MSNs and FS interneurons recorded *in vivo* (Mallet *et al.,* 2005). This stimulation protocol was applied to 5 cholinergic interneurons, and 2 of these neurons exhibited short latency responses (Table 3.2). Neuron F showed a short-latency response to the first stimulus (10.16 ms), and a reduced, but also short latency response to the second stimulus (9.21 ms; Fig. 3.5). The average response shows that both neurons fire with a greater probability to the first pulse of the paired stimulation protocol (Fig 3.6). The average latencies of response to the first and second

pulses were both under 15 ms (8.2 ms and 12.7 ms, respectively, Fig 3.6b). The probability of responding to the second pulse for neurons F and P both showed a decrease relative to their responses to the first pulse (Fig 3.6c, d). Neuron F's response to the second pulse was decreased by 20% relative to the first pulse, and neuron P's response to the second pulse was decreased by 66% (Fig 3.6d). Although only 2 neurons were examined with this stimulation protocol, the pattern is consistent.

Table 3.2. Summary of neurons recorded and stimulation protocols applied.

The prefix AJS- denotes neurons that were recorded by Dr A. Sharott, the rest were recorded by the DPhil candidate (prefix NJX-). 'Single' stimulation was 1 pulse applied every 2 s. Paired stimulation was 2 pulses with an inter-stimulus interval of 100 ms applied every 2 s. 40 Hz stimulation was 5 pulses given at a frequency of 40 Hz every 2 s. The response to the different stimulation protocols is indicated for each neuron as 1 if there was a response, 0 if there was no response, and NT if that particular stimulation protocol was not tested for that neuron.

		Cortical stimulation			Thalamic stimulation		
Neuron	**Reference for Thesis**	**Single CORTEX**	**Double CORTEX**	**40 Hz CORTEX**	**Single THALAMUS**	**Double THALAMUS**	**40Hz THALAMUS**
AJS028i	A	1	NT	NT	NT	NT	NT
AJS031a	B	1	NT	NT	NT	NT	NT
AJS031b	C	1	NT	NT	NT	NT	NT
AJS032d	D	1	NT	NT	NT	NT	NT
AJS044b	E	1	NT	NT	1	NT	NT
AJS073a	F	1	1	NT	1	1	1
AJS074g	G	0	0	NT	1	1	1
NJX009i	H	0	NT	NT	NT	NT	NT
NJX010g	I	0	NT	NT	NT	NT	NT
NJX011a	J	0	NT	NT	NT	NT	NT
NJX012d	K	0	NT	NT	0	NT	0
NJX014d	L	1	NT	NT	1	NT	NT
NJX023c	M	0	0	NT	1	NT	1
NJX026c	N	1	NT	NT	1	NT	NT
NJX027d	O	0	0	NT	1	1	1
NJX029d	P	1	1	1	1	1	1
TOTAL	**16**	**9**	**2**	**1**	**8**	**4**	**5**

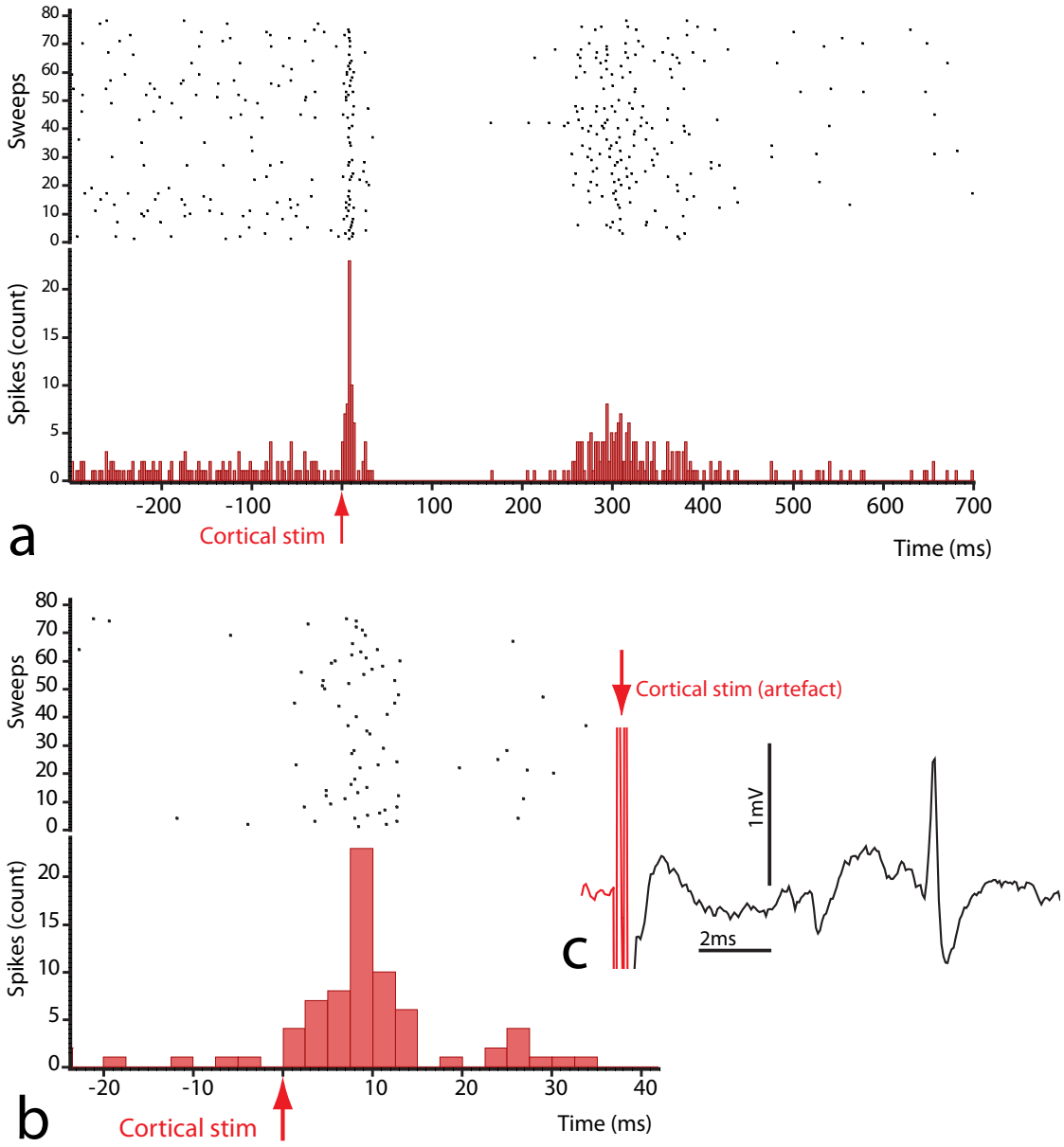


Figure 3.3. Cortical stimulation of an identified cholinergic interneuron.

a) PSTH and raster plot showing the response of neuron P to stimulation of cortex, given at time 0. (bins, 2.5ms) **b)** Enlarged section of PSTH and raster showing that this neuron responded to cortical stimulation with a peak response that had a latency of < 10 ms. ***c)*** An example of a spike in response to cortical stimulation, showing the stimulation artefact.

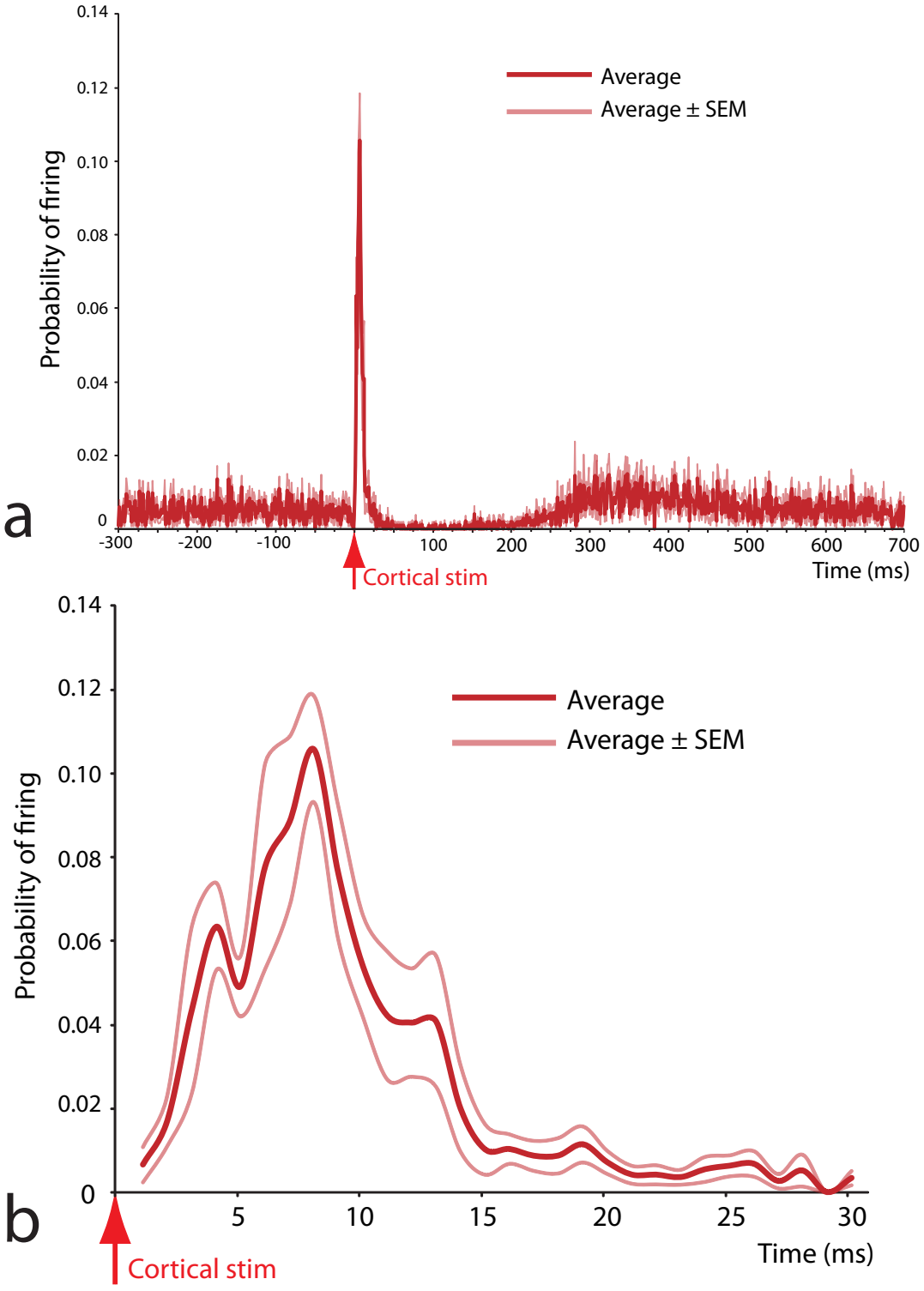


Figure 3.4. Average response to a single cortical stimulus.

a) Average response of identified cholinergic interneurons to a single cortical stimulus (n=9), an average PSTH showing spike probability (bins, 1 ms) over ~ 100 trials. The average response is shown ± SEM. ***b)*** Enlarged section of the PSTH showing the first 25 ms after cortical stimulation. The spike probability peaks at 8 ms after stimulation (bins, 1 ms).

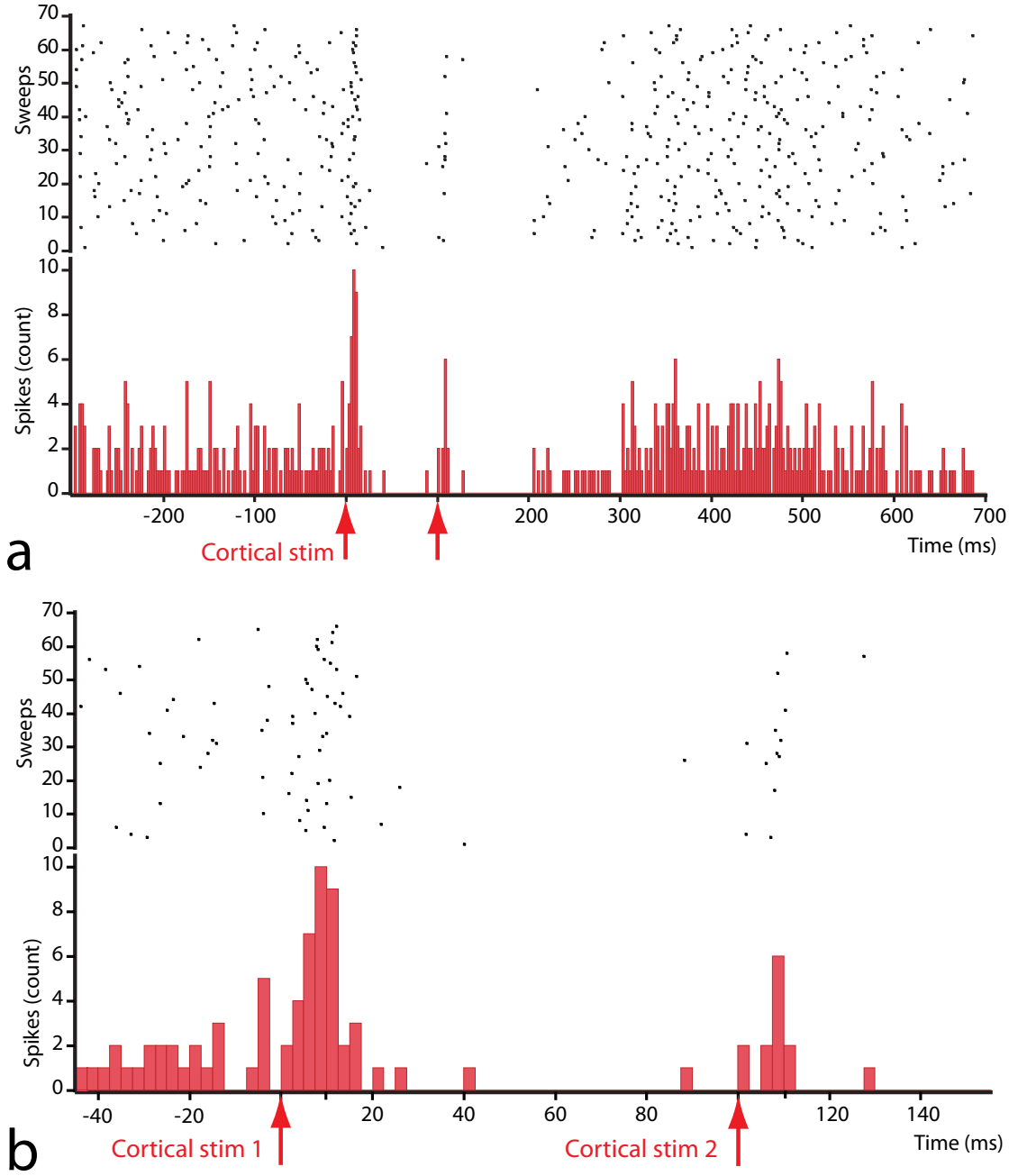


Figure 3.5. Paired cortical stimulation of an identified cholinergic interneuron.

a) PSTH and raster plot showing response of neuron F to a paired cortical stimulation, with a 100ms interval. ***b)*** Enlarged PSTH and raster plot showing that the latency to respond to both stimuli is within the 10 ms following the pulse.

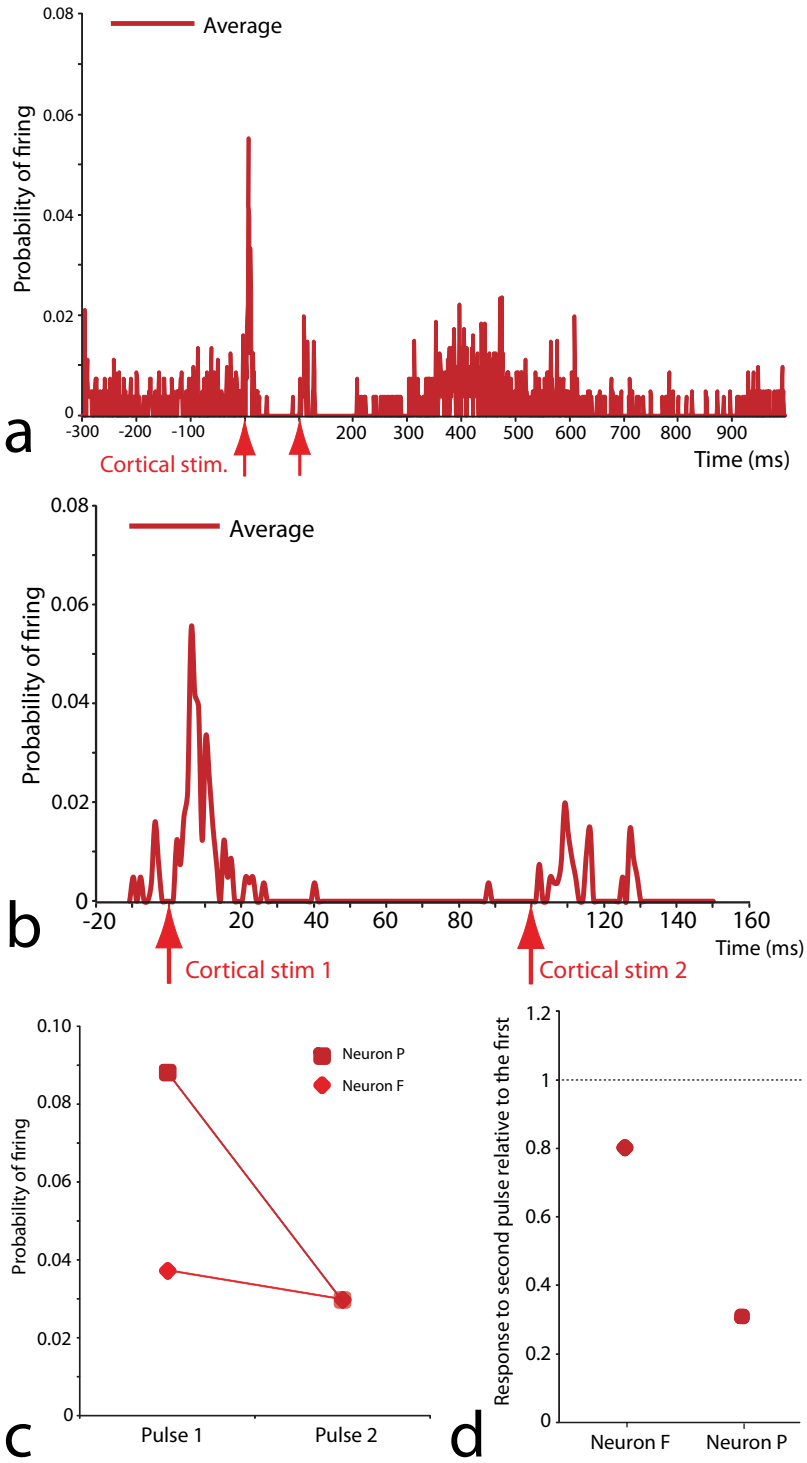


Figure 3.6. Average response to paired cortical stimulation.

a) PSTH showing average response of identified cholinergic interneurons to paired cortical stimulation (n=2; bins, 1 ms). ***b)*** Enlarged section of the average PSTH showing the response to the paired cortical stimulation. ***c)*** Plot showing the peak response to the first and second pulses of the paired stimulus protocol for neuron F (diamonds) and neuron P (squares). ***d)*** The response to the second pulse relative to the normalised first pulse (indicated by dashed line at 1) for neurons F and P.

3.3.3. Responses of cholinergic interneurons to thalamic stimulation

Thalamic stimulation (single pulse every 2 s) was applied to 9 neurons, and 8 of these neurons exhibited a short latency response (Table 3.2). The responses of cholinergic interneurons to thalamic stimulation displayed a multiphasic response. In general, this was similar to cortical stimulation, with an initial increase in firing probability followed by a decrease or suppression of firing and a rebound excitation before returning to the baseline firing rate. Cholinergic interneurons can exhibit a short-latency response to thalamic stimulation (Fig 3.7). The average response to thalamic stimulation was more variable relative to the response after cortical stimulation, but was also of a short latency (peak at 4.15ms, bins of 1 ms, n=8; Fig 3.8).

Paired thalamic stimulation, with an inter-stimulus interval of 100 ms, was applied to 4 cholinergic interneurons, and all of these interneurons responded (Table 3.2). As an example of this, Neuron F responded to both pulses within the stimulus with an increase in firing probability, followed by a suppression of firing which lasted ~200 ms (Fig 3.9). Neuron F responded to the first pulse with a peak response at a short latency following the pulse (5.15 ms; Fig 3.9), and with a longer latency response to the second pulse (28.21 ms; Figure 3.9). Neuron F responded to the second pulse of the stimulus with a greater probability of firing than to the first pulse (Fig 3.9). Note that Neuron F also responded to paired cortical stimulation (as shown in Fig 3.7), this will be examined further (see section 3.3.4). The averaged PSTH for the four neurons which responded shows that firing probability was greater after the second pulse of the paired stimulus (Fig 3.10). The latency to the peak response after the first stimulus was shorter than to the second (12.4 ± 4.7 ms and 25.5 ± 1.4 ms, respectively; Fig 3.10c). The probability to respond was greater to the second stimulus, although the response to the second pulse of the stimulus was more variable (Fig 3.10c). Three out of the four neurons showed a greater probability of firing to the second stimulus, whereas one neuron showed the opposite pattern (Figure 3.10c).

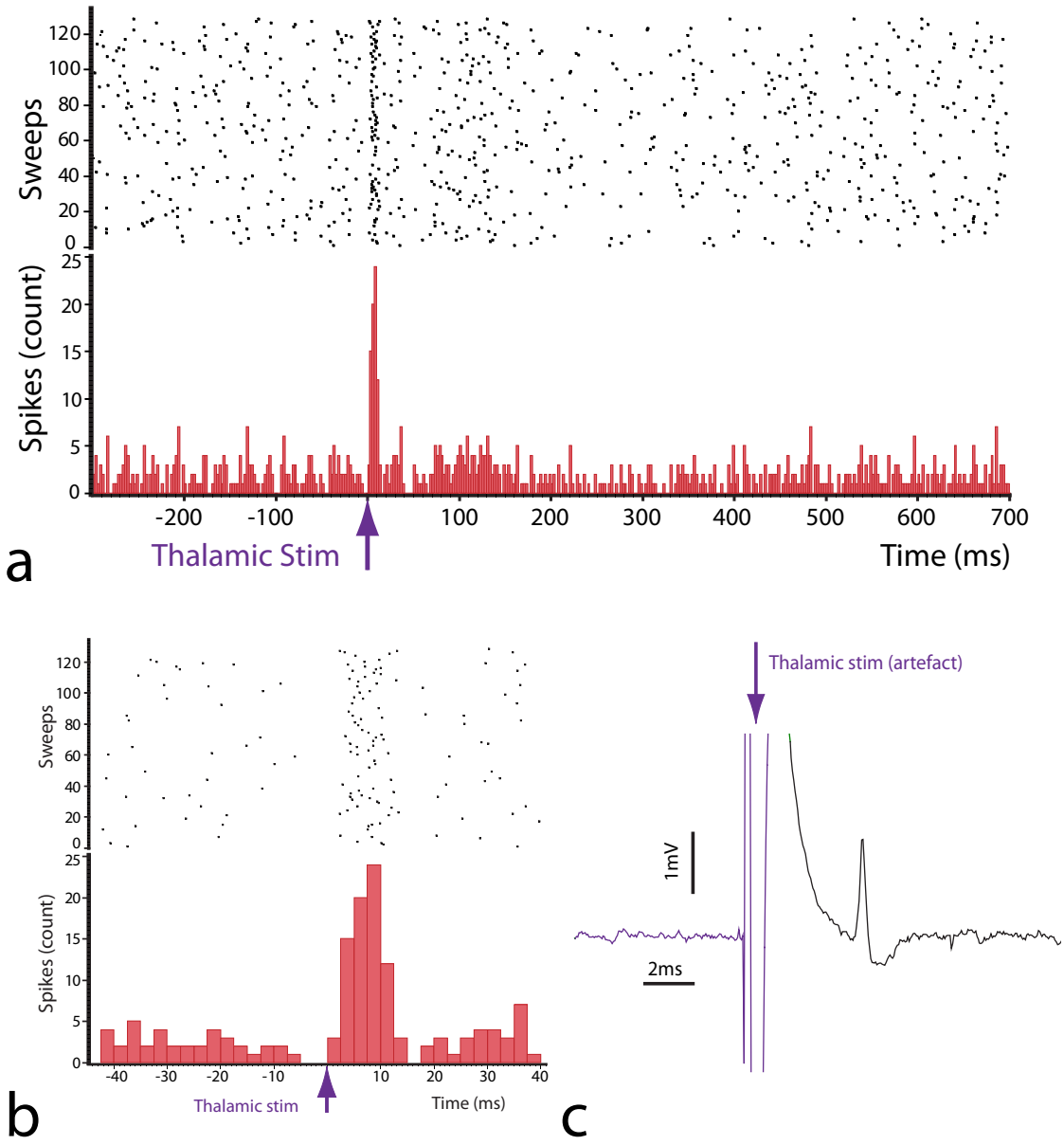


Figure 3.7. Thalamic stimulation of an identified cholinergic interneuron.

a) PSTH and raster plot showing the response of neuron M to stimulation of thalamus, given at time 0. (bins, 2.5 ms) ***b)*** Enlarged section of PSTH and raster showing that this neuron responded to cortical stimulation with a peak latency of less than 10 ms. ***c)*** An example of a spike in response to thalamic stimulation, showing the stimulation artefact.

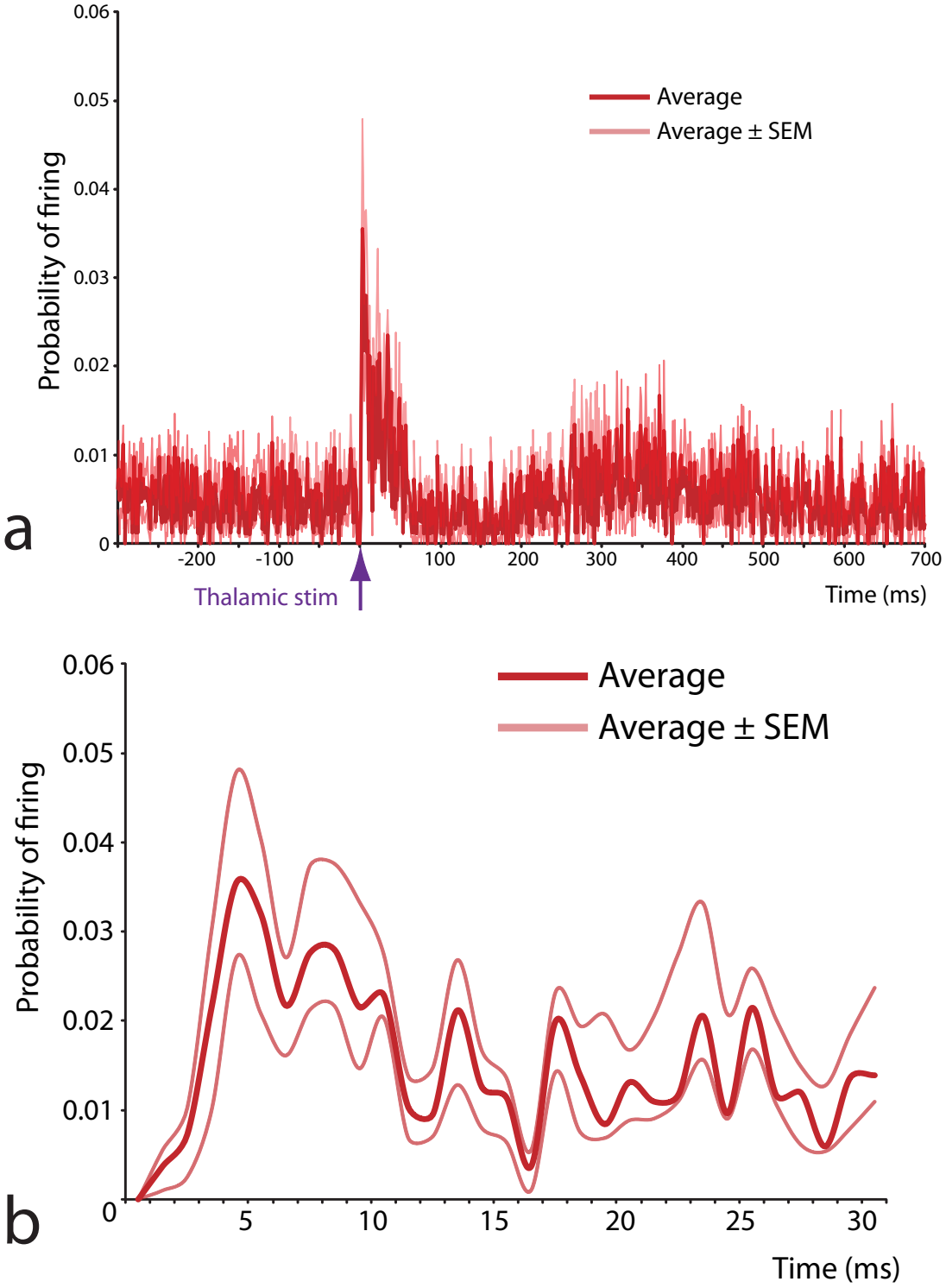


Figure 3.8. Average responses to a single thalamic stimulus.

a) Average response of identified cholinergic interneurons to a single thalamic stimulus (n=8), an average PSTH showing spike probability (bins of 1 ms). The average response is shown ± SEM. ***b)*** Enlarged section of the PSTH showing the first 30 ms after thalamic stimulation. The spike probability peaks at 4.2 ms after stimulation.

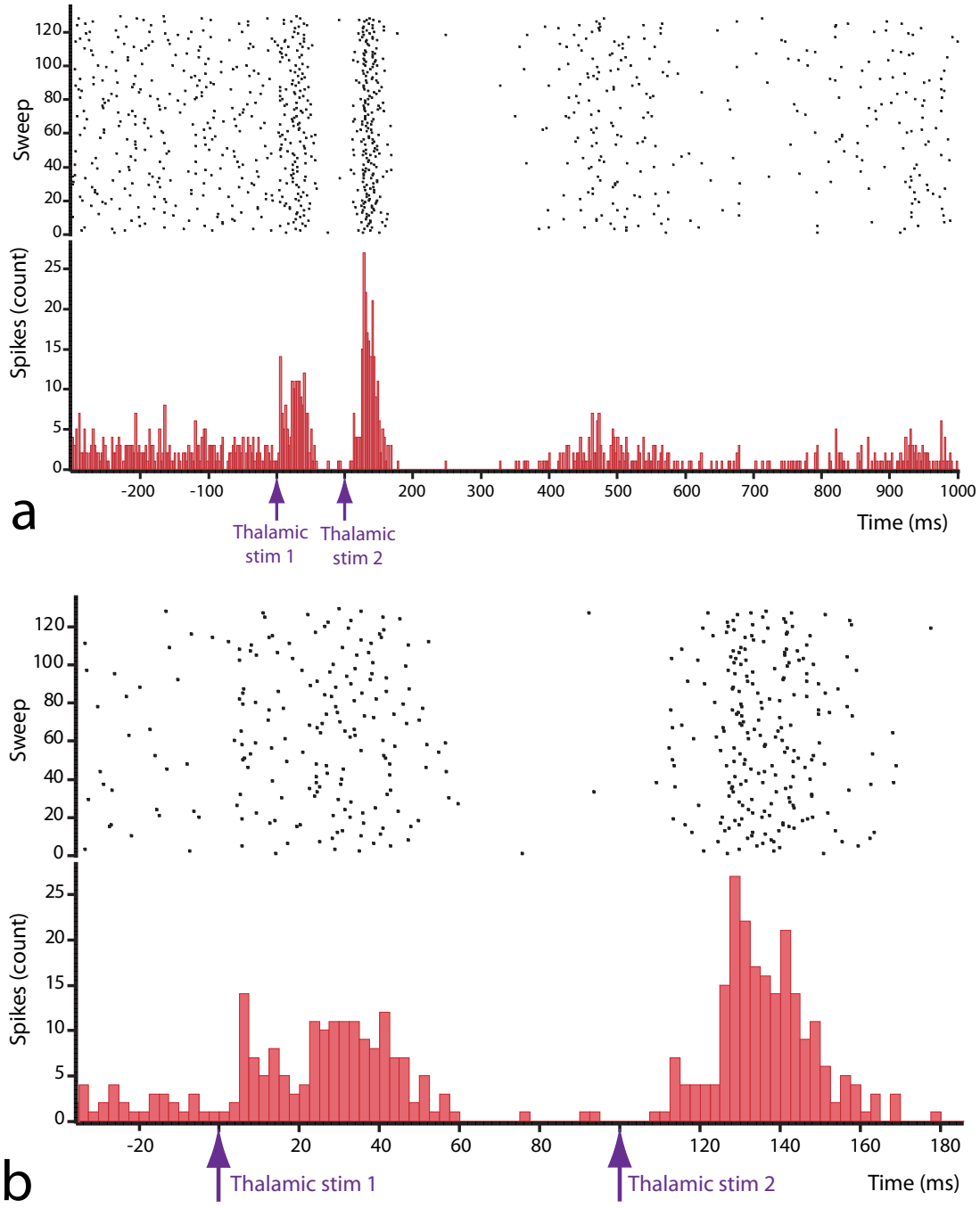


Figure 3.9. Paired thalamic stimulation of an identified cholinergic interneuron.

a) PSTH and raster plot showing response of neuron F to paired thalamic stimulation, two stimulations with a 100 ms interval. ***b)*** Enlarged PSTH and raster plot showing that the latency to respond to the first is within 10 ms, but that the latency to the second stimulation is >25 ms.

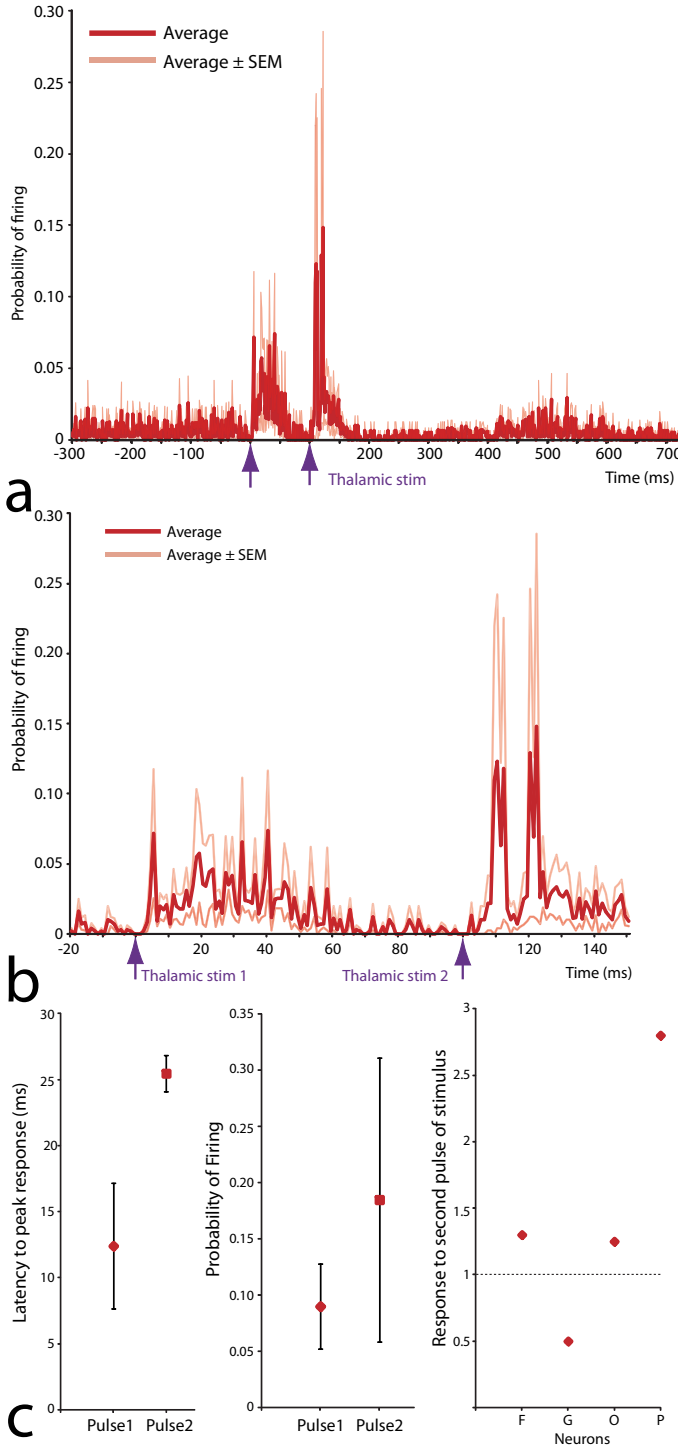


Figure 3.10. Average response to paired thalamic stimulation.

a) Average response of identified cholinergic interneurons to paired thalamic stimulation (n=4), an average PSTH showing spike probability (bins of 1 ms). The average response is shown ±SEM. ***b)*** Enlarged section of the PSTH ***c)*** The latency to the peak response to both the first and second stimulus (left), the probability of firing to each stimulus (middle), and the response of each neuron to the second pulse of the stimulus relative to the first pulse (first pulse is normalised to 1, dashed line; right).

Experiments in awake behaving Rhesus monkeys have shown that TANs respond with a higher probability of firing to high frequency stimulation of the thalamus (Nanda *et al.*, 2009). High frequency stimulation of the thalamus has also shown to be facilitating *in vitro* (Ding *et al.*, 2010). A stimulation frequency of 40 Hz was used here to further examine the nature of the thalamic innervation of cholinergic interneurons. The response of an individual identified cholinergic interneuron to a 40 Hz simulation (train of 5 pulses) is shown in figure 3.11. The neuron responds to each pulse within the train with a short latency response (< 10 ms), and exhibits the greatest probability of responding to the 3rd pulse in the train (Fig 3.11b). After the train of stimuli is given, the neuron is then silent for a period of 350 to 800 ms, as can be seen in the raster (Fig 3.11) This period of silence is the longest for the first ~20 trials, and then decreases over the subsequent trials (Fig 3.11a).

The 40 Hz stimulation protocol was applied to 6 cholinergic interneurons, and 5 showed a response (Table 3.2). The averaged PSTH shows that the neurons respond to each pulse within the stimulation train and then the firing rate decreases for > 350 ms (Fig 3.12). The probability of firing is the lowest for the first pulse in stimulus train, and is greater for rest of the pulses in the train (Fig 3.12b). The latency to peak response after each pulse within the stimulus was <10 ms (Fig 3.12c). The average latencies to peak response were shortest, and showed the least variability, to the 2nd and 5th pulses (Fig 3.12c) The probability of response was greatest to the 3rd pulse within the train, and the lowest for the 1st pulse (Fig 3.12d).

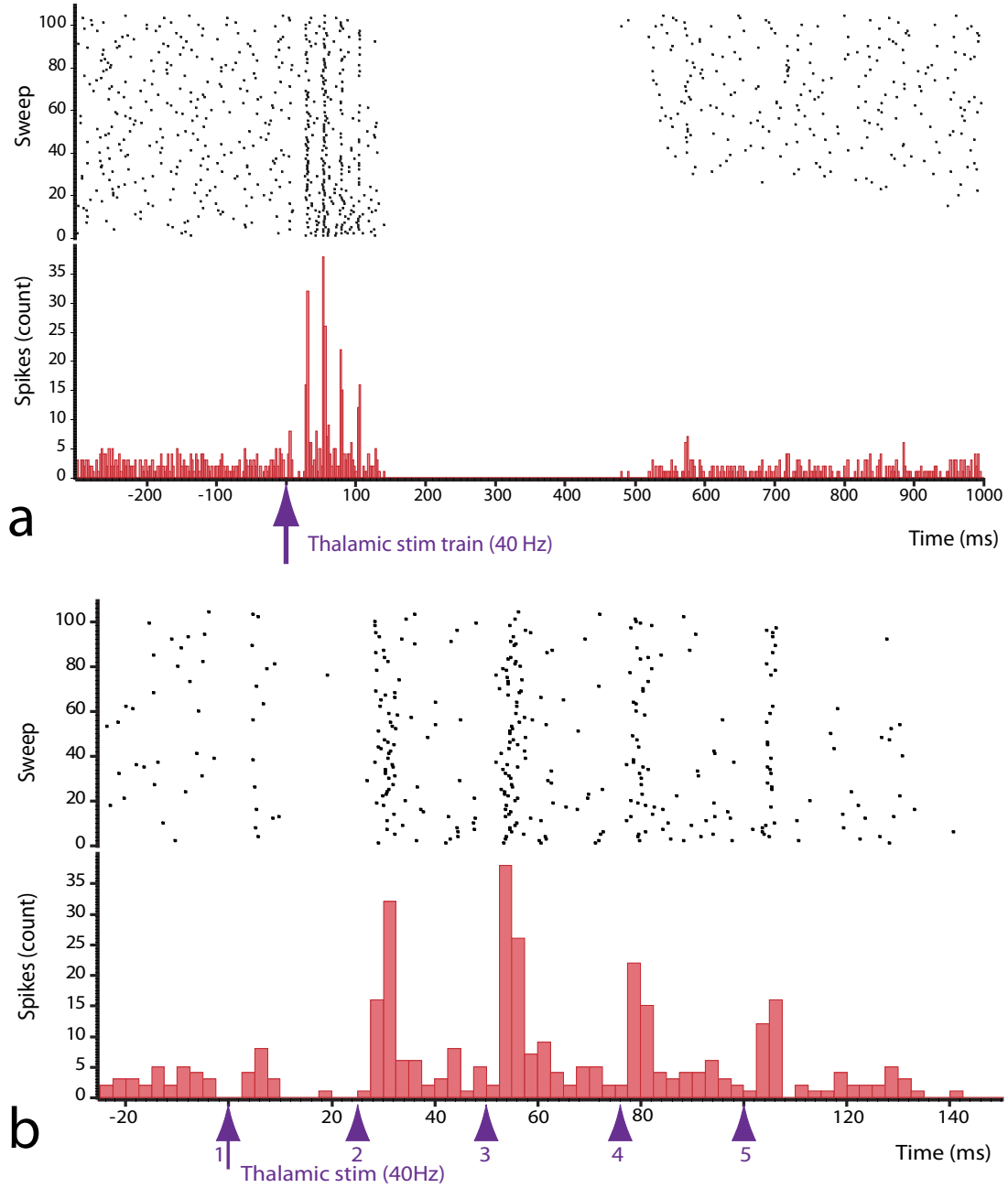


Figure 3.11. 40 Hz thalamic stimulation of an identified cholinergic interneuron.

a) PSTH and raster plot showing the response of neuron F to a 40 Hz stimulation of thalamus, given at times 0, 25, 50, 75 and 100 ms. (bins, 2.5 ms) ***b)*** Enlarged section of PSTH and raster showing the response of the neuron to each stimulus in the train (bins, 2.5 ms). The neuron's peak response to the first stimulus was at a latency of 5.15 ms, the second at 5.17 ms, the third at 4.18 ms, the fourth at 4.19 ms, and to the fifth at 5.20 ms (bins of 1ms).

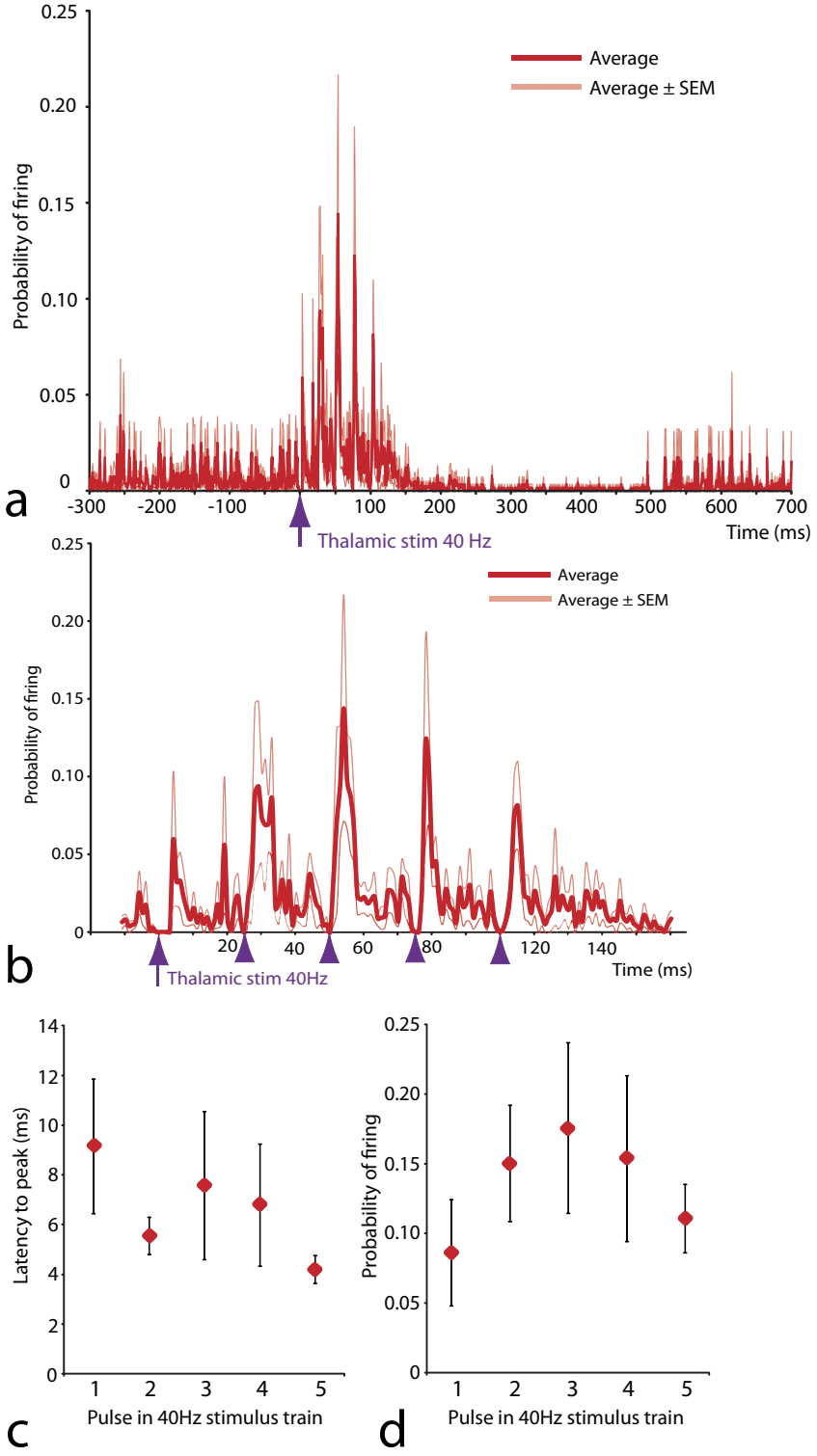


Figure 3.12. Average responses to 40 Hz thalamic stimulation.

a) Average response of identified cholinergic interneurons to 40 Hz thalamic stimulus (n=5), an average PSTH showing spike probability (bins of 1 ms). The average response is shown ±SEM. ***b)*** Enlarged section of the PSTH. ***c)*** Plot showing the average latency to the peak after each stimulus (average ±SEM). ***d)*** Plot showing the average probability of firing after each stimulus (average ±SEM).

3.3.4. Responses of cholinergic interneurons to both cortical and thalamic stimulation

In order to gain insight into how *individual* cholinergic interneurons integrate cortical and thalamic information, the responses of individual, identified, cholinergic interneurons to *both* cortical and thalamic stimulation were examined *in vivo.* Out of the 9 neurons tested with single stimulation applied to both cortex and thalamus, 5 responded to stimulation of *both* (Table 3.2). Thus, an individual neuron can respond to both cortical and thalamic stimulation (Fig 3.13). Neuron N exhibited a short latency peak response to cortical stimulation (13.16 ms; Fig 3.13b) and to thalamic stimulation (3.15 ms; Fig 3.13e). For this neuron, the patterns of response are different, neuron N responds to cortical stimulation with an initial increase in probability of firing, followed by a suppression of firing and a rebound excitation (Fig 3.13a). The response to thalamic stimulation is faster but exhibits a lesser initial increase in firing, relative to cortical stimulation, and the decrease in firing following the stimulation was less distinct although there appears to be a rebound excitation (Fig 3.13d)

For neurons that responded to both cortical and thalamic stimulation the latencies to peak response were less variable following cortical stimulation than the responses following thalamic stimulation (Fig 3.14a, c). Three out of the five neurons examined responded with a shorter latency to the cortical stimulation, one neuron responded with the same latency to both stimulations and one neuron responded with a shorter latency to thalamic stimulation (Fig 3.14a). In response to cortical stimulation, all five neurons responded with a greater probability relative to thalamic stimulation (Fig 3.14b). On average, the latency to peak response was faster following cortical stimulation, relative to thalamic, although the difference between the two groups is not significant (Fig 3.14c; $p = 0.52$, Wilcoxon signed-rank test). The average probability of firing to thalamic stimulation was significantly less than the probability of response to cortical stimulation (Fig 3.14d; $p = 0.0079$, Wilcoxon signed-rank test). Overall, the neurons responded with a shorter latency and a greater probability of firing to cortical stimulation (Fig 3.14).

A comparison of *all* the neurons for which single stimulation of either cortex or thalamus was applied reveals that the latency to peak response is longer and more variable to thalamic stimulation (Figure 3.15a, b). A comparison of the latency to peak response shows that although the thalamic responses generally exhibited a longer latency and show a wider distribution the difference between these two groups is not significant (Fig 3.15b; $p = 0.24$; Mann Whitney U test). The average latency to the first spike was also examined for all neurons for which stimulation was applied to cortex and thalamus, and the latency to first spike was faster following cortical stimulation (Fig 3.15c, d). A comparison of these two groups found that the average latency to first spike was significantly longer following thalamic stimulation (Fig 3.15d; $p = 0.015$; Mann Whitney U test). Overall, for the neurons examined, the response to cortical stimulation was generally faster relative to the response to thalamic stimulation.

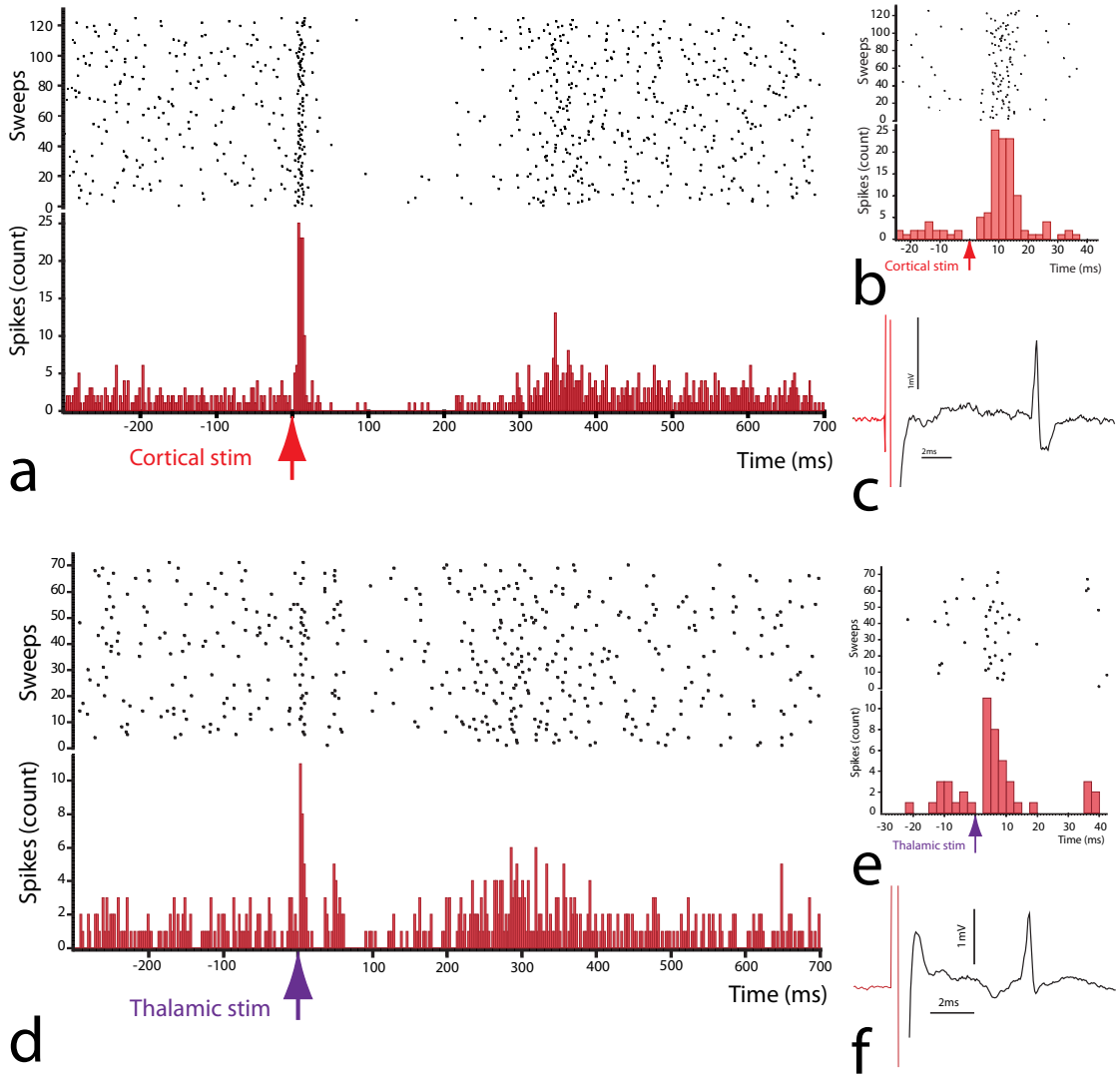


Figure 3.13. Responses of an individual identified cholinergic interneuron to cortical and thalamic stimulation.

a) PSTH and raster plot showing response of neuron N to cortical stimulation. ***b)*** Enlarged section of the PSTH showing the response to cortical stimulation. ***c)*** An example of a spike in response to cortical stimulation. ***d)*** PSTH and raster plot showing response of neuron N to thalamic stimulation. ***e)*** Enlarged section of the PSTH showing the response to thalamic stimulation. ***f)*** An example of a spike in response to thalamic stimulation

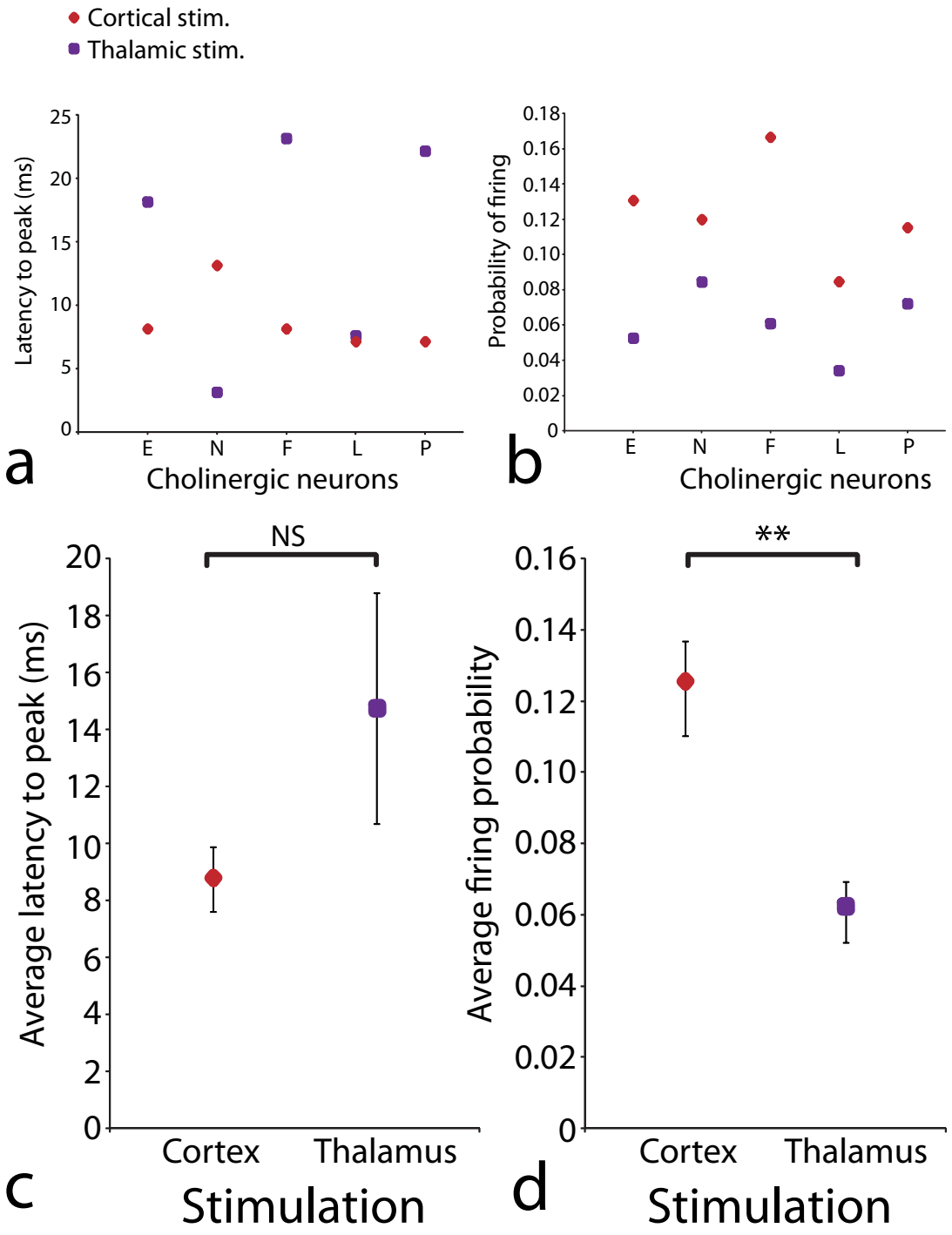


Figure 3.14. Responses of five identified cholinergic interneuron to both cortical and thalamic stimulation.

a) Latency to peak following single stimulation of cortex (red diamonds) and thalamus (purple squares) for each neuron. ***b)*** Probability of firing to cortical and thalamic stimulation for each neuron. ***c)*** Average latency to fire to cortical and thalamic stimulation (n = 5, error bars indicate SEM; NS is not significant). ***d)*** Average probability of firing to cortical and thalamic stimulation (n=5, error bars indicate SEM; ** indicates p value ≤ 0.01).

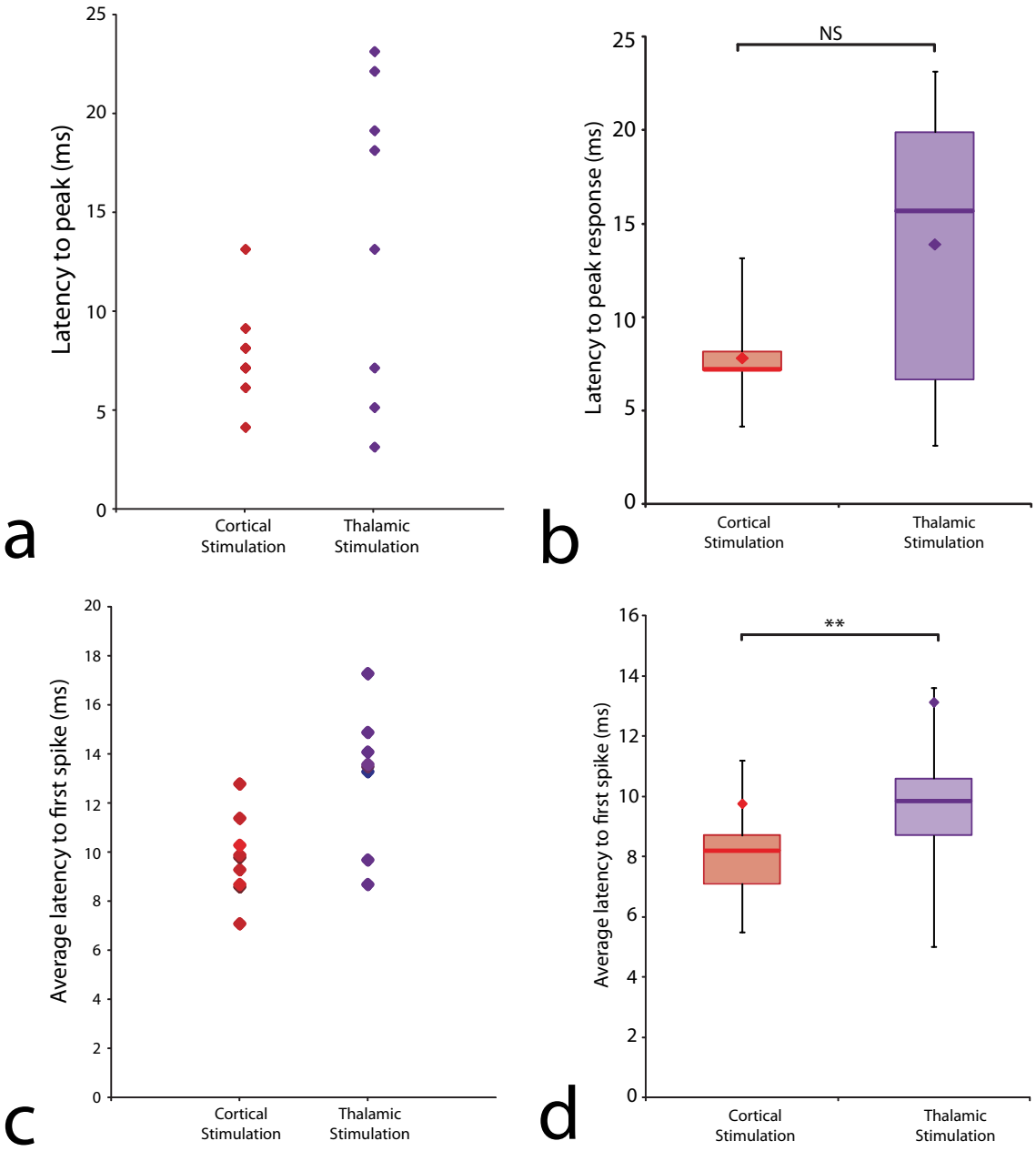


Figure 3.15. Responses of individual identified cholinergic interneurons to cortical and thalamic stimulation.

a) Plot of latencies to peak response following cortical stimulation (n=9; red diamonds) and thalamic stimulation (n=8; purple circles). ***b)*** Box and whisker plot (interquartile range) showing the latency to peak response following cortical and thalamic stimulation. Markers (diamonds) indicate the means. Thicker lines indicate the medians. (NS indicates no significant difference between the groups) ***c)*** Plot of the average latency to first spike following cortical stimulation and thalamic stimulation. ***d)*** Box and whisker plot (interquartile range) showing the average responses to first spike. Markers (diamonds) indicate the means. Thicker lines indicate the medians. (** indicates $p \leq 0.01$).

Paired cortical and paired thalamic stimulation was applied to two neurons, and they both showed responses (Table 3.2). For these two neurons, the probability of response to thalamic stimulation was greater than the response to cortical stimulation for both the first and second pulses, as shown in the averaged PSTHs (Fig 3.16). Following cortical stimulation the response is greater to the first pulse, relative to the second (Fig 3.16). The pattern is reversed following thalamic stimulation, in that the response is greater to the second pulse of the stimulus (Fig 3.16b). The latency to respond to the first pulse of the train is similar for cortical and thalamic stimulation (Fig 3.16c). For thalamic stimulation; both neurons show an increased latency to the second pulse (Fig 3.16c). For cortical stimulation; Neuron F shows a decrease in latency to the second cortical pulse, whilst neuron P shows an increase (Fig 3.16d, e). For thalamic stimulation; both neurons show a greater probability of firing to the first pulse of the stimulation (Fig 3.16d, e). For cortical stimulation; both neurons show a decrease in firing probability to the second cortical stimulus (Fig 3.16d, e).

For one neuron high frequency stimulation of both the cortex and thalamus was applied (Table 3.2). Neuron P responded to 40 Hz cortical stimulation and 40 Hz thalamic stimulation (Fig 3.17). The neuron shows a response to both cortical and thalamic stimulation, followed by a decrease in firing probability which is more evident following thalamic stimulation than cortical stimulation (>350 ms and ~200 ms, respectively; Fig 3.17). The neuron responded to the first peak of both the cortical and thalamic stimuli, but with a shorter latency to the thalamic stimulus (Fig 3.17c, d, e). The neuron then responds consistently to each stimulus within the train of the thalamic stimulus with a short latency response (< 5 ms), but only responds to the first and 3rd pulse of the cortical stimulus (Fig 3.17e). Neuron P responded to the first pulse of the cortical stimulation with the greatest probability of firing and then either did not respond or responded with very low probability to the rest of the pulses within the train (Fig 3.17f). The response of the neuron to thalamic stimulation shows that the neuron exhibited incremental firing probability up

to the 3rd and 4th pulses within the train, and the probability then decreases for the 5th pulse (Fig 3.17f). This neuron thus responds to the first pulse of the cortical stimulus and then ceases to respond but shows increasing probability to respond to thalamic stimulation as the train continues.

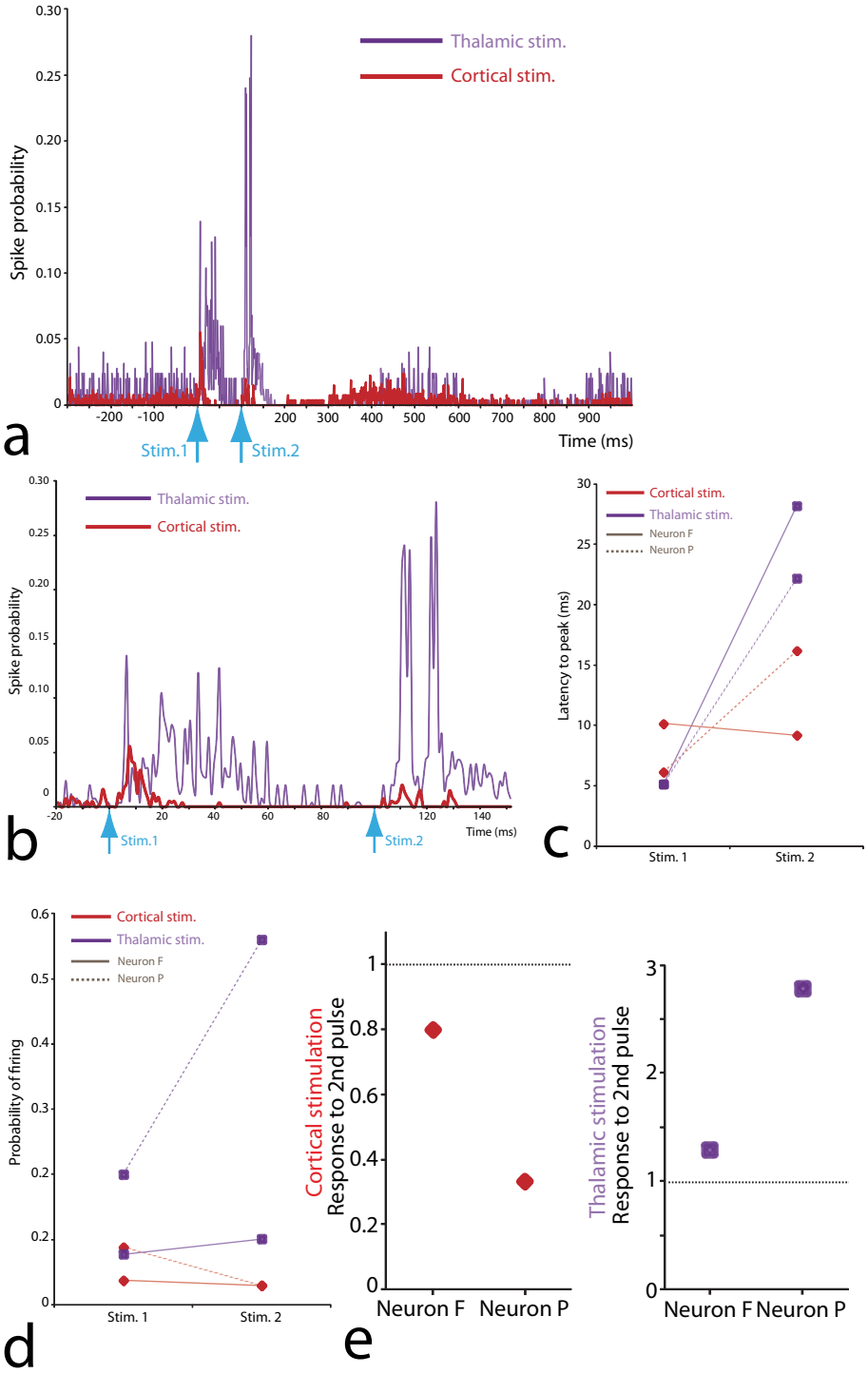


Figure 3.16. Response of two identified cholinergic interneurons to both paired cortical and thalamic stimulation.

a) Average PSTH showing the response to both paired cortical (red) and paired thalamic (purple) stimulation (n=2; bins, 1 ms). ***b)*** Enlarged section of the average PSTH. ***c)*** Latency of each of the neurons to each pulse of the cortical (red) and thalamic stimulation (dashed line is neuron F, solid line is neuron P). ***d)*** Average firing probability of each neuron to both cortical and thalamic stimulation. ***e)*** The response of each neuron to the second pulse of the stimulus, relative to the first pulse (which is indicated by the dashed lines) for cortical (left) , and thalamic (right) stimulation.

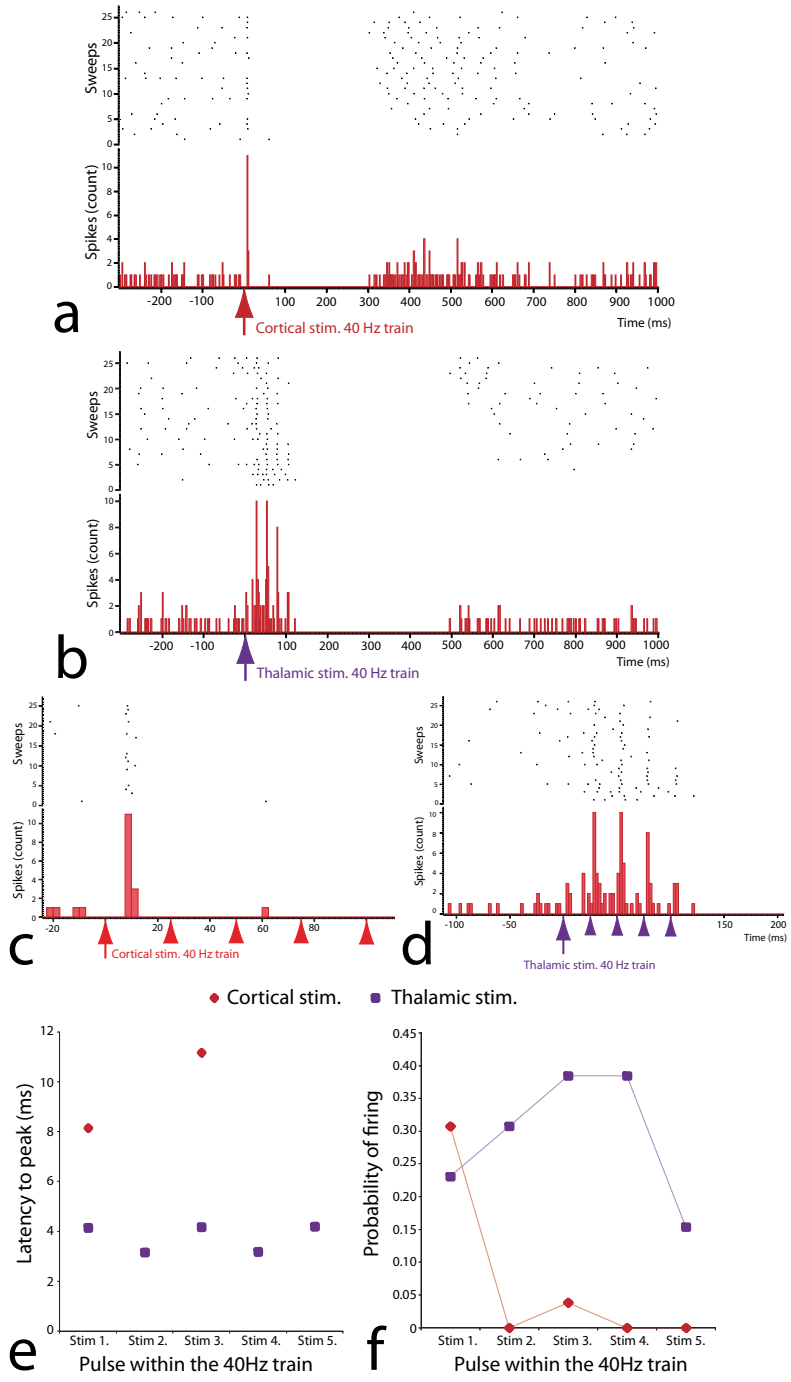


Figure 3.17. Response of one identified cholinergic interneuron to 40Hz stimulation of cortex and thalamus.

a) PSTH showing the response of neuron P to 40 Hz stimulation of cortex (bins 2.5 ms). ***b)*** Response of neuron P to 40 Hz thalamic stimulation. ***c)*** Enlarged section of the PSTH showing the response to cortical stimulation. ***d)*** Enlarged section of the PSTH showing the response to thalamic stimulation. ***e)*** The latency to peak firing to each pulse within the train to both cortical (red diamond) and thalamic (purple square) stimulation. ***f)*** The probability of firing to each pulse within the stimulus train for both cortical (red) and thalamic (purple) stimulation.

3.4. Discussion

Cholinergic interneurons have a role in reward-related behaviour and in order to carry out their role they must integrate information from different sources. The major sources of information to the striatum are from the cortex and thalamus, and the aims of this study were to examine the responses of cholinergic interneurons to stimulation of cortex and thalamus *in vivo*. Cholinergic interneurons responded to cortical and thalamic stimulation *in vivo* and the responses had differing properties. Furthermore, *individual* cholinergic interneurons can respond to both cortical and thalamic stimulation *in vivo*, and examination of these responses can give us insight into the way in which cholinergic interneurons integrate the two main inputs to striatum.

3.4.1. Cortical and thalamic stimulation of cholinergic interneurons

Cholinergic interneurons recorded in this study exhibited physiological characteristics that are consistent with those that have been described previously, such as a tonic firing rate of 2-10 Hz (Wilson *et al.*, 1990; Reynolds *et al.*, 2001; Inokawa *et al.*, 2010). All of the cholinergic interneurons included in this study were identified as immunopositive for ChAT.

The responses of cholinergic interneurons to stimulation of primary motor cortex and the Pf nucleus of the ITN were examined. The response to cortical stimulation consisted of an increase in firing probability within the first 10 ms, which is indicative of a mono-synaptic connection. This is in line with what has been described previously *in vivo* (Wilson *et al.*, 1990; Reynolds & Wickens, 2004). In most cases this response was followed by a suppression of firing that lasted ~200 ms. Single stimulation applied to the Pf resulted in a short latency increase in firing probability in cholinergic interneurons, consistent with the study by Wilson *et al.,* (1990) which reports short-latency EPSPs in TANs following stimulation of the ITN *in vivo*. The responses to thalamic stimulation, however, were more variable than the responses to cortical stimulation and on average

had a longer latency. When the average latency to first spike was examined, the latency following stimulation was significantly longer after thalamic stimulation relative to cortical stimulation. There are several possibilities for this, and also some technical considerations. Firstly, placement of the stimulation electrode in the Pf nucleus of the ITN was more difficult (relative to placement of the cortical stimulating electrode) due to the fact that it is a much smaller structure. Therefore accurate placement was less consistent, and this could contribute to the greater variability in responses. Another consideration is that neurons of the Pf also project to the cortex, and to the area of cortex which projects to a similar region of striatum (Deschênes *et al.*, 1996b; Smith *et al.*, 2004). Therefore, stimulation of the thalamus presumably results in stimulation of cortex which could then cause a depolarisation of the neurons which project to the striatum, and in turn cause a polysynaptic response in cholinergic interneurons. If the latency to respond to cortex is <10 ms and about the same for the thalamic innervation then one would expect to see two subsequent increases in firing probability, the first due directly to thalamic innervation, and the second due to the activation of corticostriatal neurons. Hence, a possibility for the greater variation in the thalamic response could be due to the subsequent activation of cortical neurons that project to striatum. However, the converse is also true: the Pf receives a cortical innervation from motor cortex layer V neurons in the rat (Cornwall & Phillipson, 1988; Van der Werf *et al.*, 2002). Although a difference in this is that the *same* neurons which project to striatum from the Pf also project to cortex, and the cortical neurons which project to Pf from cortex are thought to be of a different population to those that project to striatum (Cornwall & Phillipson, 1988). This is illustrated schematically in Figure 3.18. A possible way of dissecting this would be to stimulate Pf and temporarily inactivate motor cortex, and examine whether the variation in responses to thalamic stimulation is reduced; or the opposite, stimulate cortex whilst the ITN is inactivated. Another consideration is that stimulation in either cortex or thalamus can cause antidromic stimulation of axons within that nucleus, depending on the current spread. For example, stimulation of cortex could cause antidromic activation of Pf axons which have come via striatum (Fig 3.18), these axons could then depolarise

neurons in striatum as a result of the cortical stimulation. Likewise, stimulation in the Pf could cause antidromic stimulation of axons from cortex which through a variety of lateral interactions within the cortex could alter the responses seen in the neuron which is being recorded from (Fig 3.18). Although all these factors need to be considered, besides using reasonable stimulation intensities, it is difficult to control for all the possibilities. The introduction of newer techniques however, could greatly help reduce these issues, as will be discussed in Chapter 5.

After stimulation, of either cortex or thalamus, cholinergic interneurons showed a decrease in activity, following the initial increase, that lasted for ~200-500 ms depending on the stimulation protocol applied. This is consistent with the reports of Ding and colleagues (2010) except that they only report a suppression of firing (pause) following thalamic stimulation, and not cortical stimulation. The difference is likely to be due to the fact that *in vivo* the networks remains intact, and that inhibition is not blocked. Thus, an important difference in the results reported here is that cortical stimulation is able to elicit a suppression in firing, as well thalamic stimulation. There are many sources of GABA within striatum that could cause a decrease in firing of cholinergic interneurons, including the MSNs which receive innervation from cortex and thalamus and are thus likely to be activated at the same time as the cholinergic interneurons and therfore release GABA locally (Tepper *et al.,* 2004).

The best comparison of the different properties of cortical and thalamic input is when one *individual* cholinergic interneuron exhibits a response to both. This was observed for five cholinergic interneurons, and the probability of response to single pulse stimulation was significantly greater following cortical stimulation than to thalamic stimulation. On average the latency to peak response was longer following thalamic stimulation, although the difference was not significant; when individual neurons were examined the response latencies varied. Again there are caveats to an interpretation of this and because of limitations of recording stability the stimulation intensities were not varied extensively, and therefore the differences in probability could be a reflection of

the fact that greater stimulation intensities are required in the Pf, relative to the motor cortex. However, this suggests that there are important differences between the properties of cortical and thalamic synapses on cholinergic interneurons. Comparatively, *in vitro* recordings from MSNs have shown that cortical and thalamic synapses have distinctive properties (Smeal *et al.*, 2007; Ding *et al.*, 2008; Smeal *et al.*, 2008). The application of different stimulation protocols allowed a more detailed examination of the properties of cortical and thalamic input to cholinergic interneurons.

Paired cortical stimulation protocols were then applied; using the same stimulation protocol as reported in Mallet *et al.,* (2005) (100 ms inter-stimulus interval) who found that FS interneurons preferentially respond to the first pulse of the stimulus, whereas MSNs showed a greater firing probability to the second pulse. The authors attribute this to the fact that the FS interneurons integrate cortical information faster and then rapidly inhibit neighbouring MSNs so that they are under active inhibition at the time of the first pulse, but then able to fire to the second pulse (Mallet *et al.*, 2005). The same inter-stimulus interval was used here to examine whether cholinergic interneurons showed preferential firing to the first or the second pulse of cortical stimulation. For both neurons tested it was found that the neurons responded to both stimuli, but with a preference for the first stimulus, thus the response was depressing. However, it was only possible to carry out this stimulation protocol for two interneurons, and therefore we have to be tentative about the conclusions drawn. This indicates that cholinergic interneurons can rapidly respond to cortical stimulation, and thus are in a position to modulate the cortical input within the striatal microcircuit. There are several possibilities as to why the neurons respond less to the second stimulus, it is unlikely that this is due to active inhibition from the FS interneurons as there is no evidence for an anatomical connection (Chang & Kita, 1992). It could be inhibition from neighbouring MSNs, which also receive cortical inputs and respond within the same time frame (data not shown), or it could be due to the innate physiology of the cholinergic interneurons or the properties of the cortical synapses onto these interneurons.

In contrast to the response of cholinergic interneurons to paired cortical stimulation, cholinergic interneurons responded with a greater probability of firing to the second stimulus of paired thalamic stimulation, thus the response was facilitating. As well as the firing probability, the latency to the second stimulus was also greater. As this is different from the response to cortical stimulation it is likely to be due to the specific properties of the thalamic synapses onto these neurons. Two cholinergic interneurons responded to both paired cortical and paired thalamic stimulation. For both these neurons the cortical response was depressing, whilst the response to thalamic stimulation was facilitating. This indicates that individual cholinergic interneurons can exhibit distinct responses to stimulation of cortex and thalamus *in vivo*.

A high frequency stimulation protocol of a 40 Hz train of 5 pulses was used to further examine the response properties of cholinergic interneurons. This was carried out for five cholinergic interneurons. The neurons generally responded to each pulse in the train with a short latency response (< 10 ms), and with the greatest probability of firing to the 3rd pulse within the train. After stimulation the neurons then had a suppression of firing for > 300 ms. *In vitro*, a 50 Hz stimulation of thalamus can cause a suppression of firing in cholinergic interneurons that lasts 360 – 1300 ms (Ding *et al.*, 2010). Ding *et al.,* (2010) also describe the thalamic stimulation as facilitating, when high frequency stimulation (50 Hz) was given *in vitro* the cholinergic interneuron EPSP increased to each pulse within the stimulation. This was in direct contrast to high frequency stimulation of the cortex which did not cause an increase in the resulting EPSP (Ding *et al.*, 2010). For one of the neurons examined here it was possible to apply the high frequency (40 Hz) stimulation to both cortex and thalamus. The responses from the one neuron were remarkably disparate. The neuron responded to only the first pulse of the cortical stimulation, whereas showed the same increase in firing probability over the course of the thalamic stimulation as had been seen for the other cholinergic interneurons examined. The latency to fire to each pulse of the thalamic stimulation was short (> 5 ms) and consistent. Interestingly, the probability to fire to the first pulse was greater for the cortical stimulation compared to the thalamic stimulation. This is of particular interest since all neurons that responded to

single stimulation of both cortex and thalamus, responded to the cortical stimulation with a greater probability. This also gives further validation for the usage of several different stimulation protocols to fully examine the responses of cholinergic interneurons. Another difference between the two stimulations was that the suppression of firing after thalamic stimulation was longer compared to after cortical stimulation. After thalamic stimulation the neuron was silent for ~ 400 ms, but after cortical stimulation normal firing resumed after < 300 ms. This is also analogous to the results of Ding and colleagues (2010) who describe a prominent pause after thalamic stimulation but not after cortical stimulation.

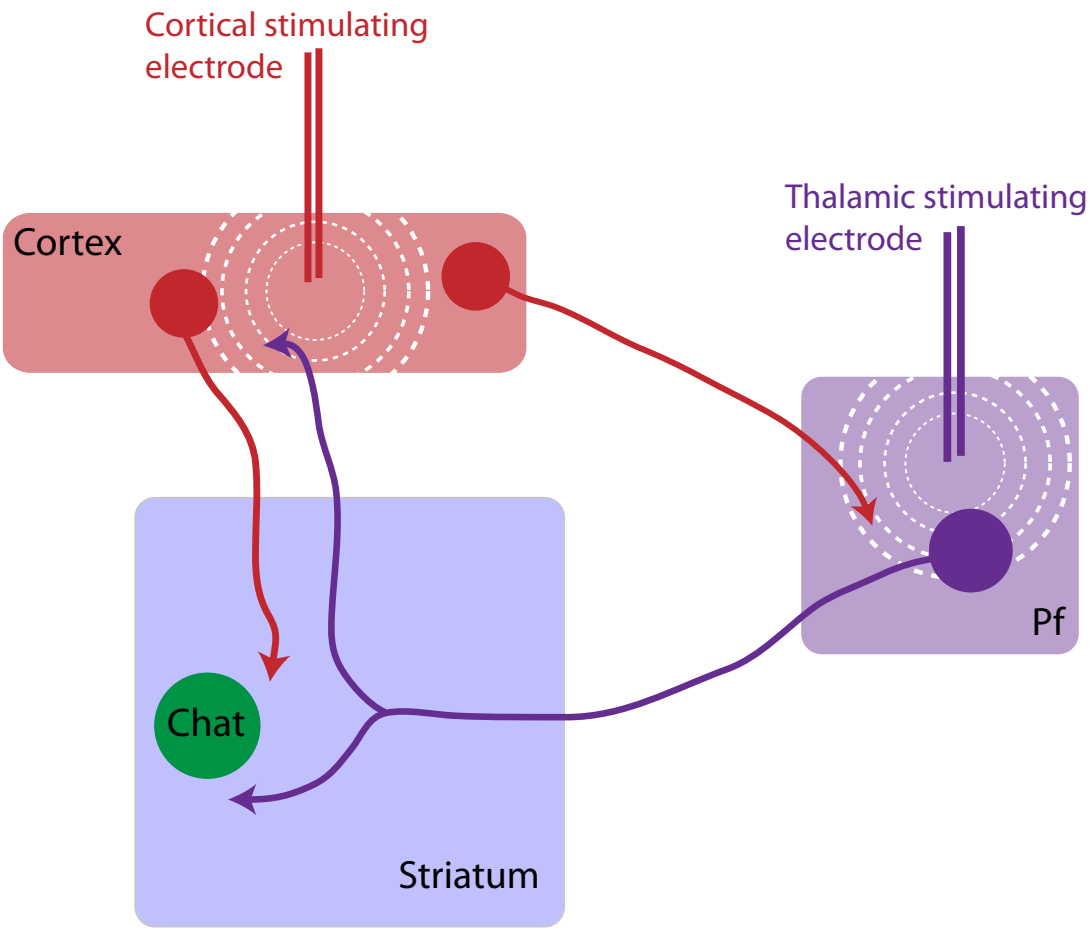


Figure 3.18. Schematic diagram indicating connectivity between the cortex, striatum and Pf nucleus.

Stimulation of the cortex or the thalamus could result in antidromic stimulation of axons, and possibly alter the responses of neurons recorded in striatum.

3.4.2. Technical considerations

The major consideration of this study was the technical challenges in recording from and labelling cholinergic interneurons that responded to *both* cortical and thalamic stimulation. First, cholinergic interneurons are already rare within the striatum contributing only ~1% of the total cell population; this is however made easier by the fact that these neurons have a distinctive physiological profile, and are very different to the much more numerous MSNs. Second, the area of recording is limited because of having to record within an area that is likely to be where the stimulation of both cortex and thalamus are effective, in this case the dorsolateral striatum. However, variation between experiments in the placement of the stimulating electrodes meant that the depth and area of recording was variable, and had to be established every experiment. Third, stability of recordings from putative cholinergic interneurons was variable, and therefore the number and length of stimulation protocols tested had to be tailored for each neuron. And finally, labelling using the juxtacellular method and recovery of the neurons *post mortem* was not always successful.

Chapter Four: Cortical and thalamic synaptic innervation of cholinergic interneurons

4.1. Introduction

Cholinergic interneurons have an important role in reward-related behaviour. Cortical and thalamic inputs converge onto the striatum, and both of these pathways carry distinct information which must then be integrated, and transmitted through the basal ganglia network. How the various subtypes of striatal neurons integrate this information shapes information processing in striatum, and thus striatal output. Cholinergic interneurons respond to cortical and thalamic stimulation with a short latency response, indicative of a monosynaptic connection, *in vivo* (Chapter 3, Wilson *et al.*, 1990; Reynolds & Wickens, 2004) and *in vitro* (Ding *et al.*, 2010). Moreover, *individual* cholinergic interneurons can respond to stimulation of both cortex and thalamus *in vivo* (Chapter 3). These physiological studies suggest a role for the cholinergic interneurons in the integration of cortical and thalamic inputs. Cholinergic interneurons are in a position to alter striatal processing through the various effects of acetylcholine on the MSNs, and thus the output of striatum.

There is strong anatomical evidence to support thalamic innervation of cholinergic interneurons from the Pf in the rat (Lapper & Bolam, 1992), and from the CM in monkeys (Sidibé & Smith, 1999). The cortical innervation has, however, been more difficult to ascertain, and if found it is sparse (Meredith & Wouterlood, 1990; Lapper & Bolam, 1992; Thomas *et al.*, 2000). To analyse the role of cholinergic interneurons in striatum it is essential to examine the relative contributions of cortical and thalamic innervation to an individual cholinergic interneuron.

The influence of dendritic architecture has been shown to have a profound role on the firing properties of a particular neuron (Mainen & Sejnowski, 1996). Thus an examination of the particular characteristics of the dendritic geometry of cholinergic interneurons can reveal important features that are specific to the neuronal cell type. Cholinergic interneurons are known to be large and extend ~500 μm in the dorsoventral and mediolateral planes, and up to 1,000 μm in the rostrocaudal plane (Bolam *et al.*, 1984; Wilson *et al.*, 1990). These figures are based on a 2-dimensional drawing, as that was

what was possible with the technology at that time. However 3-dimensional drawings can provide more detailed analyses. It is also important to note here that the 3-dimensional dendritic geometry of a neuron is necessary for biologically realistic single neuron models that can be used for computational analyses of particular neurons and their networks. The size and complexity of a neurons dendritic arbor is indicative of the tendency for that neuron to receive either many inputs from a few neurons or few inputs from many different neurons (Fiala *et al.*, 2008).

Quantitative studies of synaptic innervation can provide insight into the functions of individual neurons, and their role within networks (Gulyás *et al.*, 1999; Megias *et al.*, 2001; Henny *et al.*, 2012). The relative contribution and sub-cellular location of excitatory and inhibitory synapses is important for the computing of information within the dendrites of a neuron (Koch *et al.*, 1983; Koch, 1999). In essence, the output of a neuron is determined by the nonlinear summation of its relative inputs; therefore a detailed understanding of the innervation to an individual neuronal cell type can provide insight into function. Again, these variables are also extremely valuable for the computational analysis of specific neuron subtypes and their network connectivity.

4.1.1. Aims

Cholinergic interneurons integrate information from both cortex and thalamus in order to carry out their specific function within the striatal network. The detailed pattern of innervation to cholinergic interneurons can provide insight into how these neurons integrate information and thus contribute to striatal processing and function. Although it has been shown that cholinergic interneurons receive inputs from the ITN, there is very little anatomical evidence to support cortical innervation of these neurons, despite physiological evidence which supports this connectivity (Meredith & Wouterlood, 1990; Wilson *et al.*, 1990; Lapper & Bolam, 1992; Sidibé & Smith, 1999; Thomas *et al.*, 2000; Reynolds and Wickens, 2004).

The relative contributions of inputs to individual neurons, and the location of the synapses on the dendritic arbor can provide insight into function (Henny *et al.,* 2012).

The aim of this study was to investigate the synaptic innervation of physiologically characterised individual cholinergic interneurons. To determine the relative contribution of cortical and thalamic inputs to the various compartments of the dendritic tree, selective markers were used, VGluT1 and VGluT2 respectively. The relative contribution of asymmetric and symmetric synapses was analysed in all parts of the dendritic arbor.

4.2. Methods and Materials

4.2.1. Tissue

Four cholinergic interneurons, from four animals, were processed for electron microscopy. The first neuron was used in a pilot study to establish the immunohistochemical and electron microscopic protocols. All the neurons showed typical cholinergic interneuron firing properties, as discussed in chapter three. The four neurons used here were positive for ChAT. The responses of these neurons to stimulation of cortex and/or thalamus is also summarised in Table 3.2 (Chapter 3).

4.2.2. Immunohistochemistry

Four identified cholinergic interneurons were processed for electron microscopic analysis AJS046, neuron E, neuron H, and neuron L (See Table 3.2). Sections containing neuronal processes (lateral and medial of the section containing the soma) were isolated for EM processing; in all four cases at least 6 sections (300 μm) on either side of the cell body section were processed. A low magnification (x1.25) fluorescence image was taken of the soma at this point so that localisation of the cell body would be easier during processing. The following describes the methods used after optimisation during the pilot study. The methods used are summarised in Figure 4.1, the antibodies used during processing are summarised in Table 4.1, and the immunohistochemical protocol is summarised in Table 4.2.

Sections were washed in PBS three times and then incubated in cryoprotectant (25% sucrose, 10% glycerol) overnight at 4º. Sections (one at a time) were then placed in one well of a 6-well plate. The section was laid flat and excess cryoprotectant was removed using filter paper. The well plate was then lowered over liquid nitrogen until the section froze and went opaque. The section was then rapidly thawed using cryoprotectant which had been kept at room temperature. The sections were then incubated in cryoprotectant for at least one hour at room temperature, or until all sections had sunk to the bottom of the glass vial. The freezing process was then repeated for all of the sections and the sections

were thawed with 0.1 M PB which was kept at room temperature. All the sections were then washed in 0.1 M PB twice and three times in PBS.

Sections were incubated in PBS containing 10% NDS for 1 h at room temperature, on a shaker. The sections were then incubated in ABC (1:250; Vector; prepared according to manufactures instructions) in a 1% NDS PBS solution.

After incubation in ABC, the sections were washed three times in PBS, followed by three washes in 0.1 M PB, pH 6.0. A peroxidase reaction using tetramethylbenzidine (TMB) as the chromogen was then performed to reveal the neuron. Sections were placed for 20 min in a pre-incubation solution containing the following: 80 ml of 0.1 M PB, pH 6.0, 4 ml of ammonium paratungstate (1% in deionised H_2O), 1 ml of TMB (0.2% dissolved in absolute ethanol; Sigma-Aldrich T5525), 800 µl of ammonium chloride (0.4% in deionised H_2O), and 800 µl of D-glucose (20% in deionised H_2O). To perform the reaction, the pre-incubation solution was removed and replaced with the reaction solution, which consisted of 2 ml of the pre-incubation solution (as above) plus 2 µl of glucose oxidase (Sigma G6891). The reaction was initially carried out on the section containing the cell body in order to gauge the optimum processing time; the section was wet-mounted and checked under a microscope (X40). The reaction was then allowed to progress for all sections for between 6-8 min depending on the neuron. The reaction was stopped with 0.1 M PB, pH 6.0. Sections were then washed three times for 5 min with 0.1 M PB, pH 6.0. The reaction was then stabilised by incubation in a solution containing the following: 400 µl of ammonium chloride (0.4% in deionised H_2O), 400 µl of D-glucose (20% in deionised H2O), 800 µl of cobalt (II) chloride (1% in deionised H_2O), and 40 mg of DAB dissolved in 40 ml of 0.1 M PB, pH 6.0. The stabilisation solution was filtered before use. Sections were incubated for 15 min at room temperature. The stabilisation solution was then removed and replaced with three 10 min washes of 0.1 M PB, pH 6.0. During stabilisation, the blue-staining colour from the reaction step changes to a darker magenta colour and background staining is reduced. Sections were then washed three times in 0.1 M PB, pH 7.4.

Alternate sections were processed to reveal VGluT1 or VGluT2 labelling, using the peroxidase-anti-peroxidase (PAP) method (Bolam, 1992). Alternate sections were incubated in a primary antibody for either VGluT1 or VGluT2 (both 1:2000) at room temperature in PBS (see Table 4.1 for details). The sections were then incubated in an un-conjugated antibody (1:100; Table 4.1). Following this the sections were then washed (3X PBS) and incubated in a peroxidase-anti-peroxidase (PAP) complex (1:400; see Table 4.1). The sections were then washed in PBS three times, followed by 3 washes in Tris buffer. A peroxidase reaction using DAB as the chromogen was used to reveal VGluT1 and VGluT2 labelling in alternate sections. Sections were incubated in a solution containing DAB (0.05%) dissolved in TRIS buffer for 20 min. Hydrogen peroxidase (H_2O_2) was then added to the solution to achieve a final concentration of 0.01%. The reaction was monitored using a dissection microscope. All sections were incubated for between three and four minutes. They were then washed in Tris buffer three times, followed by three washes in 0.1M PB, pH 7.4.

Sections were then placed flat on the bottom of glass Petri dishes and post-fixed in osmium tetroxide (1% in PB; Oxkem) for 25 min. They were then washed in 0.1 M PB and dehydrated in an ascending series of ethanol dilutions [15 min in 50% ethanol, 35 min in 70% ethanol that included 1% uranyl acetate (TAAB), 15 min in 95% ethanol, and twice for 15 min in absolute ethanol]. After absolute ethanol, sections were washed twice in propylene oxide (Sigma) for 15 min, and placed into resin (Durcupan ACM; Fluka) and left overnight at room temperature. The resin was then warmed to reduce its viscosity, sections were placed on microscope slides, a cover-slip was applied, and the resin was cured at 65°C for approximately 72 h.

4.2.3. Digital reconstruction and analysis

The three-dimensional reconstruction was performed using Neurolucida (MicroBrightField, MBF), in a Nikon Eclipse microscope equipped with an x-y-z motor stage and Lucivid (MBF) using an oil immersion objective (x60). For each section the striatal contour was traced (at a lower magnification), followed by tracing the neuron

starting with the cell body section and working outwards towards the distal dendrites. For all tracing the z-axis was checked repeatedly. During the tracing 'high' and 'low' endings were labelled appropriately. An un-spliced version was saved to assist with locating dendritic fragments for re-embedding and ultramicrotoming. The tracings within the separate sections were then spliced using Neurolucida (MBF) and the final version was corrected for shrinkage in all dimensions: x (6.3%), y (6.0%) and z (8%) (Sadek *et al.*, 2007). Quantitative data from the reconstructions was then obtained using Neuroexplorer (MBF). For the Sholl analysis, radius segments of 50 μm were used. The data was then exported to Microsoft Excel (2007).

4.2.4. Re-embedding and ultramicrotoming

Light microscope images (x20) were taken through each section and then overlaid with the tracings of each section to aid with dendritic fragment localisation during re-embedding, ultramicrotoming and electron microscopy. At least one dendritic fragment was re-embedded from each sagittal section, and the 'high endings' were used wherever possible. For re-embedding the cover slips were removed, the slides were placed on a heater and a piece of tissue was removed using a scalpel and a pair of forceps, using a dissection microscope (Leica). The tissue was then glued to the top of a cylinder of resin using super-glue. It is important to retain the correct 'sidedness' of the tissue as this helps greatly with ultramicrotoming and EM.

The blocks were then trimmed using double-edged blades. The dendritic fragments within the tissue on the resin block were located and high and low endings were identified. The 'high endings' were preferentially used where possible. Ultrathin sections (50 nm) containing the pieces of dendrite were then cut on an ultramicrotome (Leica Microsystems, EM UC6), using a diamond knife. Sections were collected in a series of at least 6 sections per single slot copper, pioloform coated grid. The sections were then contrasted using lead citrate.

4.2.5. Electron microscopy

The top of the block was examined (using a x40 objective) after ultrathin sectioning to establish whether VGluT1/2 staining was still apparent. The dendritic fragments within that block were examined, and their location within the ultrathin sections was established using the electron microscope. A low magnification image of each grid was taken (X47) and the sections were numbered. The dendritic fragment(s) within each section was then imaged at a suitable magnification (x13,500 - x46,000). Each dendritic fragment was analysed through several grids, and in serial section on each grid, with a minimum of 6 sections analysed per grid. The major factor limiting the extent of dendrite that could be analysed was the penetration of the VGluT1/2 antibodies. In general only a penetration of a maximum of ~5 μm was achieved for each section. This limited the amount of dendrite able to be examined within each section.

4.2.6. Analysis

Electron micrographs were then analysed using ImageJ software (v1.41o, NIH, http://rsb.info.nih.gov/ij). To control for the possibility of VGluT-false-negative terminals only serial sections on a grid were examined if there was at least one VGluT1/2-positive profile present in one of the sections on the grid. On a random section per grid the perimeter and area of each dendritic fragment was measured. Every synapse was recorded, and the number of sections that it was apparent in; measurements were carried out on the section where the synapse was most evident. Every presynaptic terminal forming a symmetric or an asymmetric synapse with the labelled dendrite was recorded, and the perimeter and area of all presynaptic terminals was measured. The length of the post-synaptic density for every synapse formed with the cholinergic dendrite was measured. Brightness and contrast were adjusted using Adobe Photoshop (CS3, Adobe Systems inc, San Jose, CA). Synaptic density was calculated as the number of synapses divided by the length of dendrite (μm) examined (in the z-axis) and then normalised for number of synapses per 10 μm.

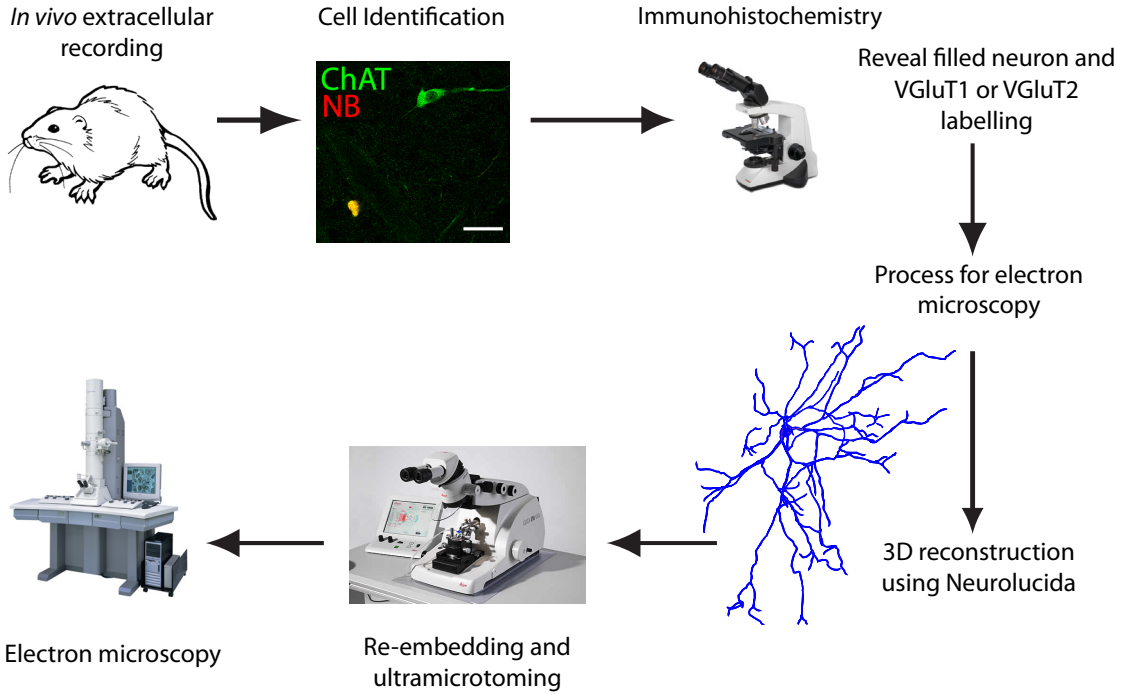


Figure 4.1. Schematic diagram illustrating the methods used.

The first stage was to record cholinergic interneurons in the anaesthetised animal (as described in Ch 3). The neuron filled with neurobiotin (NB) was then identified using an antibody for ChAT. Immunohistochemistry was then carried out to examine the neuron and alternate sections were incubated in an antibody against either VGluT1 or VGluT2. After processing for electron microscopy the neuron was reconstruction in three dimensions. Fragments of dendrite were then re-embedded and ultrathin sections ultramicrotomed so that the synaptic innervation of the dendrites could be analysed with the electron microscope.

Table 4.1. Summary of the antibodies used during processing.

Antigen	**Species**	**Manufacturer**	**Cat no**	**Dilution**	**Incubation Time**
VGluT 1	Rabbit	MAb Tech	VGT1-3	1 in 2000	Overnight
VGluT2	Rabbit	Synaptic Systems	135403	1 in 2000	Overnight
Rabbit IgG	Donkey	Jackson	711-035-152	1 in 100	> 4 hours
PAP	Rabbit	Jackson	323-005-024	1 in 400	> 4 hours

Table 4.2 Summary of the processing of the neurons

Timeline	Processing
Day 1	Neuron localised
	Low magnification fluorescence image taken (1.25X)
	Sections with neuronal processes arranged in order
	Sections incubated in cryoprotectant overnight
Day 2	Sections freeze-thawed
	Sections blocked (10% NDS) for >1 h
	Incubated overnight in ABC at a concentration of 1:250
Day 3	Peroxidase reaction (TMB) carried out to reveal the neuron
	Sections incubated for 5-8 min
	Alternate sections incubated in either VGluT1 or VGluT2 antibodies overnight
Day 4	Incubate in un-conjugated secondary antibody for > 4 h for PAP method
Day 5	Incubate in PAP for > 4 h
	Peroxidase reaction (DAB) carried out to reveal either VGluT1 or VGluT2 staining
Day 6	Osmium and dehydration
	Infiltrate with resin overnight
Day 7	Sections mounted onto slides
	Incubated in oven at 60° for ~72 h
Days 9-15	3D-reconstruction of neuron using Neurolucida (MBF)
Days 15 +	Re-embedding and ultramicrotoming
Days 16 +	Electron microscopic analysis

4.3. Results

4.3.1. Dendritic organisation of cholinergic interneurons

The dendritic arbors of three ChAT-positive striatal interneurons were reconstructed in their entirety (Figures 4.2, 4.3, and 4.4). Neuron H (Fig 4.2) has three primary dendrites, with the longest dendrite traversing over 700 μm from the soma (Figure 4.2h). Neuron E (Fig 4.3) has six primary dendrites, the longest of which traversed over 600 μm from the cell body (Fig 4.3h), and neuron L (Fig 4.4) has three primary dendrites, the longest of which was over 500 μm from the cell body (Fig 4.4h). The basic dendritic parameters of each neuron are summarised in Table 4.3. The average total dendritic length was 9,411.4 μm (± 885.0 μm), the approximate average total surface area was 16,478 μm^2 (± 2,122.3 μm^2), and the approximate average volume of the neuron was 4,564.6 μm^3 (± 895.2 μm^3) (Table 4.3).

To further examine the dendritic arbors of these neurons, a Sholl analysis was performed (Figure 4.5). Sholl analysis involves drawing concentric spheres outwards from the soma with incremental radii (Fiala *et al.*, 2008). For the analysis, the radius distance used was 50 μm. The average total dendritic length was greatest within the concentric spheres that were 150-200 μm from the soma (Fig 4.5a), and when each neuron was examined individually it is apparent that they follow the same pattern (Fig 4.5b). The average approximate surface area of the dendrites was greatest at 100-150 μm from the soma (Fig 4.5c). The approximate volume of the neurons was greatest in the first radial segment, which is within the first 50 μm from the soma; this is most likely due to the fact that neurons have the greatest dendritic diameter proximal to the cell body (Fig 4.5d). The number of branch points in each segment was also analysed, and the greatest number of branch points was between 200 to 250 μm from the soma, although this is also where the greatest variation was (Fig 4.5e). The number of intersections dendrites have with the Sholl radii is a representative measure of the overall density of the dendritic arbor (Fiala *et al.*, 2008). On average, the greatest number of intersections with the Sholl radii was at between 150-200 μm from the cell body (Fig 4.5f).

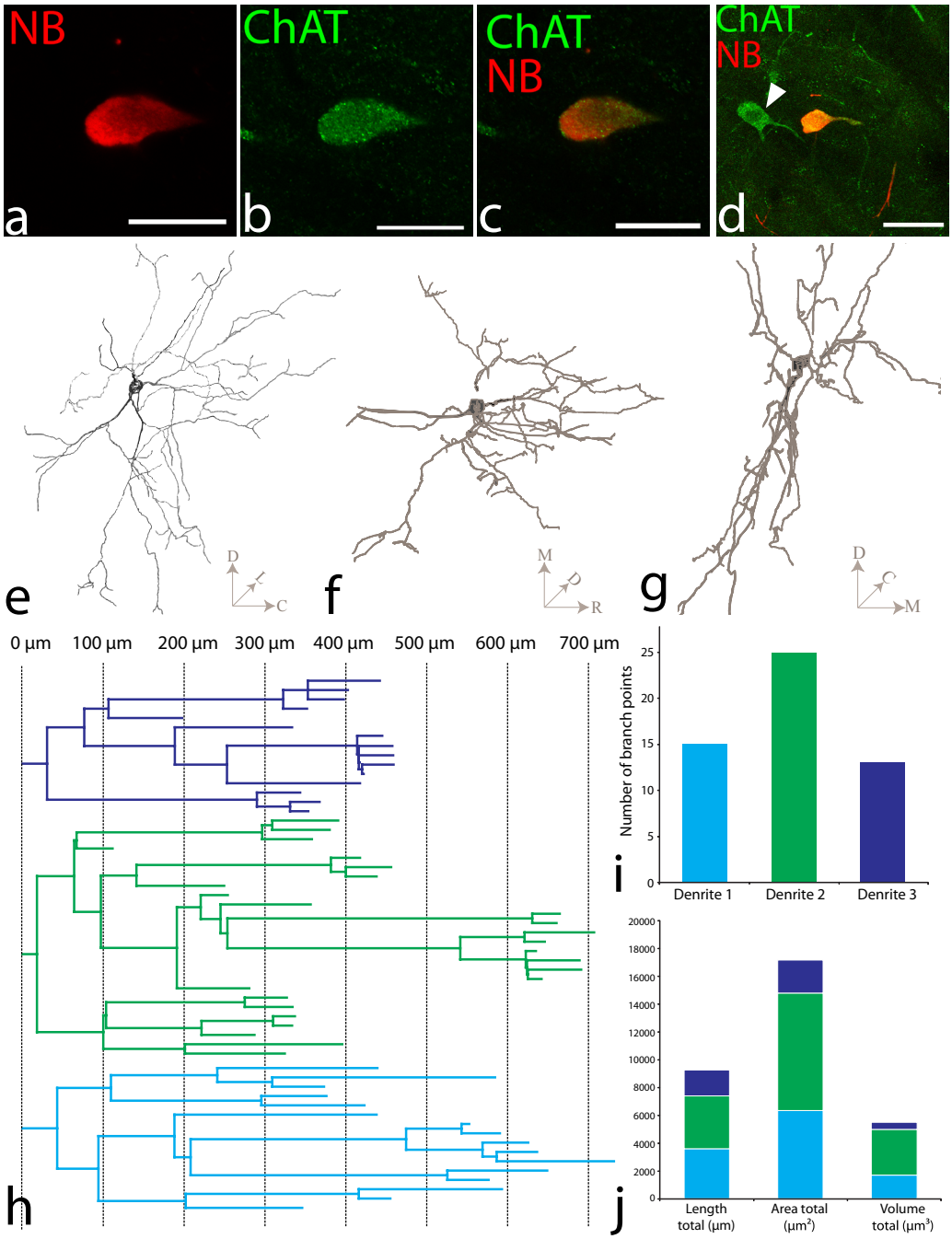


Figure 4.2. Analysis of the dendritic of an individual cholinergic interneuron, neuron H.

a) Cell body of neuron H filled with neurobiotin (NB), ***b)*** Cell body of neuron H showing ChAT immunoreactivity, ***c)*** Merged confocal fluorescence micrograph for ChAT and NB, Scale bars, 25 µm. ***d)*** Wide confocal micrograph showing the same neuron as in a, b and c and another ChAT-positive neuron that is negative for NB (arrowhead; Scale bar, 50 µm). ***e)*** Reconstruction of neuron H, frontal view, horizontal ***(f)*** and sagittal view ***(g)***. (D, dorsal; C, caudal and M, medial) ***h)*** Dendrogram of neuron H showing length and branching of the three primary dendrites, ***i)*** Total number of branch points for each primary dendrite, ***j)*** Total length, surface area and volume of neuron H showing the relative contributions of each primary dendrite; for both i and j, dendrites are coloured as in h.

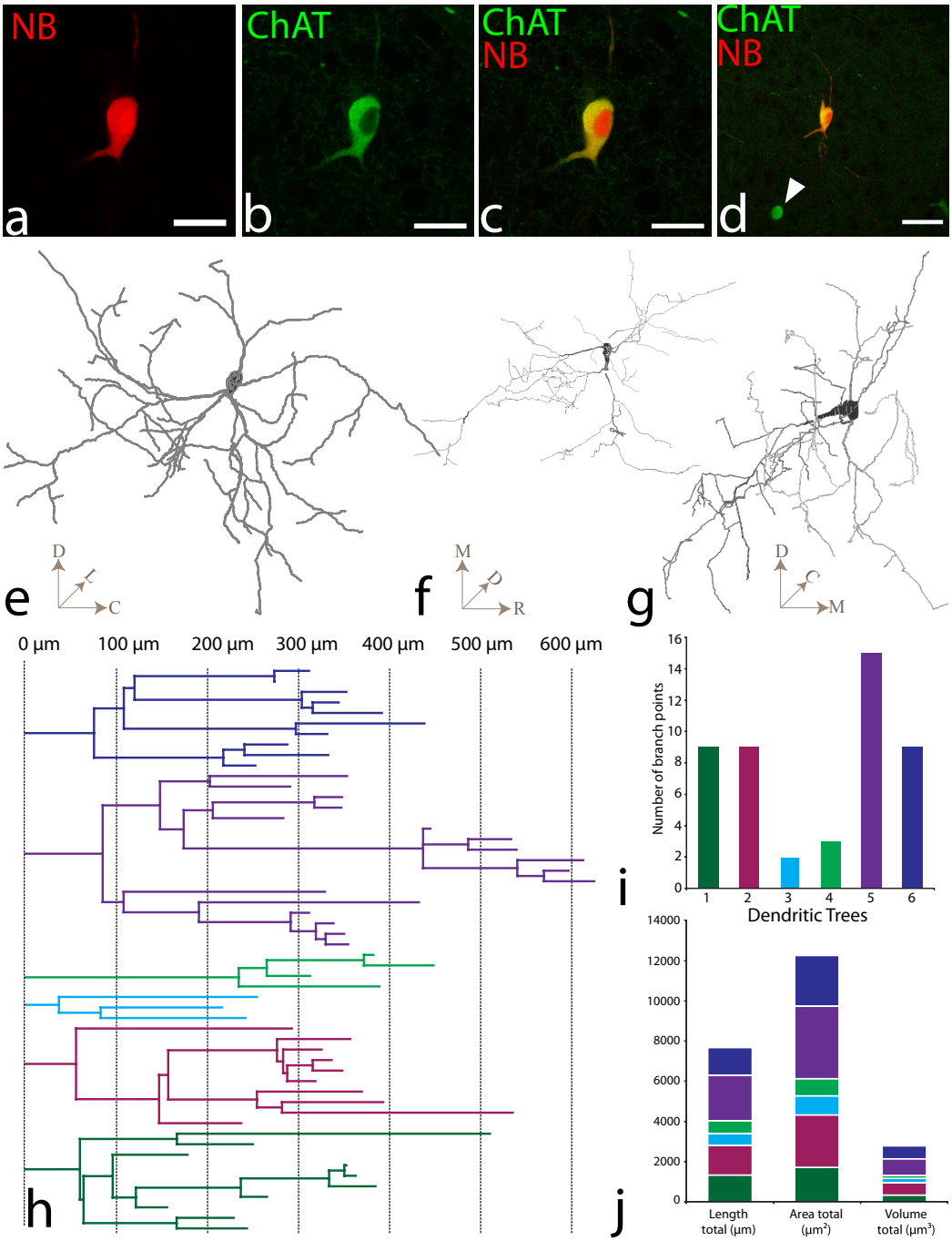


Figure 4.3.Analysis of the dendritic of an individual cholinergic interneuron, neuron E

a) Cell body of neuron E filled with neurobiotin (NB), ***b)*** Cell body of neuron E positive for ChAT immunolabelling, ***c)*** Merged confocal fluorescence micrograph for ChAT and NB (Scale bars, 25 µm). ***d)*** Wide confocal micrograph showing the same neuron as in a, b and c and another ChAT-positive neuron that is negative for NB (arrowhead; Scale bar, 50 µm). ***e)*** Reconstruction of neuron E, frontal, horizontal ***(f)*** and sagittal views ***(g)*** (D, dorsal; C, caudal and M, medial). ***h)*** Dendrogram of neuron E showing the length and branching of the three primary dendrites, ***i)*** Total number of branch points for each primary dendrite, ***j)*** Total length, surface area and volume of neuron E showing the relative contributions of each primary dendrite; for both i and j, dendrites are coloured as in h.

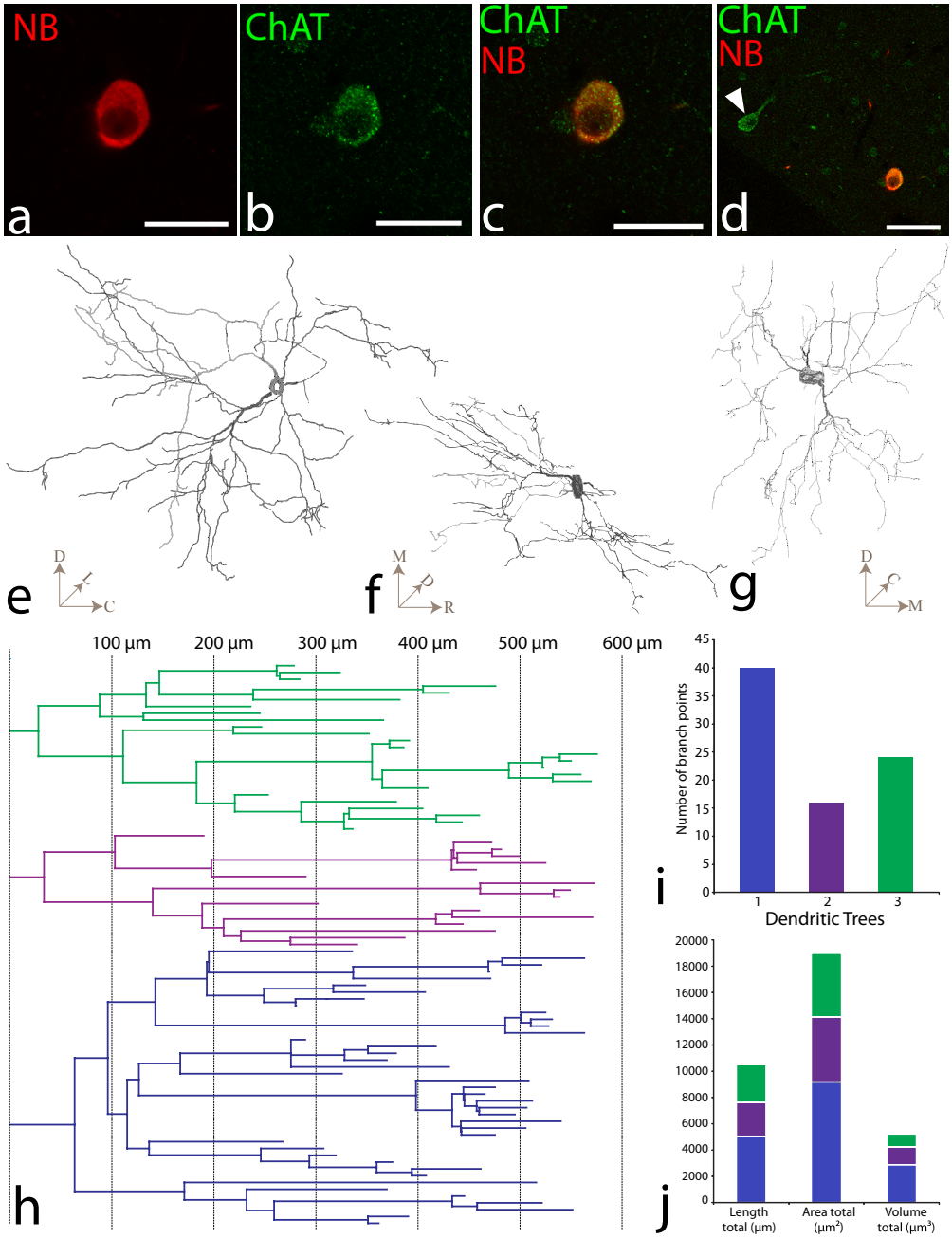


Figure 4.4. Analysis of the dendritic of an individual cholinergic interneuron, neuron L

a) Cell body of neuron L filled with neurobiotin (NB), ***b)*** Cell body of neuron L positive for ChAT immunolabelling, ***c)*** Merged confocal fluorescence micrograph for ChAT and NB (Scale bars, 25 µm). ***d)*** Wide confocal micrograph showing the same neuron as in a, b and c and another ChAT-positive neuron that is negative for NB (arrowhead) (Scale bar, 50 µm). ***e)*** Reconstruction of neuron L, frontal, horizontal ***(f)*** and sagittal views ***(g)*** (D, dorsal; C, caudal and M, medial). ***h)*** Dendrogram of neuron L showing the length and branching of the three primary dendrites, ***i)*** Total number of branch points for each primary dendrite, ***j)*** Total length, area and volume of neuron L showing the relative contributions of each primary dendrite; for both i and j, dendrites are coloured as in h.

Table 4.3. Dendritic properties of reconstructed cholinergic interneurons.

Dendritic Parameters	Neuron H	Neuron E	Neuron L	Average	± SEM
Number of primary dendrites	3	6	3	**4**	**1**
Branch points (nodes)	55	47	80	**60.67**	**9.94**
Endings	60	54	84	**66.00**	**9.17**
Total length (µm)	10,061.00	7,660.70	10,512.40	**9,411.37**	**884.98**
Approximate surface area (μm^2)	18,179.30	12,259.60	18,995.10	**16,478.00**	**2,122.31**
Approximate volume (μm^3)	5,634.35	2,771.12	5,234.18	**4,546.55**	**895.20**

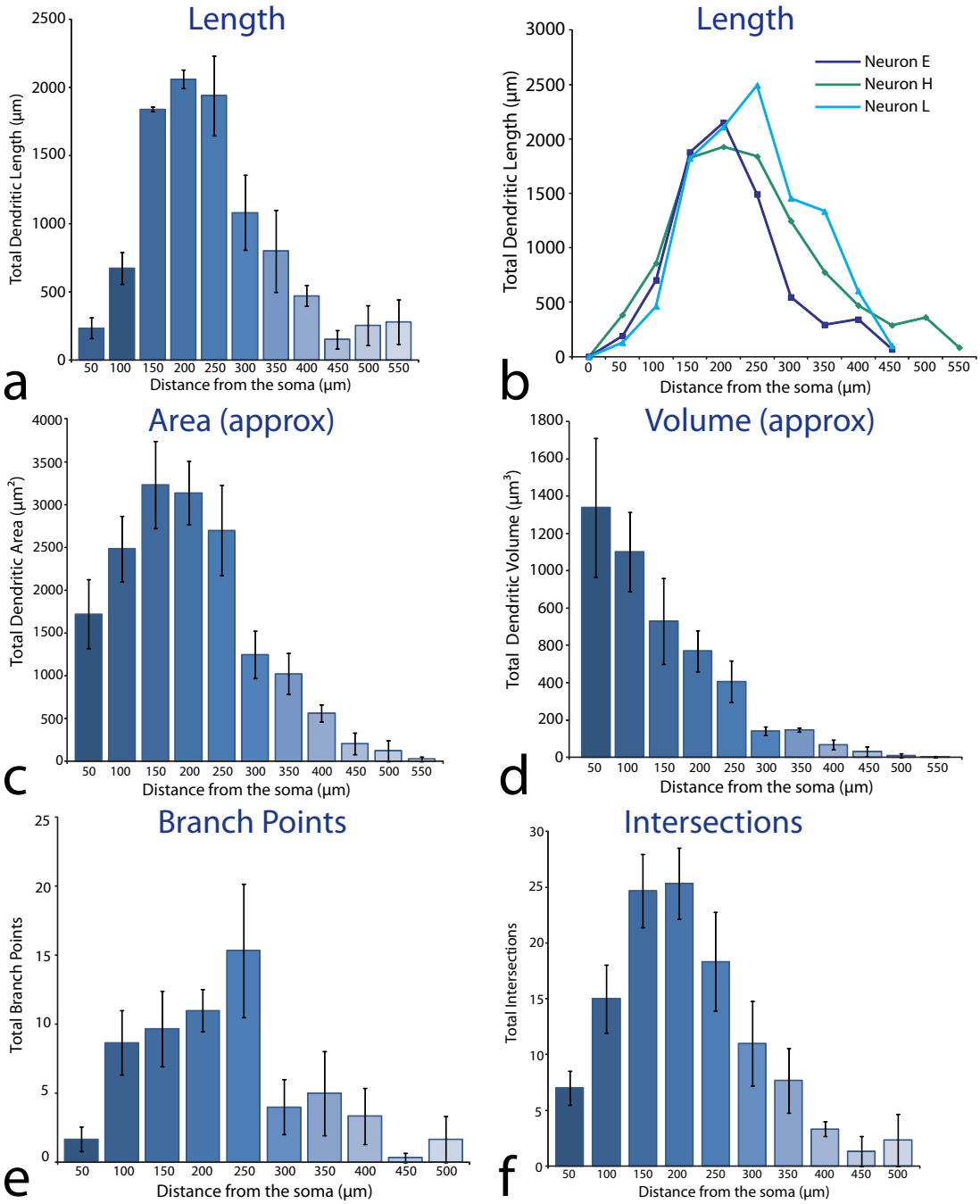


Figure 4.5. Sholl analysis of the dendrites of the reconstructed cholinergic interneurons.

a) Average length within each concentric 50 µm radial sphere from the soma, error bars indicate SEM (n=3). ***b)*** The length of neurons E, H and L within each Sholl segment. ***c)*** Average approximate surface area within each radial segment. ***d)*** Average approximate volume within each segment. ***e)*** Average number of branch points within each radial segment. ***f)*** Average number of intersections with the Sholl radii per segment.

4.3.2. Synaptic innervation of cholinergic interneurons

The synaptic innervation to two of the three reconstructed cholinergic interneurons was examined using electron microscopy; neuron H and neuron E. Fragments from all parts of the dendritic tree were analysed in serial sections in tissue labelled for either VGluT1 or VGluT2. The total number of VGluT-positive, asymmetric and symmetric synapses was counted for each fragment of dendrite. For neuron H, 20 fragments were analysed; 11 in VGluT1-labelled tissue and 9 in VGluT-2 labelled tissue (Table 4.4) and 24 fragments were analysed for neuron E; 14 in VGluT1-labelled tissue, and 10 in VGluT2-labelled tissue (Table 4.5). For each fragment, an average of 42, and 43 sections were analysed for neurons H and E, respectively (See tables 4.4 and 4.5 for number of sections per fragment). This is equivalent to ~2 μm in the z-axis (assuming each ultrathin section is 50 nm) per fragment. For each fragment, the distance from the soma was estimated using the three-dimensional reconstruction, the distance indicated is the distance from the origin of the primary dendrite *along* the dendrite to the marker indicating the fragment (Tables 4.4 and 4.5). In order to classify fragments as 'distal' or 'proximal' the distance from the soma was calculated as a percentage of the total length of the longest dendrite which was 731.7 μm for neuron H and 624.8 μm for neuron E. Fragments that were between 0 and 20% of the distance of the longest dendrite were considered to be 'proximal', and similarly dendrites within 20 to 100% of the total dendritic length were considered 'distal'.

In the dednritic fragments analysed, 90 terminals formed synapses with the dendrites of neuron H; and 120 terminals were found to form synapses with the dendrites of neuron E. For neuron H, no VGluT1-positive terminals were found to form asymmetric synapses with the dendrite, whereas 6 VGluT2-positive terminals formed asymmetric synapses with the dendrite (Table 4.4, Figure 4.6). The VGluT2-positive synapses were distributed over the dendritic tree; 2 synapses formed with proximal dendrite, whilst the other four were at distances between 36.5% and 79.8% of the total distance (Table.4.4).

Both VGluT1- and VGluT2- positive terminals were found to form asymmetric synapses with the dendrite of neuron E (Figure 4.7; Table 4.5). Neuron E formed synapses with 2 VGluT1-postive terminals and 5 VGluT-2 positive terminals (Table 4.5). One of

the VGluT-1 terminals formed a synapse with a dendritic fragment that was proximal to the cell body (Table 4.5). The VGluT2-positive synapses were formed with dendrites that were between 24% - 28% of the total dendritic distance (Table 4.5).

Unlabelled terminals also formed both asymmetric and symmetric synapses with neuron H (Fig 4.8) and neuron E (Fig 4.9). The majority of synapses formed by the dendrites of these neurons were with unlabelled terminals forming symmetric synapses; a total of 61, and 62 synapses for neurons H and E, respectively (Fig 4.10). The next largest category was unlabelled terminals forming asymmetric synapses with the dendrites of neuron H and E; 23 and 32 synapses, respectively (Fig 4.10). For both neurons symmetric synapses constituted ~2/3 of the total synaptic innervation, and ~1/3 was composed of asymmetric synapses, over the entire dendritic tree (Fig 4.10).

In order to further examine the pattern of synaptic innervation, synaptic density was examined over the different dendritic compartments (Figure 4.11). The average asymmetric synaptic density (including terminals that were VGluT-positive) was between 3.8 to 10.4 synapses per 10 μm, and was the greatest in the compartment that was 60% - 80% of the distance from the soma, and the lowest in the most distal regions examined (80% - 100%; Fig 4.11). The average symmetric synaptic density was between 10.2 to 15 synapses per 10 μm, and was greatest in the 40% - 60% compartment of the dendritic tree, and the lowest in the 60% - 80% compartment and on average showed less variation than the asymmetric synaptic density (Fig 4.11). In most compartments the symmetric synaptic density is greater than the asymmetric synaptic density, and this is especially prominent in the first 40% of dendritic tree and in the most distal compartment (80% - 100%; Fig 4.11). The average asymmetric density is marginally greater than the symmetric density in the 60% - 80% compartment (Fig 4.11). Neuron H has a higher symmetric synaptic density than asymmetric synaptic density in all compartments of the dendritic tree (Fig 4.11). Neuron E however, has a greater asymmetric synaptic density than symmetric synaptic density in the 40% - 80% compartment of the dendritic tree. Overall, both neurons have a greater symmetric synaptic density than asymmetric synaptic density in the proximal

compartment, the 20% - 40% compartment, and the most distal compartment (Fig 4.11). The overall ratios and distributions of symmetric and asymmetric synapses, and the distribution of the VGluT-positive synapses are illustrated in figure 4.12.

Table 4.4. Synaptic input to each fragment of dendrite examined for an indivdidual cholinergic interneuron, neuron H.

Distance from soma is along the dendrite, and the % of total distance is the % of the distance of the longest dendrite, 731.7 µm in this case. The column 'microns analysed' is the distance in the z-axis based on the assumption that the ultrathin sections are 50 nm thick.

Dendritic fragment	Labelling	Distance from soma (µm)	Percentage of total distance	Sections examined	Microns analysed (z-axis)	Asymmetric synapses	VGluT-positive synapses	Symmetric synapses
1	**VGLUT1**	2.10	0.29	45	2.3			
2		5.20	0.71	82	4.1	2		5
3		74.6	10.20	49	2.5			6
4		193.8	26.49	14	0.7	1		
5		233.5	31.91	32	1.6	1		1
6		238.3	32.57	29	1.5	3		4
7		277.1	37.87	24	1.2	1		1
8		418.3	57.17	36	1.8	2		3
9		483.2	66.04	31	1.6			1
10		611.2	83.53	28	1.4	1		2
11		619.5	84.67	37	1.9	0		2
12	**VGLUT2**	84.5	11.55	58	2.9	2	1	6
13		89.3	12.20	56	2.8	1	1	2
14		103.6	14.16	65	3.3	2		6
15		266.9	36.48	42	2.1		1	7
16		287.2	39.25	56	2.8		1	2
17		309.6	42.31	46	2.3	1		5
18		499.0	68.20	69	3.5	2	1	4
19		583.9	79.80	26	1.3	3	1	2
20		583.9	79.80	24	1.2	1		2
	TOTAL			**849**	**42.45**	**23**	**6**	**61**

Table 4.5 Synaptic input to each fragment of dendrite examined for an individual cholinergic interneuron E.

Distance from soma is along the dendrite, and the % of total distance is the % of the distance of the longest dendrite, 624.8 µm in this case. The column 'microns analysed' is the distance in the z-axis based on the assumption that the ultrathin sections are 50 nm thick.

Dendritic fragment	Labelling	Distance from soma (µm)	Percentage of total distance	Sections examined	Microns analysed (z-axis)	Asymmetric synapses	VGluT-positive synapses	Symmetric synapses
1	**VGLUT1**	34.1	5.46	80	4	3		2
2		65.0	10.40	15	0.8			1
3		70.5	11.28	33	1.7	1		4
4		86.0	13.76	36	1.8	1		2
5		97.0	15.52	45	2.3	2	1	
6		152.6	24.42	47	2.4	1		4
7		207.6	33.23	40	2			2
8		266.1	42.59	23	1.2	4	1	3
9		285.8	45.74	45	2.3	1		5
10		296.9	47.52	40	2	2		
11		307.7	49.25	21	1.1	1		1
12		315.4	50.48	40	2	2		1
13		377.1	60.36	52	2.6	3		2
14		563.1	90.12	55	2.7	1		5
15	**VGLUT2**	0.1	0.00	41	2.05	2		6
16		46.5	7.44	41	2.05	3		4
17		148.7	23.80	70	3.5	1		1
18		152.4	24.39	36	1.8		3	1
19		152.4	24.39	46	2.3			6
20		152.4	24.39	52	2.6			3
21		159.0	25.45	73	3.65		1	6
22		169.7	27.16	9	0.45		1	
23		417.7	66.85	67	3.35	3		3
24		507.6	81.24	32	1.6	1		
	TOTAL			**1039**	**51.6**	**32**	**7**	**62**

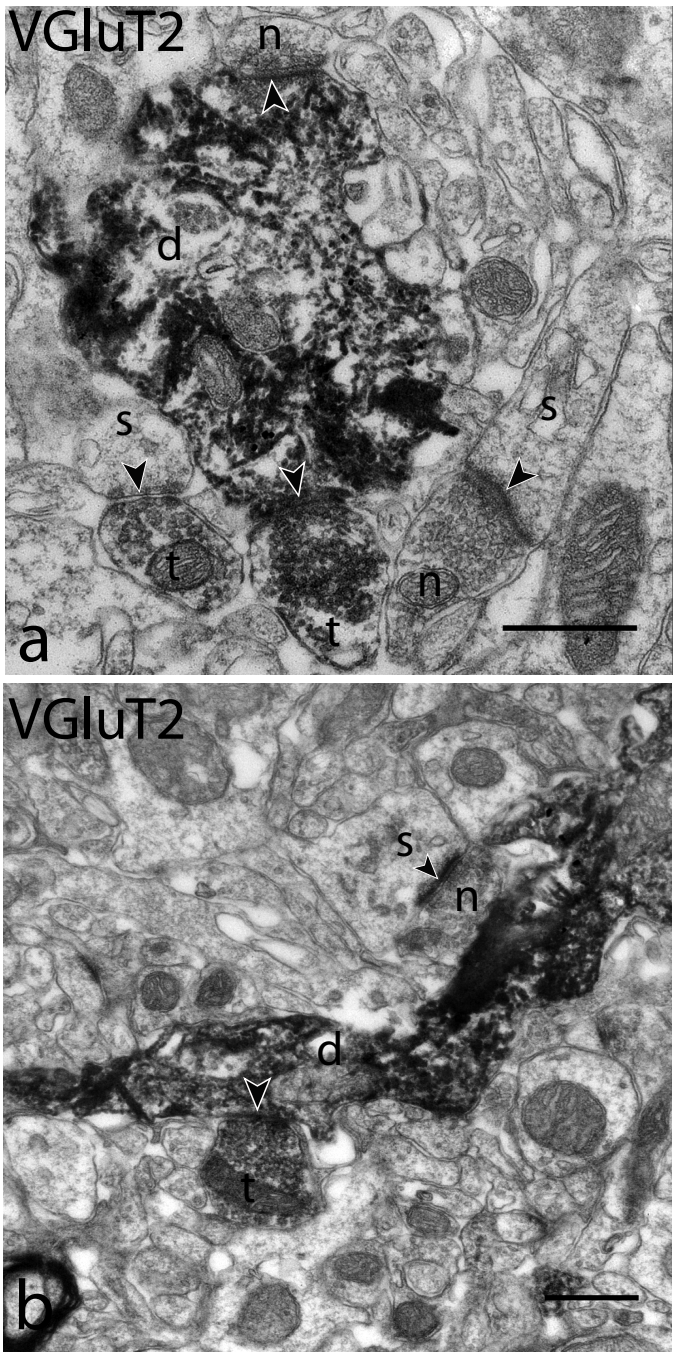


Figure 4.6. VGluT2-positive terminals form asymmetric synapses with the dendrites of a cholinergic interneuron.

a) A VGluT2-positive terminal (t) forms an asymmetric synapse (arrowhead) with a dendrite of neuron H (d). A negative terminal (n) is also forming an asymmetric synapse (arrowhead) with the dendrite. A positive terminal (t) is also seen to form an asymmetric synapse (arrowhead) with a spine (s), and an unlabelled terminal (n) forms an asymmetric synapse (arrowhead) with another spine (s). ***b)*** A labelled terminal (t) forms an asymmetric synapse (arrowhead) with a dendrite of neuron H (d). An unlabelled terminal (n), directly adjacent to the dendrite forms an asymmetric synapse (arrowhead) with a spine (s). Scale bars, 0.25 μm

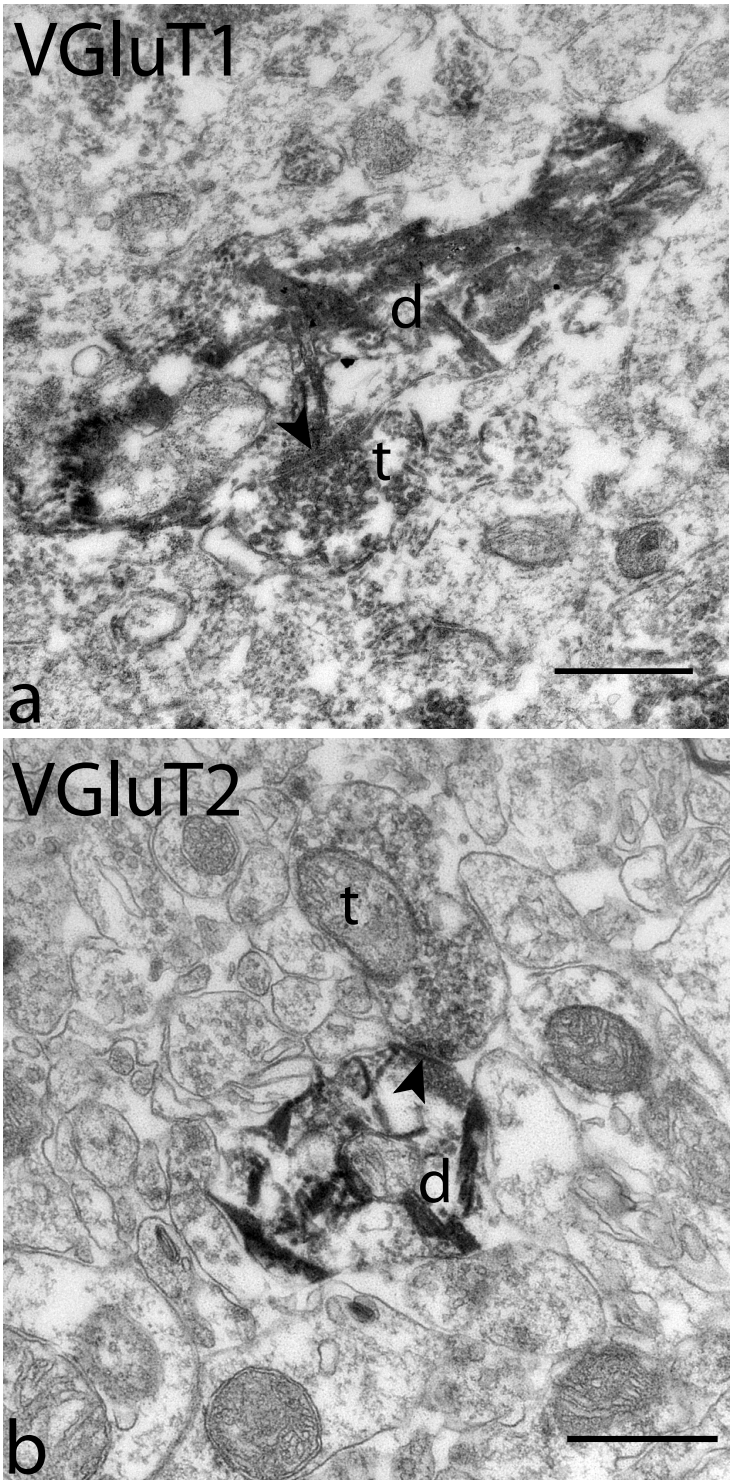


Figure 4.7. VGluT1 and VGluT2-positive terminals form synapses with the dendrites of an individual cholinergic interneuron.

a) A VGluT1-positive terminal (t) forms an asymmetric synapse (arrowhead) with a labelled dendrite of neuron E (d). ***b)*** A VGluT2-positive terminal (t) forms an asymmetric synapse (arrowhead) with a dendrite of neuron E (d). Scale bars, 0.25 μm.

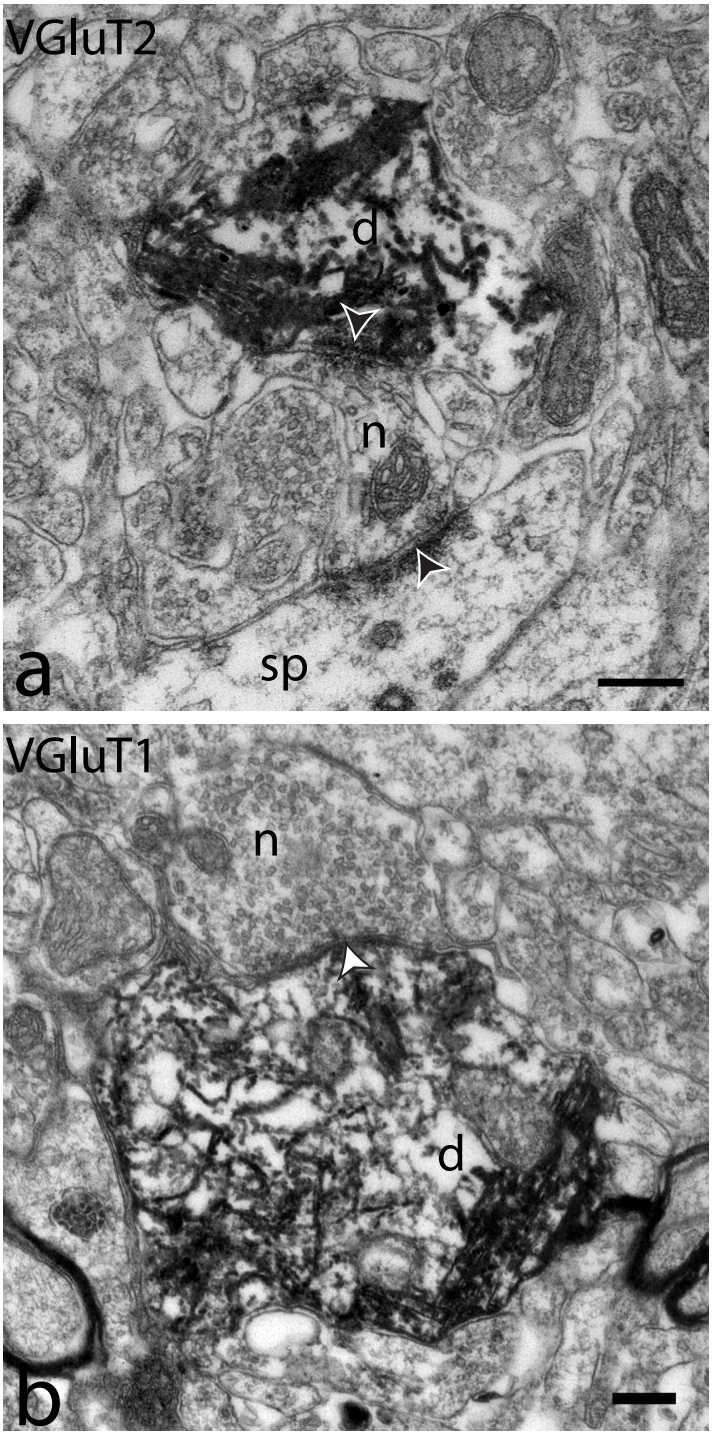


Figure 4.8. Unlabelled terminals form asymmetric and symmetric synapses with the dendrites of a cholinergic interneuron, neuron H.

a) An unlabelled terminal (n) forms asymmetric synapses (black arrowheads) with a dendrite of neuron H (d) and a spine (sp), in tissue labelled for VGluT2. ***b)*** An unlabelled terminal (n) forms a symmetric synapse (white arrowhead) with a dendrite of neuron H (d) in tissue labelled for VGluT1. Scale bars, 0.25 μm

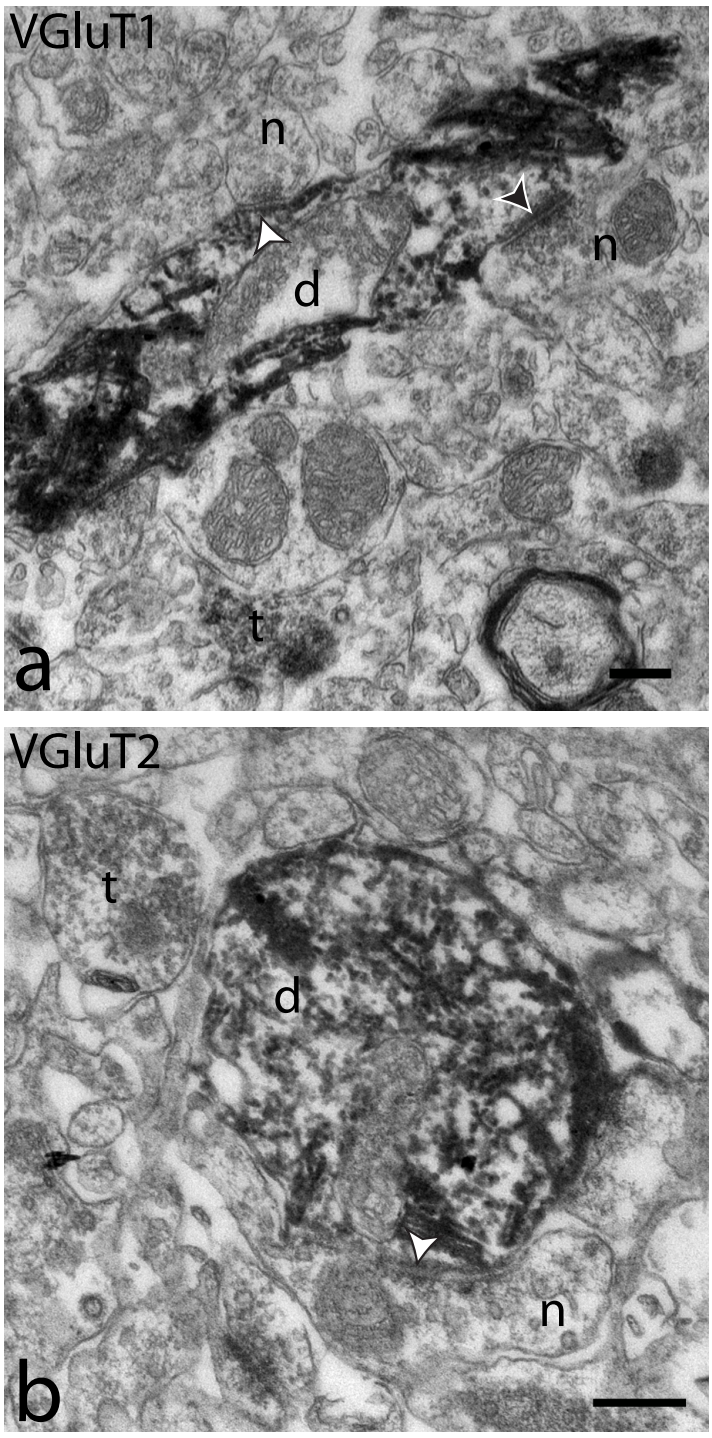


Figure 4.9. Unlabelled terminals form asymmetric and symmetric synapses with the dendrites of a cholinergic interneuron, neuron E.

a) Unlabelled terminals (n) form asymmetric (black arrowhead) and symmetric (white arrowhead) synapses with a dendrite of neuron E (d), in VGluT1 labelled tissue. Note the VGLuT1-positive terminal (t) within the frame. ***b)*** An unlabelled terminal (n) forms a symmetric synapse (white arrowhead) with a dendrite of neuron E (d) in tissue labelled for VGluT2. Note the VGluT2-posiotive terminal (t) within the frame. Scale bars, 0.25 μm.

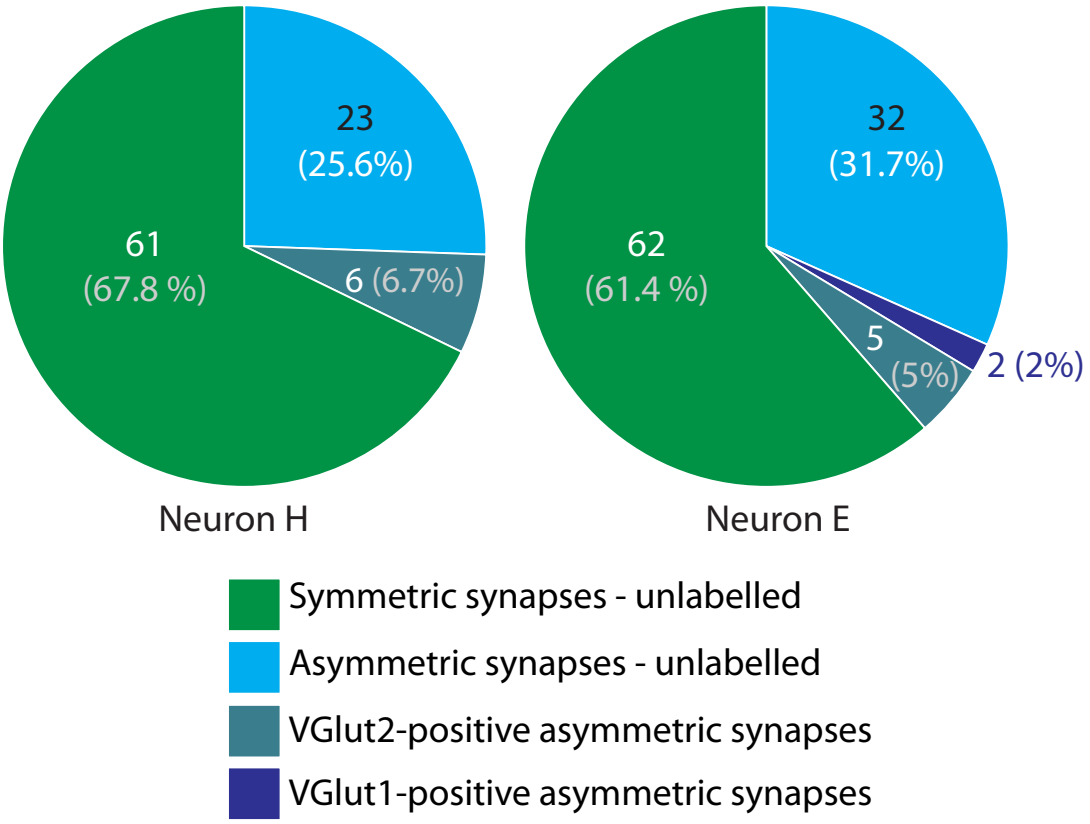


Figure 4.10. Proportions of synapses onto the dendrites of two cholinergic interneurons, neurons H and E.

For neuron H, 90 terminals formed synapses with the dendrites; of these 61 were symmetric synapses (67.8%), and 29 were asymmetric (32.3%) and out the asymmetric synapses 6 were positive for VGluT2 (6.7% of total; left). For neuron E, 101 terminals formed synapses with the dendrites; 62 were symmetric (61.4%), 39 were asymmetric (38.7%) and out of the terminals forming asymmetric synapses 5 were positive for VGluT2 (5% of total), and 2 were positive for VGluT1 (2% of total; right).

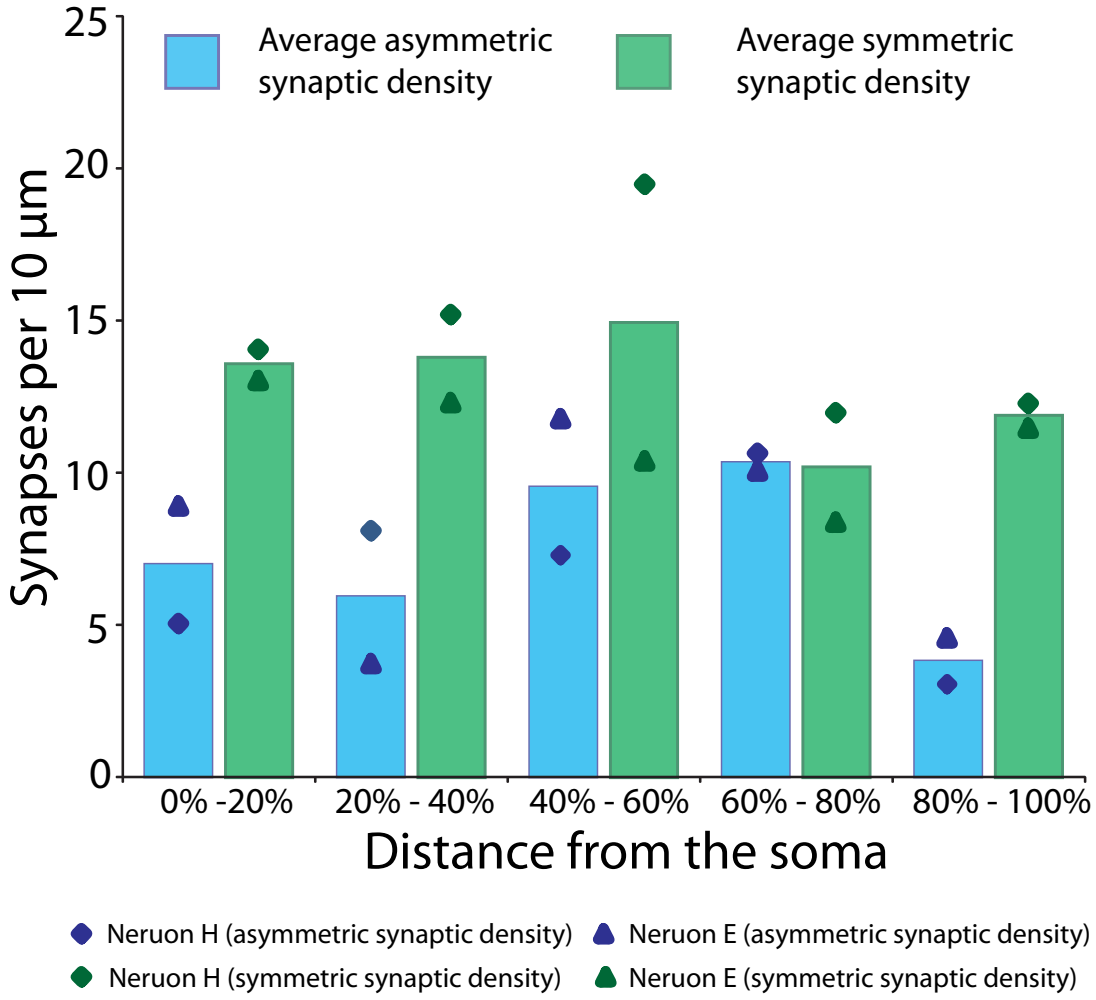


Figure 4.11. Synaptic density of symmetric and asymmetric synapses in the different dendritic compartments, examined for two cholinergic interneurons

The number of synapses (per 10 µm) for asymmetric (blue) and symmetric (green) synapses was averaged between the two neurons examined (bar chart), for each incremental 20% of the distance from the soma. The relative synaptic densities for neuron H (diamonds) and neuron E (triangles) are plotted. The asymmetric densities include the VGluT-positive terminals.

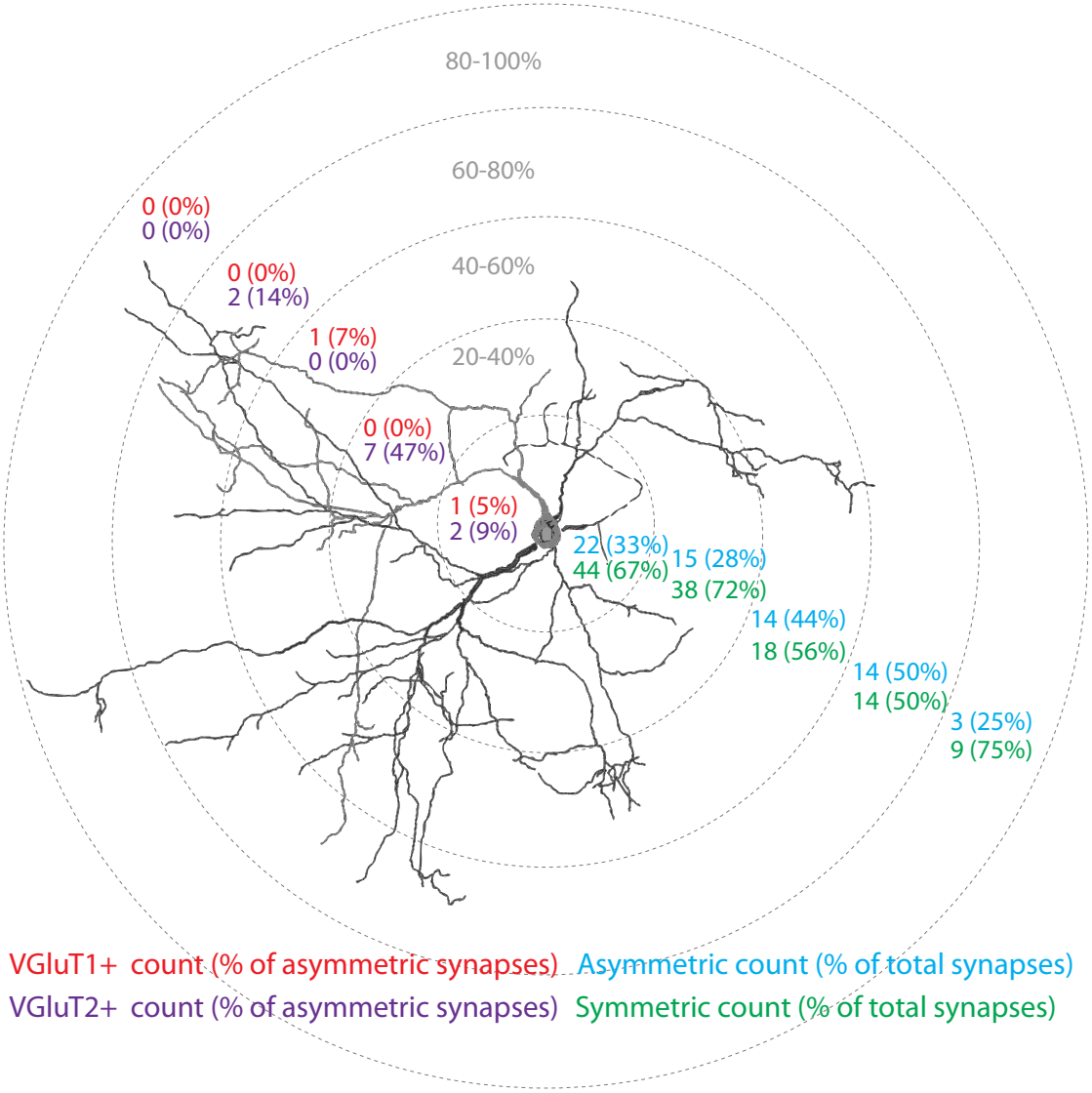


Figure 4.12. Average proportion and distribution of all synapses examined.

The number (count) of synapses and the percentage of the total synapses for asymmetric (blue) and symmetric (green) synapses within each 20% incremental distance from the cell body, for both neurons combined. The number (and percentage of the total asymmetric synapses) of VGluT1 (red) and VGluT2 (purple) positive synapses is also shown.

4.4. Discussion

The way in which cholinergic interneurons integrate their afferent inputs is dependent on the proportion and distribution of synapses on their dendritic tree. In this study the dendritic structure of cholinergic interneurons was examined, and the number of synapses formed, both asymmetric and symmetric, within the different dendritic compartments was quantified. A detailed examination of the cortical (VGluT1) and thalamic (VGlut2) inputs was carried out. The results reveal that cortical and thalamic axons can form synapses with an *individual* cholinergic interneuron. Both neurons examined in this study formed a greater proportion of symmetric synapses than asymmetric synapses, and this is especially prominent in the proximal and most distal regions of the dendritic tree.

4.4.1. Dendritic structure of cholinergic interneurons

Despite the huge amount of variation within the brain, for very few neuronal cell types is there a clear relationship between dendritic architecture and function; i.e. one cannot deduce the functional roles of a neuron from its structure alone. One example of where this relationship is obvious is for retinal ganglion cells, where the length and breadth of their dendritic arbor determines the area over which they can receive visual input (Koch, 1999). Dendritic branching is known to have an effect on electrical activity, as per the cable theory of a neuron, as proposed by Rall in the 1950s, which can be modified for extended dendritic structures (Borst & Egelhaaf, 1994; Koch, 1999). Investigations into the relationship between dendritic geometry and electrical activity are often carried out using computational models, where it is possible to probe questions which are technically difficult to examine experimentally. The purpose of the dendrite is to receive inputs over a certain area, and indeed the size and complexity of the dendrite is a reflection of its synaptic innervation (Fiala *et al.*, 2008). The size, pattern and features of the dendritic structures of the cholinergic interneurons examined in this study are consistent with previous reports of physiologically recorded and filled TANs (Wilson *et al.*, 1990). These neurons are large, and have dendrites that extend over long distances (up to 700 μm) from the soma; in comparison to MSNs which have dendritic fields of ~400

μm (DiFiglia *et al.*, 1976; Preston *et al.*, 1980; Kincaid *et al.*, 1998). The total dendritic length of a cholinergic interneuron, as described in this study (~9,400 μm), is about the same as that of a cerebellar Purkinje neuron in the guinea pig (Fiala *et al.*, 2008). The Purkinje neuron, however, has about 440 branch points (Fiala *et al.*, 2008) whereas the cholinergic interneuron has an average of 66; therefore the cholinergic interneuron has the same dendritic length over which to integrate inputs, but is much less complex. The cholinergic neuron does however have more branch points than a CA1 pyramidal cell (rat) or a starburst amacrine cell (rhesus monkey) (Fiala *et al.*, 2008). The cholinergic interneurons therefore have a unique set of features represented in its dendritic geometry that allow it to carry out its role within the striatum.

One of the main advantages of 3-dimensional reconstructions of neurons is in the implementation of biologically realistic computer models. This is the first 3-dimensional reconstruction of a striatal cholinergic interneuron, and consequently could be useful for models that aim to understand the functions of this particular cell type, and its role within a network.

4.4.2. Synaptic innervation of cholinergic interneurons

The way in which a neuron is interconnected with other neurons gives valuable information about its particular role within a network, and can provide insight into the physiological responses of a particular neuron type *in vivo* (Henny *et al.*, 2012). The aim of this study was to examine the cortical and thalamic innervation to individual, electrophysiologically characterised and neurochemically identified cholinergic interneurons. Neuron H formed 6 asymmetric synapses with thalamic terminals (VGluT2-positive) out of the 29 asymmetric synapses examined (20.7 %). These synapses were distributed over the dendritic compartments. Over all the dendritic fragments examined in this study, this neuron received no input from cortical terminals, which is consistent with previous a previous study (Lapper & Bolam, 1992). Neuron E formed 5 synapses with thalamic terminals (VGlut2-positive) and 2 synapses with cortical terminals (VGluT1), out of the 39 asymmetric synapses examined (12.8 % and 5.1%, respectively). One of the

cortical synapses was proximal to the cell body. This neuron responded to cortical and thalamic stimulation *in vivo* and therefore the fact that it receives synaptic innervation from both the cortex and thalamus is supportive of the physiological data presented (Chapter 3). This work therefore provides evidence that an individual cholinergic interneuron can receive innervation from both the cortex and the thalamus. The cortical synapses were however, less numerous than the thalamic synapses, which again is in line with previous anatomical examinations of these neurons (Meredith & Wouterlood, 1990; Lapper & Bolam, 1992). This could be attributed to the fact that cortical (VGluT1) terminals are known to form the vast majority of their synapses with dendritic spines (> 99%) in rat striatum, whereas thalamic input (VGluT2) forms a greater percentage with dendritic shafts (~30%) in the rat striatum (Lacey *et al.*, 2005). Therefore, based on this pattern, the overall likeliness for cortical innervation of cholinergic interneurons would be less than the thalamic innervation. This would however assume a lack of selectivity, and this is unlikely considering the specific roles of different neuronal subtypes. For example, PV-interneurons in the striatum receive cortical synaptic innervation onto their proximal dendrites that is very powerful *in vivo,* which indicates selective innervation (Lapper *et al.*, 1992; Bennett & Bolam, 1994; Mallet *et al.*, 2005) Also, asymmetric synapses account for ~80% of the total synapses within striatum (Ingham *et al.*, 1998).

The total numbers of VGluT-positive terminals forming synapses with the cholinergic interneurons was a small proportion of the total number of asymmetric synapses examined. Even on the basis that VGluT-negative terminals in one section could be positive for the other VGluT-marker, the numbers are still lower than would be expected. There are several possibilities for this; it could be due to technical issues, such as the unlabelled terminals could be false-negatives for either VGluT-marker, which would indicate that the numbers reported are an underestimate. The issue of false-negatives was attempted to be controlled for in the method of analysis; serial sections of dendritic fragments were only examined if there was a VGluT-positive terminal within the frame on at least one section on the grid being examined. Another possibility is that the unlabelled terminals forming synapses with the dendrite were positive for neither VGluT1 nor VGluT2. A percentage

of terminals that form asymmetric synapses within the striatum are negative for both known markers of glutamatergic terminals, and this can be up to 30% of terminals (Lacey *et al.*, 2005; Raju *et al.*, 2008). Based on the assumption that the unlabelled terminals are glutamatergic, then there could be an as yet unknown marker for glutamatergic terminals, and it could be these terminals that selectively innervate the dendrites of the cholinergic interneurons. However, in the CNS, not all terminals that form asymmetric synapses are glutamatergic, as 5-HT and cholinergic terminals can form asymmetric synapses; although cholinergic terminals in striatum form symmetric synapses. However, this point must be considered, although for the sake of this study the assumption was that the vast majority of asymmetric synapses were glutamatergic.

The rest of the synapses formed with each of the neurons were unlabelled, forming either asymmetric (putative excitatory) or symmetric (putative inhibitory) synapses. Overall, the cholinergic interneuron dendrites formed more symmetric synapses than asymmetric ones, this is in agreement with an examination of the distal dendrite of a cholinergic interneuron (Sizemore *et al.*, 2010). This is markedly different from the innervation of MSNs, each MSN forms ~10,000 asymmetric synapses and ~2500 symmetric synapses (Wilson, 2007). Within the striatum asymmetric synapses make up ~ 80% of the total synapses formed (Ingham *et al.*, 1998). Altogether, the ratio of asymmetric to symmetric synapses on the cholinergic interneuron is very different from the MSN, and must be selective, and central to the properties and role of the cholinergic interneurons. The innervation to cholinergic interneurons also has a different pattern to other neurons, such as that of pyramidal neurons in the CA1 region of the hippocampus. Pyramidal neurons have differing ratios of excitatory input to inhibitory input in the different layers of the hippocampus, and in the different dendritic compartments (Megias *et al.*, 2001). The pyramidal neurons studied received overall greater excitatory innervation and inhibition was only greater proximally (Megias *et al.*, 2001). Gulyás and colleagues (1999) also examined the innervation of the different interneuron populations within the hippocampus, and found that dependent on neuronal type the dendrite received differing ratios of excitatory vs. inhibitory innervation. For all the interneuronal cell types,

excitatory innervation was greater than inhibitory, and this was especially prominent for PV-interneurons where only 6.4% of the synapses examined were inhibitory (Gulyás *et al.*, 1999). And again, the synaptic innervation was specific within the different layers and dendritic compartments (Gulyás *et al.*, 1999). It is interesting in the present study that for the cholinergic interneurons there were more symmetric (putative inhibitory) synapses overall and that there was no obvious specificity related to dendritic compartment. On the assumption that majority of the symmetric synapses formed are GABAergic this means that these neurons are receiving more inhibitory than excitatory input over the entire dendritic tree. A recent examination of dopaminergic neurons in the SNpc found that dendrites of these neurons form ~50% of their synapses with GABA-positive terminals, and ~30% with glutamatergic terminals (Henny *et al.*, 2012). The number of inhibitory terminals was region specific, the dendrites that extended into the SNpr received a relatively greater number of synapses with GABAergic terminals (Henny *et al.*, 2012). Furthermore the numbers of GABAergic terminals received was correlated with the inhibitory responses of these neurons to aversive stimuli *in vivo* (Henny *et al.*, 2012). Henny *et al.,* (2012) thus describe a distinct relationship between dendritic architecture, number and distribution of inhibitory inputs and physiological characteristics.

Besides GABAergic terminals there are however, other subtypes of neurons which are likely to form symmetric synapses with cholinergic interneurons. Dopaminergic axons originating in the SNpc are likely to constitute a proportion of the terminals forming symmetric synapses on the dendrites of the cholinergic neurons (Kubota *et al.*, 1987; Chang, 1988). Although, dopaminergic terminals form synapses infrequently and dopamine is also able to have its effect via volume transmission (Ingham *et al.*, 1998; Moss & Bolam, 2008). Therefore the actual contribution of dopaminergic axons to the terminals forming symmetric synapses is likely to be small. Other sources of axons forming symmetric synapses include GABAergic terminals. The PV interneurons are not likely to contribute as there is no evidence for synaptic connectivity (Chang & Kita, 1992). The NOS interneurons have been shown to contact cholinergic interneurons, therefore these terminals may to contribute to the numbers of symmetric synapses examined (Vuillet *et*

al., 1992). Another source of GABAergic terminals to cholinergic interneurons are the MSNs, which are known to make synaptic connections with cholinergic interneurons (Bolam *et al.*, 1986; Martone *et al.*, 1992). Neurons that give rise to both the direct and indirect pathways form synapses with cholinergic interneurons (Bolam *et al.*, 1986; Martone *et al.*, 1992). Axon collaterals of direct pathway MSNs (D_1 and substance P expressing) form synapses with cholinergic interneurons more frequently than those of the indirect pathway (D_2 and enkephalin expressing) (Martone *et al.*, 1992). Also, cholinergic interneurons are also known to form synapses with other cholinergic interneurons (Chang & Kita, 1992). A more detailed assessment of the possible sources of innervation to cholinergic interneurons is required.

Cholinergic interneurons are capable of tonic firing in the absence of any synaptic input (Bennett & Wilson, 1999). Nonetheless, excitatory input to cholinergic interneurons *in vitro* can modify the pattern of firing, via AMPA receptors (Bennett & Wilson, 1998). Inhibitory input is able to delay the generation of action potentials, and thus can alter the overall firing rate (Bennett & Wilson, 1998). Therefore the predominance of inhibitory synaptic input could possibly be a necessity for the control of the firing rate. However the functional significance of the ratio of asymmetric to symmetric synapses is difficult to interpret as the relative weights of the synapses are not able to be distinguished. For example, Bennett and Wilson (1998) found that the $GABA_A$ IPSPs recorded *in vitro* were sparse, which is counterintuitive to the anatomical data presented here. This discrepancy is also illustrated by the MSNs, which receive a much greater number of asymmetric synapses but are very effectively influenced by inhibition, such as by the input from the PV interneurons (Koos & Tepper, 1999). In the case of the cholinergic interneurons it is likely that their unique physiological characteristics and pattern of synaptic innervation renders them sensitive to a few excitatory inputs, and this is demonstrated in their responses to stimulation *in vivo* (Chapter 3).

4.4.3. Technical considerations

With extensive anatomical processing and analysis there are many technical considerations that need to be addressed. The neurons are filled with neurobiotin using the juxtacellular method, and the extent of filling can vary from neuron to neuron. Although the most effectively modulated neurons were chosen for anatomical processing there is still a chance that there is incomplete filling of the dendritic arbor. The neurons were left for a period of time to attempt to control for this. The implication of this is that the compartment referred to as most 'distal' (80% -100% of total dendritic length) is not in fact the most distal region of the dendrites.

There are several technical considerations with the immunohistochemical processing. In order to preserve the tissue ultrastructure the sections were freeze-thawed but although this increases penetration, the penetration of the antibodies against the VGluT markers was not great, generally up to about 5 μm from the surface of the tissue. This means that dendrite that can be sampled is restricted to the surface regions of the tissue. This is important as it increases the likelihood of encountering false negatives terminals for either VGluT marker. Care was taken to only sample the regions near the surface where labelling was still evident. This was also controlled for at the level of analysis as dendrites were only examined within serial sections that had at least one frame where a VGluT-positive terminal was present.

Although the analysis of synaptic density is based on the assumption that the ultrathin sections are 50 nm thick, this is most likely an average thickness, as there is variation. There is also shrinkage introduced through the processing and ultrathin sectioning that was not accounted for in the estimations of synaptic density. However whatever shrinkage was introduced was likely to be consistent overall, and therefore affect all parts of the dendritic tree and all synapses examined. One major consideration is that in terms of sampling the dendritic tree, only a small fraction can be examined due to the labour intensity of the sectioning, electron microscopy and analysis.

Chapter Five: General Discussion

5.1. General Discussion

The striatum is the computational hub of the basal ganglia, and has a major role in the processing and transmission of information. Two major excitatory inputs converge onto striatum; from the cortex and the thalamus. Examination of the way in which the cortical and thalamic afferents innervate different subtypes of striatal neurons gives us insight into how these neurons process information. In this thesis, a combination of approaches was used to examine the cortical and thalamic inputs to subtypes of striatal neurons.

The cortical and thalamic innervation of the different subtypes of MSNs was analysed using quantitative electron microscopic techniques. The separation of MSNs into two populations is a central tenet of models of basal ganglia function. Hence understanding how the two major inputs to striatum innervate these populations is critical for our understanding of the underlying rules of connectivity of the basal ganglia. The results of this study provide evidence that axons of the cortico- and thalamo- striatal pathways form synaptic connections with neurons of both the direct and indirect pathways. Moreover, the proportions of connections formed by both the cortical and thalamic axons onto the direct and indirect pathway neurons were the same. This indicates that cortical information is transmitted to both direct and indirect pathway neurons, and similarly for thalamic information. Therefore, despite heterogeneity within the cortical and thalamic projections, when the populations are considered as a whole their contribution to the innervation of direct and indirect pathway neurons is of the same magnitude. The MSNs of both the direct and indirect pathways have low baseline firing rates and are generally hyperpolarised and require excitatory innervation to drive firing, which is predominantly from cortex and thalamus. Therefore, in light of the work here, inputs from the cortex and the thalamus are in equal positions to be able to depolarise the population of MSNs of either pathway. The way in which the afferent inputs influence individual MSNs is dependent on the more intricate details of their connectivity. Although the *overall* thalamic projection does not selectively innervate direct or indirect pathway neurons, there is

evidence that the axons from the CM selectively innervate indirect pathway neurons, in the squirrel monkey (Sidibé & Smith, 1996). Consequently, for a sub-set of indirect pathway neurons, in order for these neurons to fire, coordinated input from the CM may be required, irrespective of cortical activity. Another possibility is that all MSNs receive convergent innervation and that the cortical *or* thalamic inputs are in equal positions to depolarise these neurons; *or* perhaps coincident input from both cortex and thalamus is required to depolarise the MSNs from their relatively hyperpolarised resting state. Evidence from physiological studies suggests that MSNs do indeed receive convergent inputs from cortex and thalamus (Kocsis *et al.*, 1977; Ding *et al.*, 2008). Moreover, Ding *et al.,* (2008) report that 26% of MSNs recorded *in vitro* responded to stimulation of *both* cortex and thalamus, whereas 44% responded to cortical stimulation only and 30% to thalamic stimulation only. This is of course dependent on the site of stimulation and other caveats, but indicates that a proportion of MSNs receive convergent inputs (this will be discussed below).

The detailed electron microscopy performed in this study allowed examination of other fundamental issues of connectivity, such as the convergence and divergence of cortical and thalamic inputs. This study provides qualitative evidence for the divergence of cortical information to neurons of both the direct and indirect pathway. Likewise, a single thalamic afferent was found to innervate a neuron of the direct pathway and a neuron of the indirect pathway. This suggests that an individual cortical, or thalamic, neuron can selectively target neurons of both pathways. Thereby information from the cortex or thalamus is diverging within the striatum; and can be selectively processed by neurons of each pathway. As neurons of each pathway are differentially modulated within the striatal microcircuit, by the levels of neurotransmitter, and indeed different expression of receptors, the information processing is dependent on the specifics of the neuron subtype. If this is extrapolated it could mean that neurons of the direct and indirect pathways are receiving the ‘same’ information and the integration and transmission of this information is entirely dependent on the dynamics within the striatal microcircuit. In order to examine this issue further, the quantitative extent of divergence needs to be

analysed.

The issue of convergence of information was also able to be examined in this study. The qualitative evidence from this study suggests that neurons of the direct, or indirect pathway can receive convergent information from both the cortex and the thalamus. Although, the extent of convergence remains to be examined, this suggests that one individual neuron is receiving distinct information from two sources. Therefore neurons of both the pathways are in a position to assimilate the information from both of the two major sources of innervation to the striatum. The principles of connectivity presented here suggest that the cortical and thalamic innervation to the striatum is integrated by both direct and indirect pathway neurons. This study brings to light some issues that need to be examined further, and this will be discussed below.

The cortical and thalamic input to cholinergic interneurons was analysed in vivo, *in the anaesthetised rat*. Cholinergic interneurons are involved in reward-related behaviour; in order to carry out their role they must assimilate information from different sources. The two most prominent sources of information to the striatum are from the cortex and the thalamus. To examine how cholinergic interneurons integrate these inputs, extracellular recordings of cholinergic interneurons were carried out in dorsolateral striatum, and stimulation was applied to the motor area of cortex, and the Pf nucleus of the ITN. Cholinergic interneurons responded to cortical and thalamic stimulation with short latency excitatory responses, indicative of monosynaptic connections; this is in agreement with previous data recorded *in vivo*, although in previous studies the neurons were not identified as being immunopositive for ChAT (Wilson *et al.*, 1990; Reynolds & Wickens, 2004). This indicates that both the cortical and thalamic inputs are in a position to activate the cholinergic interneurons. There were some apparent differences between the responses to cortical and thalamic stimulation. These differences remained evident when the responses were recorded from individual cholinergic interneurons, i.e. they are not due to variability between neurons. This study provides evidence for important distinctions between the properties of cortical and thalamic synapses onto cholinergic interneurons *in*

vivo. There are several possible reasons for these differences; one possibility is that they could be due to differing ratios of glutamate AMPA and NMDA receptors, as has been reported for MSNs *in vitro* (Ding *et al.*, 2008; Smeal *et al.*, 2008), however the caveats of anaesthetic usage must be noted here, as ketamine is an NMDA receptor antagonist.

The application of various stimulation protocols allowed a further examination of these differences. For both paired and high frequency protocols, stimulation of cortex and thalamus resulted in disparate responses in the cholinergic interneurons. For paired cortical stimulation, cholinergic interneurons responded preferentially to the first pulse of the stimulation, and the pattern was reversed for thalamic stimulation. The cholinergic interneurons responded with increasing probability of firing to the first 1-4 pulses of high frequency thalamic stimulation, and then this probability decreased to the 5th pulse. For one neuron, high frequency stimulation of both cortex and thalamus was applied, this neuron responded to only the first pulse of the cortical stimulation, but to every pulse of the thalamic stimulation with the same pattern as seen for the other cholinergic interneurons. This suggests that the overall probability of responding to thalamic stimulation increases with increasing trains of stimuli, but shows the opposite pattern for cortical stimulation. Although the numbers of neurons for which these protocols were tested are low, the data indicates that the thalamic stimulation is 'facilitating', whereas the cortical stimulation is 'depressing'. A possible explanation for these distinctions is differing release probabilities of the cortical and thalamic terminals innervating the cholinergic interneurons. Another possibility is that it could be due to the specific properties of the synapses onto the neurons. Indeed, a recent study by Ding and colleagues (2008) describes similar disparities; furthermore, the responses recorded from cholinergic interneurons were distinct from those of neighbouring MSNs (Ding *et al.*, 2010). Despite the origins of these differences, it is interesting that they are distinct; although it is not entirely surprising considering differences in the anatomy and functions of these pathways are well documented. This study indicates that cortical and thalamic inputs can result in different responses in the cholinergic interneurons, and thereby can affect the timing and probability of the release of acetylcholine. Acetylcholine is an important striatal neuromodulator and has differential

effects on the subtypes of neurons within the striatal microcircuit, and is important for modulating the release of dopamine.

Cholinergic interneurons were silent for a period following stimulation, and this was particularly prominent following high frequency stimulation of the thalamus. This period of silence following initial excitation is similar to the 'pause' response of these neurons, which has been described *in vitro* and *in vivo* in behaving animals (Aosaki *et al.*, 1994b; Matsumoto *et al.*, 2001; Ding *et al.*, 2010; Schulz *et al.*, 2011). In behaving monkeys the thalamic innervation to cholinergic interneurons is essential for their ability to pause (Matsumoto *et al.*, 2001). The thalamostriatal projection is involved in transmitting information about sensory events (Smith *et al.*, 2011). The projection to the cholinergic interneurons may therefore provide a mechanism whereby this information can be integrated into the striatal microcircuit, and this could be mediated by the pause. The mechanism(s) which contribute to the pause in firing are difficult to dissect. In this study, the fact that the pause was more prominent after thalamic, rather than cortical, stimulation is consistent with previous studies, and reinforces the importance of the thalamic innervation. Currently, there is no consensus on whether the pause is a result of active inhibition or due to an activation of the innate properties of the cholinergic interneuron; it is likely to be a combination of factors. There are a few possibilities as to why the thalamic input is able to induce the pause, but not the cortical input. The thalamic input to the striatum must either cause the pause via an innate mechanism of the cholinergic interneurons or innervate another neuron type which in turn causes a cessation of firing in the cholinergic neurons. A recent review by Goldberg and Reynolds (2011) highlight three mechanisms by which this could occur. First, GABAergic interneurons could be coincidentally depolarised by thalamic inputs and then inhibit the cholinergic interneurons in a feed-forward manner (Goldberg & Reynolds, 2011). The population of GABAergic interneurons would most likely be the NOS interneurons based on known anatomical connections, however, the extent and nature of thalamic inputs to these neurons needs to be examined further. A recent study has however, illustrated that the relationship between NOS and ChAT neurons is of functional significance in shaping the

dynamics of the striatal microcircuit (English *et al.*, 2011). A second possibility is that the thalamic inputs cause an increase in dopamine release which then acts on the cholinergic interneurons to suppress firing (Goldberg & Reynolds, 2011). Although this would help explain the requirement of dopamine for the pause, it fails to describe a mechanism which is exclusive to the thalamostriatal system, as glutamate release from cortical terminals can also increase the release of dopamine. Finally, the pause may be due to the innate properties of the cholinergic interneurons, which are initiated by thalamic inputs. Goldberg and Reynolds (2011) propose either a deactivation of a hyperpolarisation-activated current, or activation of the slow AHP. The data presented here suggest that the properties of the synapses from cortex and thalamus are different, and therefore the thalamic input could result in activation of innate mechanisms that are not activated by the cortical inputs. Although the aim of this study was not to examine the mechanisms of the pause response the data presented reinforces the importance of the role of thalamic inputs to cholinergic interneurons.

The synaptic innervation to two physiologically characterised and neurochemically identified cholinergic neurons was examined using electron microscopy. The integrative properties of an individual neuron or neuronal cell type are dependent on the numbers and distribution of inputs on their dendritic arbor. Using selective markers, the relative contributions of cortical and thalamic inputs to cholinergic interneurons was examined in the different dendritic compartments. One of the neurons examined formed synapses with both cortical and thalamic afferents; although the thalamic terminals were more numerous than the cortical ones. This indicates that the two major sources of input to the striatum can converge onto an individual neuron, and thus both inputs are in a position to modulate the processing of information by this neuron. The other neuron examined in this study, formed synapses with thalamic afferents, whilst no cortical afferents were seen to form synaptic contacts with the dendrites. In both of these cases it is evident that the thalamic afferents form synapses more frequently than the cortical afferents, if the cortical ones do at all. This indicates that overall, the thalamic innervation is in a position to exert a greater influence over the cholinergic interneurons. This is consistent with evidence that

the thalamic inputs are essential for the conditioned pause response, as discussed above.

Although the thalamic input is likely to be more influential, a synaptic cortical input is still evident, at least to one of the neurons examined. Furthermore, unlike previous studies, the cortical synapses were not distal; one was proximal to the soma which indicates that it is in a strong position to be able to alter the firing properties of the cholinergic interneuron. The functional relevance of this cortical input is difficult to ascertain. From the physiological evidence reported here, and elsewhere, this connection is monosynaptic and able to illicit a short latency response (Chapter 3; Reynolds & Wickens, 2004). Indeed, the physiological data presented here suggests that the 'power' of the cortical input is of the same magnitude as that of the thalamic input, although the caveats of electrical stimulation must be considered. A possible explanation is that a specific population of cortical neurons innervate the cholinergic interneurons, and supply them with particular information that is transmitted with high fidelity. Although sparse, the cortical inputs could still be selective and of great importance to the role of the cholinergic interneurons. Elucidating the origins and roles of the cortical input to these neurons needs further examination.

5.1.1. Future work

There are several issues that have been brought to light by the data presented here and that need further examination. For the first part of the study (Chapter 2) the populations of cortical and thalamic inputs were considered as a whole; further examination of the specific innervation to the direct and indirect pathway neurons from different populations and regions of cortex and thalamus needs to be carried out. Also the extent of divergence and convergence needs to be quantified, as this could provide insight into striatal processing. One way in which this could be addressed would be to use a similar approach as used in Chapter 4 for direct and indirect pathway neurons. This would provide information about whether individual direct or indirect pathway neurons were receiving convergent information, and to what extent. Another way to address these questions is through the use of newer techniques; one way in which this could be done would be to

use a marker that allows monosynaptic tracing of a neuron's presynaptic inputs, such as a modified rabies virus (Choi & Callaway, 2011; Miyamichi *et al.*, 2011) or a DNA vector (Rancz *et al.*, 2011). By targeting these genetic manipulations to an individual direct or indirect pathway MSN, the entirety of their inputs could be examined. The results would indicate whether one neuron receives input from specific cortical and/or thalamic regions, and would also provide insight into the extent of convergence onto an individual neuron. This approach could also be used for the cholinergic interneurons, and would theoretically be less labour intensive than the methodology used in this study (Chapter 4), and it could be carried out on more neurons than described here. This approach could also establish whether or not a specific population of cortical neurons innervate the cholinergic interneurons. A thorough examination of all the different sources of innervation to the cholinergic interneurons, both excitatory and inhibitory would be possible using these techniques. A benefit of this approach would also be that the neurons could be recorded *in vivo* and therefore they could be electrophysiologically characterised prior to assessment of their various inputs (Rancz *et al.*, 2011).

One particular limitation of the examination of the responses of cholinergic interneurons to stimulation *in vivo* was the likelihood that stimulation of thalamus resulted in cortical stimulation and *vice versa*. One way of overcoming this would be the usage of optogenetic techniques to selectively activate or inhibit cortical or thalamic inputs. This could be done *in vitro* by targeting specific populations of thalamic nuclei and recording the responses of the cholinergic interneurons. This technique has been used to examine the differential role of histamine of cortical and thalamic inputs to striatum (Ellender *et al.*, 2011). Ideally, this would be carried out *in vivo* although this is more technically challenging with the current approaches. The aim would be to dissect the influence of the cortical and thalamic inputs to the cholinergic interneurons (although it could also be possible to examine all other neurons subtypes in striatum). One way to examine this *in vivo* would be to temporarily inactivate the cortex; this could be achieved through the usage of muscimol, or removal of the cortex. The results could then provide further insight as to the discrete roles of the cortical and thalamic inputs.

Using similar approaches to the ones described in this thesis it would also be possible to examine the other striatal interneurons. Although TANs were preferentially recorded *in vivo* other interneuron types and MSNs were also recorded and stimulation applied in some cases. This data, although preliminary can serve as a basis for which to compare the cortical and thalamic innervation to different subtypes of striatal neurons. Differences and similarities in the responses to cortical and thalamic innervation between different neuron types could provide insight into how these neurons contribute to striatal processing. Furthermore, as was described for this thesis, the neurons can be filled with neurobiotin after recording and neurochemically identified *post-mortem* and detailed analysis of their synaptic innervation can be examined using electron microscopy.

5.1.2. General conclusions

The results described in this thesis provide insight into how the two major excitatory afferents to the striatum innervate different subtypes of neurons. Firstly, the two populations of MSNs were examined and it was found that overall the subtypes of both pathways form similar numbers of synapses with cortical and thalamic afferents. This suggests that neurons of both pathways are in similar positions to receive and process information from both cortex and thalamus. The extent of both divergence and convergence of cortical or thalamic information could greatly influence the way in which the striatum processes information. Although, as discussed, certain features of this work need to be examined further, these results shed light on how the principal neuronal cell type in striatum is innervated by the two major striatal inputs.

Cholinergic interneurons have been shown to have an important role in reward-related behaviour; the way in which these neurons assimilate information from the two major sources is vital to their role in striatum. The results from the electrophysiological recordings *in vivo* suggest that these neurons can respond to both cortical and thalamic stimulation with a short latency response, indicative of a monosynaptic connection. Through the application of various stimulation protocols it was able to be ascertained that the cholinergic interneurons showed differing responses to cortical and thalamic inputs,

suggesting important distinctions between these two inputs onto these neurons. These distinctions could be central to the role of cholinergic interneurons in the striatum, and indeed could provide insight into how the thalamic input is shown to be essential for the conditioned pause response. A thorough characterisation of the synaptic innervation onto individual, neurochemically identified cholinergic interneurons was carried out, using selective markers of cortical and thalamic inputs. The results indicate that individual neurons can receive synaptic input from the cortex and thalamus, but that the thalamic innervation forms synapses more frequently than the cortical input. This is in line with the central role of the thalamus in the conditioned pause response. The way in which a particular neuron type integrates information is dependent on the number and distribution of synapses on their dendritic arbor; therefore the results of this study provide critical information about the role of cholinergic interneurons in the striatal microcircuit.

References

Ade, K.K., Janssen, M.J., Ortinski, P.I. & Vicini, S. (2008) Differential tonic GABA conductances in striatal medium spiny neurons. *J Neurosci*, **28**, 1185-1197.

Adewale, A.S., Macarthur, H. & Westfall, T.C. (2005) Neuropeptide Y induced modulation of dopamine synthesis in the striatum. *Regul Pept*, **129**, 73-78.

Albin, R.L., Young, A.B. & Penney, J.B. (1989) The functional anatomy of basal ganglia disorders. *Trends Neurosci*, **12**, 366-375.

Alexander, G.E. & Crutcher, M.D. (1990) Functional architecture of basal ganglia circuits: neural substrates of parallel processing. *Trends Neurosci*, **13**, 266-271.

Alexander, G.E., DeLong, M.R. & Strick, P.L. (1986) Parallel organization of functionally segregated circuits linking basal ganglia and cortex. *Annu Rev Neurosci*, **9**, 357-381.

Aoki, C. & Pickel, V.M. (1990) Neuropeptide Y in cortex and striatum. Ultrastructural distribution and coexistence with classical neurotransmitters and neuropeptides. *Ann N Y Acad Sci*, **611**, 186-205.

Aosaki, T., Graybiel, A.M. & Kimura, M. (1994a) Effect of the nigrostriatal dopamine system on acquired neural responses in the striatum of behaving monkeys. *Science*, **265**, 412-415.

Aosaki, T., Tsubokawa, H., Ishida, A., Watanabe, K., Graybiel, A.M. & Kimura, M. (1994b) Responses of tonically active neurons in the primate's striatum undergo systematic changes during behavioral sensorimotor conditioning. *J Neurosci*, **14**, 3969-3984.

Apicella, P. (2007) Leading tonically active neurons of the striatum from reward detection to context recognition. *Trends Neurosci*, **30**, 299-306.

Aronin, N., Chase, K. & DiFiglia, M. (1986) Glutamic acid decarboxylase and enkephalin immunoreactive axon terminals in the rat neostriatum synapse with striatonigral neurons. *Brain Res*, **365**, 151-158.

Bagetta, V., Picconi, B., Marinucci, S., Sgobio, C., Pendolino, V., Ghiglieri, V., Fusco, F., Giampa, C., and Calabresi, P., (2011) Dopamine-dependent long-term depression is expressed

in striatal spiny neurons of both direct and indirect pathways: implications for parkinson's disease. *J Neurosci,* **31**, 12513–12522

Barnes, N.M. & Sharp, T. (1999) A review of central 5-HT receptors and their function. *Neuropharmacology*, **38**, 1083-1152.

Barroso-Chinea, P., Castle, M., Aymerich, M.S. & Lanciego, J.L. (2008) Expression of vesicular glutamate transporters 1 and 2 in the cells of origin of the rat thalamostriatal pathway. *J Chem Neuroanat*, **35**, 101-107.

Bennett, B.D. & Bolam, J.P. (1993) Characterization of calretinin-immunoreactive structures in the striatum of the rat. *Brain Res*, **609**, 137-148.

Bennett, B.D. & Bolam, J.P. (1994) Synaptic input and output of parvalbumin-immunoreactive neurons in the neostriatum of the rat. *Neuroscience*, **62**, 707-719.

Bennett, B.D., Callaway, J.C. & Wilson, C.J. (2000) Intrinsic membrane properties underlying spontaneous tonic firing in neostriatal cholinergic interneurons. *J Neurosci*, **20**, 8493-8503.

Bennett, B.D. & Wilson, C.J. (1998) Synaptic regulation of action potential timing in neostriatal cholinergic interneurons. *J Neurosci*, **18**, 8539-8549.

Bennett, B.D. & Wilson, C.J. (1999) Spontaneous activity of neostriatal cholinergic interneurons in vitro. *J Neurosci*, **19**, 5586-5596.

Berendse, H.W. & Groenewegen, H.J. (1990) Organization of the thalamostriatal projections in the rat, with special emphasis on the ventral striatum. *J Comp Neurol*, **299**, 187-228.

Berke, J.D. (2011) Functional properties of striatal fast-spiking interneurons. *Front Syst Neurosci*, **5**, 45.

Berke, J.D., Okatan, M., Skurski, J. & Eichenbaum, H.B. (2004) Oscillatory entrainment of striatal neurons in freely moving rats. *Neuron*, **43**, 883-896.

Berretta, S., Parthasarathy, H.B. & Graybiel, A.M. (1997) Local release of GABAergic inhibition

in the motor cortex induces immediate-early gene expression in indirect pathway neurons of the striatum. *J Neurosci*, **17**, 4752-4763.

Bevan, M.D., Booth, P.A., Eaton, S.A. & Bolam, J.P. (1998) Selective innervation of neostriatal interneurons by a subclass of neuron in the globus pallidus of the rat. *J Neurosci*, **18**, 9438-9452.

Bevan, M.D., Hallworth, N.E. & Baufreton, J. (2007) GABAergic control of the subthalamic nucleus. *Progress in Brain Research*, **160**, 173-188.

Bevan, M.D., Magill, P.J., Terman, D., Bolam, J.P. & Wilson, C.J. (2002) Move to the rhythm: oscillations in the subthalamic nucleus-external globus pallidus network. *Trends Neurosci*, **25**, 525-531.

Blomeley, C. & Bracci, E. (2005) Excitatory effects of serotonin on rat striatal cholinergic interneurones. *J Physiol*, **569**, 715-721.

Blomeley, C. & Bracci, E. (2008) Substance P depolarizes striatal projection neurons and facilitates their glutamatergic inputs. *J Physiol*, **586**, 2143-2155.

Blomeley, C.P. & Bracci, E. (2009) Serotonin excites fast-spiking interneurons in the striatum. *Eur J Neurosci*, **29**, 1604-1614.

Blomeley, C.P. & Bracci, E. (2011) Opioidergic interactions between striatal projection neurons. *J Neurosci*, **31**, 13346-13356.

Blomeley, C.P., Kehoe, L.A. & Bracci, E. (2009) Substance P mediates excitatory interactions between striatal projection neurons. *J Neurosci*, **29**, 4953-4963.

Bolam, J.P. (ed) (1992) *Experimental Neuroanatomy*. Oxford University Press, Oxford, UK.

Bolam, J.P., Brown, M.T., Moss, J. & Magill, P.J. (2009) Basal Ganglia: Internal Organization. In Squire, L.R. (ed) *Encyclopaedia of Neuroscience*. Academic Press, Oxford, pp. 97-1104.

Bolam, J.P., Hanley, J.J., Booth, P.A. & Bevan, M.D. (2000) Synaptic organisation of the basal ganglia. *Journal of Anatomy*, **196** 527-542.

Bolam, J.P., Ingham, C.A., Izzo, P.N., Levey, A.I., Rye, D.B., Smith, A.D. & Wainer, B.H. (1986) Substance P-containing terminals in synaptic contact with cholinergic neurons in the neostriatum and basal forebrain: a double immunocytochemical study in the rat. *Brain Res*, **397**, 279-289.

Bolam, J.P. & Izzo, P.N. (1988) The postsynaptic targets of substance P-immunoreactive terminals in the rat neostriatum with particular reference to identified spiny striatonigral neurons. *Exp Brain Res*, **70**, 361-377.

Bolam, J.P. & Smith, Y. (1990) The GABA and substance P input to dopaminergic neurones in the substantia nigra of the rat. *Brain Res*, **529**, 57-78.

Bolam, J.P., Wainer, B.H. & Smith, A.D. (1984) Characterization of cholinergic neurons in the rat neostriatum. A combination of choline acetyltransferase immunocytochemistry, Golgi-impregnation and electron microscopy. *Neuroscience*, **12**, 711-718.

Borst, A. & Egelhaaf, M. (1994) Dendritic processing of synaptic information by sensory interneurons. *Trends Neurosci*, **17**, 257-263.

Bromberg-Martin, E.S., Matsumoto, M. & Hikosaka, O. (2010) Dopamine in motivational control: rewarding, aversive, and alerting. *Neuron*, **68**, 815-834.

Brown, M.T., Henny, P., Bolam, J.P. & Magill, P.J. (2009) Activity of neurochemically heterogeneous dopaminergic neurons in the substantia nigra during spontaneous and driven changes in brain state. *J Neurosci*, **29**, 2915-2925.

Calabresi, P., Gubellini, P., Centonze, D., Sancesario, G., Morello, M., Giorgi, M., Pisani, A. & Bernardi, G. (1999) A critical role of the nitric oxide/cGMP pathway in corticostriatal long-term depression. *J Neurosci*, **19**, 2489-2499.

Calabresi, P., Maj, R., Pisani, A., Mercuri, N.B. & Bernardi, G. (1992) Long-term synaptic depression in the striatum: physiological and pharmacological characterization. *J Neurosci*, **12**, 4224-4233.

Calabresi, P., Picconi, B., Tozzi, A. & Di Filippo, M. (2007) Dopamine-mediated regulation of corticostriatal synaptic plasticity. *Trends Neurosci*, **30**, 211-219.

Calabresi, P., Pisani, A., Mercuri, N.B. & Bernardi, G. (1996) The corticostriatal projection: from synaptic plasticity to dysfunctions of the basal ganglia. *Trends Neurosci*, **19**, 19-24.

Castle, M., Aymerich, M.S., Sanchez-Escobar, C., Gonzalo, N., Obeso, J.A. & Lanciego, J.L. (2005) Thalamic innervation of the direct and indirect basal ganglia pathways in the rat: Ipsi- and contralateral projections. *J Comp Neurol*, **483**, 143-153.

Cepeda, C., André, V.M., Yamazaki, I., Wu, N., Kleiman-Weiner, M. & Levine, M.S. (2008) Differential electrophysiological properties of dopamine D1 and D2 receptor-containing striatal medium-sized spiny neurons. *Eur J Neurosci*, **27**, 671-682.

Chang, H.T. (1988) Dopamine-acetylcholine interaction in the rat striatum: a dual-labeling immunocytochemical study. *Brain Res Bull*, **21**, 295-304.

Chang, H.T. & Kita, H. (1992) Interneurons in the rat striatum: relationships between parvalbumin neurons and cholinergic neurons. *Brain Res*, **574**, 307-311.

Charpier, S. & Deniau, J.M. (1997) In vivo activity-dependent plasticity at cortico-striatal connections: evidence for physiological long-term potentiation. *Proc Natl Acad Sci U S A*, **94**, 7036-7040.

Choi, J. & Callaway, E.M. (2011) Monosynaptic inputs to ErbB4-expressing inhibitory neurons in mouse primary somatosensory cortex. *J Comp Neurol*, **519**, 3402-3414.

Cornwall, J. & Phillipson, O.T. (1988) Afferent projections to the parafascicular thalamic nucleus of the rat, as shown by the retrograde transport of wheat germ agglutinin. *Brain Res Bull*, **20**, 139-150.

Cowan, R.L. & Wilson, C.J. (1994) Spontaneous firing patterns and axonal projections of single corticostriatal neurons in the rat medial agranular cortex. *J Neurophysiol*, **71**, 17-32.

Cowan, R.L., Wilson, C.J., Emson, P.C. & Heizmann, C.W. (1990) Parvalbumin-containing GABAergic interneurons in the rat neostriatum. *J Comp Neurol*, **302**, 197-205.

Day, M., Wokosin, D., Plotkin, J.L., Tian, X. & Surmeier, D.J. (2008) Differential excitability and modulation of striatal medium spiny neuron dendrites. *J Neurosci*, **28**, 11603-11614.

Del Bel, E.A., Guimaraes, F.S., Bermudez-Echeverry, M., Gomes, M.Z., Schiaveto-de-souza, A., Padovan-Neto, F.E., Tumas, V., Barion-Cavalcanti, A.P., Lazzarini, M., Nucci-da-Silva, L.P. & de Paula-Souza, D. (2005) Role of nitric oxide on motor behavior. *Cell Mol Neurobiol*, **25**, 371-392.

Deniau, J.M., Mailly, P., Maurice, N. & Charpier, S. (2007) The pars reticulata of the substantia nigra: a window to basal ganglia output. *Prog Brain Res*, **160**, 151-172.

Deschênes, M., Bourassa, J., Doan, V.D. & Parent, A. (1996a) A single-cell study of the axonal projections arising from the posterior intralaminar thalamic nuclei in the rat. *Eur J Neurosci*, **8**, 329-343.

Deschênes, M., Bourassa, J. & Parent, A. (1996b) Striatal and cortical projections of single neurons from the central lateral thalamic nucleus in the rat. *Neuroscience*, **72**, 679-687.

Di Giovanni, G., Di Matteo, V., Pierucci, M. & Esposito, E. (2008) Serotonin-dopamine interaction: electrophysiological evidence. *Prog Brain Res*, **172**, 45-71.

DiFiglia, M., Aronin, N. & Martin, J.B. (1982) Light and electron microscopic localization of immunoreactive Leu-enkephalin in the monkey basal ganglia. *J Neurosci*, **2**, 303-320.

DiFiglia, M., Pasik, P. & Pasik, T. (1976) A Golgi study of neuronal types in the neostriatum of monkeys. *Brain Res*, **114**, 245-256.

Dimova, R., Vuillet, J., Nieoullon, A. & Kerkerian-Le Goff, L. (1993) Ultrastructural features of the choline acetyltransferase-containing neurons and relationships with nigral dopaminergic and cortical afferent pathways in the rat striatum. *Neuroscience*, **53**, 1059-1071.

Ding, J., Peterson, J.D. & Surmeier, D.J. (2008) Corticostriatal and thalamostriatal synapses have distinctive properties. *J Neurosci*, **28**, 6483-6492.

Ding, J.B., Guzman, J.N., Peterson, J.D., Goldberg, J.A. & Surmeier, D.J. (2010) Thalamic gating of corticostriatal signaling by cholinergic interneurons. *Neuron*, **67**, 294-307.

Dubé, L., Smith, A.D. & Bolam, J.P. (1988) Identification of synaptic terminals of thalamic or cortical origin in contact with distinct medium-size spiny neurons in the rat neostriatum. *J Comp Neurol*, **267**, 455-471.

Ebrahimi, A., Pochet, R. & Roger, M. (1992) Topographical organization of the projections from physiologically identified areas of the motor cortex to the striatum in the rat. *Neurosci Res*, **14**, 39-60.

Ellender, T.J., Huerta-Ocampo, I., Deisseroth, K., Capogna, M. & Bolam, J.P. (2011) Differential modulation of excitatory and inhibitory striatal synaptic transmission by histamine. *J Neurosci*, **31**, 15340-15351.

English, D.F., Ibanez-Sandoval, O., Stark, E., Tecuapetla, F., Buzsaki, G., Deisseroth, K., Tepper, J.M. & Koos, T. (2011) GABAergic circuits mediate the reinforcement-related signals of striatal cholinergic interneurons. *Nat Neurosci*, **15**, 123-130.

Fiala, J.C., Spacek, J. & Harris, K.M. (2008) Dendritic Structure. In Stuart, G., Spruston, N., Hausser, M. (eds) *Dendrites*. Oxford University Press, Oxford, pp. 1-41.

Figueredo-Cardenas, G., Morello, M., Sancesario, G., Bernardi, G. & Reiner, A. (1996) Colocalization of somatostatin, neuropeptide Y, neuronal nitric oxide synthase and NADPH-diaphorase in striatal interneurons in rats. *Brain Res*, **735**, 317-324.

Flaherty, A.W. & Graybiel, A.M. (1991) Corticostriatal transformations in the primate somatosensory system. Projections from physiologically mapped body-part representations. *J Neurophysiol*, **66**, 1249-1263.

Flaherty, A.W. & Graybiel, A.M. (1994) Input-output organization of the sensorimotor striatum in the squirrel monkey. *J Neurosci*, **14**, 599-610.

Foerde, K., Poldrack, R.A., Khan, B.J., Sabb, F.W., Bookheimer, S.Y., Bilder, R.M., Guthrie, D., Granholm, E., Nuechterlein, K.H., Marder, S.R. & Asarnow, R.F. (2008) Selective corticostriatal dysfunction in schizophrenia: examination of motor and cognitive skill learning. *Neuropsychology*, **22**, 100-109.

Francois, C., Percheron, G., Parent, A., Sadikot, A.F., Fenelon, G. & Yelnik, J. (1991) Topography of the projection from the central complex of the thalamus to the sensorimotor striatal territory in monkeys. *J Comp Neurol*, **305**, 17-34.

Fremeau, R.T., Jr., Troyer, M.D., Pahner, I., Nygaard, G.O., Tran, C.H., Reimer, R.J., Bellocchio, E.E., Fortin, D., Storm-Mathisen, J. & Edwards, R.H. (2001) The expression of vesicular glutamate transporters defines two classes of excitatory synapse. *Neuron*, **31**, 247-260.

Fremeau, R.T., Jr., Voglmaier, S., Seal, R.P. & Edwards, R.H. (2004) VGLUTs define subsets of excitatory neurons and suggest novel roles for glutamate. *Trends Neurosci*, **27**, 98-103.

Fujiyama, F., Kuramoto, E., Okamoto, K., Hioki, H., Furuta, T., Zhou, L., Nomura, S. & Kaneko, T. (2004) Presynaptic localization of an AMPA-type glutamate receptor in corticostriatal and thalamostriatal axon terminals. *Eur J Neurosci*, **20**, 3322-3330.

Fujiyama, F., Sohn, J., Nakano, T., Furuta, T., Nakamura, K.C., Matsuda, W. & Kaneko, T. (2011) Exclusive and common targets of neostriatofugal projections of rat striosome neurons: a single neuron-tracing study using a viral vector. *Eur J Neurosci*, **33**, 668-677.

Fujiyama, F., Unzai, T., Nakamura, K., Nomura, S. & Kaneko, T. (2006) Difference in organization of corticostriatal and thalamostriatal synapses between patch and matrix compartments of rat neostriatum. *Eur J Neurosci*, **24**, 2813-2824.

Gage, G.J., Stoetzner, C.R., Wiltschko, A.B. & Berke, J.D. (2010) Selective activation of striatal fast-spiking interneurons during choice execution. *Neuron*, **67**, 466-479.

Galarraga, E., Vilchis, C., Tkatch, T., Salgado, H., Tecuapetla, F., Perez-Rosello, T., Perez-Garci, E., Hernandez-Echeagaray, E., Surmeier, D.J. & Bargas, J. (2007) Somatostatinergic modulation of firing pattern and calcium-activated potassium currents in medium spiny neostriatal neurons. *Neuroscience*, **146**, 537-554.

Galvan, A. & Smith, Y. (2011) The primate thalamostriatal systems: Anatomical organization, functional roles and possible involvement in Parkinson's disease. *Basal Ganglia*, **1**, 179-189.

Gardiner, T.W. & Kitai, S.T. (1992) Single-unit activity in the globus pallidus and neostriatum of the rat during performance of a trained head movement. *Exp Brain Res*, **88**, 517-530.

GENSAT (2009) The Gene Expression Nervous System Atlas (GENSAT) Project. NINDS, Contracts N01NS02331 & HHSN271200723701C, The Rockerfeller University (New York, NY), http://www.gensat.org/index.html.

Gerfen, C.R. (1989) The neostriatal mosaic: striatal patch-matrix organization is related to cortical lamination. *Science*, **246**, 385-388.

Gerfen, C.R. (1992) The neostriatal mosaic: multiple levels of compartmental organization in the basal ganglia. *Annu Rev Neurosci*, **15**, 285-320.

Gerfen, C.R., Engber, T.M., Mahan, L.C., Susel, Z., Chase, T.N., Monsma, F.J., Jr. & Sibley, D.R. (1990) D1 and D2 Dopamine Receptor-Regulated Gene Expression of Striatonigral and Striatopallidal Neurons. *Science*, **250**, 1429-1432.

Gerfen, C.R. & Surmeier, D.J. (2011) Modulation of striatal projection systems by dopamine. *Annu Rev Neurosci*, **34**, 441-466.

Gertler, T.S., Chan, C.S. & Surmeier, D.J. (2008) Dichotomous anatomical properties of adult striatal medium spiny neurons. *J Neurosci*, **28**, 10814-10824.

Gittis, A.H., Nelson, A.B., Thwin, M.T., Palop, J.J. & Kreitzer, A.C. (2010) Distinct roles of GABAergic interneurons in the regulation of striatal output pathways. *J Neurosci*, **30**, 2223-2234.

Goldberg, J.A. & Reynolds, J.N. (2011) Spontaneous firing and evoked pauses in the tonically active cholinergic interneurons of the striatum. *Neuroscience*, **198**, 27-43.

Gong, S., Zheng, C., Doughty, M.L., Losos, K., Didkovsky, N., Schambra, U.B., Nowak, N.J., Joyner, A., Leblanc, G., Hatten, M.E. & Heintz, N. (2003) A gene expression atlas of the central nervous system based on bacterial artificial chromosomes. *Nature*, **425**, 917-925.

Graybiel, A.M. (2005) The basal ganglia: learning new tricks and loving it. *Curr Opin Neurobiol*, **15**, 638-644.

Graybiel, A.M. (2008) Habits, rituals, and the evaluative brain. *Annu Rev Neurosci*, **31**, 359-387.

Graybiel, A.M. & Rauch, S.L. (2000) Toward a neurobiology of obsessive-compulsive disorder. *Neuron*, **28**, 343-347.

Grillner, S., Hellgren, J., Menard, A., Saitoh, K. & Wikstrom, M.A. (2005) Mechanisms for selection of basic motor programs--roles for the striatum and pallidum. *Trends Neurosci*, **28**, 364-370.

Groenewegen, H.J. & Berendse, H.W. (1994) The specificity of the 'nonspecific' midline and intralaminar thalamic nuclei. *Trends Neurosci*, **17**, 52-57.

Gulyás, A.I., Megias, M., Emri, Z. & Freund, T.F. (1999) Total number and ratio of excitatory and inhibitory synapses converging onto single interneurons of different types in the CA1 area of the rat hippocampus. *J Neurosci*, **19**, 10082-10097.

Haber, S.N. & Calzavara, R. (2009) The cortico-basal ganglia integrative network: the role of the thalamus. *Brain Res Bull*, **78**, 69-74.

Hassani, O.K., Francois, C., Yelnik, J. & Feger, J. (1997) Evidence for a dopaminergic innervation of the subthalamic nucleus in the rat. *Brain Res*, **749**, 88-94.

Hauber, W. (1998) Involvement of basal ganglia transmitter systems in movement initiation. *Prog Neurobiol*, **56**, 507-540.

Henny, P., Brown, M.T., Northrop, A., Faunes, M., Ungless, M.A., Magill, P.J. & Bolam, J.P. (2012) Structural correlates of heterogeneous in vivo activity of midbrain dopaminergic neurons. *Nat Neurosci*, **15,** 613-619.

Herkenham, M. & Pert, C.B. (1981) Mosaic distribution of opiate receptors, parafascicular projections and acetylcholinesterase in rat striatum. *Nature*, **291**, 415-418.

Hersch, S.M., Ciliax, B.J., Gutekunst, C.A., Rees, H.D., Heilman, C.J., Yung, K.K., Bolam, J.P., Ince, E., Yi, H. & Levey, A.I. (1995) Electron microscopic analysis of D1 and D2 dopamine receptor proteins in the dorsal striatum and their synaptic relationships with motor corticostriatal afferents. *J Neurosci*, **15**, 5222-5237.

Herzog, E., Bellenchi, G.C., Gras, C., Bernard, V., Ravassard, P., Bedet, C., Gasnier, B., Giros, B. & El Mestikawy, S. (2001) The existence of a second vesicular glutamate transporter specifies subpopulations of glutamatergic neurons. *J Neurosci*, **21**, RC181.

Hikosaka, O. (2007) GABAergic output of the basal ganglia. *Prog Brain Res*, **160**, 209-226.

Hope, B.T., Michael, G.J., Knigge, K.M. & Vincent, S.R. (1991) Neuronal NADPH diaphorase is a nitric oxide synthase. *Proc Natl Acad Sci U S A*, **88**, 2811-2814.

Humphries, M.D., Wood, R. & Gurney, K. (2010) Reconstructing the three-dimensional GABAergic microcircuit of the striatum. *PLoS Comput Biol*, **6**, e1001011.

Ibanez-Sandoval, O., Tecuapetla, F., Unal, B., Shah, F., Koos, T. & Tepper, J.M. (2011) A Novel Functionally Distinct Subtype of Striatal Neuropeptide Y Interneuron. *J Neurosci*, **31**, 16757-16769.

Ingham, C.A., Hood, S.H., Taggart, P. & Arbuthnott, G.W. (1998) Plasticity of synapses in the rat neostriatum after unilateral lesion of the nigrostriatal dopaminergic pathway. *J Neurosci*, **18**, 4732-4743.

Inokawa, H., Yamada, H., Matsumoto, N., Muranishi, M. & Kimura, M. (2010) Juxtacellular labeling of tonically active neurons and phasically active neurons in the rat striatum. *Neuroscience*, **168**, 395-404.

Izzo, P.N. & Bolam, J.P. (1988) Cholinergic synaptic input to different parts of spiny striatonigral neurons in the rat. *J Comp Neurol*, **269**, 219-234.

Janssen, M.J., Ade, K.K., Fu, Z. & Vicini, S. (2009) Dopamine modulation of GABA tonic conductance in striatal output neurons. *J Neurosci*, **29**, 5116-5126.

Jiang, Z.G. & North, R.A. (1992) Pre- and postsynaptic inhibition by opioids in rat striatum. *J Neurosci*, **12**, 356-361.

Jones, E.G. (1985) *The Thalamus*. Plenum, New York.

Jones, E.G. (2007) *The Thalamus*. Cambridge University Press, Cambridge.

Joshua, M., Adler, A., Mitelman, R., Vaadia, E. & Bergman, H. (2008) Midbrain dopaminergic neurons and striatal cholinergic interneurons encode the difference between reward and aversive events at different epochs of probabilistic classical conditioning trials. *J Neurosci*, **28**, 11673-11684.

Kaneko, T. & Fujiyama, F. (2002) Complementary distribution of vesicular glutamate transporters in the central nervous system. *Neurosci Res*, **42**, 243-250.

Kasanetz, F., Riquelme, L.A. & Murer, M.G. (2002) Disruption of the two-state membrane potential of striatal neurones during cortical desynchronisation in anaesthetised rats. *J Physiol*, **543**, 577-589.

Kawaguchi, Y. (1997) Neostriatal cell subtypes and their functional roles. *Neurosci Res*, **27**, 1-8.

Kawaguchi, Y., Wilson, C.J., Augood, S.J. & Emson, P.C. (1995) Striatal interneurones: chemical, physiological and morphological characterization. *Trends Neurosci*, **18**, 527-535.

Kawaguchi, Y., Wilson, C.J. & Emson, P.C. (1989) Intracellular recording of identified neostriatal patch and matrix spiny cells in a slice preparation preserving cortical inputs. *J Neurophysiol*, **62**, 1052-1068.

Kawaguchi, Y., Wilson, C.J. & Emson, P.C. (1990) Projection subtypes of rat neostriatal matrix cells revealed by intracellular injection of biocytin. *J Neurosci*, **10**, 3421-3438.

Kelland, M.D., Soltis, R.P., Anderson, L.A., Bergstrom, D.A. & Walters, J.R. (1995) In vivo characterization of two cell types in the rat globus pallidus which have opposite responses to dopamine receptor stimulation: comparison of electrophysiological properties and responses to apomorphine, dizocilpine, and ketamine anesthesia. *Synapse*, **20**, 338-350.

Kemp, J.M. & Powell, T.P. (1970) The cortico-striate projection in the monkey. *Brain*, **93**, 525-546.

Kemp, J.M. & Powell, T.P. (1971a) The site of termination of afferent fibres in the caudate nucleus. *Philos Trans R Soc Lond B Biol Sci*, **262**, 413-427.

Kemp, J.M. & Powell, T.P. (1971b) The termination of fibres from the cerebral cortex and thalamus upon dendritic spines in the caudate nucleus: a study with the Golgi method. *Philos Trans R Soc Lond B Biol Sci*, **262**, 429-439.

Kimura, M., Rajkowski, J. & Evarts, E. (1984) Tonically discharging putamen neurons exhibit set-dependent responses. *Proc Natl Acad Sci U S A*, **81**, 4998-5001.

Kincaid, A.E. & Wilson, C.J. (1996) Corticostriatal innervation of the patch and matrix in the rat neostriatum. *J Comp Neurol*, **374**, 578-592.

Kincaid, A.E., Zheng, T. & Wilson, C.J. (1998) Connectivity and convergence of single corticostriatal axons. *J Neurosci*, **18**, 4722-4731.

Kita, H. (2007) Globus pallidus external segment. *Prog Brain Res*, **160**, 111-133.

Kita, H. & Kitai, S.T. (1994) The morphology of globus pallidus projection neurons in the rat: an intracellular staining study. *Brain Res*, **636**, 308-319.

Kita, H., Kosaka, T. & Heizmann, C.W. (1990) Parvalbumin-immunoreactive neurons in the rat neostriatum: a light and electron microscopic study. *Brain Res*, **536**, 1-15.

Kita, T., Kita, H. & Kitai, S.T. (1984) Passive electrical membrane properties of rat neostriatal neurons in an in vitro slice preparation. *Brain Res*, **300**, 129-139.

Koch, C. (1999) *Biophysics of computation : information processing in single neurons*. Oxford University Press, Oxford.

Koch, C., Poggio, T. & Torre, V. (1983) Nonlinear interactions in a dendritic tree: localization, timing, and role in information processing. *Proc Natl Acad Sci U S A*, **80**, 2799-2802.

Kocsis, J.D., Sugimori, M. & Kitai, S.T. (1977) Convergence of excitatory synaptic inputs to caudate spiny neurons. *Brain Res*, **124**, 403-413.

Koos, T. & Tepper, J.M. (1999) Inhibitory control of neostriatal projection neurons by GABAergic interneurons. *Nat Neurosci*, **2**, 467-472.

Koos, T., Tepper, J.M. & Wilson, C.J. (2004) Comparison of IPSCs evoked by spiny and fast-spiking neurons in the neostriatum. *J Neurosci*, **24**, 7916-7922.

Kramer, P.F., Christensen, C.H., Hazelwood, L.A., Dobi, A., Bock, R., Sibley, D.R., Mateo, Y. & Alvarez, V.A. (2011) Dopamine D2 receptor overexpression alters behavior and physiology in Drd2-EGFP mice. *J Neurosci*, **31**, 126-132.

Kreitzer, A.C. (2009) Physiology and pharmacology of striatal neurons. *Annu Rev Neurosci*, **32**, 127-147.

Kreitzer, A.C. & Malenka, R.C. (2007) Endocannabinoid-mediated rescue of striatal LTD and motor deficits in Parkinson's disease models. *Nature*, **445**, 643-647.

Kubota, Y., Inagaki, S., Shimada, S., Kito, S., Eckenstein, F. & Tohyama, M. (1987) Neostriatal cholinergic neurons receive direct synaptic inputs from dopaminergic axons. *Brain Res*, **413**, 179-184.

Kusnoor, S.V., Parris, J., Muly, E.C., Morgan, J.I. & Deutch, A.Y. (2010) Extracerebellar role for Cerebellin1: modulation of dendritic spine density and synapses in striatal medium spiny neurons. *J Comp Neurol*, **518**, 2525-2537.

Lacey, C.J., Bolam, J.P. & Magill, P.J. (2007) Novel and distinct operational principles of intralaminar thalamic neurons and their striatal projections. *J Neurosci*, **27**, 4374-4384.

Lacey, C.J., Boyes, J., Gerlach, O., Chen, L., Magill, P.J. & Bolam, J.P. (2005) GABA(B) receptors at glutamatergic synapses in the rat striatum. *Neuroscience*, **136**, 1083-1095.

Lanciego, J.L., Gonzalo, N., Castle, M., Sanchez-Escobar, C., Aymerich, M.S. & Obeso, J.A. (2004) Thalamic innervation of striatal and subthalamic neurons projecting to the rat entopeduncular nucleus. *Eur J Neurosci*, **19**, 1267-1277.

Lapper, S.R. & Bolam, J.P. (1992) Input from the frontal cortex and the parafascicular nucleus to cholinergic interneurons in the dorsal striatum of the rat. *Neuroscience*, **51**, 533-545.

Lapper, S.R., Smith, Y., Sadikot, A.F., Parent, A. & Bolam, J.P. (1992) Cortical input to parvalbumin-immunoreactive neurones in the putamen of the squirrel monkey. *Brain Res*, **580**, 215-224.

Larsson, M. & Broman, J. (2005) Different basal levels of CaMKII phosphorylated at Thr286/287 at nociceptive and low-threshold primary afferent synapses. *Eur J Neurosci*, **21**, 2445-2458.

Lei, W., Jiao, Y., Del Mar, N. & Reiner, A. (2004) Evidence for differential cortical input to direct pathway versus indirect pathway striatal projection neurons in rats. *J Neurosci*, **24**, 8289-8299.

Llewellyn-Smith, I.J., Pilowsky, P. & Minson, J.B. (1993) The tungstate-stabilized tetramethylbenzidine reaction for light and electron microscopic immunocytochemistry

and for revealing biocytin-filled neurons. *J Neurosci Methods*, **46**, 27-40.

Lobo, M.K., Karsten, S.L., Gray, M., Geschwind, D.H. & Yang, X.W. (2006) FACS-array profiling of striatal projection neuron subtypes in juvenile and adult mouse brains. *Nat Neurosci*, **9**, 443-452.

Lopez-Huerta, V.G., Tecuapetla, F., Guzman, J.N., Bargas, J. & Galarraga, E. (2008) Presynaptic modulation by somatostatin in the neostriatum. *Neurochem Res*, **33**, 1452-1458.

Magill, P.J., Bolam, J.P. & Bevan, M.D. (2000) Relationship of activity in the subthalamic nucleus-globus pallidus network to cortical electroencephalogram. *J Neurosci*, **20**, 820-833.

Mahon, S., Deniau, J.M. & Charpier, S. (2001) Relationship between EEG potentials and intracellular activity of striatal and cortico-striatal neurons: an in vivo study under different anesthetics. *Cereb Cortex*, **11**, 360-373.

Mahon, S., Vautrelle, N., Pezard, L., Slaght, S.J., Deniau, J.M., Chouvet, G. & Charpier, S. (2006) Distinct patterns of striatal medium spiny neuron activity during the natural sleep-wake cycle. *J Neurosci*, **26**, 12587-12595.

Mailly, P., Charpier, S., Menetrey, A. & Deniau, J.M. (2003) Three-dimensional organization of the recurrent axon collateral network of the substantia nigra pars reticulata neurons in the rat. *J Neurosci*, **23**, 5247-5257.

Mainen, Z.F. & Sejnowski, T.J. (1996) Influence of dendritic structure on firing pattern in model neocortical neurons. *Nature*, **382**, 363-366.

Mallet, N., Le Moine, C., Charpier, S. & Gonon, F. (2005) Feedforward inhibition of projection neurons by fast-spiking GABA interneurons in the rat striatum in vivo. *J Neurosci*, **25**, 3857-3869.

Martone, M.E., Armstrong, D.M., Young, S.J. & Groves, P.M. (1992) Ultrastructural examination of enkephalin and substance P input to cholinergic neurons within the rat neostriatum. *Brain Res*, **594**, 253-262.

Matsuda, W., Furuta, T., Nakamura, K.C., Hioki, H., Fujiyama, F., Arai, R. & Kaneko, T. (2009) Single nigrostriatal dopaminergic neurons form widely spread and highly dense axonal arborizations in the neostriatum. *J Neurosci*, **29**, 444-453.

Matsumoto, N., Minamimoto, T., Graybiel, A.M. & Kimura, M. (2001) Neurons in the thalamic CM-Pf complex supply striatal neurons with information about behaviorally significant sensory events. *J Neurophysiol*, **85**, 960-976.

McGeorge, A.J. & Faull, R.L. (1989) The organization of the projection from the cerebral cortex to the striatum in the rat. *Neuroscience*, **29**, 503-537.

McHaffie, J.G., Stanford, T.R., Stein, B.E., Coizet, V. & Redgrave, P. (2005) Subcortical loops through the basal ganglia. *Trends Neurosci*, **28**, 401-407.

Megias, M., Emri, Z., Freund, T.F. & Gulyas, A.I. (2001) Total number and distribution of inhibitory and excitatory synapses on hippocampal CA1 pyramidal cells. *Neuroscience*, **102**, 527-540.

Meredith, G.E. & Wouterlood, F.G. (1990) Hippocampal and midline thalamic fibers and terminals in relation to the choline acetyltransferase-immunoreactive neurons in nucleus accumbens of the rat: a light and electron microscopic study. *J Comp Neurol*, **296**, 204-221.

Minamimoto, T., Hori, Y. & Kimura, M. (2005) Complementary process to response bias in the centromedian nucleus of the thalamus. *Science*, **308**, 1798-1801.

Minamimoto, T. & Kimura, M. (2002) Participation of the thalamic CM-Pf complex in attentional orienting. *J Neurophysiol*, **87**, 3090-3101.

Miyamichi, K., Amat, F., Moussavi, F., Wang, C., Wickersham, I., Wall, N.R., Taniguchi, H., Tasic, B., Huang, Z.J., He, Z., Callaway, E.M., Horowitz, M.A. & Luo, L. (2011) Cortical representations of olfactory input by trans-synaptic tracing. *Nature*, **472**, 191-196.

Molina-Hernandez, A., Nunez, A., Sierra, J.J. & Arias-Montano, J.A. (2001) Histamine H3 receptor activation inhibits glutamate release from rat striatal synaptosomes. *Neuropharmacology*, **41**, 928-934.

Morello, M., Reiner, A., Sancesario, G., Karle, E.J. & Bernardi, G. (1997) Ultrastructural study of nitric oxide synthase-containing striatal neurons and their relationship with parvalbumin-containing neurons in rats. *Brain Res*, **776**, 30-39.

Morris, G., Arkadir, D., Nevet, A., Vaadia, E. & Bergman, H. (2004) Coincident but distinct messages of midbrain dopamine and striatal tonically active neurons. *Neuron*, **43**, 133-143.

Moss, J. & Bolam, J.P. (2008) A dopaminergic axon lattice in the striatum and its relationship with cortical and thalamic terminals. *J Neurosci*, **28**, 11221-11230.

Moss, J., Ungless, M.A. & Bolam, J.P. (2011) Dopaminergic axons in different divisions of the adult rat striatal complex do not express vesicular glutamate transporters. *Eur J Neurosci*, **33**, 1205-1211.

Murer, M.G., Tseng, K.Y., Kasanetz, F., Belluscio, M. & Riquelme, L.A. (2002) Brain oscillations, medium spiny neurons, and dopamine. *Cell Mol Neurobiol*, **22**, 611-632.

Nambu, A., Tokuno, H. & Takada, M. (2002) Functional significance of the cortico-subthalamo-pallidal 'hyperdirect' pathway. *Neurosci Res*, **43**, 111-117.

Nanda, B., Galvan, A., Smith, Y. & Wichmann, T. (2009) Effects of stimulation of the centromedian nucleus of the thalamus on the activity of striatal cells in awake rhesus monkeys. *Eur J Neurosci*, **29**, 588-598.

Navailles, S. & De Deurwaerdere, P. (2011) Presynaptic control of serotonin on striatal dopamine function. *Psychopharmacology (Berl)*, **213**, 213-242.

Nisenbaum, E.S. & Wilson, C.J. (1995) Potassium currents responsible for inward and outward rectification in rat neostriatal spiny projection neurons. *J Neurosci*, **15**, 4449-4463.

Ondracek, J.M., Dec, A., Hoque, K.E., Lim, S.A., Rasouli, G., Indorkar, R.P., Linardakis, J., Klika, B., Mukherji, S.J., Burnazi, M., Threlfell, S., Sammut, S. & West, A.R. (2008) Feed-forward excitation of striatal neuron activity by frontal cortical activation of nitric oxide signaling in vivo. *Eur J Neurosci*, **27**, 1739-1754.

Oorschot, D.E. (1996) Total number of neurons in the neostriatal, pallidal, subthalamic, and substantia nigral nuclei of the rat basal ganglia: a stereological study using the cavalieri and optical disector methods. *J Comp Neurol*, **366**, 580-599.

Pakhotin, P. & Bracci, E. (2007) Cholinergic interneurons control the excitatory input to the striatum. *J Neurosci*, **27**, 391-400.

Parent, A., Charara, A. & Pinault, D. (1995) Single striatofugal axons arborizing in both pallidal segments and in the substantia nigra in primates. *Brain Res*, **698**, 280-284.

Parthasarathy, H.B. & Graybiel, A.M. (1997) Cortically driven immediate-early gene expression reflects modular influence of sensorimotor cortex on identified striatal neurons in the squirrel monkey. *J Neurosci*, **17**, 2477-2491.

Partridge, J.G., Janssen, M.J., Chou, D.Y., Abe, K., Zukowska, Z. & Vicini, S. (2009) Excitatory and inhibitory synapses in neuropeptide Y-expressing striatal interneurons. *J Neurophysiol*, **102**, 3038-3045.

Patel, Y.C. (1999) Somatostatin and its receptor family. *Frontiers in Neuroendocrinology*, **20**, 157-198.

Paxinos, G. & Watson, C. (1986) *The rat brain in stereotaxic coordinates*. Academic Press, Sydney, Australia.

Phelps, P.E., Houser, C.R. & Vaughn, J.E. (1985) Immunocytochemical localization of choline acetyltransferase within the rat neostriatum: a correlated light and electron microscopic study of cholinergic neurons and synapses. *J Comp Neurol*, **238**, 286-307.

Pickel, V.M., Chan, J. & Sesack, S.R. (1992) Cellular basis for interactions between catecholaminergic afferents and neurons containing Leu-enkephalin-like immunoreactivity in rat caudate-putamen nuclei. *J Neurosci Res*, **31**, 212-230.

Pinault, D. (1996) A novel single-cell staining procedure performed in vivo under electrophysiological control: morpho-functional features of juxtacellularly labeled thalamic cells and other central neurons with biocytin or Neurobiotin. *J Neurosci Methods*, **65**, 113-136.

Planert, H., Szydlowski, S.N., Hjorth, J.J., Grillner, S. & Silberberg, G. (2010) Dynamics of synaptic transmission between fast-spiking interneurons and striatal projection neurons of the direct and indirect pathways. *J Neurosci*, **30**, 3499-3507.

Plenz, D. & Kital, S.T. (1999) A basal ganglia pacemaker formed by the subthalamic nucleus and external globus pallidus. *Nature*, **400**, 677-682.

Pollard, H., Moreau, J., Arrang, J.M. & Schwartz, J.C. (1993) A detailed autoradiographic mapping of histamine H3 receptors in rat brain areas. *Neuroscience*, **52**, 169-189.

Preston, R.J., Bishop, G.A. & Kitai, S.T. (1980) Medium spiny neuron projection from the rat striatum: an intracellular horseradish peroxidase study. *Brain Res*, **183**, 253-263.

Raju, D.V., Ahern, T.H., Shah, D.J., Wright, T.M., Standaert, D.G., Hall, R.A. & Smith, Y. (2008) Differential synaptic plasticity of the corticostriatal and thalamostriatal systems in an MPTP-treated monkey model of parkinsonism. *Eur J Neurosci*, **27**, 1647-1658.

Raju, D.V., Shah, D.J., Wright, T.M., Hall, R.A. & Smith, Y. (2006) Differential synaptology of VGluT2-containing thalamostriatal afferents between the patch and matrix compartments in rats. *J Comp Neurol*, **499**, 231-243.

Ramanathan, S., Hanley, J.J., Deniau, J.M. & Bolam, J.P. (2002) Synaptic convergence of motor and somatosensory cortical afferents onto GABAergic interneurons in the rat striatum. *J Neurosci*, **22**, 8158-8169.

Rancz, E.A., Franks, K.M., Schwarz, M.K., Pichler, B., Schaefer, A.T. & Margrie, T.W. (2011) Transfection via whole-cell recording in vivo: bridging single-cell physiology, genetics and connectomics. *Nat Neurosci*, **14**, 527-532.

Redgrave, P., Prescott, T.J. & Gurney, K. (1999) The basal ganglia: a vertebrate solution to the selection problem? *Neuroscience*, **89**, 1009-1023.

Reiner, A., Medina, L. & Veenman, C.L. (1998) Structural and functional evolution of the basal ganglia in vertebrates. *Brain Res Rev*, **28**, 235-285.

Reynolds, J.N., Hyland, B.I. & Wickens, J.R. (2001) A cellular mechanism of reward-related learning. *Nature*, **413**, 67-70.

Reynolds, J.N. & Wickens, J.R. (2004) The corticostriatal input to giant aspiny interneurons in the rat: a candidate pathway for synchronising the response to reward-related cues. *Brain Res*, **1011**, 115-128.

Rudkin, T.M. & Sadikot, A.F. (1999) Thalamic input to parvalbumin-immunoreactive GABAergic interneurons: organization in normal striatum and effect of neonatal decortication. *Neuroscience*, **88**, 1165-1175.

Rymar, V.V., Sasseville, R., Luk, K.C. & Sadikot, A.F. (2004) Neurogenesis and stereological morphometry of calretinin-immunoreactive GABAergic interneurons of the neostriatum. *J Comp Neurol*, **469**, 325-339.

Sadek, A.R., Magill, P.J. & Bolam, J.P. (2007) A single-cell analysis of intrinsic connectivity in the rat globus pallidus. *J Neurosci*, **27**, 6352-6362.

Sadikot, A.F., Parent, A. & Francois, C. (1992a) Efferent connections of the centromedian and parafascicular thalamic nuclei in the squirrel monkey: a PHA-L study of subcortical projections. *J Comp Neurol*, **315**, 137-159.

Sadikot, A.F., Parent, A., Smith, Y. & Bolam, J.P. (1992b) Efferent connections of the centromedian and parafascicular thalamic nuclei in the squirrel monkey: a light and electron microscopic study of the thalamostriatal projection in relation to striatal heterogeneity. *J Comp Neurol*, **320**, 228-242.

Sadikot, A.F. & Rymar, V.V. (2009) The primate centromedian-parafascicular complex: anatomical organization with a note on neuromodulation. *Brain Res Bull*, **78**, 122-130.

Salin, P. & Kachidian, P. (1998) Thalamo-striatal deafferentation affects preproenkephalin but not preprotachykinin gene expression in the rat striatum. *Brain Res Mol Brain Res*, **57**, 257-265.

Sammut, S., Park, D.J. & West, A.R. (2007) Frontal cortical afferents facilitate striatal nitric oxide transmission in vivo via a NMDA receptor and neuronal NOS-dependent mechanism. *J Neurochem*, **103**, 1145-1156.

Schultz, W. (1998) Predictive reward signal of dopamine neurons. *J Neurophysiol*, **80**, 1-27.

Schulz, J.M., Oswald, M.J. & Reynolds, J.N. (2011) Visual-induced excitation leads to firing pauses in striatal cholinergic interneurons. *J Neurosci*, **31**, 11133-11143.

Shen, W., Flajolet, M., Greengard, P. & Surmeier, D.J. (2008) Dichotomous dopaminergic control of striatal synaptic plasticity. *Science*, **321**, 848-851.

Sherman, S.M. & Guillery, R.W. (1996) Functional organization of thalamocortical relays. J

Neurophysiol, 76, 1367-1395.

Shink, E., Bevan, M.D., Bolam, J.P. & Smith, Y. (1996) The subthalamic nucleus and the external pallidum: two tightly interconnected structures that control the output of the basal ganglia in the monkey. *Neuroscience*, **73**, 335-357.

Shuen, J.A., Chen, M., Gloss, B. & Calakos, N. (2008) Drd1a-tdTomato BAC transgenic mice for simultaneous visualization of medium spiny neurons in the direct and indirect pathways of the basal ganglia. *J Neurosci*, **28**, 2681-2685.

Sidibé, M. & Smith, Y. (1996) Differential synaptic innervation of striatofugal neurones projecting to the internal or external segments of the globus pallidus by thalamic afferents in the squirrel monkey. *J Comp Neurol*, **365**, 445-465.

Sidibé, M. & Smith, Y. (1999) Thalamic inputs to striatal interneurons in monkeys: synaptic organization and co-localization of calcium binding proteins. *Neuroscience*, **89**, 1189-1208.

Sizemore, R.J., Reynolds, J.N. & Oorschot, D.E. (2010) Number and type of synapses on the distal dendrite of a rat striatal cholinergic interneuron: a quantitative, ultrastructural study. *Journal of Anatomy*, **217**, 223-235.

Smeal, R.M., Gaspar, R.C., Keefe, K.A. & Wilcox, K.S. (2007) A rat brain slice preparation for characterizing both thalamostriatal and corticostriatal afferents. *J Neurosci Methods*, **159**, 224-235.

Smeal, R.M., Keefe, K.A. & Wilcox, K.S. (2008) Differences in excitatory transmission between thalamic and cortical afferents to single spiny efferent neurons of rat dorsal striatum. *Eur J Neurosci*, **28**, 2041-2052.

Smith, A.D. & Bolam, J.P. (1990a) The neural network of the basal ganglia as revealed by the study of synaptic connections of identified neurones. *Trends Neurosci*, **13**, 259-265.

Smith, Y., Bennett, B.D., Bolam, J.P., Parent, A. & Sadikot, A.F. (1994) Synaptic relationships between dopaminergic afferents and cortical or thalamic input in the sensorimotor territory of the striatum in monkey. *J Comp Neurol*, **344**, 1-19.

Smith, Y., Bevan, M.D., Shink, E. & Bolam, J.P. (1998) Microcircuitry of the direct and indirect

pathways of the basal ganglia. *Neuroscience*, **86**, 353-387.

Smith, Y. & Bolam, J.P. (1990b) The output neurones and the dopaminergic neurones of the substantia nigra receive a GABA-containing input from the globus pallidus in the rat. *J Comp Neurol*, **296**, 47-64.

Smith, Y. & Kieval, J.Z. (2000) Anatomy of the dopamine system in the basal ganglia. *Trends Neurosci*, **23**, S28-33.

Smith, Y. & Parent, A. (1986) Neuropeptide Y-immunoreactive neurons in the striatum of cat and monkey: morphological characteristics, intrinsic organization and co-localization with somatostatin. *Brain Res*, **372**, 241-252.

Smith, Y., Raju, D., Nanda, B., Pare, J.F., Galvan, A. & Wichmann, T. (2009a) The thalamostriatal systems: anatomical and functional organization in normal and parkinsonian states. *Brain Res Bull*, **78**, 60-68.

Smith, Y., Raju, D.V., Pare, J.-F. & Sidibé, M. (2004) The thalamostriatal system: a highly specific network of the basal ganglia circuitry. *Trends Neurosci*, **27**, 520-527.

Smith, Y., Surmeier, D.J., Redgrave, P. & Kimura, M. (2011) Thalamic contributions to Basal Ganglia-related behavioral switching and reinforcement. *J Neurosci*, **31**, 16102-16106.

Smith, Y., Villalba, R.M. & Raju, D.V. (2009b) Striatal spine plasticity in Parkinson's disease: pathological or not? *Parkinsonism Relat Disord*, **15 Suppl 3**, S156-161.

Somogyi, P., Bolam, J.P. & Smith, A.D. (1981) Monosynaptic cortical input and local axon collaterals of identified striatonigral neurons. A light and electron microscopic study using the Golgi-peroxidase transport-degeneration procedure. *J Comp Neurol*, **195**, 567-584.

Somogyi, P., Priestley, J.V., Cuello, A.C., Smith, A.D. & Takagi, H. (1982) Synaptic connections of enkephalin-immunoreactive nerve terminals in the neostriatum: a correlated light and electron microscopic study. *J Neurocytol*, **11**, 779-807.

Stephenson-Jones, M., Samuelsson, E., Ericsson, J., Robertson, B. & Grillner, S. (2011) Evolutionary conservation of the basal ganglia as a common vertebrate mechanism for action selection. *Curr Biol*, **21**, 1081-1091.

Steriade, M. (2000) Corticothalamic resonance, states of vigilance and mentation. *Neuroscience*, **101**, 243-276.

Stern, E.A., Jaeger, D. & Wilson, C.J. (1998) Membrane potential synchrony of simultaneously recorded striatal spiny neurons in vivo. *Nature*, **394**, 475-478.

Surmeier, D.J., Ding, J., Day, M., Wang, Z. & Shen, W. (2007) D1 and D2 dopamine-receptor modulation of striatal glutamatergic signaling in striatal medium spiny neurons. *Trends Neurosci*, **30**, 228-235.

Tepper JM, Koós T, Wilson CJ. (2004) GABAergic microcircuits in the neostriatum. *Trends Neurosci*, **27**, 662-669.

Tepper, J.M., Tecuapetla, F., Koos, T. & Ibanez-Sandoval, O. (2010) Heterogeneity and diversity of striatal GABAergic interneurons. *Front Neuroanat*, **4**, 150.

Thomas, T.M., Smith, Y., Levey, A.I. & Hersch, S.M. (2000) Cortical inputs to m2-immunoreactive striatal interneurons in rat and monkey. *Synapse*, **37**, 252-261.

Valjent, E., Bertran-Gonzalez, J., Herve, D., Fisone, G. & Girault, J.A. (2009) Looking BAC at striatal signaling: cell-specific analysis in new transgenic mice. *Trends Neurosci*, **32**, 538-547.

Van der Werf, Y.D., Witter, M.P. & Groenewegen, H.J. (2002) The intralaminar and midline nuclei of the thalamus. Anatomical and functional evidence for participation in processes of arousal and awareness. *Brain Res Brain Res Rev*, **39**, 107-140.

Vandermaelen, C.P. & Kitai, S.T. (1980) Intracellular analysis of synaptic potentials in rat neostriatum following stimulation of the cerebral cortex, thalamus, and substantia nigra. *Brain Res Bull*, **5**, 725-733.

Vincent, S.R., Johansson, O., Hokfelt, T., Skirboll, L., Elde, R.P., Terenius, L., Kimmel, J. & Goldstein, M. (1983) NADPH-diaphorase: a selective histochemical marker for striatal neurons containing both somatostatin- and avian pancreatic polypeptide (APP)-like immunoreactivities. *J Comp Neurol*, **217**, 252-263.

Vuillet, J., Dimova, R., Nieoullon, A. & Kerkerian-Le Goff, L. (1992) Ultrastructural relationships between choline acetyltransferase- and neuropeptide y-containing neurons in the rat striatum. *Neuroscience*, **46**, 351-360.

Vuillet, J., Kerkerian, L., Kachidian, P., Bosler, O. & Nieoullon, A. (1989) Ultrastructural correlates of functional relationships between nigral dopaminergic or cortical afferent fibers and neuropeptide Y-containing neurons in the rat striatum. *Neurosci Lett*, **100**, 99-104.

Wainer, B.H., Bolam, J.P., Freund, T.F., Henderson, Z., Totterdell, S. & Smith, A.D. (1984) Cholinergic synapses in the rat brain: a correlated light and electron microscopic immunohistochemical study employing a monoclonal antibody against choline acetyltransferase. *Brain Res*, **308**, 69-76.

Wang, Z., Kai, L., Day, M., Ronesi, J., Yin, H.H., Ding, J., Tkatch, T., Lovinger, D.M. & Surmeier, D.J. (2006) Dopaminergic control of corticostriatal long-term synaptic depression in medium spiny neurons is mediated by cholinergic interneurons. *Neuron*, **50**, 443-452.

Webster, K.E. (1961) Cortico-striate interrelations in the albino rat. *Journal of Anatomy*, **95**, 532-544.

West, A.R., Galloway, M.P. & Grace, A.A. (2002) Regulation of striatal dopamine neurotransmission by nitric oxide: effector pathways and signaling mechanisms. *Synapse*, **44**, 227-245.

Wickens, J.R. (2009) Synaptic plasticity in the basal ganglia. *Behav Brain Res*, **199**, 119-128.

Wilson, C.J. (1993) The generation of natural firing patterns in neostriatal neurons. *Prog Brain Res*, **99**, 277-297.

Wilson, C.J. (2007) GABAergic inhibition in the neostriatum. *Prog Brain Res*, **160**, 91-110.

Wilson, C.J., Chang, H.T. & Kitai, S.T. (1990) Firing patterns and synaptic potentials of identified giant aspiny interneurons in the rat neostriatum. *J Neurosci*, **10**, 508-519.

Wilson, C.J. & Goldberg, J.A. (2006) Origin of the slow afterhyperpolarization and slow rhythmic bursting in striatal cholinergic interneurons. *J Neurophysiol*, **95**, 196-204.

Wilson, C.J. & Groves, P.M. (1980) Fine structure and synaptic connections of the common spiny neuron of the rat neostriatum: a study employing intracellular inject of horseradish peroxidase. *J Comp Neurol*, **194**, 599-615.

Wilson, C.J. & Groves, P.M. (1981) Spontaneous firing patterns of identified spiny neurons in the rat neostriatum. *Brain Res*, **220**, 67-80.

Wilson, C.J. & Kawaguchi, Y. (1996) The origins of two-state spontaneous membrane potential fluctuations of neostriatal spiny neurons. *J Neurosci*, **16**, 2397-2410.

Wu, Y. & Parent, A. (2000) Striatal interneurons expressing calretinin, parvalbumin or NADPH-diaphorase: a comparative study in the rat, monkey and human. *Brain Res*, **863**, 182-191.

Wu, Y., Richard, S. & Parent, A. (2000) The organization of the striatal output system: a single-cell juxtacellular labeling study in the rat. *Neurosci Res*, **38**, 49-62.

Xu, Z.C., Wilson, C.J. & Emson, P.C. (1989) Restoration of the corticostriatal projection in rat neostriatal grafts: electron microscopic analysis. *Neuroscience*, **29**, 539-550.

Xu, Z.C., Wilson, C.J. & Emson, P.C. (1991) Restoration of thalamostriatal projections in rat neostriatal grafts: an electron microscopic analysis. *J Comp Neurol*, **303**, 22-34.

Yamada, T., McGeer, P.L., Baimbridge, K.G. & McGeer, E.G. (1990) Relative sparing in Parkinson's disease of substantia nigra dopamine neurons containing calbindin-D28K. *Brain Res*, **526**, 303-307.

Yung, K.K., Smith, A.D., Levey, A.I. & Bolam, J.P. (1996) Synaptic connections between spiny neurons of the direct and indirect pathways in the neostriatum of the rat: evidence from dopamine receptor and neuropeptide immunostaining. *Eur J Neurosci*, **8**, 861-869.

Yung, K.K.L., Bolam, J.P., Smith, A.D., Hersch, S.M., Ciliax, B.J. & Levey, A.I. (1995) Immunocytochemical localization of D1 and D2 dopamine receptors in the basal ganglia of the rat: Light and electron microscopy. *Neuroscience*, **65**, 709-730.

Zheng, T. & Wilson, C.J. (2002) Corticostriatal combinatorics: the implications of corticostriatal axonal arborizations. *J Neurophysiol*, **87**, 1007-1017.

Zhou, F.M., Wilson, C.J. & Dani, J.A. (2002) Cholinergic interneuron characteristics and nicotinic properties in the striatum. *J Neurobiol*, **53**, 590-605.